

Report NADC 76238 30

Vol. I & Vol. II

Volume I

LEVEL

25

DDC
RECEIVED
NOV 1 1978

METALCLAD AIRSHIP HULL STUDY

9 F

AD A060637

DDC FILE COPY

TURBOMACHINES, INC.
17342 EASTMAN ST., IRVINE, CALIF. 92705

This document has been approved
for public release and sale; its
distribution is unlimited.

L. R. Campbell, V. H. Pavlecka, J. W. Roda,
E. V. Stephens and G. Szuladzinski

DECEMBER, 1976

FINAL REPORT

PREPARED FOR

NAVAL AIR DEVELOPMENT CENTER

WARMINSTER, PENNSYLVANIA 18974

NADC-31P3

78 10 16 073

19 REPORT DOCUMENTATION PAGE		READ INSTRUCTIONS BEFORE COMPLETING FORM	
1. REPORT NUMBER NADC 76238-38-1	2. GOVT ACCESSION NO.	3. RECIPIENT'S CATALOG NUMBER	
4. TITLE (and Subtitle) METALCLAD AIRSHIP STUDY, Volume I and Volume II.	5. TYPE OF REPORT & PERIOD COVERED Final Report.	6. PERFORMING ORG. REPORT NUMBER R-MC1276-01	
7. AUTHOR(s)	8. CONTRACT OR GRANT NUMBER(s) N62269-76-C-0500	9. PROGRAM ELEMENT, PROJECT, TASK AREA & WORK UNIT NUMBERS UDI-H-21353A (AE-219E)	
10. CONTROLLING OFFICE NAME AND ADDRESS Turbomachines, Inc. 17342 Eastman St. Irvine, Calif. 92714	11. REPORT DATE December 1976	12. NUMBER OF PAGES Vol I 380-Vol II 7 Dwgs.	
13. MONITORING AGENCY NAME & ADDRESS (if different from Controlling Office) Lighter-Than-Air Project Office (30P3) Naval Air Development Center Warminster, Pa. 18974	14. SECURITY CLASS. (of this report) Unclassified	15. DECLASSIFICATION/DOWNGRADING SCHEDULE	
16. DISTRIBUTION STATEMENT (of this Report) Approved for Public Release; Distribution Unlimited			
17. DISTRIBUTION STATEMENT (of the abstract entered in Block 20, if different from Report) L. R. Campbell, V. H. Pavlecka, J. W. Roda, E. V. Stephens E. Szuladzinski			
18. SUPPLEMENTARY NOTES Contract Monitor was Mr. Thomas E. Hess, Advanced Technology Section, Aero Structures Division, Air Vehicle Technology Department, Naval Air Development Center			
19. KEY WORDS (Continue on reverse side if necessary and identify by block number) Airships Lighter-Than-Air Aircraft Structures Shell Structures			
20. ABSTRACT (Continue on reverse side if necessary and identify by block number) This report determines the structural weights (lifting structure only) of five Metalclad airship hulls of 10 to 20 million cubic feet displacement and capable of 100 knots airspeed. The in- dividual hull weights are then related to the gross displacement lift producing a ratio denoted λ (lambda), which indicates the merit of each hull for lifting useful load. To determine the hull weights it was necessary to analyze the hull strength with			

DD FORM 1 JAN 73 1473

EDITION OF 1 NOV 65 IS OBSOLETE
S/N 0102- LF-014-6601

SECURITY CLASSIFICATION OF THIS PAGE (When Data Entered)

393 094

12

(20) Abstract (continued)

respect to maximum loading moments. This process required the computation of stresses in the shell skin and analysis of the interaction of the skin with the hull structure. In the course of these background investigations, prior structural concepts were refined, flexible diaphragms for containment of gas proposed and internal operating air pressures determined.

Hull form shapes, design of structure, including materials and processes, construction methods and parameters of operation are necessarily covered in this report.

Present, as well as, new materials and technology were applied to obtain a very low coefficient compared to historic skeletal rigid airships. This coupled with a higher and broader variation of internal pressures, resulted in a conclusion that Metal-clad airships are technically and operationally feasible, economically viable and reliable under adverse conditions.

Summa

Accession for	
NTIS	White Section <input type="checkbox"/>
DDC	Buff Section <input type="checkbox"/>
UNANNOUNCED	
JUSTIFICATION	
BY DISTRIBUTION/AVAILABILITY CODES	
Dist.	and/or SPECIAL
A	

SUMMARY

The purpose of this study is to reliably determine the weights of Metalclad airship hulls in the range of gross displacements between 10 million and 20 million cubic feet. The parameter expressed by Lambda (λ), the ratio of the weight of a hull to its gross displacement lift, is of basic significance to the justification for pursuing airship development.

To arrive at a valid conclusion for the value of Lambda, it was necessary to propose a design architecture of structures suitable for Metalclad hulls and to analyze typical examples of it; to analyze the effect of maximum external loads on the hulls; to determine the thicknesses of the hull shell skin and design efficient joining seams; to explore the interaction of the skin with the hull structure; to determine hull air pressures; to consider the division of the hull volume into sub-volumes and gas cells and devise means for inflating the hull with as little contamination by air as possible; to investigate the extreme case of loss of pressure and lift of the maximum volume cell during flight.

All these exploratory studies were performed with what is considered positive and encouraging results, substantiating the calculated weights of skin, structure, cell membranes and diaphragms for each hull. The work was carried throughout with a conservative approach which was deliberate with respect to the analytical procedures and in the case of the hull skin, was enforced by limitations of the availability of skin gages in the catalog of standard thicknesses of light aluminum alloy sheet metal. This observation is important because in all past experience with Metalclad principles, there always existed an impression that the quoted hull weights were optimistic. This report is definitely conservative in its approach to the determination of weights; it concludes with the expectation that the ultimate weight of hulls designed in detail, with more painstaking analytical preparation, will be actually less than determined in this study.

The work on the substance of the study also lead to other important conclusions, some of which share equal importance with low hull weight. Foremost among them is the determination of relatively high hull air pressure, compared to the initial Metalclad airship development, when with low strength aluminum alloys and poor efficiencies of seam joints, the air pressure had to be uncomfortably low. The report concludes that the hull pressure in a large Metalclad hull with present technology would be at least ten times higher and could vary between its maximum value and a value at least thirty five per cent lower than was previously possible without losing tension.

in the hull skin even under the most severe flight bending moment.

Another by-product of the study is the determination of a Metalclad architecture of structures for Metalclad hulls which are cellular in principle, never used before in rigid airships; the study determined that these structures are light in weight, capable of functioning in harmony with elastic deformations of the skin and are highly redundant both, in loading (since they are continuous circular beams) as well as incidental damage. Cellular structures are also easier to fabricate. The elastic compatibility of interaction between skin and structure is an important conclusion of this study; it was analyzed and determined with the aid of a computer that the shell skin and the hull structure directly attached to it, can be made elastically compatible in their relative deformations at all their interfaces, as mentioned immediately above without any complexity, in fact, without additional weight.

One expected conclusion relates to the soundness of the principle of using external longerons, without any explicit joints with the internal frame structure, yet with firm attachment to it through the hull skin. Had the orthodox method of connecting structural elements been followed; i.e., by re-joining them after cutting for attachment to another element, the structural weight would have been greater, with the Lambda parameter reaching values of over $\lambda > .30$, even in the largest hulls, not to mention the complexity and cost of such construction.

Determination of weights required a serious study of cell sizes and of the functioning of cell membranes. The prior concept of providing gas cells in Metalclad hulls was confirmed in its overall practicability for the containment of gas, with a number of advantages, including the minimum conceivable area of membrane material required for the purpose. Although there has been a noticeable improvement in specific weights of membranes within the last ten years, this weight is still too high for internal membranes; further development needs to be accomplished with the aim of devising membranes specifically for Metalclad hulls, within which cell membranes are particularly well protected.

An important conclusion has emerged with respect to the form of the hulls. It is known that large rigid airship hulls vibrated in the stern portion. This vibration was induced beyond doubt by separation of the boundary layer (BL) with resulting shedding of vortices that caused force instabilities over the stern hull surface; similar vibrations are also known in sea-going ships, especially at high speeds. Once this was

accepted as a reasonable explanation of the cause of hull vibrations, the importance of the BL control in airships became basic. Originally, the hull drag was expected to be reduced by BL control; this objective has now taken second place, and delay of air mass separation around the stern has now the priority over drag reduction, as desirable as the latter also is. Metalclad hulls would suffer more severely from shedding of vortices than fabric covered skeletal rigid hulls. One result of the recognition of this danger, besides the need for BL control, is to provide a slowly sloping hull form toward the stern which in turn also increases the lift volume where it has always been inadequate; this departure from slender sterns of past hulls also had a favorable, although unsought, influence on the Lambda parameter.

The study on Metalclad hulls ends with several recommendations as follows:

1. Detailed design study of the distribution of skin gages, more closely differentiated than present standards permit.
2. Further analytical study of structure-skin interaction for the purpose of deriving simple and direct relations for design use. This is not a problem but a condition, well understood, looking for design directives.
3. Analytical and experimental model study for determining critical (elastic) buckling stresses in the skin as a function of all gore panel parameters, with the aim of improving still further the prospects for making the skin thinner, or the spacing of longerons greater, or both.
4. A thorough design study and model testing of Metalclad cellular main frame structures, known now to be heavier than necessary.
5. Analytical and experimental model stability work on the possibility of using one instead of two secondary frames between two main frames.
6. Design study of a Metalclad hull with structures for local weight load support as well as structures of convenience included, with the aim of reducing some longitudinal external hull structure by indispensable internal load support structures.
7. Further comprehensive analysis and tests of riveted-bonded skin seams, including fatigue testing.

8. Development of new concepts for cell membranes for Metalclad hulls.
9. Examination of prospects for use of carbon fiber/epoxy composites for Metalclad structures, including many sections of weight load carrying structures, tanks, containers, etc., possibly also main frames.
10. Review of maximum external loads on airship hulls, including the determination of more precise loading procedures for the final hull design; the present methods are too arbitrary and empirical.
11. Comprehensive testing of airship hulls at high Reynolds numbers, possibly in a water tunnel and also with BL control simulation.

During the completion of this report, but before its final issue, much attention was given to the validity of the basis for determination of hull skin thickness. It was felt that the maximum hull pressures were too high and particularly that the ratio between the maximum and minimum pressure was unnecessarily too large (over six). Old photographs of doflated ZMC-2 reveal that elastic buckling of the hull skin was approximately uniform in appearance, regardless of the spacing of longerons. This suggests that once the critical buckling appears, it is not much different in panels or gores, of different widths; the critical buckling parameter used as the basis of determination of skin thickness, where valid for the determination of the critical buckling stress, has only a distant relation to the degree of buckling, as old photographs indicate.

This discovery showed that the thickness of the hull skin could be safely reduced and the ratio between maximum and minimum pressure lowered. This was done for MC-200, resulting in a 37.5% weight saving of the hull skin with a maximum pressure of 8.75 in. of water column and maximum-minimum pressure ratio still at comfortable 3.5. The Lambda parameter was reduced to $\lambda = .2439$ from $\lambda = .2758$.

This points to the future direction of determining the skin thickness with further substantiation by tests of the validity of this conclusion.

TABLE OF CONTENTS

VOLUME I

	Page
1. Introduction	17
1.1 Description of Metalclad Hull Design Principles	17
1.2 Criteria for Flight Forces, Stability, Function and Construction of Metalclad Structure	30
1.3 Hull Data Analyzed for all Hull Sizes	33
1.4 Limitations of the Analysis	47
1.5 Explanation of the Hull Form	49
1.6 Factors of Safety	52
1.7 Function of Individual Components	53
1.8 Determination of the Size of Cells	55
2. Load Analysis	63
2.1 External Loads, Aerodynamic Moment, Gust Moment	63
2.2 Internal Loads	63
2.3 Loads Due to Surging	69
3. Main Frame Analysis	72
3.1 Section Characteristics	72
3.2 Case No. 23, Segment 0 - θ	76
3.3 Case No. 23, Segment θ - π	76
3.4 Frame Behavior	81
3.5 Diametral Deformation of Main Frame No. 334.50 of MC-200 (largest diameter frame)	81

TABLE OF CONTENTS - VOLUME I - (continued)

	Page
4. Secondary Frames	87
4.1 Description	87
5. Longeron Description	88
5.1 Introduction	88
5.2 Computer Analysis Typical Longeron	88
5.3 Hull Geometry, MC-200	96
5.4 Finite-Element Model of Longeron	103
5.5 Force and Displacement Input	121
5.6 Results of Computer Analysis	123
5.7 Flight Condition with Deflated Cell, MC-200	129
5.8 Local Reinforcements Required	131
5.9 Pressure Condition, MC-100	131
5.10 Flight Condition with Deflated Cell, MC-100	141
5.11 Determination of the Size of Longerons	149
6. Bulkhead Diaphragms	161
6.1 Diaphragms between the Cells	161
7. Hull Shell Skin Thickness	165
7.1 Skin Thickness Variation	165
7.2 Relative Elasticity of Skin and Structure	198
8. Skin Seams	207
8.1 Type, Strength, and Weight	207
8.2 Length of Seams in the Hulls	208

TABLE OF CONTENTS - VOLUME I - (continued)

	Page
9. Hull Openings and Reinforcement of Bow	232
9.1 Description	232
9.2 Opening Reinforcement	232
9.3 Bow Structure	232
10 Hull Structure Weights	234
10.1 Weights of Hull Components	234
10.2 Weight Determination of Frames and longerons	235
10.2.1 Main Frames	236
10.2.2 Secondary Frames	242
10.2.3 Longerons	246
10.3 Hull Skin Weight Summary	263
10.4 Seams	269
10.5 Diaphragm and Cell Weights	270
10.6 Corrugations	289
10.7 Paint and Primer Weights	291
10.8 Structure Weight	293
10.9 Graphite Fibre Epoxy Composites	295
11. Method of Construction	296
11.1 Description	296
12. Evaluation of Study and Comments	298

TABLE OF CONTENTS - Volume I - (continued)

	Page
REFERENCES	307
GLOSSARY OF TERMS	309
APPENDIX A Model for Pressure Loading of Main Frame	311
APPENDIX B Model Sizing of Main Frame	319
APPENDIX C Model of Main Frame Section	322
APPENDIX D Model of Longeron Sizing	325
APPENDIX E Sizing of I-Beam with Thin Web	342
APPENDIX F Fixity of Long Edges in Membrane Plates	345
APPENDIX G Theory of Local Skin Bending near Longerons	347
APPENDIX H Geometrical Properties of Tri- angular Sections	352
APPENDIX I Bending of Longeron	355
APPENDIX J Standards	367
APPENDIX K Notations	373
APPENDIX L Ellipses and Ellipsoids	378

VOLUME II

APPENDIX M Hull Layouts	
APPENDIX N Construction Layouts	

LIST OF ILLUSTRATIONS

FIGURE NO.	LEGEND	Page No.
1	Skeletal Main Frame	19
2	Typical Main Frame Section	20
3	Typical Secondary Frame Section	21
4	Typical Longeron Section	22
5	Longitudinal Corridor on Top of the Hull	29
6	Envelope - Maximum Bending Moment	64
7	Skin Element	65
8	Cell Pressure Diagram	70
9	Loading of a Main Frame	73
10	MC-200: Frame 334.5 Under Weight Loading	74
11	MC-200: Frame 334.5 Under Weight Loading - Shear and Bending Moment Curves	80
12	Section of MC-200 Main Frame @ Station 334.50	82
13	Typical Main Frame Under Radial Deflection of the Hull Shell	84
14	Longeron Geometry	88
15	Main Frame Section Geometry	89
16	Typical Hull Structure Relationships	90
17	Computer Analysis Model	92
18	Computer Model of Gap Between Skin and Frame	94
19	Typical Longeron Section	102

ILLUSTRATIONS (continued)

FIGURE NO.	LEGEND	Page No.
20	Longeron Height Variation	102
21	Typical Frame Bay	105
22	Numbering Sequence Frame Bays	106
23	Longeron Loading Pattern	130
24	Spacing - Secondary Frames	133
25	Longeron Cross-Section	133
26	Main Frame Cross-Section	134
27	Secondary Frame Cross-Section	135
28	Longeron Segment	136
29	Longeron Doubler	145
30	Element Model	147
31	Hull Cross-Section	150
32	Hull Skin Cross-Section	154
33	Gas Cell and Ballonet Arrangement for MC-200 (Typ. All Hulls)	163
34	Diaphragm Fabric	164
35	MC-100 Skin Thickness Diagram	193
36	MC-125 Skin Thickness Diagram	194
37	MC-150 Skin Thickness Diagram	195
38	MC-175 Skin Thickness Diagram	196
39	MC-200 Skin Thickness Diagram	197
40	Types of Seam Joints	210
41	Reinforced Metalclad Hull Bow	233
42	Hull Skin Schematic	264
43	Longeron Corrugation	289

ILLUSTRATIONS (continued)

FIGURE NO.	LEGEND	Page No.
44	Weight to Displacement Chart	294
-APPENDIX-		
A1	Pressure Forces on A-Frame Model	311
A2	Notation for A Hull Section	312
A3	Identification of Distributed Loads from Pressure	314
A4	Distribution of Lift and Weight Forces	316
A5	Notation for Axial Forces	316
A6	Distribution of Axial Forces Along the Hull Perimeter	318
B1	Main Frame	319
C1	Spacing of Frames	322
C2	Area Distribution in a Main Frame	323
D1	Model of a Girder	325
D2	Model of a Longeron	326
D3	Area Distribution in a Longeron	330
D4	Skin Deflection Relative to a Frame	335
D5	Forces Between Skin and Frame	336
E1	I-Beam Schematic	342
F1	Model of Membrane	345
H1	Typical Structural Section, with $\alpha < 30^\circ$	353

ILLUSTRATIONS (continued)

-APPENDIX-

FIGURE NO.	LEGEND	Page No.
I1	Loading of a Beam on Elastic Foundation	355
I2	Skin Deflection Between Longerons	357
I3	Loading on Skin	358
I4	Skin Between Longerons	359
I5	Skin Bending Along a Frame	360

LIST OF TABLES

TABLE NO.	HEADING	Page
1	Bending Moments, 0° - 180°	78
2	Radial Shear, 0° - 180°	78
3	Total Lift Force On Each Main Frame	86
4	Stiffness of Foundation Springs	91
5	Longeron Deflection	95
6	Hull Parameters, I	97
7	Hull Parameters, II	100
8	Spring Constants	107
9	Gap Discontinuity	121
10	Longeron Stress	123
11	Frame Stress	127
12	Skin Ring Constants	137
13	Typical Longeron Forces	139
14	Spring Forces	139
15	Computer Analysis Results	140
16	Secondary Frame Results	141
17	Longeron Sizes - MC-200	151
18	Longeron Sizes - MC-100	152
19	Longeron Section Properties	159
20	MC-100: Seams-Weight per Foot, 1b	211
21	MC-125: Seams-Weight per Foot, 1b	212
22	MC-150: Seams-Weight per Foot, 1b	213
23	MC-175: Seams-Weight per Foot, 1b	214

LIST OF TABLES (continued)

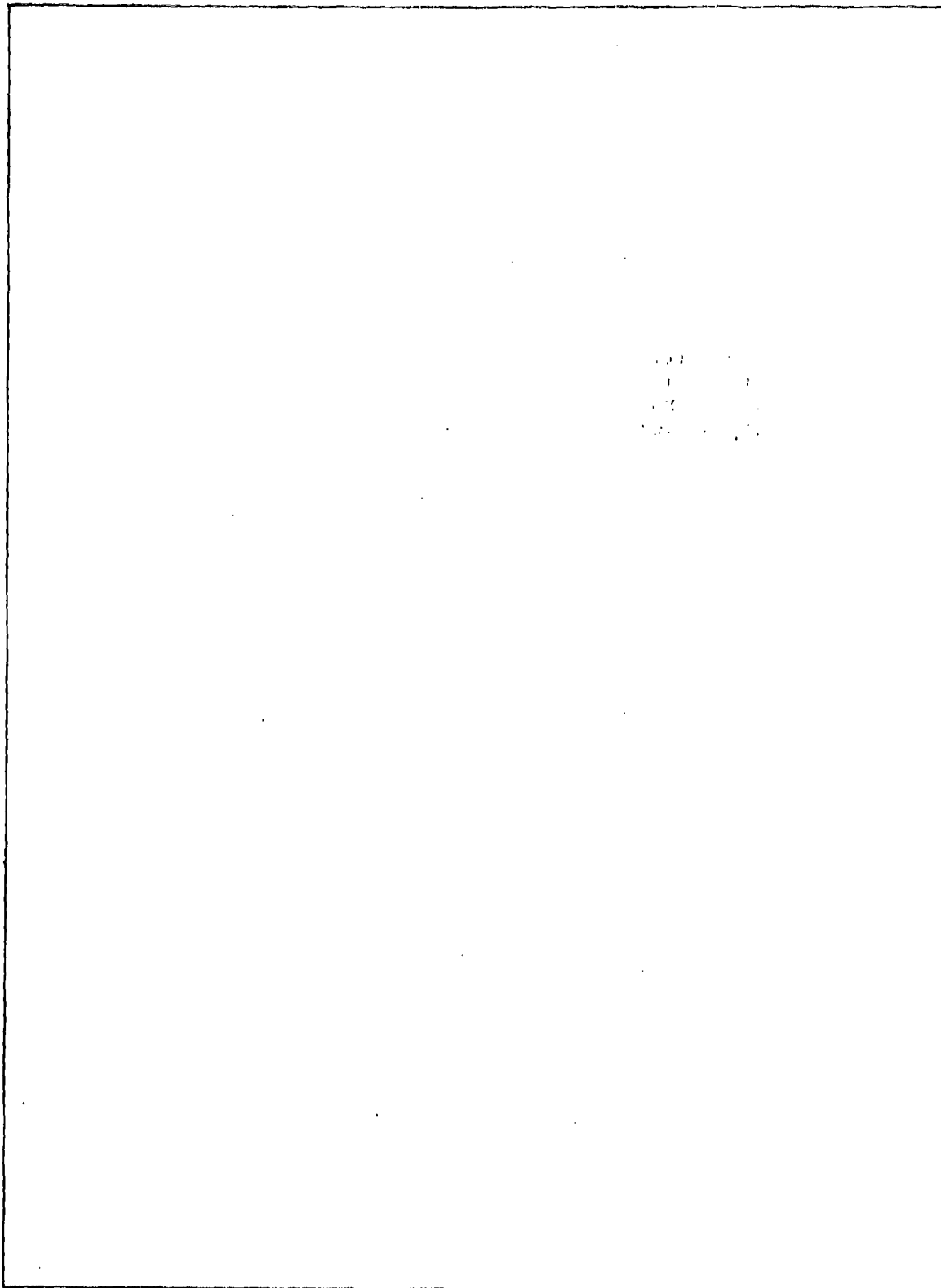
TABLE NO.	HEADING	Page
24	MC-200: Seams-Weight per Foot, 1b	215
25	MC-200: Type I Lap Joint	216
26	MC-200: Type II Lap Joint	217
27	MC-200: Type II Lap Joint, Secondary Frames	218
28	MC-200: Type II Lap Joint, Longerons	220
29	MC-200: Type III Lap Joint, Skin Panels	222
30	MC-200: Type IV Lap Joint	229
31	MC-200: Butt Joint	230
32	MC-200: Main Frame Weights	236
33	MC-200: Secondary Frame Weights	242
34	MC-200: Longerons Weights	246
35	MC-100: Main Frame Weight Calculations	252
36	MC-100: Secondary Frame Weight Calculations	256
37	MC-100: Longerons Calculations	260
38	Weight Summary-All Hull Skin MC-100	265
39	Weight Summary-All Hull Skin MC-200	267
40	Weight of Seams	269
41	MC-100 Diaphragms	270
42	MC-100 Gas Cell Membrane Weights	270
43	MC-125 Diaphragms	274

LIST OF TABLES (continued)

TABLE NO.	HEADING	Page
44	MC-125 Cell Membrane Weights	274
45	MC-150 Diaphragms	278
46	MC-150 Cell Membrane Weights	278
47	MC-175 Diaphragms	282
48	MC-175 Cell Membrane Weights	282
49	MC-200 Diaphragms	286
50	MC-200 Cell Membrane Weights	286
51	Paint and Primer Weights	291
52	Summary - Weight	293

-APPENDIX-

B-I	Bending Moment	320
F-I	Membrane Pressures And Stresses	346



1. INTRODUCTION

1.1 DESCRIPTION OF METALCLAD HULL DESIGN PRINCIPLES.

Metalclad Airship hull principles were laid down approximately fifty years ago by R. H. Upson in several references as noted a.

In the simplest definition, a Metalclad hull has a rigid internal structure capable of supporting an elastically deformable thin, gas-tight metal skin shell in deflated state, without lifting gas in the hull. The skin is elastically deformed between its structural boundaries and supports, with deep buckles visible all over its surface, caused either by the weight of the skin or by shear deformations from the supports of the hull; generally, the elastic buckling is a combination of both of these deformations and during erection, the appearance may give an impression of concern for the integrity of the hull.

The supporting structure is made rigid by the firmly attached shell skin and supports this metal skin without harm to it. The structure is comprised of three distinct elements: The main frames, which are rigid rings with the ultimate purpose of transferring weight loads into the skin by shear. The secondary frames, which are approximately equidistantly spaced between the main frames. The longerons, running fore and aft along the hull contour are spaced at equal distances peripherally and are firmly attached to the main frames and secondary frames. All structure is attached to the skin. This assembly of structural girders and skin comprises all the lifting Metalclad hull structure. The girder structure alone, without the skin, is not capable of self-support and would collapse if not stabilized by the skin. The skin alone, in deflated condition, would collapse without the support of the girder structure. However, in combination, attached to each other, the girders and the skin shell form an overall rigid body in deflated condition with harmless local elastic instability of the skin.

The secondary frames and the longerons are essential to the hull structure during erection and also when the hull is deflated; they are not essential to the inflated hull under pressure. The main frames are essential to the hull structure during erection, assembly and when the hull is deflated; they hold the longerons and the skin in place and support their weight. When the hull is inflated, the main frames are the principal structure for transfer of weight loads into the hull skin shell by shear.

Due to inflation with gas and principally by supercharge air pressure, the thin metal shell becomes taut with tension.

a. See references, Page 307.

All elastic buckles disappear and the hull body becomes rigid locally in addition to overall rigidity inherent in the structure without pressure.

All structural girders in the ZMC-2^{b.} were curved to the local hull form and directly attached to the skin. They were not straight as in skeletal Zeppelin type hulls. It is a fundamental distinction of Metalclad hulls that the structure is everywhere directly attached to the skin and is fitted to the skin curvature. In deflated condition, the skin is supported by the structure; in inflated state, the structure complements the skin strength and deforms elastically with the skin to various degrees, almost completely in the case of secondary frames and longerons and less at the main frames. In Metalclad structures, this is recognized and provided for to assure gradual skin restraint from the structure, as is described in section 1.2.

The principle of conformity of the structure to the hull form in a combination with the hull skin, gives the lightest and also the simplest structure. This is so, even when under compression loads in a deflated hull, because the curved girder deformation is restrained everywhere by the skin in tension in transverse as well as longitudinal direction. Although curvature raises the slenderness ratio of a curved girder, the skin effectively reduces it, for instance in the case of secondary frames and longerons, even when the hull is deflated.

The principle of structural conformity to the hull curvature requires a new solution of all structures, particularly main frames. The skeletal girder truss structure can be used with the base girders curved and the truss girders straight, as shown in Fig. 1. This system has the advantage of good flexibility of the base girders which allows them to deform with reduced restraint in respect to the skin radial deformation, caused by internal hull pressure. In cylindrical shells, the circumferential extension of skin is twice as great as the extension in the longitudinal direction under internal pressure, therefore, the recognition of this fact is important. Not favorable to the skeletal structure of Fig. 1, is the complexity of it, the weight of special joints and the unavoidable loading of straight girders in bending superimposed on compression loads. The skeletal main frame construction deserves further consideration and at this time, is not being excluded from use in Metalclad construction.

The hull study described in this report is based on cellular principles in all structure. This approach is consistent with the Metalclad concept of indivisible attachment of structure to the skin as well as with modern light structures. A typical

b. ZMC-2 U.S. Navy all metal airship, 1929.

main frame of a Metalclad hull is shown in Fig. 2, and a typical girder for Metalclad secondary frames and longerons is shown in Fig. 3 and 4 respectively.

A typical main frame, Fig. 2, is in itself a Metalclad structure, composed of corrugated side walls as surfaces of frustum cones, riveted to either extruded or rolled circumferential base cornices attached directly through the base skin to the external longerons. At the apex, the cornice is composed of two circumferential curved sections, attached together with the corrugated sidewalls to make a curved apex girder of high stability. All cornices are held fixed, element by element, by corrugated sloping sides. The base cornices are also stabilized by the base plates, which are thicker than the local hull skin. All three cornices will support high compression stresses without buckling, due to the high degree of fixity of their elemental support and resulting stability.

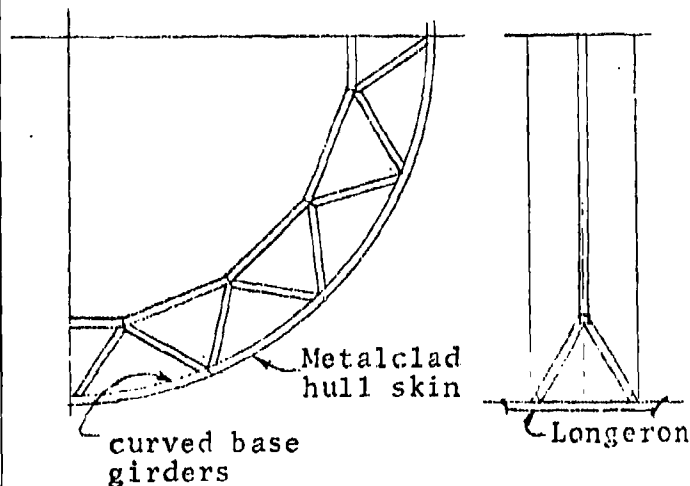


FIGURE 1. Skeletal Main Frame

Past experience indicates that in similar configurations, the cornices ultimately fail at stresses near the yield point of the metal in compression.

The main frame, instead of being a skeletal frame is actually a continuous circular beam with lighter or heavier cornices where bending moments demand it and with corrugations of

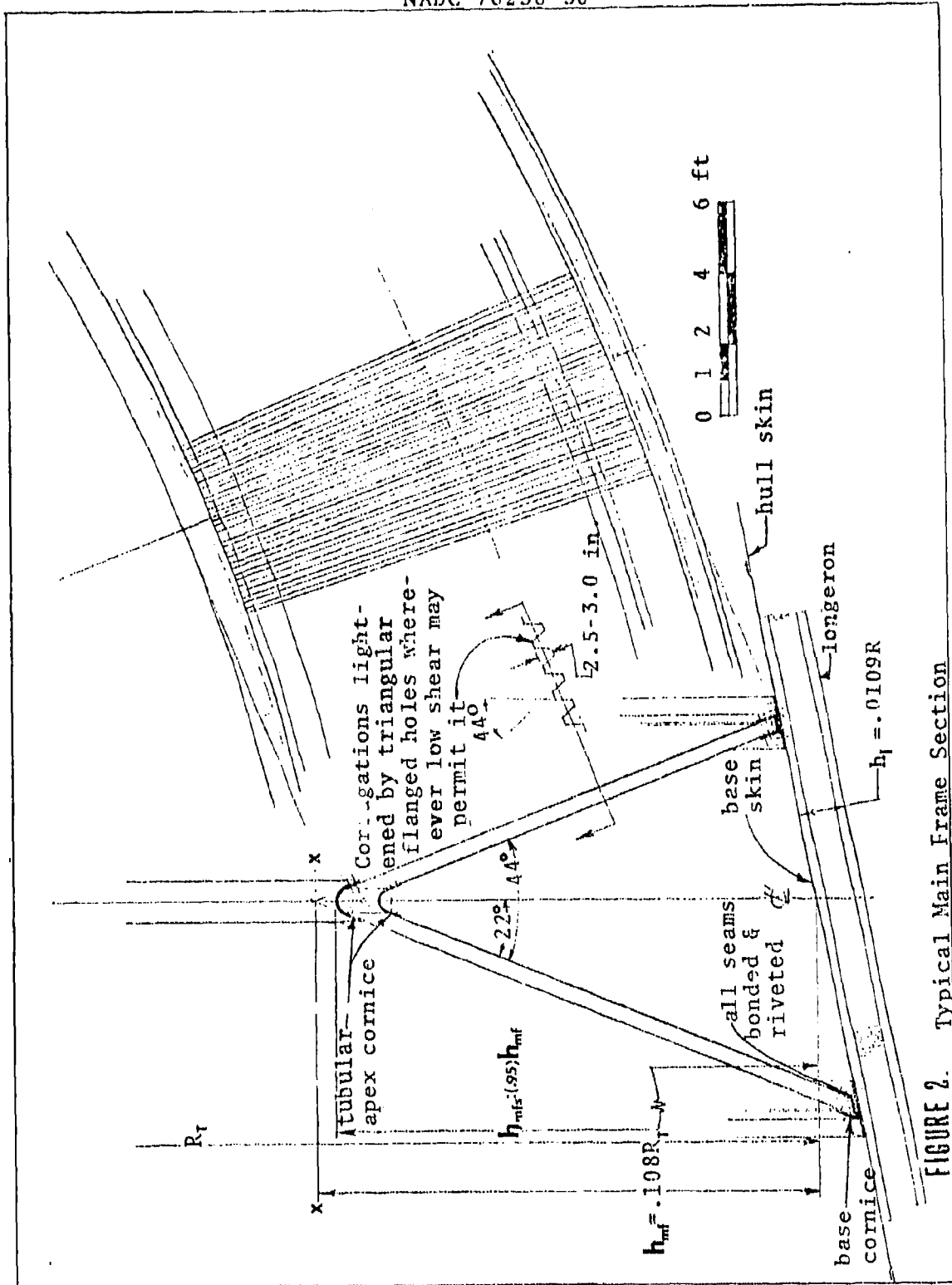


FIGURE 2. Typical Main Frame Section

FIGURE 3. Typical Secondary Frame Section

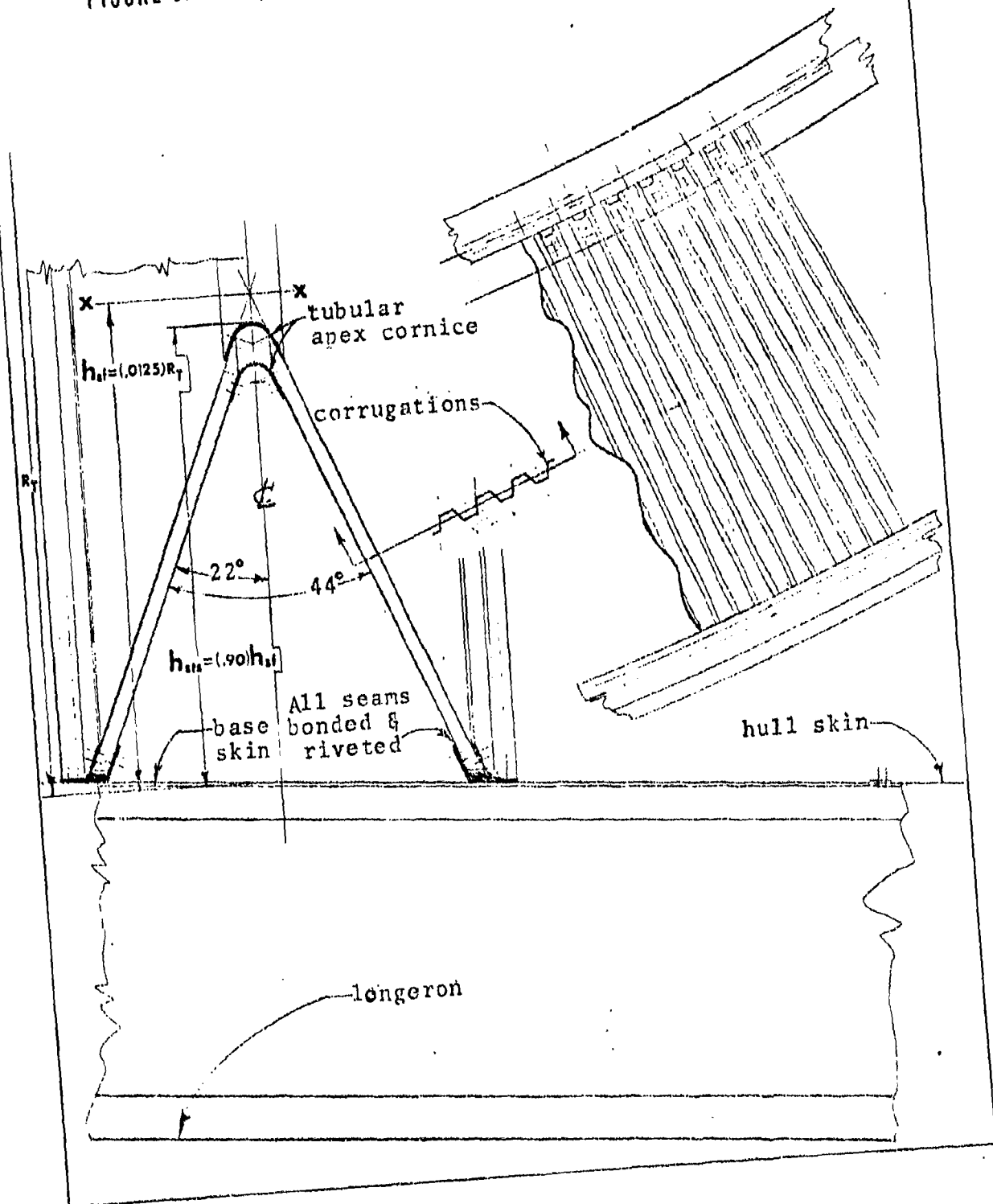
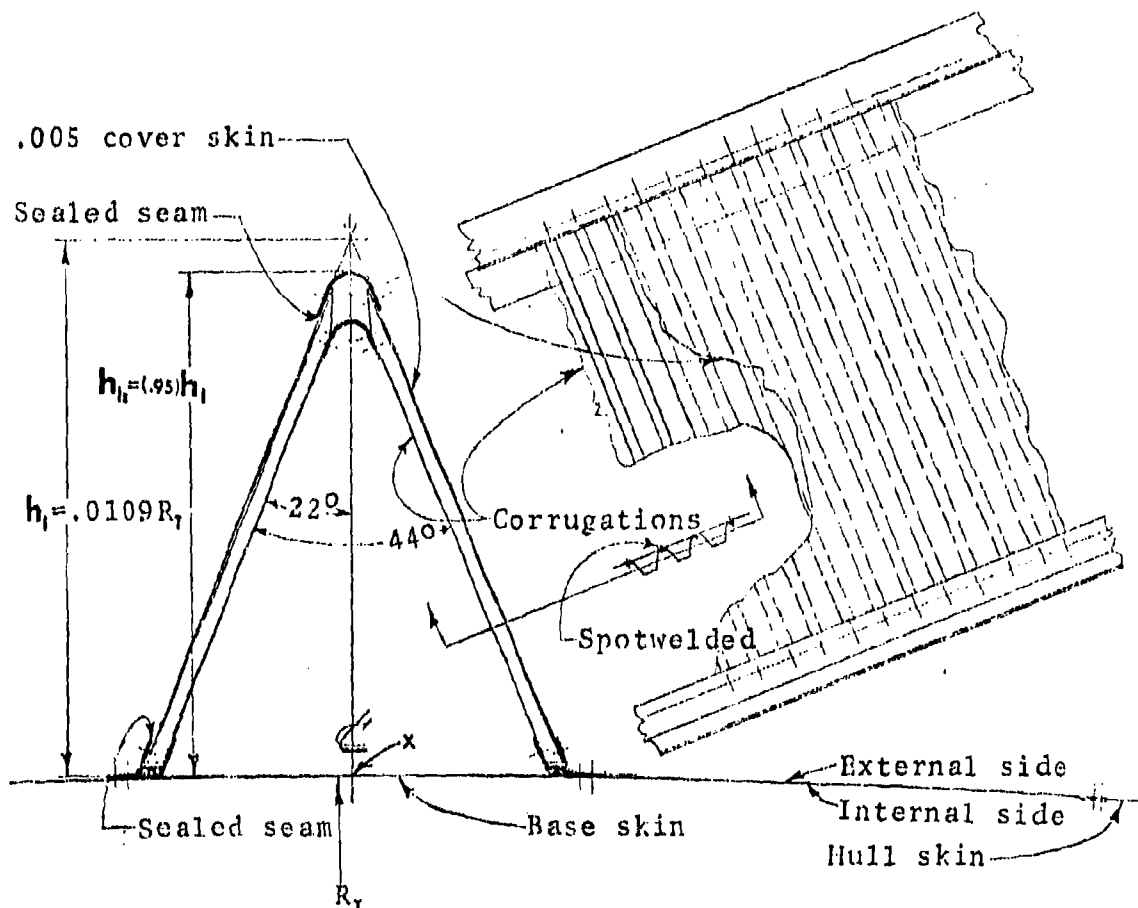


FIGURE 4. Typical Longeron Section



thickness according to local shear loads. Section 3 shows a simplified analysis of the largest main frame of the MC-200^c and also main frame models are described in Appendices A, B, and C.

On the respective drawings of the hulls (Refer to appendix M.) are shown these main frames in some detail, only as the initial approach to their actual design. The corrugations of main frames of MC-200 are provided with lightening holes in frame segments where shears are always light, instead of going to very thin gages more vulnerable by human contact. The upper halves of all main frames will have thin sheet covers spotwelded to the corrugations and riveted

- c. MC-200: 20,000,000 cubic feet in volume.
- MC-100: 10,000,000 cubic feet in volume.

by sealed joints to the cornices to provide gas tight bulk-heads for the cells. In the air space, below the hull equator, the corrugations have no sheet covers with the exception of the three mainframes supporting compartment sealing diaphragms. All main frames in all hulls have a constant height parameter of $(.108) \times R_T$,^d except far forward in the bow and far aft in the stern, where main frames with the above parameter would be too low in height for human access. The minimum actual height (apex cornice to base) of any main frame is 86 in. for any hull. The cornices of the main frames can be easily spliced and also reinforced by doublers where needed. There are no girder cross joints, only riveted seams. All rivets are to be flush on the external sides of all internal structures and all cornice edges are to be rounded-off to reduce scuffing of cell membranes. All external rivets are flush to decrease drag. All rivet lines are openly accessible and staggered for ease of reaching by tools. The main frame structure is easily accessible for attachments of any kind, structural supports for equipment, ladders, platforms etc. Manholes, if needed, may be placed anywhere.

The frame apex included angle is 44° for structural reasons because the corrugated sides are in effect large Belleville springs with relatively low spring constants. This allows the frame to adjust with little force to the elastic growth of skin perimeter when the hull is inflated. Due to the radially outward directed forces caused by internal pressure, the corrugated sides of the frame will rotate slightly toward the center plane of the frame, tending to decrease the apex angle thus adjusting the diameter of the frame to some mean value of the total radial skin deformation. A larger apex angle would be adverse to this adjustment. The smaller apex angle is also justified because the main frames of Metalclad hulls will not have to resist high gas and air surge forces on the radial nets and diaphragms in the plane of the main frames. These surge forces will be greatly reduced because the Metalclad hulls are subdivided longitudinally into four air spaces. An incidental advantage of the "slender" 44° main frame, is its lower geometrical volume compared to a 60° apex angle frame, yet, the internal space of even the minimum height 86 in. frame is more than adequate for all access and equipment installation purposes.

The base skin of the mainframes is thicker than the local hull skin thickness, to relieve the slope of the skin deflection curve between the free skin and the rigidity of the frame, as shown in Fig. 2. The frame itself and its base skin are in effect, two springs acting elastically to reduce the differential between the relatively low radial deformation of main

- d.
h: Frame height = apex to base
 R_T : Hull radius at frame station

frames and the greater deformation of the local skin. The radial diaphragm net will be anchored at 48 stations along the apex cornice of the main frames. At these stations, the corrugations will be locally of thicker gage, directing the pull forces toward the longerons and in shear to the adjacent corrugated webs. A typical pivoting arm attachment through the main frame is shown in simple terms on hull layouts (appendix M.). These attachments require small openings in the corrugated sides which can be easily reinforced while the apex cornice will be everywhere continuous.

The main frame structure is also basic to other hull structures viz. the secondary transverse frames and the longerons; both are derived from the main frame structure, as is described further on. The guiding principle is to obtain light, simple structures in all cases, with simplicity of construction, high redundancy and the most efficient use of material in fabrication.

A typical secondary frame, Fig. 3, is constructed as a triangular girder of 44° apex angle with two corrugated shear web sides riveted to an apex cornice made of outer and inner rolled profile. At the base, the corrugations are riveted to extruded or rolled cornices, which in turn are riveted to the base skin. The base skin is thicker than the local hull skin. Similarly as in the case of main frames, this provides a transition from a more rigid frame to a less rigid skin, both in the deflated state when the skin is elastically buckled, as well as in the inflated state when the skin is extended radially more than the secondary frame. This is illustrated in Fig 3. The circumferential skin extension will exert a radially distributed force on the base cornices of the frames, causing an angular rotation of the corrugated shear webs toward the frame centerline, diminishing the apex angle and thereby providing a second spring adjustment to the radial skin deformation. The first one being the deformation of the thicker-than-skin base plate of the frame. In effect, two elastic springs are provided to accomodate the relative difference in local deformation of the skin and of the frame. Individual hull layout drawings (Refer to appendix M) show typical secondary frames with dimensions.

In all hull studies of this report, another fundamental principle is used, viz, to eliminate, as much as possible, all structural joints necessary for the crossing of structural elements. This is a new concept to Metalclad construction and is a logical step in its progressive development. Splicing joints cannot be eliminated and are not unduly heavy, nor complex. On the other hand, joints required for the crossing of structure, e.g., the main or secondary frame crossing

a longeron, are always complex, heavy, expensive and insecure. Structures generally fail first at joints.

In the studied hulls the longerons are external to the hull while all main and secondary frames are internal. Between the frames and the longerons the thicker base skin of all frame structures of a Metalclad hull are serving as an incidental gusset plate at each structural crossing. The structures are as firmly joined as conceivable by simple by-pass crossing without discontinuity of girders. All studied hulls require a relatively large number of longerons (Refer to section 7.1). The increase of drag from external longerons is due to friction and is minimal, estimated at no more than 2%-3% of the total hull friction resistance. The gain in weight reduction with this type construction will be significant, although not quantified at the time of this report because of the complexity of the task. The principal advantages are in the simplicity of structure and increased structural integrity of the hull. Equally as advantageous is the circumferential smoothness of the internal walls of Metalclad hulls. The cell membranes will not encounter longitudinal ridges over which to drag, nor will there arise any air spaces entrapped between the cell membranes and internal longerons during inflation. Fig. 4 shows a typical longeron in its section, almost identical to although lower in height than a transverse frame, again composed of internal and external apex cornices joined by corrugations into a highly stable section capable of sustaining high bending compression stresses. The corrugated external sides of the longerons are covered by an approximately .005 in. thick flat sheet spotwelded on the outer side of the corrugations with sealed seams to diminish the drag and prevent moisture accumulating in the longeron. At all main frame and longeron crossovers a hole in the base skin of the frame will connect the internal volume of each, to prevent air pressure forces arising in the longerons. The longerons are sufficient to support the hull during construction and also during flight in case of loss of all pressure in a hull sub-volume. The hull structure and consequent weight summations are based on this longeron structure capability.

In summation the Metalclad main frames, secondary frames and longerons are very efficient structures. The base cornices are stabilized element-by-element by the base skin of greater thickness than the local hull skin, and by the corrugated sides of the complete section. The apex cornice is stabilized also element-by-element, by the corrugated side webs; both, the apex and the base cornices will reach high compressive stresses approaching the compression yield point of the metal. The small apex included angle of 44° in all structures will accommodate the elastic deformation of the skin by diminishing

in the primary and secondary frames and increasing in the longerons, thereby partially adjusting and unloading the girder to the deformed hull dimensions. When under pressure, if the apex angle were larger, the girder would be stiffer against such deformations, which is undesirable. The 44° angle is still sufficient for high stability, while less restraining to radial deformations at the base of all structures. Deformability of the skin does not hinder the precise joining of the plating to the hull structure, because of precision assembly techniques as described in Section 11. When supercharged with air pressure, the elastic skin becomes taut, the wrinkles and buckles totally disappear and the hull becomes a smooth body, with exact compound curvature all over. The longerons "float" with the skin in its radial deflection as do the secondary frames; all become generally unloaded from weight loads and loaded by forces from elastic deformation of the skin shell and impose small restraining forces on the skin as described in Section 2 and 5. The main frames put more restraint on the skin under pressure and provisions as described above and in section 1.2, are made for this.

The framework is the principal structure during construction for supporting the deflated hull. Inflated with air and gas pressure, the hull structure changes its character; the skin then becomes the principal structure, while the main frames serve the purpose of introducing weight loads into the skin by shear as well as restraining by diaphragms, the air and gas loads in the longitudinal direction. In both states, deflated as well as inflated, a Metalclad hull is a rigid airship hull. Under pressure, the inflated hull (with lifting gas) remains circular if the lift load is balanced by weight load shears. This was analytically shown by Upson in 1924 (See Ref. a) The Metalclad airship hull principles were demonstrated by the airship ZMC-2, in 1929. Its hull was constructed of 2024 Alclad, .0095 in. thick over all the hull surface. The parameter $D/t = 624 \text{ in.} / .0095 \text{ in.} = 65,684^e$ of the ZMC-2 is among the highest known in shell structures. The longeron and secondary frame structure was made of a 2 in. high "hat" section of $D/L = 624 \text{ in.} / 2 \text{ in.} = 312^f$. The main frames were approximately 10 in. high with each frame wire braced in its plane. The inflation-deflation cycle was repeated innumerable times through the almost 12 years of life of the ZMC-2 without discernible fatigue of the skin metal at any location. The hull of the ZMC-2 during construction was manhandled more severely before splicing the stern and bow sections together than is expected to happen during the construction of Metalclad hulls considered in this report.

e. $D/t = \text{Max. hull dia/skin thickness}$

f. $D/L = \text{max. hull dia/height of section}$

In spite of the structural lightness, as indicated by the above parameters, not the slightest harm was done to the hull structure by this severe handling before inflation.

The hulls of this report are subdivided into a number of individual, independent cells for the containment of the lifting gas. Section 1.9 and 6 describes the cells in detail. It should be pointed out that the hull skin itself contains the gas directly in the upper portion of the gas cell between radial intersections with the hull diameter at 7.5° above the equator (MC-200) on the starboard and port sides. These intersections correspond to the location of their respective longerons and below this intersection the gas is contained by a pliable floating membrane. The membrane is securely attached to the hull skin at these longitudinally running stations by a replaceable gas-tight joint shown schematically on hull layouts. The membranes are at least as large, from 7.5° above the equator on port to 7.5° above the equator on the starboard side, as the lower portion of the hull and are free to lie on the inner wall of the bottom of the hull with 100% gas inflation. In the transverse plane of each main frame is positioned an elastic disc-like net, anchored circumferentially to the apex cornice of the frame. Above the 7.5° intersections, the net is a part of a sealed diaphragm or semi-bulkhead, separating two adjacent cells. Below the 7.5° intersections the disc-like net is open and the cell wall is a free, semi-circular diaphragm attached along its semi-perimeter to the cylindrical part of the longitudinal cell membrane forming a complete cell. In effect, the top part of the cell is fixed, while the lower part is free-floating, capable of being drawn tightly by suction against the inner wall of the hull in preparation for inflation. This will insure a minimal dilution of the lifting gas with entrapped air during evacuation and inflation. In case of puncture of the top hull skin by an unforeseen cause, the cell membrane would be lifted by air under pressure against the inner wall of the hull, cover the opening and still maintaining internal air pressure; only in the extreme case of a tear in the membrane as well, would the pressure be reduced or lost in the air subvolume where the damage occurred. Typical cells are shown on layouts of the hulls (Refer to appendix M.). In at least three main frames along the length of a hull, the whole inner area of the frame is a sealed diaphragm, dividing the hull into four air sub-volumes, each with its number of gas cells. These sub-volumes contain air below the cells. The bow and the stern air volume is serving the purpose of ballonnets for trim and also as compensating space for dilation of the lifting gas. The second and the third air sub-volume is

for gas dilation only. The additional purpose of division of the hull volume into four air sub-volumes is to diminish the total surge of gas and air during hull pitching, which in turn reduces the loads on elastic net diaphragms in all main frames.

At equator, on both port and starboard sides, all adjacent cells are interconnected by controlled valve ducts, which will permit transfer of gas from one cell to its adjacent cell, in response to ballonnet fullness, when needed.

The hull skin is projected to be bonded and riveted to the thicker base skin at the bases of all structures, as is shown on the hull layouts, (appendix M.) and described in Section 11. All skin panel seams are to be butt joints with flush riveted and bonded back-up strip. The seams of all structures are described in section 8. It is also proposed to use bonding for structural seams to secure higher stability of the assembly between rivet centers.

All hull structures in this report are proposed to be controlled by dynamic thrusters in Z and Y coordinates; the thrusters will be located in the bow and stern on the main frames. No weight allowance has been made for the structure restraining the forces of the controlling thrusts because these forces are not a part of the gas lifting equilibrium. It is to be noted however, that the thruster control forces will act, in most cases, as couples and their moments on the hull will be considerably smaller than the moments from rudders or elevators.

The size of the hulls suggests that it would be practical for access purposes to provide a low height (86 in. max) internal longitudinal keel at station π of a hull, as is indicated in Fig. 5. This is to be considered in the future and would replace the topmost external longeron. The cell diaphragm would not be hindered in any way as it would fold around it and the corridor would provide ducts for hydrogen, if used as a supplementary fuel, and access for inflation of cells with lifting gas. An additional advantage would be that in the case of loss of air or gas pressure, the hull could travel at higher speed because the bending strength of the deflated section of the hull would be higher with the internal keel than with longerons alone. Disadvantage would be the weight of the top keel and a small reduction of lift gas volume.

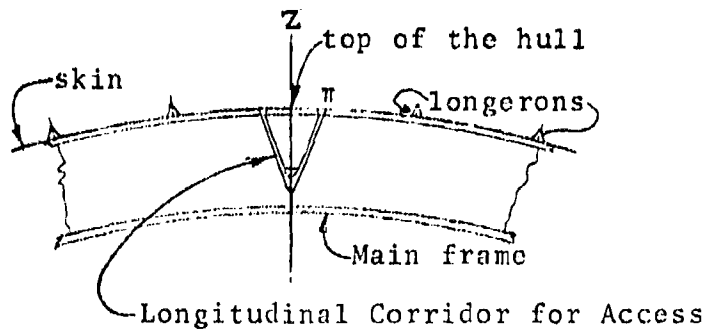


FIGURE 5. Longitudinal Corridor at Top of the Hull

It is shown further on in this Report (Refer to Section 2.1) that Metalclad hulls are more than adequate for the highest gust bending moments with a factor of safety larger than two, although two is the minimum factor of safety of design for all hulls. Also, the supercharge air pressure in all hulls is high enough to be dependably controllable and can be in fact reduced before the factor of safety, with respect to external loading, would be reached. This is a most noteworthy development of Metalclad technology when compared to the era of the ZMC-2, when the air pressures were declining to low values with the increase in size of the hulls, reaching values that would have been doubtful in reliability.

Appendices A through I in this report, deal with a variety of structural problems. Although reference to them is made in various sections of the report, they are not a direct part of the presented analysis and rather reflect the development of understanding of the problems they relate to; due to their developmental nature they often are numerically different from the text, while still expressing the concept. Their merit is in dealing with principles rather than in specific results.

1.2 CRITERIA FOR FLIGHT FORCES, STABILITY, FUNCTION AND CONSTRUCTION OF METALCLAD STRUCTURE. A skeletal airship hull has to satisfy only one set of strength criteria from external forces, viz., the flight loads. All Metalclad hulls have to satisfy two criteria of external forces. One is the rigidity and strength of the full structure during erection when the hull shell must be self-supporting without gas and air pressure. These forces are due to the local weight of the hull, principally the skin and longerons acting as external loads. The other one is the same set of strength criteria as for skeletal hulls. These two distinct criteria are not exclusive of each other; in fact there is a joint effect in the case of loss of lifting gas in a cell and ultimately, also of air pressure, during flight. In this situation a Metalclad hull would be subject to weight loads due to its own local skin and structure as well as to aerodynamic moments at reduced speed of travel. During erection of Metalclad hulls, the main frames will be self-supporting on the assembly stand, as discussed in section 11.

The skin between the main frames must be supported by the structure during assembly. This structure consists of two main frames, two secondary frames and the longerons crossing them. The longerons support the skin panels as a uniformly distributed load (in the first approximation) and are in turn, supported by the main frames and stabilized by the secondary frames. Neither the secondary frames nor the longerons are needed when the hull is inflated except when pressure is lost. If a gas cell should lose its lifting gas, the cell membrane will lift up against the inside of the hull skin and keep it under longitudinal and transverse tension with air pressure; the air pressure is normally much higher than the gas pressure, even at the top of the hull. Should the membrane be torn as well in an unlikely but possible situation, due for instance to cutting by sharp edges of structure or a tear in the metal hull skin; the air pressure will be reduced in that sub-volume of the hull or conceivably, it may not be possible to maintain it at all. In that case the longerons will be loaded by bending moments on the hull in addition to having to support the weight of the skin in the length of the hull. The hull will have a reduced section modulus which has to be still high enough to resist a maximum moment at the maximum speed at which the hull can then travel. Section 1.8 establishes that the travel speed of the hull would still be between 50% and 60% of the maximum speed in level flight. The secondary frames stabilize and support the longerons by collecting the weight of the skin and longerons and transferring it to the adjacent main frame by skin shear. The skin is capable of shear transfer even in a "slack" condition as was demonstrated by the deflated ZMC-2. A Metalclad hull has longitudinal curvature along its length.

This geometry imparts higher rigidity to the longerons in bending than their section properties give to them alone; this is described in Section 5. On top of the hull, longitudinal compression deflects the longerons outwardly against the weight of the skin and especially, against the restraining circumferential forces of the circular hull skin surface, or transverse tension of the skin, even in the slack state. Experience with the ZMC-2 structure supports this assumption. The analysis of such a structural system is not known, by Turbomachines, Inc., to have been accomplished. C. B. Bienzeno⁸ (See references, page) has developed an analysis of a curved bar under compression with one restraining force at the middle opposing the deflection. At this time it is assumed that the longerons will be capable of sustaining compression stresses on the order of $\sigma_c = 15,000 \text{ lb/in}^2$ maximum and additive bending stresses of $\sigma_b = 15,000 \text{ lb/in}^2$ maximum for the purpose of this study. The analytical solution of a curved longeron in compression, loaded and restrained by distributed forces along its length opposing the deflection from the end load, is a much desired tool to be developed in the near future. Discussion in this direction is described in section 5 and also in section 1.7, indicating the magnitude of this stabilizing effect of the skin and the relief of the bending moment on the longerons especially on top of the hull. The longerons at stations lower than π (at the top), are loaded progressively less by compression as well as bending (in the deflated hull condition), but more in torsion, toward station $\pi/2$ at the equator, as indicated in Appendix D. The longerons are rigid in torsion, especially with the hull skin stabilizing them. This case is not discussed further in this report.

Due to radial growth of the hull shell under pressure, the longerons, being attached to the main frames, will be subjected to bending loads between frames. Local "doubler" reinforcements are needed inside their apex cornices to limit the stresses at each frame. This was also investigated by a computer program and is reported in section 5. The construction process of a Metalclad hull is described in section 11, and at this point it need only be stated that the progressive assembly of the hull will not have to contend with excessive deformations of the uncompleted peripheral structure because of a jury-structure used to unload the structure of the hull. A light jury structure will also be used for fixing the dimensions between two adjacent main frames to alleviate the loading conditions during the partially completed hull assembly. The investigation under section 1.2 discusses the capability of the structure at the top of a completed hull to carry static loads when not under pressure. During construction, the loading of the longerons and secondary frames will not be as high as noted

⁸ C.B. Bienzeno, Z. Angew. Mathematics, Mechanics Vol. 18, 1938

above, in the "loss of pressure" condition. The external flight loads were investigated on the MC-200 for a pitched flight condition but were not completed when it was clear that the hull moments, such as turning and yaw were much lower than the maximum aerodynamic moment. (This is especially true when considering the gust moment.) The "envelope" moment, as suggested by D. E. Woodward,^h was used for the purpose of analysis in this report. Within this "envelope" moment are contained all controls moments. This moment, actually two moment envelopes, one with, and one without the pressure is the determining criterion for the hull design in the inflated condition, as well as the deflated condition with flight at reduced speed.

Note: "Envelope" is shown in Section 2, page 64 Figure 6.

^h. Proceedings of the interagency Workshop on LTA Vehicles, FTL Report F75-2 , January, 1975 .

1.3 HULL DATA ANALYZED FOR ALL HULL SIZES.

- See The Following Tables -

1.3 HULL DATA ANALYZED FOR ALL HULL SIZES.

<u>Item</u>		<u>MC-100</u>
Number of main frames	z_{mf}	9
Number of secondary frames	z_{sf}	19
Number of longerons	z_l	42
Maximum hoop stress, top of the hull	$\sigma_{TST}, \text{ lb/in}^2$	32,850
Maximum hoop stress, bottom of the hull	$\sigma_{TSB}, \text{ lb/in}^2$	32,661
Maximum longitudinal tension stress top of the hull	$\sigma_{LST}, \text{ lb/in}^2$	21,642
Maximum longitudinal stress bottom of the hull	$\sigma_{LSB}, \text{ lb/in}^2$	21,250
External hull surface area	$A_h, \text{ ft}^2$	297,467
Surface length, bow to stern	$L_s, \text{ ft}$	774.1
Volume of maximum size cell	$V_c, \text{ ft}^3 (10)^6$	1.689
Total weight of skin	$W_s, \text{ lb}$	100,690
Total weight of seams	$W_{se}, \text{ lb}$	included in the weight of the skin
Total weight of main frames	$W_F, \text{ lb}$	30,328
Total weight of secondary frames	$W_f, \text{ lb}$	7,881
Total weight of longerons	$W_l, \text{ lb}$	35,528
Total weight of cell diaphragm	$W_d, \text{ lb}$	17,538
*Total weight of lifting hull	$W_o, \text{ lb}$	191,965
Maximum height of longerons	in.	9.53
Longeron area/Skin area		.14236
Fullness of cells at sl for 5,000 ft ceiling		.86163.
*Unpainted		

<u>MC-125</u>	<u>MC-150</u>	<u>MC-175</u>	<u>MC-200</u>
9	9	9	9
19	19	19	19
42	44	46	48
32,850	32,850	32,850	32,850
28,166	31,585	28,574	31,172
21,005	21,328	19,968	19,968
20,237	20,304	20,382	20,382
345,220	389,799	431,981	472,201
833.9	886.1	932.8	975.3
2.115	2.538	2.961	3.369
124,143	148,434	173,638	199,794
included in the weight of skin			
37,910	45,492	53,073	60,655
9,852	11,822	13,792	15,763
41,227	46,556	51,594	56,398
20,354	22,982	25,469	27,841
233,486	275,286	317,566	360,451
10.27	10.9	11.5	12.0
.14236	.15333	.15545	.17105
.86163	.86163	.86163	.86163

<u>Item</u>		<u>MC-100</u>
Radial deformation of the skin due to maximum pressure with Poisson's effect	ΔR , in	1.9780
Specific weight of skin per ft^3 of displacement	w_{sv} , lb/ft^3	0.01007
Specific weight of skin per ft^2	w_{sa} , lb/ft^2	0.33849
Specific weight of hull per ft^3	w_o , lb/ft^3	0.01920
Reynolds' number, at s_1	Re_o , $(10)^8$	7.80964
Reynolds' number, at 10,000ft altitude	Re_{10} , $(10)^8$	6.10611
Dynamic pressure at s_1	q_o , lb/ft^2	33.903
Dynamic pressure at 5,000 ft altitude	q_5 , lb/ft^2	29.214
Dynamic pressure at 10,000ft altitude	q_{10} , lb/ft^2	25.037
Approximate drag of hull, at s_1 , 100 knots	D_o , lb	23,605.0
Approximate drag of hull at 5,000 ft altitude, 100knots	D_5 , lb	20,340.0
Approximate drag of hull at 10,000 ft altitude, 100 knots	D_{10} , lb	17,432.0
Area of maximum diameter hull section	A , ft^2	20,588.0
Drag coefficient of hull alone	C_D	0.015*
Power at s_1 , 100 knots	N_o , THP	7,249.0
Power at 10,000 ft altitude, 100 knots	N_{10} , THP	5,253.0

* Refer to page 61.

<u>MC-125</u>	<u>MC-150</u>	<u>MC-175</u>	<u>MC-200</u>
2.562	2.760	3.087	3.228
0.00993	0.00990	0.00992	0.00999
0.35961	0.3808	0.40196	0.4231
0.01868	0.01835	0.01815	0.01802
8.41266	8.93988	9.41118	9.83954
6.57761	6.98982	7.35831	7.69323
33.903	33.903	33.903	33.903
29.213	29.213	29.213	29.213
25.037	25.037	25.037	25.037
27,391.0	30,931.0	34,279.0	37,470.0
23,602.0	26,652.0	29,537.0	32,287.0
20,228.0	22,842.0	25,314.0	27,671.0
23,890.0	26,978.0	29,898.0	32,682.0
0.015	0.015	0.015	0.015
8,412.0	9,499.0	10,527.0	11,507.0
6,212.0	7,015.0	7,774.0	8,498.0

<u>Item</u>		<u>MC-100</u>
Gross volume of the hull	$V_o, (10)^6 \text{ ft}^3$	10.002
Gross displacement lift at s ₂	$L, (10)^5 \text{ lb}$	6.53657
Maximum diameter	$D, \text{ ft}$	161.91
Length	$L, \text{ ft}$	728.58
Distance of maximum Dia station from bow	$a_B, \text{ ft}$	262.29
Distance of maximum Dia station from stern	$a_S, \text{ ft}$	466.29
Fineness ratio	L/D	4.5
Prismatic coefficient		.6667
Volume ratio, $V_{100} = 1.0$	V_i/V_{100}	1.00
Length ratio, $L_{100} = 1.0$	L_i/L_{100}	1.00
Diameter ratio, $D_{100} = 1.0$	D_i/D_{100}	1.00
Center of buoyancy from bow	$l_{CB}, \text{ ft}$	338.79
Maximum aerodynamic moment	$M_{ae}, (10)^6 \text{ ftlb}$	22.931
Maximum gust moment	$M_m, (10)^6 \text{ ftlb}$	23.759
Maximum gas head moment	$M_g, (10)^6 \text{ ftlb}$	1.7634
Fullness of cells at s ₁ for 10,000 ft ceiling		.73878
Maximum air pressure in hull	$p, \text{ lb/in}^2$.6143
Maximum flight air pressure in the hull	$p, \text{ in wc}$	17.0
Maximum skin thickness	$t, \text{ in}$.020
Number of gas cells	Z_c	9
Number of air sub-volumes	Z_a	4



NADC-76238-30

<u>MC-125</u>	<u>MC-150</u>	<u>MC-175</u>	<u>MC-200</u>
12.500	15.000	17.500	20.000
8.16875	9.80250	11.43625	13.07000
174.41	185.34	195.11	203.99
784.83	834.02	877.99	917.95
282.54	300.25	316.07	330.46
502.29	533.77	561.91	587.49
4.5	4.5	4.5	4.5
.6667	.6667	.6667	.6667
1.25	1.50	1.75	2.00
1.0772	1.1447	1.2051	1.2599
1.0772	1.1447	1.2051	1.2599
364.92	387.83	408.26	426.85
28.545	35.638	40.129	45.864
29.588	35.638	41.577	47.520
2.3745	3.0280	3.7188	4.4436
.73878	.73878	.73878	.73878
.60106	.62968	.59464	.56125
16.64	17.43	16.46	15.54
.022	.024	.024	.024
9	9	9	9
4	4	4	4

Note:

Useful Load = lift at a given altitude ceiling minus the deadweight of the hull.

<u>Item</u>		<u>MC-100</u>
Total lift for 5,000 ft ceiling	$L_5, 1b$	551,879.0
Useful load for 5,000 ft ceiling	$U_5, 1b$	359,914.0
Useful load for 5,000 ft ceiling/Hull weight	U_5/W_0	1.8749
Total lift for 10,000 ft ceiling	$L_{10}, 1b$	473,199.0
Useful load for 10,000 ft ceiling	$U_{10}, 1b$	281,234.0
Useful load at sea level/hull weight	U_0/W_0	2.3362
Useful load for 10,000 ft ceiling/Hull weight	U_{10}/W_0	1.4650
Power at 5,000 ft Alt, 100 knots	N_5, THP	6,240.0
Speed at 5,000 ft Alt, with sl power	$u_5, knots$	116.06
Maximum available lift gas volume	V_g, ft^3	$(9.8)(10)^6$
Ratio: $\frac{\text{Lift for 5,000 ft}}{\text{Lift for 10,000 ft}}$	L_5/L_{10}	1.1663
Air space in the hull to lift % gross displacement	$V_a, \%$	2.00
Useful load for 5,000 ft ceiling/Lift for 5,000 ft ceiling	U_5/L_5	0.65216

<u>MC-125</u>	<u>MC-150</u>	<u>MC-175</u>	<u>MC-200</u>
692,665.0	833,478.0	974,264.0	1,115,021.0
459,179.0	558,192.0	656,698.0	754,520.0
1.9666	2.0277	2.0679	2.0934
593,844.0	714,651.0	835,365.0	956,055.0
360,358.0	439,365.0	517,799.0	595,604.0
2.4426	2.5135	2.5606	2.5897
1.5434	1.5960	1.6305	1.6524
7,240.0	8,178.0	9,060.0	9,904.0
116.06	116.06	116.06	116.06
(12.3)(10) ⁶	(14.8005)(10) ⁶	(17.3005)(10) ⁶	(19.8)(10) ⁶
1.1663	1.1663	1.1663	1.1663
1.60	1.33	1.14	1.00
0.66292	0.66971	0.67404	0.67669

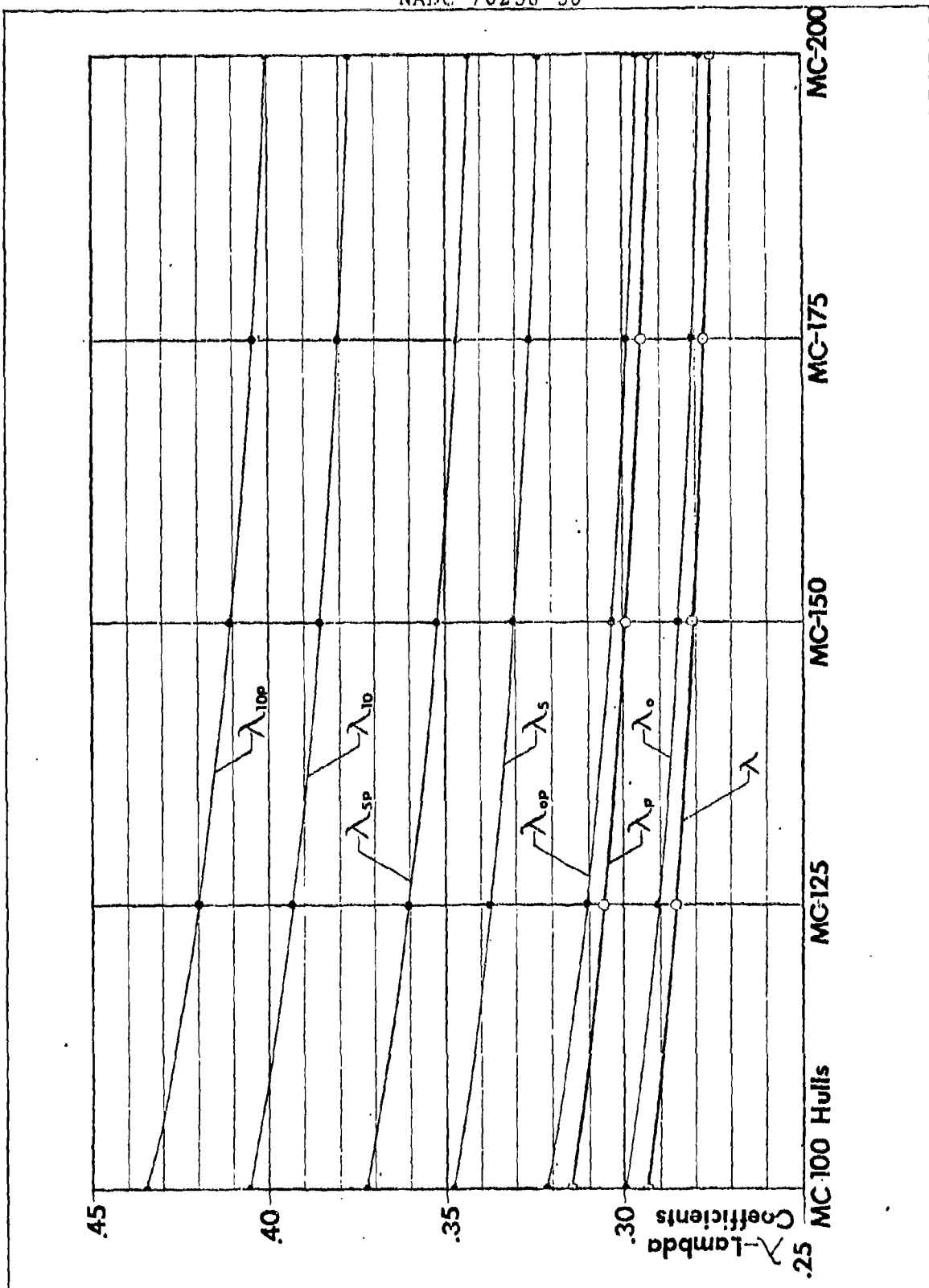
<u>Item</u>		<u>MC-100</u>
Useful load for 10,000 ft ceiling/Lift for 10,000 ft ceiling	U_{10}/L_{10}	0.59432
Weight of primer and paint, external hull surface and longerons	W_{pe} , lb	10,236.0
Weight of primer, internal air space surface	W_{pi} , lb	3,576.0
Ratio of painted hull weight/Unpainted hull weight	W_{op}/W_o	1.0719
Weight of hull with paint	W_{op} , lb	205,777.0
Lift at sea level, fully inflated, (for reference)	L_o , lb	640,430.0
Useful load at s_1 , (for reference)	U_o , lb	448,465.0
Useful load at s_1 /Hull weight	U_o/W_o	2.3362
Useful load at s_1 /Lift at s_1	U_o/L_o	0.7003
Useful load at s_1 /Useful load at 5,000 ft ceiling	U_o/U_5	1.2460
Useful load at s_1 /Useful load at 10,000 ft ceiling	U_o/U_{10}	1.5946
Ratio: Lift at 5,000 ft ceiling/Lift at s_1	L_5/L_o	0.8617
Ratio: Lift at 10,000 ft ceiling/Lift at s_1	L_{10}/L_o	0.7389
Speed at 10,000 ft altitude, with s_1 power	u_{10} , knots	135.42

<u>MC-125</u>	<u>MC-150</u>	<u>MC-175</u>	<u>MC-200</u>
0.60682	0.61480	0.61985	0.62300
11,814.0	13,393.0	14,971.0	16,549.0
4,123.0	4,668.0	5,214.0	5,761.0
1.0683	1.0656	1.0636	1.0610
249,423.0	293,347.0	337,751.0	382,767.0
803,805.0	967,221.0	1,130,588.0	1,293,930.0
570,319.0	691,935.0	813,022.0	933,473.0
2.4426	2.5135	2.5601	2.5897
0.70952	0.71538	0.71911	0.72142
1.2420	1.2396	1.2380	1.2372
1.5826	1.5748	1.5701	1.5673
0.86173	0.86173	0.86173	0.86173
0.73879	0.73887	0.73888	0.73888
135.42	135.42	135.42	135.42

<u>Item</u>		<u>MC-100</u>
Total hull weight / gross displacement lift	$W_o/L = \lambda$	0.29375
Total hull weight(painted)/ gross displacement lift	$W_{op}/L = \lambda_p$	0.31488
Total hull weight/lift at sea level	$W_o/L_o = \lambda_o$	0.29974
Total hull weight(painted)/ lift at sea level	$W_{op}/L_o = \lambda_{op}$	0.32131
Total hull weight/lift for 5000 ft ceiling	$W_o/L_5 = \lambda_5$	0.34784
Total hull weight(painted)/ lift for 5000 ft ceiling	$W_{op}/L_5 = \lambda_{5p}$	0.37287
Total hull weight/lift for 10,000 ft ceiling	$W_o/L_{10} = \lambda_{10}$	0.40567
Total hull weight(painted)/ lift for 10,000 ft ceiling	$W_{op}/L_{10} = \lambda_{10p}$	0.43486

Note: L_o, L_5, L_{10} are based on gross displacement lift(L)
minus air space.

<u>MC-125</u>	<u>MC-150</u>	<u>MC-175</u>	<u>MC-200</u>
0.28583	0.28083	0.27768	0.27578
0.30534	0.29926	0.29533	0.29285
0.29048	0.28462	0.28089	0.27857
0.31030	0.30329	0.29874	0.29581
0.33710	0.33029	0.32595	0.32327
0.36009	0.35196	0.34667	0.34328
0.39318	0.38520	0.38006	0.37702
0.42001	0.41048	0.40432	0.40035



1.4 LIMITATIONS OF THE ANALYSIS The analysis is deliberately limited to the lifting structure of the hulls and excludes all other structure needed for the support of weight loads, control forces, landing forces, etc., except the main frames, which are loaded by weight loads corresponding to the lift acting on them. The lifting hulls must be capable of a speed of 100 knots and will sustain all external loads and moments related to this speed. A maximum ceiling of 10,000 ft. is assumed in the report where it is applicable. The MC-100 and MC-200 are considered as two boundary hulls and are analyzed in greater depth than the MC-125, MC-150 and MC-175. The significant weight values for these latter hulls are interpolated from the values of the two boundary hulls. All results are tabulated for access and comparison and some are plotted. This exploratory analysis is designed to determine loading and weight parameters with increasing hull size. The exploratory nature of the analysis leads at times to a degree of inconsistency of results, particularly due to the changing concepts of design during the work of generating and assembling the output material for this report. However, in weight statement preparation, these discrepancies do not exist.

A Metalclad system of structures in a Metalclad hull and the elastic interaction between the structure and the skin is defined in this report. This was of secondary importance in ZMC-2, due to its small size and greater-than-needed skin thickness. In the hulls considered in this report, this is of primary importance. Careful attention was paid to the determination of skin weight, the largest part of the total weight, by proportioning the thickness over the surface of a hull not only in the longitudinal direction but also circumferentially, to the greatest extent possible. Standard skin gauges were specified in all cases. The skin thickness is greater on top than on the bottom of the hulls, because in low fineness ratio hulls, the gas head is significant in its influence on the value of transverse stress. More thorough computer analysis is needed to define the elastic interaction of the skin and the structure under internal pressure. Results of this analysis will lead to some weight reduction of the structure.

Similar weight reduction can be expected from the future use of non-standard sheet gages for the hull shell skin; in this report only standard gages are used. The use of standard gages compels the use of the next higher gage with an unnecessary weight increase. Non-standard gages will permit greater differentiation of skin thickness distribution over the hull surface, without adversely affecting the required strength of the skin. The amount of skin sheet required for construction of Metalclad hulls is large enough to justify the use of non-standard gages.

The weight study used conservative values wherever a degree of uncertainty appeared. In an actual design this conservative influence would be reduced and a most careful control of weights throughout the design would be instituted.

The weight analysis completely disregards structures that have no relation to lift. This implies a conservative limitation of the results in an actual hull design because structure necessary for functional reasons will contribute to flight strength; particularly, to the strength of the deflated hull if pressure should be irreparably lost in a major volume cell. One such structure will be at the bottom of the hull for habitation and weight load support. Another structure will provide an access corridor at the top of the hull, connecting all main frames, as noted in section 1.1. These structures will eliminate the need for longerons at their local peripheral stations because the skin will be supported in a deflated condition by them indirectly. In the weight analysis, all these potentially useful contributions of internal structures are disregarded.

1.5 EXPLANATION OF THE HULL FORM The hull form of Metalclad airships has been given a thorough study. The first consideration in these studies was that Metalclad airships should not have high fineness ratios but rather favor ratios in the range of 4 to 5, where the drag coefficient is almost constant as far as is known, even in very large sizes. Next, several forms of hulls were considered, among them envelopes based on NASA 64-021,¹ and 65,3-018¹ profiles; these were discarded due to their low prismatic coefficients and large slopes of the profile toward the stern trailing tip. This latter consideration has gained importance in modern times because it is strongly suspected that vibrations of airship hulls experienced in the stern region were caused by shedding of vortices as the boundary layer (BL) separated at random, especially at high speed of flight. Stern vibrations are well known in marine ships; in some instances, they were so violent that the sterns had to be reinforced. In the past, these vibrations were uniformly blamed on the propellers. Propellers are turbomachines and when they function properly, they do not vibrate as violently as indicated by ship hulls; on the other hand, if the water enters them in a turbulent state, caused by separation along the rapidly converging sides of the stern, the propellers will run with induced vibrations, the origin of which is not in their nature but in the turbulence.

Similar circumstances exist along airship hulls as the air mass flows toward the stern. The BL separates in a random pattern, causing shedding of vortices which induces powerful forces to arise on the hull surface, and in turn causes dynamic impact on the stern part of the hull and vibrations of its structure. These vibrations existed in all skeletal airships, in spite of the damping effect of their fabric cover. In Metalclad airships, they would be more severe, due to the rigidity of the surface of the inflated hull. This consideration has guided the thinking about the form of the stern of Metalclad hulls more than any other. The obvious countermeasure is the suppression or at least reduction, of the BL separation; this has now become a major factor in Metalclad hull design and the study tacitly assumes that all five hulls of this report would have controlled BL, to some useful extent.

There are several ways to achieve this end. Some of them are complementary and all but one, outside the scope of this report. One promising method is the suction of the BL into

i. NASA Report No. 824, 1945.

the hull by an internal propulsion power plant, which then imparts momentum to this air mass and jets it through a tunnel duct at the end of the stern; the motion of the free jet (cold air) has a second effect on accelerating the BL suggested in the paper by Carmen J. Mazza.^j

A hull using this method can be more full in the stern part with consequent reduction of the hull stern envelope slopes, thereby displacing the station separation further aft (Schlichting^k). This is the method considered within this report. Greater fullness of the hull stern provides higher lift than do hulls with pointed sterns. The best envelope curve that fits into this requirement is an ellipsoid therefore the hull form is composed of a bow ellipsoid with its major axis equal to the distance from the bow to the station of the maximum diameter and a stern ellipsoid with its major axis length from the station of maximum diameter to the tip of the stern. Prior stern envelope surveys were composed of a hyperboloid, commencing at the maximum diameter station and joining an ellipsoid at the stern. This form was not used on the hulls of this report because it does not have adequately slow slopes along the hull curve. The maximum diameter station was moved from the original (.40)L location to (.36)L location from the bow to adjust the slopes of the stern ellipsoid. The hull ellipsoids have not only the first derivatives on a smooth curve at all longitudinal stations, but the second derivative is also a smooth curve, without any discontinuities in the rate of change or hull envelope slopes.

Considered also was the hull envelope curve described by Pake and Pipitone,^l a deviation from airfoil sections designed for complete BL removal. It is difficult to resist the attractiveness of these forms, particularly because they are also suitable for stern located power plants of the concept mentioned above, however not enough is known at this time to base a comparative study on this hull form.

Originally, the removal of the BL was looked upon as the gain in reducing the hull drag coefficient. This purpose continues to be valid but the BL removal has acquired a new importance in its power to suppress or at least, to reduce the stern vibrations which in Metalclad hulls must be a prime consideration. The proposed hulls are drawn up with

j. C. J. Mazza - Proceedings of the Interagency Workshop on LTA Vehicles, MIT, 1975, P. 133.

k. Schlichting- Boundary Layer Theory, 1955, McGraw-Hill.

l. F. A. Pake and S. T. Pipitone - Proceedings on LTA Vehicles FTL Report - R75-2, Jan. 1975, Page 147.

these factors in mind while an additional improvement from this effort has appeared, viz., the higher prismatic coefficient of the studied Metalclad hulls, with greater lift in the stern, where most prior airships were always deficient in lifting power.

1.6 **FACTORS OF SAFETY.** The hulls are projected to be made of Alclad 7050-T76 sheets and extrusions. The mechanical properties of 7050-T76 Alclad are noted below:^m

Alloy Form Temper			7050 Alclad Sheet T76
Thickness, in.	.015-.039		.040-.187
σ_{tu} , lb/in ²	L	73,000	75,000
σ_{ty} , lb/in ²	L	64,000	66,000
σ_{cy} , lb/in ²	L	61,000	64,000
τ_{su} , lb/in ²		44,000	45,000
ϵ	% LT	7	8
E , 10 ⁶ , lb/in ²		10.2	
E_c , 10 ⁶ , lb/in ²		10.6	
E , 10 ⁶ , lb/in ²		10.4	(Used in this report)

The factor of safety used in this report is two (2), with respect to σ_{tu} and 1.5, with respect to σ_{ty} . The latter case will apply in tension as well as compression and shear.

The maximum allowable stresses are:

Load Stress:		7050-T76 sheet thickness	
		.015-.039	.040-.187
σ_{tu} , lb/in ²	L	36,500	37,500
σ_{ty} , lb/in ²	L	42,667	44,000
σ_{cy} , lb/in ²	L	40,667	42,667
τ_{su} , lb/in ²		22,000	22,500

The minimum gage of .015 in., given in reference ^m of this report is too high for some hull skin areas and sheet-corrugation panel assemblies. Sheets thinner than this limitation would have to be produced in the Alclad form down to a minimum

^m. Naval Air Systems Command Report: N00019-74-C-0065
January, 1976.

thickness of .005 in. All seams between hull shell skin gore panels, base skin of the structure and also seams joining components of girders are specified (Section 8. and 8.1) as bonded and riveted for reasons of sealing and increase of strength due to continuous adhesion of thin components with thicker cornice materials that join into thick assemblies along the seams. In past experience, absence of adhesion in longitudinal seams of girders has caused failing by premature buckling between rivets.

Riveted-bonded seams are described in Section 8. and all seams are designed with higher than 100% efficiency, which is possible with bonding. In strength-weight analysis this is decreased to .90 of the ultimate strength of the metal.

All structures use 7050-T76 extrusions. Extruded 7050 alloy of different tempers than T76 is reported in Reference ⁿ. The mechanical properties of extruded 7050 alloy are higher than of Alclad 7050 but this is neglected in this report and the same property values are used for extrusions as well as for Alclad.

1.7 FUNCTION OF INDIVIDUAL COMPONENTS: MAIN FRAMES, SECONDARY FRAMES AND LONGERONS. The principal component of a Metalclad hull shell is the skin, bonded by leak-proof seams joining individual gore panels between longerons. The function of the skin is to contain the lifting gas and the super-charging air. The lifting forces of the gas press on the skin, the main frames, and the intermediate frames to hold the hull shell circular. This compels the lift forces to generate shears on the sides of the hull. In turn, this transfers the lift loads to the main frames, where the lift forces are resisted by the weight loads. The longerons play a role in stabilizing the skin in shear. This role increases as the internal pressure decreases and the secondary frames and longerons take up loads with slackening skin due to a drop in pressure or the complete loss of pressure in flight. During the construction of the hull the longerons provide support in the absence of pressure. The hull shell must be built of as light a gage of skin as possible, because the major part of the hull weight is in the skin. This precondition also determines, as the next step, the necessary number of longerons to support the skin adequately in its slack state. The background for this is the experience with the ZMC-2 expressed by a parameter which ties together the skin thickness, its unsupported width, and the radius of its curvature, Section 7. The least possible thickness of skin also determines the hull air pressure at which the maximum allowable transverse stress

ⁿ. Alcoa Green Letter, April, 1976, Aluminium Co. of America.

can be set up. Therefore, the skin thickness is determined by the highest acceptable internal air pressure, the practical manufacturing and handling characteristics of thin plates, a reasonable number of longerons and the consideration of slope of deformation of skin as the more rigid structure is approached.

It is inherent in Metalclad structures that the number of longerons be larger than in the historically large skeletal airship hulls. It is not known to what lower value the parameter ξ can be reduced. Indications are that it is now too high, yet there is no experimental evidence on how much lower it can reasonably be.

There are no singular values for the determination of Metalclad hulls and their structural members. Design relations have to be arrived at by successive approximations for what can be considered the optimum compromise of weight, simplicity, comparative rigidity, stability and strength under all conditions of construction as well as flight operation.

1.8 DETERMINATION OF THE SIZE OF CELLS The largest volume cell inevitably is located at or near the maximum hull diameter. Cells forward and aft of this location are smaller in volume, principally due to a limiting length of longerons between two main frames with radial cell bulkheads.

If the largest cell should lose its inflation gas, a sagging bending moment will occur, resisted by longerons which must be sufficiently strong and rigid to sustain this loading as well as some value of the maximum, aerodynamic or gust bending moment at a reduced speed of flight, to return to the home base. In Metalclad airships a second emergency condition may arise, if in addition to the loss of lift of the largest cell, the air sub-volume in which it is located, should also lose a part or all of its air pressure. The loading of longerons in this case is discussed under Section 5.

This section of the report considers the determination of the size of the maximum cell volume. The loss of lift from deflation of this cell will have to be made up by one or more of the following lifting forces:

1. Lift of the hull at a pitch angle in flight at reduced speed, at full propulsion power.
2. Lift of downward aiming thrustors, no more than 80% of their total downward capacity. *
3. Heating of lifting gas by fuel, no more than 60% of the total remaining lifting gas volume. *
4. Dumping of fuel; (no ballast is expected to be carried, because with thrustors, none is necessary).

Of these four lifting measures, heating of gas is least effective; dynamic lift and the lift of thrustors are most effective. Dumping of fuel is undesirable except in extreme emergency. At full power and with heating of gas, fuel consumption will increase at an abnormal rate and in this respect, maintenance of lift equilibrium is going to be assisted.

To reduce largest cell volume would lead to closer spacing of main frames near the maximum hull diameter station. Future work will require a compromise solution. Closer spacing of main frames near the maximum diameter station will result in

* Reasonable estimates based on preliminary calculations.

several cells of identical volume but smaller than the largest cell of this study. This is not a requirement of the present study.

MC-100

The analysis proceeds on the assumption that the largest cell volume (or volumes) is inflated for a 10,000 ft ceiling, and the cell lift is determined on the following basis:

The volume of the cell is:

$$V = \pi R^2 l = (3.14159)(80.953)^2(83.0) = 1.7088(10)^6 \text{ ft}^3$$

Lift of this cell at 10,000 ft altitude is:

$$L = K_{10} V = (.04828)(1.7088)(10)^6 = 8.250(10)^4 \text{ lb}$$

This force must be replaceable via emergency measures.

Upon loss of gas tight integrity of the largest gas cell a sequence similar to the following will occur. In practice they will initiate almost simultaneously, but are taken as separate functions for purpose of clarity.

1. From 10,000 ft, the airship will drop to near sea level height.
2. Angle of pitch on the bow is + 20°.
3. Full power is maintained.
4. 80% of the thrust of downward directed thrustors is applied.
5. At least 60% of the remaining gas volume is heated to 20°F above ambient temperature.

Drag and lift coefficients are taken from NACA TR394, page 14, Figure 16(A) (reference to page 59) for fineness ratio of 4.8, which is close to 4.5, for this purpose. The graphs of Figure 16(A) indicate a drag coefficient $C_D = .020$ at $\theta = 0^\circ$.
(modified to $C_D = .015$ on page 61).

Hull drag at sea level,

$$D_o = C_D \frac{\gamma}{2g} V^{2/3} u^2, \text{ lb}$$

$$D_o = (.015) \frac{.076475}{64.348} (10.0024048 \times 10^6)^{2/3} (168.9)^2$$

$$D_o = \frac{(1.519169)(10)^6}{64.348} = 23,609, \text{ lb in level flight}$$

The speed of flight at $\theta = 20^\circ$, $C_D = .055$

$$u^2 = \frac{2D_o g}{\gamma V^{2/3} C_D} = \frac{(2)(23,609)(32.174)}{(.076475)(10.0024048 \times 10^6)^{2/3}(.055)}$$

$$u^2 = 7780.2666$$

$$u = 88.205819 \text{ ft/sec.}$$

$$u = (.5921)(88.205819) = 52.23 \text{ knots}$$

At this speed, $\theta = 20^\circ$, $C_L = .165$ the hull dynamic lift is :

$$L = (.165) \frac{.076475}{64.348} (10.0024048 \times 10^6)^{2/3} (7780.2666)$$

$$L = 70,827 \text{ lb}$$

Net total lift of the hull

$$L_{100} = (.95)(10)^7 (.048279) = L_{100} = 458,653 \text{ lb}$$

Downward directed thrustors capacity

$$(.10)(L_{100}) = (.10)(458,653) = 45,865 \text{ lb}$$

80% of thrustors effective

$$(.85)(45,863) = 38,984 \text{ lb}$$

Heating of gas

$$\text{state at ambient temperature } \gamma_o = \frac{P}{R T_o}$$

$$\text{state at elevated temperature } \gamma_1 = \frac{P}{R T_1}$$

at higher temperature, lift of gas $k = \gamma_{\text{Air}} - \gamma_{\text{He}}$

$$\text{for } \lambda_{\text{Air}} = \text{constant } \frac{k_1}{k_o} = \frac{T_1}{T_o}$$

k_o , lift of He at ambient temperature

k_1 , lift of He at 20°F higher than ambient

$$k_1 = k_o = \frac{T_1}{T_o} = (.06535) \frac{538.69}{518.69} = .0678698 \text{ lb/ft}^3, \text{ at sea level}$$

$$\Delta k = .0678698 - .06535 = .0025198 \text{ lb/ft}^3$$

Gain in lift by heating to 538.69 from 518.69 $^\circ\text{R}$ at sea level



Net gas volume at 10,000 altitude

$$\begin{array}{rcl} 9,500,000 & \text{ft}^3 & \text{full hull of gas (approximate)} \\ -1,708,800 & " & \text{lost cell} \\ \hline 7,792,200 & " & \text{at 10,000 ft} \end{array}$$

At sea level:

$$\frac{.04828}{.06535}(7.7922)(10)^6 = (5.756808)(10)^6 \text{ ft}^3$$

$$60\% \text{ of the gas volume heated } (.6)(5.756808)(10)^6 = (3.45408)(10)^6 \text{ ft}^3$$

Lifting forces due to $\Delta t = 20^\circ\text{F}$ temperature rise of gas

$$(.0025198)(3.45408)(10)^6 = 8,703 \text{ lb}$$

hull lift 70,827 lb

thrusters 38,984 lb

Lift due to $\frac{8,703 \text{ lb}}{\text{superheated gas } 118,514 \text{ lb}}$

Required lift: $\frac{-82,501 \text{ lb}}{\text{Excess margin: } 36,013 \text{ lb}}$

No fuel needs to be dumped due loss of lift of the largest cell. Drag due to the air columns of thruster jets, the reduced speed of flight, and therefore the hull lift will be reduced and some fuel may have to be dumped. The analysis becomes complex at this point for fuel consumed at high rates will compensate favorably for the drag of the thruster jets.

MC-200

An analysis for the maximum cell of hull is made for MC-200.

$$V = \pi R^2 l = (3.14159)(101.9945)^2(104.0) = 3.398884(10)^6 \text{ ft}^3$$

Lift of the cell at 10,000 ft altitude is

$$L = k_{10} V = (.04828)(3.398884)(10)^6 = 16.4098(10)^4 \text{ lb}$$

As in the case of MC-100, with emerging loss of the longest cell, the airship will drop to near sea level height, while pitching up to $\theta = 20^\circ$, maintaining full power, and putting into action 80% of the thrust of downward-directed thrusters while heating at least 60% of the remaining gas volume by 20°F above ambient temperature.

From NACA TR 394, Page 14, Figure 16(A), for fineness ratio of 4.8, which is close to 4.5 for this purpose, the graphs of Figure 16(A) indicate a drag coefficient of $C_D = .020$

$$C_D = .015 \text{ at } \theta = 0^\circ \text{ (modified from } C_D = .020 \text{ (see page 61))}$$

Hull drag at sea level

$$D_o = C_D \frac{\gamma}{2g} v^{2/3} u^2 \text{ lb}$$

$$D_o = (.015) \frac{.076475}{64.348} (20.0000288 \times 10^6)^{2/3} (168.9)^2$$

$$D_o = (5.085515)(10)^{-1} (7.36807)(10)^4$$

$$D_o = 37,470 \text{ lb}$$

The speed of flight at $\theta = 20^\circ$, $C_D = .055$

$$u^2 = \frac{2D_o g}{\gamma v^{2/3} C_D} = \frac{(2)(37,470)(32.174)}{(.076475)(20.0000288 \times 10^6)^{2/3} (.055)}$$

$$u^2 = (7.7800574)(10)^3$$

$$u = 88.204633 \text{ ft/sec.}$$

$$u = (.5921)(88.204633) = 52.23 \text{ knots}$$

At this speed, $\theta = 20^\circ$, $C_L = .165$ and dynamic lift of the hull:

$$L = (.165) \frac{.076475}{64.348} (20.0000288 \times 10^6)^{2/3} (7780.0574)$$

$$L = 112,410 \text{ lb}$$

Capacity of the thrusters

net lift of the hull at 10,000 ft (approximately)

$$L_{200} = (.95)(10)^7 (2)(.048264) = L_{200} = 917,016 \text{ lb}$$

Downward directed thrustors capacity:

$$(.10)(L_{200}) = (.10)(917016) = 91702 \text{ lb}$$

Heating of Gas

$$\text{equation of state at ambient temperature } \gamma_0 = \frac{p}{RT_0}$$

$$\text{at higher temperature } \gamma_1 = \frac{p}{RT_1}$$

Lift of gas $k = \gamma_{\text{Air}} - \gamma_{\text{He}}$

$$\text{For } \gamma_{\text{Air}} = \text{constant} \quad \frac{k_1}{k_0} = \frac{T_1}{T_0}$$

k_0 , lift of He at ambient temperature

k_1 , lift of He at 20° higher than ambient temperature

$$k_1 = k_0 \frac{T_1}{T_0} = (.06535) \frac{538.69}{518.69} = .0678698 \text{ lb/ft}^3$$

$$\Delta k = .0678698 - .06535 = .0025198 \text{ lb/ft}^3$$

Gain in lift by heating to 538.69 from 518.69 OR

Net gas volume at 10,000 ft altitude

$(19)(10)^6 \text{ ft}^3$ full hull of gas (approximately)

$$- \frac{(3.398884)(10)^6 \text{ ft}^3}{(15.601116)(10)^6 \text{ ft}^3 \text{ at } 10,000 \text{ ft}}$$

At sea level:

$$\frac{.04828}{.06535} (15.601116)(10)^6 = (11.526)(10)^6 \text{ ft}^3$$

$$60\% \text{ of the remaining gas heated } (.6)(11.526)(10)^6 = (6.9156)(10)^6 \text{ ft}^3$$

Lifting force due to $\Delta t = 20^\circ\text{F}$ temperature

$$\text{Rise of gas } (.0025198)(6.9156)(10)^6 = 17426 \text{ lb}$$

Hull lift	112,410 lb
Thrustors	91,702 lb
Lift due to superheated gas	<u>17,426 lb</u>
	221,538 lb
Required lift	<u>-164,098 lb</u>
Excess margin	57,440 lb

No fuel needs to be dumped in case of loss of the maximum volume cell of MC-200. It can be safely assumed that similar relations can be obtained with other sizes of hulls therefore the subject is not discussed further.

The source of the drag coefficient used in this section is the NACA TR number 394 (1931)^o, particularly the tests of airship hulls carried out in the closed throat variable density tunnel, shown in Figure 16(A) for a FR = 4.8; this ratio of tested hulls is closest to FR=4.5, of the studied hulls.

The drag coefficient for a bare hull is $C_D = .020$ for $\theta = 0^\circ$, as noted in Figure 16(A). This value was manipulated to a lower value of $C_D = .015$ for this study only, in view of the following considerations:

1. The TR 394 notes that the drag coefficient slightly increases for bare hulls when the FR decreases, refer to Figures 13(A) and (B). Between FR of 4.8 and 4.5, this increase should be very small.
2. The TR 394 notes that surface roughness has a powerful influence on the C_D , especially at higher Reynolds' numbers, refer to Figure 20. Metalclad hulls will be smooth, their surface undistorted under loading; wind tunnel test C_D of model is expected to be close to the actual C_D of a full size Metalclad hull, at equivalent Reynolds' number.
3. Schlichting^P shows in his Figure 13.14, that suction over an airfoil can reduce the C_D by at least 50%, according to tests by Pfenninger. Propulsion of Metalclad hulls is expected to be inseparably associated with BL control by suction, but the

^oNACA Technical Report No. 394, 1931

^PBoundary Layer Theory, Schlichting, 1955, McGraw-Hill
Pfenninger, Page 239 Figure 13.14 .

reduction of the C_D as hoped for is not going to be as effective as with the airfoil of Figure 13.14. It appears possible that the propulsion involvement with BL reduction could be expected to reduce the C_D , obtained by wind tunnel tests of TR 394, by 25%. This is to be done by two inputs of energy into the hull BL; first one, by suction at approximately 70 - 75% of hull length and the second one, by the momentum of the cold air thrust stream at the stern end.

4. At this time and only tentatively, the coefficient of hull drag is taken as $C_D = .0150$ with the expectation that apart from the control gondola, there will be no other protrusions external to the hull. The effect of external longerons on the value of C_D is as yet unknown. They increase the hull friction surface area by approximately 10% or less; on the other hand, it is likely that external longerons may have a limiting influence on the separation of vortices. These complex relations can be determined only by wind tunnel testing.
5. Figures 17, 18 and 19 of TR 394 show the C_D still noticeably decreasing even at the highest Reynolds' number of tested hull models, $Re_m = (.49)(10)^8$. The Reynolds' numbers of studied hulls are 15 to 21 times higher than of the models in TR 394; in view of this, it can be confidently expected that the assumed value of $C_D = .0150$, will be approached by actual hulls even without BL control.

2. LOAD ANALYSIS

2.1 EXTERNAL LOADS, AERODYNAMIC MOMENT, GUST MOMENT.

During construction without internal pressure, a hull is loaded locally by its own weight to various degrees of severity; these loads will be taken up by light jury structure during erection and the construction loads on the hull structure will be low. The top longerons support the skin and their own weight in bending between main frames, with intermediate support from secondary frames.

In flight, the hull may be subjected to the aerodynamic moment, expressed by:

$$M_{ae} = (.02) \frac{\gamma}{2g} u^2 V^{2/3} L \text{ ftlb} \quad \text{or}$$

to a gust moment, expressed by

$$M_m = (.01) \frac{\gamma}{2g} u c V^{2/3} L \text{ ftlb}$$

with $c = 35.0$ ft/s gust velocity; the M_m M_{ae} and is used as the maximum design moment in an envelope of moments suggested by Woodward^h, and shown in Fig. 6 for MC-100 and MC-200, respectively.

$$q = \gamma/2g u^2 = 33.9034 \text{ lb, constant, for all hulls. (100 knots)}$$

The turning, yaw and pitch moments on a hull were also analyzed, but for this report, were abandoned when it became evident that they were always lower than the M_m moment. The aerodynamic pressure, q , will be provided for in the bow by double hull plating with cellular structure backup in between, as indicated on hull layouts (See appendix M). This structure will also be relied upon for distribution of anchoring loads directly into the skin, also into the longerons. Longerons cross sectional areas are disregarded in determining the tension stresses in the skin, a conservative measure, because they also carry tension in addition to the skin.

2.2 INTERNAL LOADS. When inflated, the hull is loaded by a gas head which induces higher transverse and longitudinal tension stresses on the top of the hull, compared with the transverse and longitudinal tensions on the bottom of the hull, due to supercharge air pressure.

^h: Proceedings of the Interagency Workshop on LTA Vehicles, FTL Report R75-2, January, 1975, p. 169.

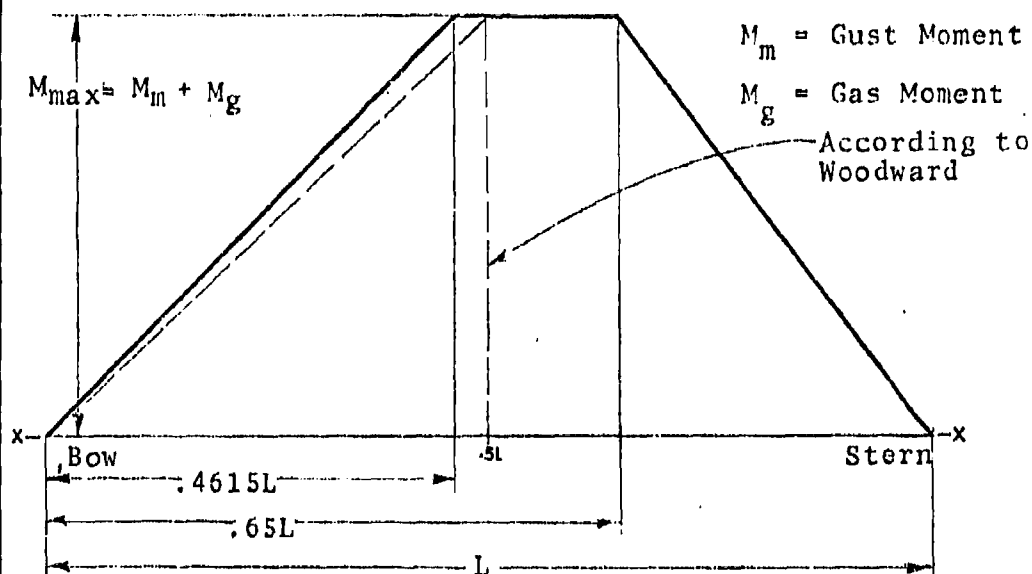


FIGURE 6 Envelope- Maximum Bending Moment

Envelope of maximum bending moments according to Donald E. Woodward:

h. Proceedings of Workshop on LTA Vehicles, FTL Report R75-2, January, 1975.

The Woodward envelope of maximum moments is specified as reaching its highest value between $(.5)L$ and $(.65)L$, while L is the length of the hull.

In the Woodward type diagram above, the maximum moment is reached at $(.4615)L$, which is another of several conservative assumptions taken in this report; eventually, this limit can be raised to Woodward's limit of $(.5)L$ with some weight reduction.

The gas as well as the air pressure cause transverse and longitudinal tensions in the skin of the hull shell, σ_T and σ_L , respectively. In Fig.7 is shown a skin element $ds_T ds_L$, under pressure p , loading it by a force $p ds_T ds_L$, causing a transverse (hoop) tension load $\sigma_T t ds_L$ and a longitudinal tension load $\sigma_L t ds_T$.

The equilibrium of forces on the skin element (without imposed shear) is:

$$\sigma_L t ds_T d\beta + \sigma_T t ds_L d\alpha = p ds_T ds_L$$

$$ds_L = R_L d\beta \text{ and } ds_T = R_T d\alpha$$

finally,
$$\frac{\sigma_L}{R_L} + \frac{\sigma_T}{R_T} = \frac{p}{t} \quad (1)$$

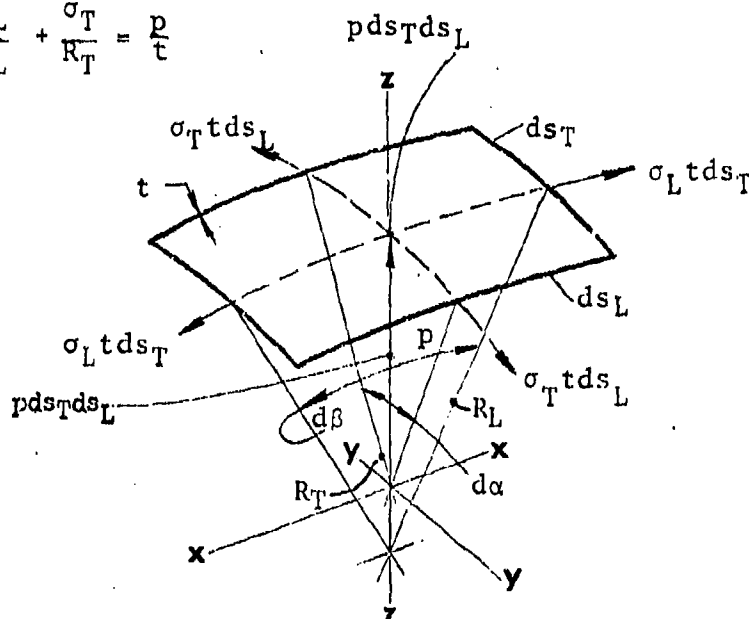


FIGURE 7. Skin Element

In a cylinder, $R_L = \infty$ and Eq.(1) reduces to:

$$\sigma_T = \frac{p R_T}{t} \quad (2)$$

In hulls having continuous longitudinal curvature, as in the case of all hulls in this report, Eq.(1) is valid. From the relations in a cylinder,

$$\sigma_T = 2\sigma_L \quad (3)$$

It can be assumed that the longitudinal length of a skin element is so small that Eq.(3) still applies, while the longitudinal curvature is included. From Eq.(1) the transverse or hoop stress in a hull under internal air pressure can then be expressed.

$$\frac{\sigma_T}{R_T} = \frac{p}{t} - \frac{\sigma_L}{R_L}$$

Introducing $\sigma_L = \frac{pR_T}{2t}$,

$$\frac{\sigma_T}{R_T} = \frac{p}{t} - \frac{pR_T}{2tR_L}$$

$$\text{and } \sigma_T = \frac{pR_T}{t} - \frac{pR_T^2}{2tR_L} = \frac{pR_T}{2t} \left[2 - \frac{R_T}{R_L} \right] \quad (4)$$

If $R_L \rightarrow \infty$, Eq. reduces to: $\sigma_T = \frac{pR_T}{t}$, which is Eq.(2)

In the analysis of this report, another form is used, putting $\sigma_T/2 = \sigma_L$ in Eq. (1)

$$\frac{\sigma_T}{R_T} + \frac{\sigma_T}{2R_L} = \frac{p}{t}$$

$$\sigma_T \left[\frac{1}{R_T} + \frac{1}{2R_L} \right] = \frac{p}{t}$$

$$\sigma_T \left[\frac{2R_L + R_T}{2R_LR_T} \right] = \frac{p}{t}$$

$$\text{and } \sigma_T = \frac{p}{t} \left[\frac{2R_LR_T}{2R_L + R_T} \right] \quad (5)$$

At all stations along the hull length.

Eq. (5) checks with Eq.(4) within a small decimal error. The hulls of this report are ellipsoids and the radius of curvature R_L is computed at any station from:

$$R_L = \frac{[b^4x^2 + a^4y^2]^{2/3}}{a^4b^4}, \quad (6)$$

for bow and stern ellipsoids.

For the maximum diameter section, R_L forward of this station is:

$$R_{LB} = \frac{a_B^2}{b} \quad \text{and aft of this station:}$$

$$R_{LS} = \frac{a_S^2}{b}; \quad R_{LB} \text{ and } R_{LS} \text{ are radii of the osculatory}$$

circles for the bow and stern ellipsoids, respectively.

The hulls considered are large, and have a low fineness ratio (F.R. = 4.5); their gas head therefore, is greater than in historical airships and is included in determining the air supercharge pressure in order not to exceed the highest allowable stress in hoop tension on top of the hulls. Eq.(5) remains as is for the bottom of the hull and is modified as follows for the upper half of the hull shell:

$$\sigma_T = \frac{2kR_T + p}{t} \left[\frac{2R_T R_L}{2R_L + R_T} \right] \quad (7)$$

All skin stresses are based on sea level state, as must be the case. At the same time, full cell inflation will rarely if ever, occur at sea level and therefore this design assumption is conservative.

As the altitude of flight increases, the hull supercharge pressure will diminish to satisfy the desire for keeping the hoop stresses substantially constant with altitude. It will be desirable to control the hull air pressure from stress sensors connected to the hull skin for monitoring the transverse stresses. This is the most direct control of air pressure possible.

From skin stress analysis of section 7.1, it is evident that the hull air pressure is not a narrow value to be continuously concerned with and maintained within tight limits.

The establishment of this fact is one of the most important results of this hull study and is emphasized here.

During calm weather, the air pressure can be reduced in flight to lower values without danger of skin wrinkles appearing anywhere. Even in turbulent weather, when near maximum gust moments might be expected, the air pressure in the studied hulls could be reduced down to 64% of the value of pressure at maximum allowable hoop stress, in the case of MC-200 and MC-100, and by interpolation, all other hulls. This reduction in pressure would not endanger the hull structure or cause skin wrinkles to appear.

This does not mean that the hulls are overdesigned; rather these margins are the consequence of using the minimum practical gages of skin to maximum allowable stress, with a factor of safety of 2 on the ultimate tensile strength of Alclad 7050-T76 Alloy. In effect, this design factor of safety is lower than that which can exist at a lower air pressure.

The purpose of this comment is to bring forth awareness that there is nothing sensitive about the maintenance of air pressure within close limits and also, that the hulls are more tolerant of air pressure variations and in fact stronger than required even for the highest gust moments at full speed. The maximum air pressure is approximately 15 to 16 in. of water column in all hulls and is very satisfactory for control purposes, particularly with modern means of rapid response controls with their accuracy and dependability.

NASA Standard^r air pressure ratio between sea level and 10,000 ft design ceiling of the studied hulls is:

$$\frac{1455.33}{2116.22} = .6877$$

The sea level supercharge hull pressure would reduce with altitude to $(15.539)(.6877) = 10.686$ in. maximum of water column for MC-200, still a relatively large number for pressure, that could be reduced still further to $(10.686)(9357/15380) = 6.501$ in. of water before wrinkles would commence to appear under maximum bending moment loading. All of these numbers, taken from section 8.1, neglect the presence of longerons. The air pressure is lower in MC-200 than in other hulls, because the skin on top is the same thickness as on MC-175 and MC-150 hulls, for the reason of having to use a standard sheet gage. Therefore, there is nothing demanding in the control of hull air pressure at sea level or with altitude, even in the least favorable case of the MC-200.

The above comments apply only to the hull structure for lifting, excluding all structures for convenience that will inevitably be inside all hulls of actual airships. It is in this region that the hulls will be well provided with structure for the purposes of supporting weight loads. This structure will also unload the skin by supporting bending loads that would otherwise reduce the skin longitudinal tension. These effects will be positive but their magnitude is not known at this time.

^r. NACA 1235 - Standard Atmosphere, 1955

The skin on the top of the hull is thicker than on the bottom, commencing 30° below the equator on the port side, around the circular perimeter of the hull to 30° below the equator on the starboard side; in addition, a gas head hogging moment is generated, increasing the tension on top of the hull; this moment is expressed by:

$$M_g = \frac{1}{4} \pi k R^4 \text{ ftlb, at maximum hull section.}$$

In part this moment is expected to be compensated for by fixed weight load distribution in the hull to at least 0.8 of its maximum value; the design head moment is then:

$$M_{g_{des}} = (.2) \pi k R^4 \text{ ftlb}$$

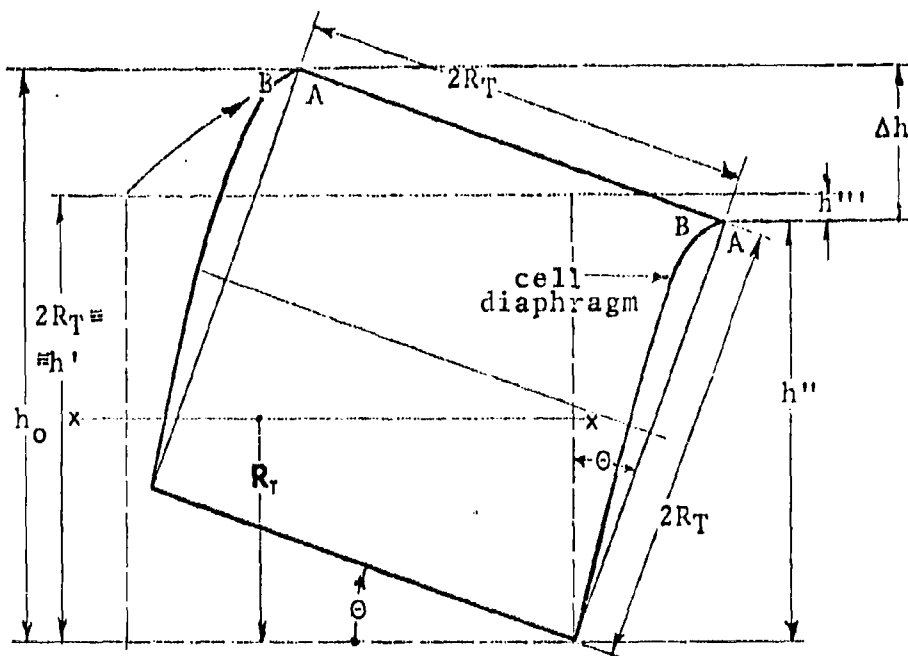
This moment is used as a contributing load in section 7.1, in determining the longitudinal skin stresses of MC-100 and MC-200. By interpolation, the skin stresses in the other intermediate hulls, are closely comparable to the stresses in the two boundary hulls.

The weight loads are collected directly and also indirectly by structure at the bottom of the hull and transferred into the circular continuous beam main frames which distribute and transfer these loads as shear, into the hull shell skin. The skin is supporting the gas lift forces opposing the weight loads. In this transfer of forces, shear in the hull shell skin is the principal mechanism of equilibrium between lift and weight loads.

Upson proved analytically in 1924^s that a Metalclad hull lifted by a gas will retain its transverse circular form as long as the lift forces are resisted by shears in the hull shell skin and that, in effect, no frames are necessary. The main circular frames deliver shear to the skin and are indispensable for this function. The secondary frames are needed during construction of the hull and especially in the adverse case of loss of gas pressure or even of air pressure in an air sub-volume of the hull.

2.3 LOADS DUE TO SURGING. The lifting gas volume is sub-divided into cells by radial diaphragms and cell "floating" semi-cylindrical envelopes, pressing on radial network in the planes of all main frames. When the hull is in pitched attitude, the gas head in each cell increases, Fig. 8

^s General Calculations and Formulas for Metalclad Airship Design, 1929, Aircraft Development Corp. Technical Report #29



$$h_0 = 2R_T(\sin\theta + \cos\theta)$$

$$\Delta h = h_0 - h'' = 2R_T(\sin\theta + \cos\theta) - 2R_T\cos\theta$$

$$\text{Pressure on side B: } p_B = 2kR_T\cos\theta$$

$$\text{Pressure on side A: } p_A = 2kR_T(\sin\theta + \cos\theta)$$

$$\text{Pressure between A and B: } \Delta p_{A-B} = 2kR_T\sin\theta$$

$$\text{for } \theta = 20^\circ, \Delta p_{A-B} = .342(2kR_T)$$

The pressure bulging the diaphragm at B will be 34% higher than in level flight.

FIGURE 8 Cell Pressure Diagram

simply due to the increased vertical difference between the top and bottom of a cell compartment. This causes a non-equilibrium loading on top of the radial network which, in the upper half of the inner area of main frames, is integral with the diaphragm. The diaphragm is forced to bulge and the forces arising from this load are resisted by frames. C.P. Burgess^t analyzed this case, also with a deflated cell, for ZR-1. In reference ^t, is shown that unbalanced gas loads do not lead to stresses in the main frames that require additional structure or reinforcements of frames; the frames are inherently structurally adequate to sustain these loads in a typical case and at this time, no further attention was given to this source of internal loading. The cellular Metalclad main frames are expected to be particularly effective in resisting this loading, because the network loads are going to be more rapidly dissipated into continuous beam frame structure, than would be the case in skeletal truss frames. The analysis of gas and air surging is not considered at the present time. At this time radial network in the main frames is thought to be sufficiently elastic and energy absorbing. Should subsequent work conclude that hydraulic shock absorbers must be used, they can be placed at each anchor joint on main frames between the ball socket and the pivoting horn attached to the network; this joint is shown on the layout of the MC-200 (Appendix M-5).

^t. The U.S. Navy Design Memorandum No.35-C.P. Burgess.

3. MAIN FRAME ANALYSIS

3.1 SECTION CHARACTERISTICS.* All main frames have a triangular cross-section, with the circumferential base being a base skin, thicker than the adjoining local hull skin. The apex is connected to the base by continuous, sloping shear webs made of straight-sided corrugations.

All main frames are continuous circular beams. This is a departure from the skeletal deep frames of R-101 and of the AKRON and MACON airships. In Metalclad construction, the main frames are loaded continuously along their periphery, by lift forces, shear forces and weight (load) forces. This basic character of loading calls for a continuous circular beam which can support all these forces continuously, element-by-element of its periphery and is the lightest structure for this purpose. A view of a main frame is shown in Figure 2, section 1.1, and is typical for all main frames in all hulls.

The geometric height (base to apex of sides) of all main frames is $h_{mf} = .108 R_T$, except with a minimum of $h_{mf} = 96$ in. This latter height is then constant at all hull radii that would call for a lower height of frame for the convenience of human access. The structural height is set at $h_{mfs} = (.95)h_{mf}$. This is the height from the base, on center line of the section, to the top of the apex cornice. The apex angle of all frames is 44° total, 22° on each side of the section center line.

The apex cornice is composed of two rolled sections, as illustrated, joined together by the corrugated sides of the frame. The apex cornice is, in effect, a non-circular tube in its section, curved to the radius of the apex cornice relative to the hull curvature. The base cornices are preferably extrusions, curved to the local hull radius and riveted to the corrugated sides of the frame. The base structure is a part of the hull shell skin, although thicker than the local skin, as is described in section 5.** An essential component of the base structure are the longerons, located externally with respect to the skin, but attached to the base skin of the frames as well as to the base cornices.

Each main frame is directly attached to the skin at every element of its perimeter and receives the lift loads from the skin as well as transfers loads to it by shear. The weight loads are (at this time) assumed to be at the lowest part of each frame, as a distributed load of high intensity. The analysis assumes the weight load to be concentrated at two stations on the bottom of each frame $x = 22.50$ on each side from $x = 0^\circ$, as shown in Figure 9. This is a highly conservative assumption. Similar conservative measures are taken

* Also refer to Appendices A, B, and C. **Figure 16

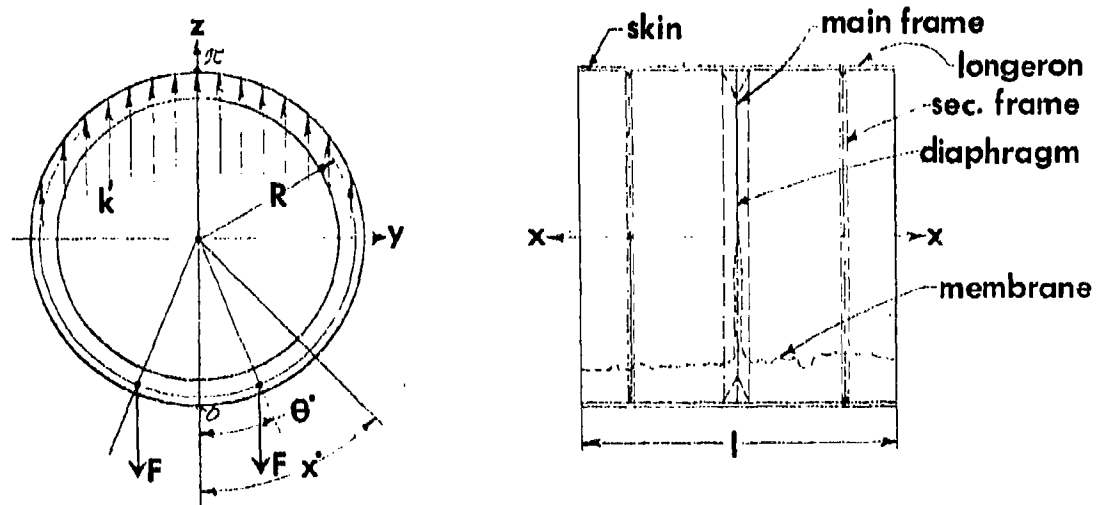


FIGURE 9 Loading of a Main Frame

often in this report. In the final design of each hull, some weight can be eliminated in the lifting structure and taken up by the weight-load supporting structure.

No solution was found in existing literature researched by TI for a circular beam (Main) frame, loaded by a distributed weight-load at its lowest arc and unloaded by shear flow into the hull skin all along its perimeter. The shear flow into the skin is indicated in Figure 10-B, on one half of a frame, typical for both sides of the frame. The shear load on each side of the frame is $V/2$ (or $F/4$) of what is shown in Figure 10-B. The shear load into the skin is zero at station 0 and π . At station $\pi/2$, the shear load into the skin is maximum and equal to $F/2$, or $F/4$ on each side of the frame. A frame, loaded in this manner will have high negative bending moments at the station of load "F" application; along the rest of the frame perimeter, the bending moments will be lower, as indicated schematically in Figure 10-A.

The solution to the analysis of the above frame loading problem was resolved by using a known solution, based on the assumption that all lifting forces are directly on the frame instead of on the hull skin. The loading is indicated on Figure 9. Equations for a circular beam of Figure 9, are in R. J. Roark's book "Formulas For Stress And Strain,"^u

^u Formulas For Stress And Strain, R. J. Roark, Fourth Edition, McGraw-Hill, 1965.

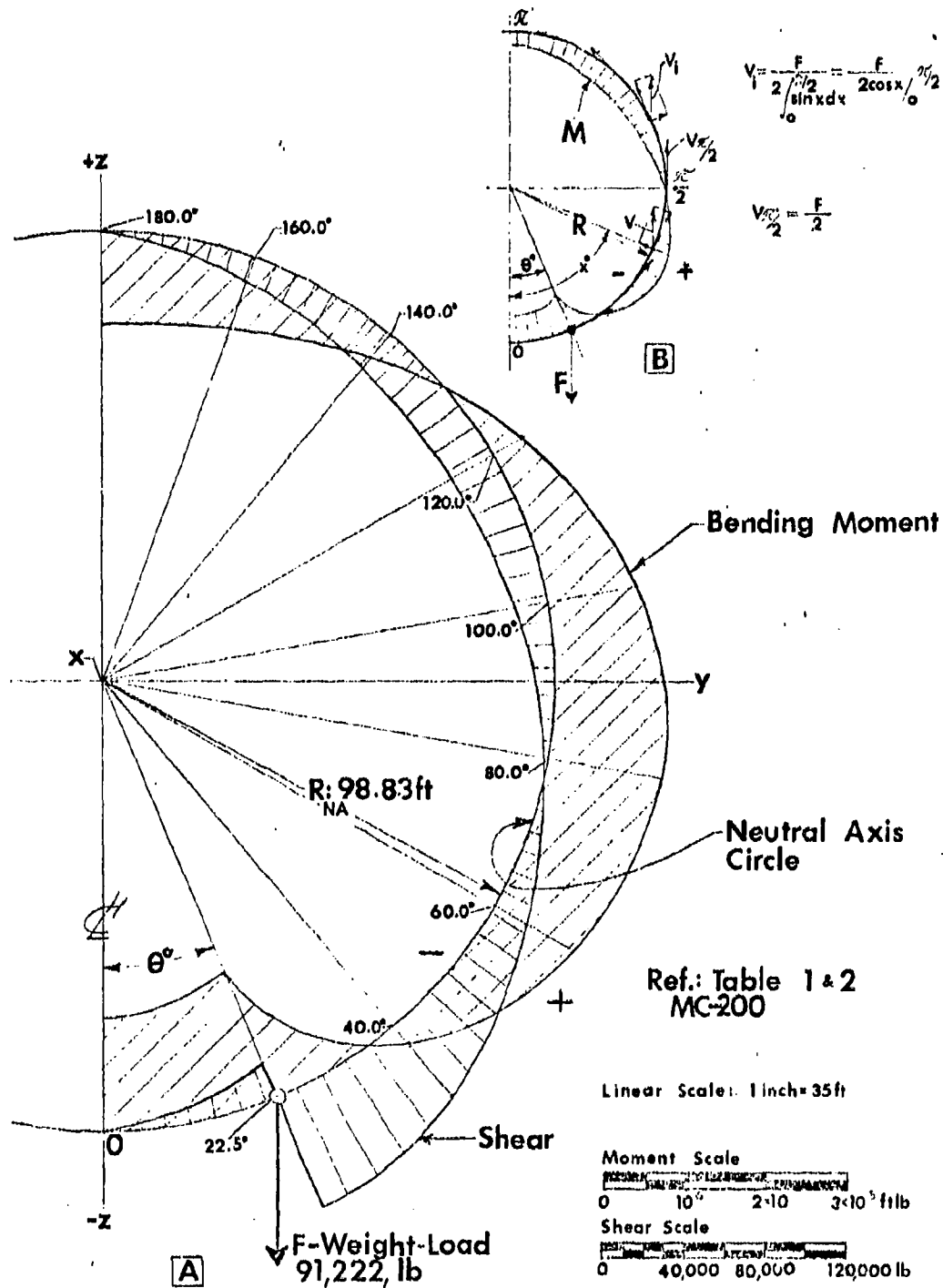


FIGURE 1.0 Frame 334.5 (MC-200) Under weight Loading

page No. 177, Case No. 23, for $\beta = \pi$.

The formulas for Case No. 23 are used for computing bending moments, shears and diametral deformations of main frame 334.50 of MC-200 hull, by way of example. The Case No. 23 is directly applicable for a Metalclad hull, with k , (specific lift) negative and force F reversed in direction. The formulas of Case No. 23 are repeated here for record. The analysis itself is not included. Case No. 23, as shown in Figure 10-A, compared to the actual loading of main frames in a Metalclad hull, is unduly severe; yet, the frame of the example is more than adequate to support the loading with only very small deformations. The severity of the frame loading is first caused by the concentrated weight-load at one station, θ^0 , which will not likely happen due to the nature of weight-load carried by airships; the second cause of high loading is due to the tacit assumption that all available lift is acting directly on the frame, instead of on the hull skin and in reality, is always unloaded into the skin by shear flow from the frame beginning immediately at station θ^0 . In the assumed loading case No. 23, all lift is acting on frame segment $\pi/2 - \pi$, where in actual loading, only $1/2 F$ is acting at station $\pi/2$ and from then on, is directed into the hull plating, so that all hull shear from weight-load F , is zero at station π .

The specific lift k' , as shown in formulas under 3.2 and 3.3, is a reduced nominal specific lift at s_1 , due to the direct lift of the hull structure by the gas; in effect, the lift on the frame, supporting weight loads, is reduced by the weight of: (See Figure 9)

1. The main frame.
2. Weight of skin of the hull section corresponding to the frame.
3. Weight of two secondary frames.
4. Weight of longerons of the hull section.
5. Weight of diaphragm and membranes of the hull section.

The sum of these weights is lifted directly by the gas and is deducted from the total lift of the hull section, based on the gross displacement volume of the hull section minus air volume contained inside the main frame.

3.2 CASE 23 - SEGMENT 0-θ

For frame segment between station $x = 0$ and station $x = \theta$, for fully inflated hull, (segment $0 - \theta$):

Bending Moment:

$$M_{(0 - \theta)} = M_1 + \left[-T_1 R(1 - \cos x) = k' R^3 \left((.5)x \sin x + 1.0 - \cos x \right) \right] (1), \text{ ft lb}$$

Shear:

$$V_{(0 - \theta)} = \left[-T_1 \sin x + k' R^2 \left((.5)x \cos x + (1.5) \sin x \right) \right] (1), \text{ lb}$$

Where:

$$M_1 = k' R^3 \left[-.249928 + (.50)(1 + \cos \theta + \theta \sin \theta - (3.14159) \sin \theta + \sin^2 \theta) \right] (2), \text{ ft lb}$$

$$T_1 = k' R^2 (1.250025) + (.31831) F \sin^2 \theta = k' R^2 (1.250025 + (.5) \sin^2 \theta), \text{ lb/ft}$$

$$F = (.5) \pi k' R^2 = (1.570796) k' R^2, \text{ lb/ft}$$

3.3 CASE 23 - SEGMENT $\theta - \pi$

For frame segment from station $x = \theta$ to station $x = \pi$, for fully inflated hull, (segment $\theta - \pi$):

$$M_{(\theta - \pi)} = M_1 + \left[-T_1 R(1 - \cos x) + k' R^3 \left((.5)x \sin x + 1.0 - \cos x \right) - FR(\sin x - \sin \theta) \right] (1), \text{ ft lb}$$

Shear:

$$V_{(\theta - \pi)} = \left[-T_1 \sin x - F \cos x + k' R^2 \left((.5)x \cos x + (1.5) \sin x \right) \right] (2), \text{ lb}$$

Values of M_1 , T_1 and F , are the same as for segment $0 - \theta$.

For a main frame at maximum hull diameter of MC-200, the above weights are:

	<u>lb</u>
1.	9,383
2.	17,810
3.	2,596
4.	4,928
5.	<u>3,885</u>

ΣW: 38,602 lb

Total volume of the hull section of length l : 3,399,251 ft³

Air space in frame V_F : 16,754 ft³

Lift of hull section of length l :

$$L_T = k(V_O - V_F) = .06535(3,399,251 - 16,754), \text{ lb}$$

$$= .06535 (3,382,497), \text{ lb}$$

$$L_T = 221,046 \text{ lb at sea level, fully inflated hull.}$$

Net lift on the main frame:

$$L_N = k(V_O - V_F) - \Sigma W = 182,444 \text{ lb}$$

Effective specific lift for the support of weight loads on the main frame:

$$k' = \frac{L_N}{V_O - V_F} = \frac{182,444}{3,382,497} = .0539377, \text{ lb/ft}^3 \text{ at sea level}$$

Weight load "F" is assumed to be concentrated at one station, $\theta = 22.5^\circ$, on each half of the main frame,

$$F = \frac{L_N}{2} = \frac{182,444}{2} = 91,222 \text{ lb, as shown in Figure 10.}$$

This is a very conservative assumption and is taken deliberately in this case.

With the aid of equations referenced in 3.2 and 3.3 above, moments and shears were computed at ten stations along the semi-periphery of the frame, using the radius of the neutral

axis of the frame in the inflated hull, $R = R_{NA} = 98.8283$ ft.

The computed moments and shears are tabulated in Table 1 and Table 2 respectively.

TABLE 1 Bending Moments $0^\circ - 180^\circ$

<u>Station x°</u>	<u>$M(0 - x)$, ft lb</u>
0	-1,401,834
22.5	-1,675,048
40.0	+ 3,110
60.0	+1,125,595
80.0	+1,439,252
100.0	+1,137,136
120.0	+ 423,488
140.0	- 352,084
160.0	- 939,054
180.0	-1,156,437

TABLE 2 Radial Shear $0^\circ - 180^\circ$

<u>Station x°</u>	<u>$V(0 - x)$, lb</u>
0	0
22.5	79,438 — $\begin{cases} (0 - \theta): -17,978 \text{ lb} \\ (0 - \pi): +61,460 \text{ lb} \end{cases}$
40.0	+45,032
60.0	+20,282
80.0	- 1,233
100.0	-16,165
120.0	-22,710
140.0	-20,857
160.0	-12,287
180.0	0

The moments and shears are plotted along the frame neutral axis circle in Figure 10 and on a straight abscissa equal to semi-perimeter, in Figure 11.

The highest bending moment arises at $\theta = 22.5^\circ$ station of concentrated weight force "F", $M_{22.5} = -1,675,048$ ft lb. In an actual condition of hull loading, this weight force would be distributed between at least $\pm 30^\circ$ stations along the frame perimeter, with respect to station 0, and the moment would be lower.

Maximum stress in the frame at station $\theta = 22.5^\circ$ is compression in the apex cornice of the frame:

$$\sigma_{A_\theta} = \frac{M_\theta C_F}{I_F} = \frac{(1,675,048)(12)(80.92)}{44,742.7} = 36,353 \text{ lb/in}^2 \text{ compression}$$

This stress is higher than maximum allowable, $\sigma_{des} = 32,850 \text{ lb/in}^2$; considering the severity of loading assumption, it should not be necessary to reinforce the apex cornice.

At station $x = 110^\circ$, where the next highest bending moment is, tension in the apex cornice would be:

$$\sigma_{A_{110}} = \frac{(1,439,252)(12)(80.92)}{44,742.7} = 31,235 \text{ lb/in}^2 \text{ tension}$$

At this station as in other perimetral stations, the apex cornice will not require reinforcement. The frame can be reduced in height all along its perimeter from its present structural overall height of 118.98 in. to no more than 100.0 in. with considerable weight saving. Instead of the geometrical height of main frames equal to $(.108) R_T$, which is the given criteria for analysis as shown in Figure 2 Section 1.1 and 3.1 it is proposed to make it in actual design $(.0925) R_T$.

The moment distribution in Figure 10-A, indicates that the main frame should have a constant height all along its perimeter. However, Figure 10-B suggests that all main frames should be designed deeper at and around station $x = 0^\circ$, and progressively less deep toward station π . The most attractive solution would be to place the center of the apex cornice circle above the center of the circle of the base cornices. Whether the gain in lightness will justify the cost of this design will have to be demonstrated.

The corrugated shear sides of the frame cross-section triangle will be made heavier locally around station $x = 0^\circ$, the highest shear load on each side of the frame above the equator is approximately 1,100 lb/ft, which is well within the capability of .032 in. thick shear sides and also points

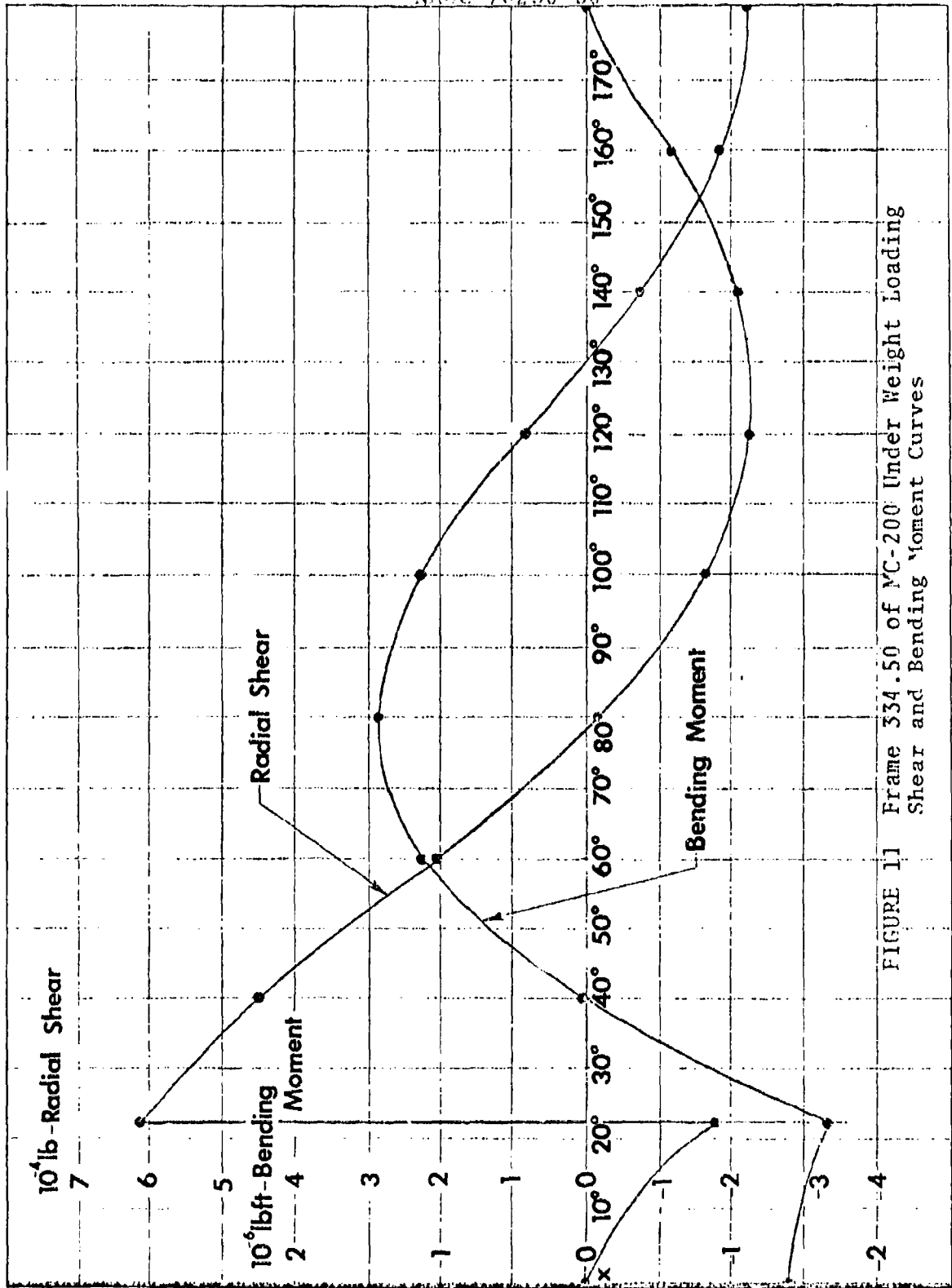


FIGURE 11 Frame 334.50 of MC-200 Under Weight Loading
Shear and Bending Moment Curves

toward reducing the height of the frame, as noted above.

Preliminary analysis tends to confirm the justification of reducing the weights of all main frames to 80% of their computed values as stated in Section 10. The weight reduction will be probably even more favorable in the final analysis, once the method of computing frames based on Figure 10-B is developed.

3.4 FRAME BEHAVIOR. The main as well as secondary frames in metalclad hulls have a unique behavior. When the hull is deflated and without pressure, the base skin along the frame perimeter is practically inactive. Neglecting for the time the effective width of the base skin, the neutral axis of the frame section is located very closely at mid-height of the frame cross-section.

When the hull is inflated with pressure, the base skin of all frames (as well as of longerons), becomes fully effective structurally. The frames are then capable of supporting compressive stresses in their base skin to almost the full value of the allowable stress ($\sigma_{AL} = 32,350 \text{ lb/in}^2$), because this stress is equal to the hoop tension stress due to pressure. The effective area of the frame section increases at the base and the moment of inertia of the frame is higher. The neutral axis of the inflated frames moves toward the base, and its new location is approximately 1/3 of the structural height of the frame. The distance to the apex cornice increases, but the apex cornice stress remains almost constant. However, the rigidity of the frame is greater under hull pressure than when the hull is deflated. This is an important factor in reducing the radial deformations of all main frames; as the inflated airship is being loaded in preparation for flight the outwardly displacement of the neutral axis of main frames to a greater radius, is a powerful factor in making the frames more rigid under weight loads, because frame deformations are a function of the fifth power of the frame neutral axis radius.

3.5 DIAMETRICAL DEFORMATION OF MAIN FRAME NO. 334.50 Of MC-200 (largest diameter frame). The typical main frame analysis as described above is dealt with as if the frame were loaded alone, without a metal hull; this is the first highly conservative basis, because in the hull, the frame will be unloaded by shear on the sides of the hull, which is a far more favorable condition than loading it by distributed lift at the top of the frame, as the analysis assumes. The second conservative assumption is the concentrated weight loading at the bottom of the frame; this load is going to be more distributed and the high bending moment and shear in this vicinity will be alleviated, although the rest of the frame circumference should not be affected too noticeably by better

distribution of weight loads at the bottom. The third conservative assumption is the frame height parameter $(.108R_T)$; analysis shows this to be more realistic at $.0925 R_T$ along its total perimeter. The skin shear unloads the frame rapidly into hull skin and the frame will not be as severely loaded in the hull as is assumed in the analysis according to Case No. 23^u from which the frame deformation formulas are used.

From Figure 12, the moment of inertia of a main frame of MC-200, at station $\theta = 22.5^\circ$, is $I = 44,742.7 \text{ in}^4$.

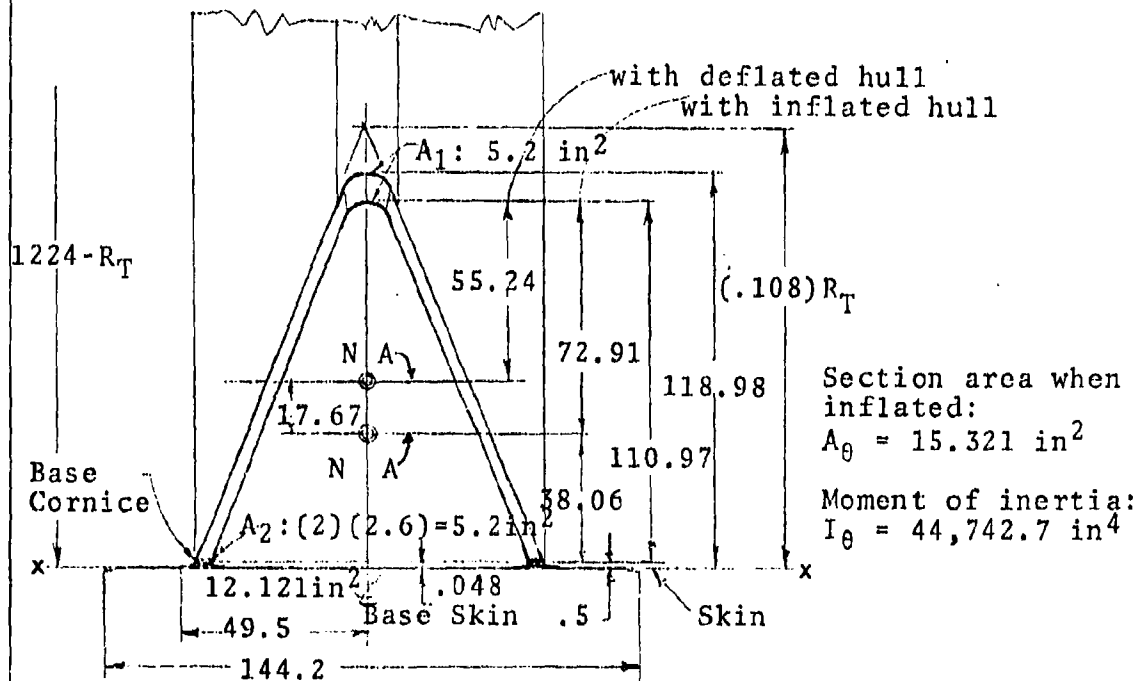


FIGURE 12 Section Of Frame No. 334.5 Of MC-200 At Station $\theta = 22.5^\circ$, Maximum Moment Station

In the absence of more realistic analysis, the deflections as determined below are used to determine the weights of main frames in other than MC-200 hulls, by extrapolation. However, as explained in Section 10 these weights have been "Adjusted."

In Figures 12 and 13 are shown a typical main frame with the hull inflated and deflated. The width of base will not alter significantly with changes of inflation, but the base skin will move radially outward under hoop tension, (shown at full value of the hull skin). Although the thicker base skin will reduce the base radial deformation to between one half to one third of the nearby skin deformation, even in this overstated

3.5.1 Diametral Deformation - Case No. 23^u

"Y"-Axis (horizontally)

$$D_y = \frac{kR^5}{EI} \left\{ \frac{1}{\pi} \left[-2\pi + \pi(\theta \sin \theta + \cos \theta - (.875)\pi - (.25)\pi \sin^2 \theta) \right] + 2.0 + (.625)\pi \right\} (1), \text{ in.}$$

For main frame 334.5, Figures 9, 10, 11, and 13, using the above equation:

$$D_y = -34.712 \text{ in., diametrically}$$

Radial deformation, at equator:

$$\Delta R_y = -17.356 \text{ in.}$$

Then,

$$\frac{\Delta R_y}{\Delta R_T} = \frac{17.356}{1224.0} = .014179 \text{ or } 1.4179\% \text{ of the hull radius.}$$

This deformation under very severe loading assumptions (concentrated weight load and no shear unloading from the frame into the hull skin), is small and indicates again the already reached conclusion that the frame height can be reduced.

"Z" Axis (vertically)

$$D_z = \frac{kR^5}{EI} \left\{ \frac{1}{\pi} \left[-2\pi + \pi(\theta \sin \theta + \cos \theta) \right] + 2.0 - (.125)\pi^2 + (.25)\pi(\theta + \sin \theta \cos \theta - 2\sin \theta) \right\} (2), \text{ in.}$$

For main frame 334.5, Figures 9, 10, 11 and 13, using the above equation:

$$D_z = -34.7118, \text{ in. total diametral frame deformation.}$$

This is a very small deformation, considering the diameter of the frame ($D_T = 2,448 \text{ in.}$) and the comment made with respect to horizontal deformation of this frame applies also in the case of the vertical deformation.

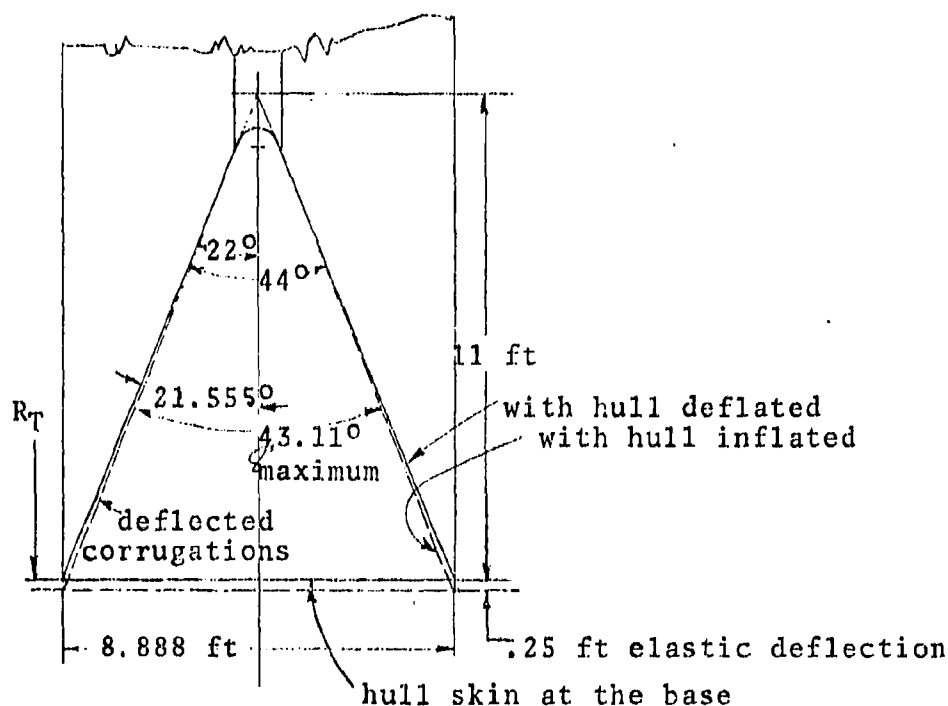


FIGURE 13 Typical Main Frame Under Radial Deflection Of The Hull Shell.

example, the corrugated sides of the frame will deflect elastically less than one half a degree in a length of 11.863 feet.

In Figure 12, is indicated the change of section properties, typical of all structures attached to skin in metalclad hulls; with pressure in the hull, the base skin (thicker than local skin) comes into effect and the neutral axis moves radially outward from its location in deflated hull; in this case, the neutral axis moves 17.67 in. The moment of inertia increases outwardly from deflated to inflated state; the maximum bending stress remains substantially unchanged, while the frame rigidity increases.

The maximum bending moment stress on frame 334.5 at sta. $\theta = 22.5^\circ$ is:

$$\sigma_{\theta} = 36,353 \text{ lb/in}^2, \text{ computed in Section 3.1,}$$

under the severe assumption that all weight is concentrated at two stations $\theta: + 22.5^\circ$. If this stress should actually exist, the apex cornices at these two stations would be

locally reinforced and everywhere else along the whole frame perimeter the cornice areas would reduce to $A_1 = 3.17 \text{ in}^2$ minimum, or a mean value of reduction of:

$$\frac{(3.17)(2) + (5.2)(2)}{2} = 8.37 \text{ in}^2 \text{ Total mean cornice area.}$$

The cornice area of the frame section can be scaled down to:

$$\frac{8.37}{10.40} = .8048, \text{ or}$$

80% of the maximum section area, for the determination of frame weight. The effect of the corrugations contribution to the cornice strength was disregarded at this time. The apex cornice is effectively a tube and the base cornices are extrusions.

The major characteristic of all Metalclad frames is the capability to easily adjust to radial skin deformations due to inflation pressure. At the same time, their stiffness in all transverse directions is increased by a large factor without significant change in the maximum bending stress. This is a desirable quality of Metalclad shell structures.

In Table 3 are arranged all gas lift loads on all main frames in each hull for sea level lift with fully inflated hull. These maximum static lift loads, corresponding to each frame are total lift loads, before the weights of directly lifted structures are deducted, as is done in the example case of Frame No. 334.5 of MC-200, of this section.

The hulls cannot fly with fully inflated cells at sea level, yet the frame analysis is based on this condition, because for test purposes in the dock, this case will arise, with a hull tethered at each main frame.

Normally, the hulls will be always inflated to less than their complete fullness, for flight below a fixed ceiling altitude.

TABLE 3 Total Lift Force On Each Main Frame, lb (e S.L. With Full Inflation)

Main Frame	MC-200	MC-175	MC-150	MC-125	MC-100
I	15,312 (18.38)	13,398 (13.72)	11,484 (13.03)	9,570 (12.26)	14,595 (19.25)
II	144,772 (121.87)	126,675 (112.70)	108,579 (107.06)	90,482 (100.74)	63,288 (97.10)
III	202,003 (229.5)	176,752 (215.98)	151,502 (205.61)	126,252 (193.06)	98,240 (179.30)
IV	221,036 (334.5)	193,406 (316.075)	165,777 (300.25)	138,148 (282.54)	110,307 (262.287)
V	212,939 (438.81)	186,322 (416.17)	159,704 (395.33)	133,087 (372.02)	105,523 (345.20)
VI	190,635 (543.16)	166,806 (515.65)	142,980 (489.83)	119,147 (460.94)	99,508 (425.94)
VII	156,137 (646.46)	136,620 (614.45)	117,106 (583.68)	97,586 (549.26)	84,892 (516.54)
VIII	106,103 (751.64)	92,840 (715.06)	79,579 (679.25)	66,314 (639.19)	64,937 (607.98)
IX	42,961 (853.08)	37,591 (812.08)	32,221 (771.41)	26,351 (752.92)	
	(1,293,868)	(1,130,410)	(968,932)	(806,937)	(641,290)

4. SECONDARY FRAMES

4.1 DESCRIPTION Secondary frames serve the purpose of stabilizing the longerons in deflated hulls. With pressure in the hull, their presence is entirely redundant. The principal stabilizing structure for the longerons is the skin, and if relied upon exclusively, the skin would have a tendency to become non-circular in hull cross section when deflated and the stabilizing restraint on the longerons would disappear. Secondary frames hold the skin to a substantially circular hull cross section and therefore, the longerons are also held radially to their peripheral locations. The importance of this structural function becomes clear when it is understood that as long as the longerons are positioned radially by the frames, main as well as secondary, they maintain along their length a positive longitudinal curvature. Any axial compressive load on them will cause them to deflect outwardly with respect to the hull surface and this deflection, however small, even in a deflated hull, will be resisted tangentially by the skin thus stabilizing the longerons.

The function of all secondary frames is principally to hold the hull skin to a circular cross section. This function requires that secondary frames have sufficient height in section to obtain as high a moment of inertia with as little weight as possible. In this analysis, the computer program was a good guide and the height of all secondary frames was established at $(.0125) R_T$ at all stations. A typical cross section of a secondary frame is shown in Figure 3 of Section 1. It is similar in design to the main frames, but lower in height and uniform in section all along its perimeter. The upper half of each secondary frame is submerged in lifting gas, while the lower half is in the air space. At a small angle above equatorial plane on each side of the hull, the secondary frames are divided by an internal, bulkhead, pressed out of sheet metal, acting as a separator between gas and air spaces, and serving as a back-up for the attachment of the cell membrane to the secondary frame, a typical installation appears on the layout of MC-200.

A typical secondary frame is a continuous circular beam of cellular concept, composed of an apex cornice, two base cornices and two corrugated shear webs connecting the apex to the base cornices with a 44° angle at the apex.

All secondary frames have a thicker gage than the local skin base to reduce the slopes of deflection of the skin on both sides of each secondary frame. When inflated, the base skin becomes an integral part of the frame similarly as happens in main frames.

5. LONGERON DESCRIPTION

5.1 INTRODUCTION. Most of this section is devoted to the analysis of a longeron in a hull subjected to uniform pressure. For MC-200 the calculations extend over nearly the whole length of hull, while for MC-100 they are limited to only three frame bays.

A longeron is treated as a beam on an elastic foundation provided by skin. The frames constitute a row of interacting elastic elements. The effect of the axial force due to the longitudinal pressure component is important, because it gives the system an additional stiffness in the radial direction. The presence of an axial force makes the system nonlinear and necessitates the use of iterative solution.

A condition is also considered, where pressure completely escapes from one cell. This causes the longerons to lose much of the support the skin is providing. A conservative approach is taken to clearly demonstrate the adequacy of the structure, when acted upon by a gust.

5.2 COMPUTER ANALYSIS OF TYPICAL LONGERON SEGMENT UNDER INTERNAL PRESSURE. The hull is uniformly pressurized with $p = 0.976 \text{ lb/in}^2$. The geometry shown here does not exactly correspond to any part of the ship and should be treated merely as an illustration of the method of analysis.

Structural Components. (Refer to Appendices "D" "H" & "I" for longeron models).

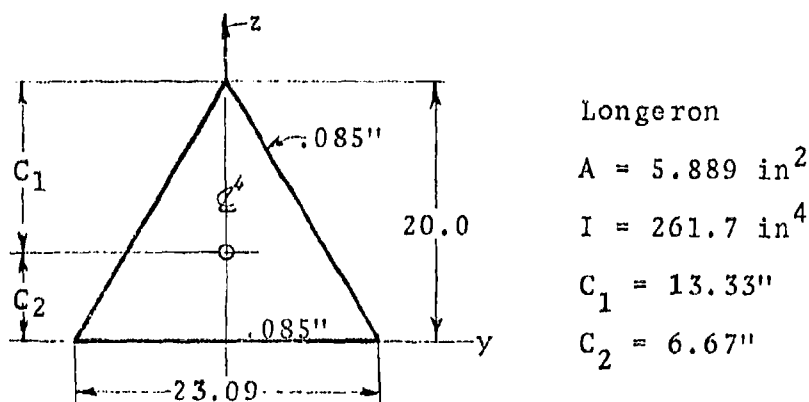


FIGURE 14 Longeron Geometry

Section is considered to be constant along the length.

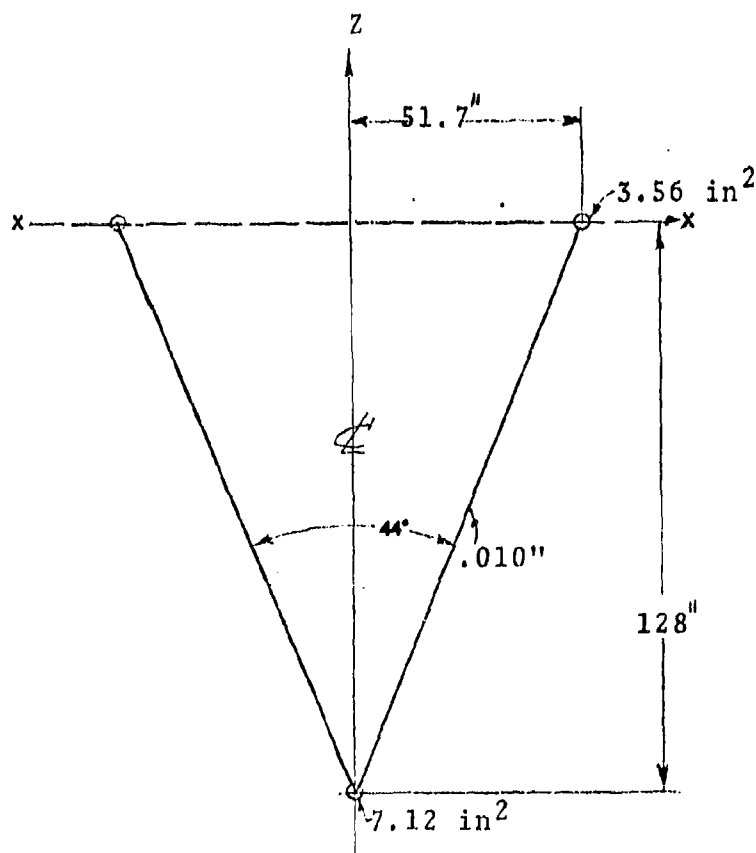
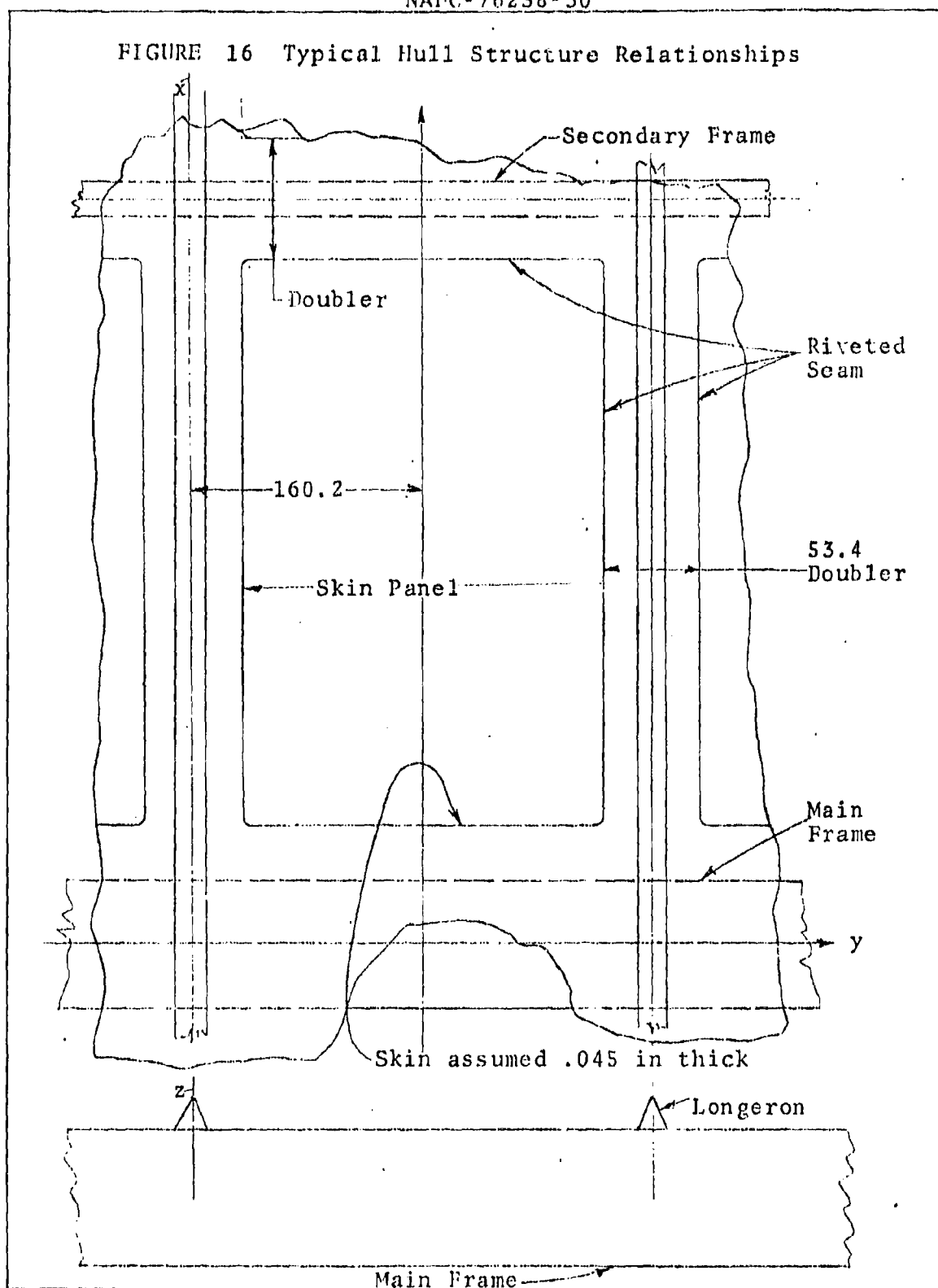


FIGURE 15 Main Frame Section Geometry

Longerōn spacing = $320.4''$ (on circumference) for 24 Longerons
 Frame spacing = $432''$ (av.)

If this geometry was duplicated at every frame bay, this analysis would be valid.

FIGURE 16 Typical Hull Structure Relationships



5.2.1 Stiffness of Foundation Springs. The curvature of skin, which results in its stiffness in radial direction is accounted for in the model by a series of equivalent springs supporting the longeron (see Figure 17).

The spring constant of skin is given by:

$$k_o = \frac{2\pi Et}{zR} \quad (\text{per unit length of hull})$$

When this is multiplied by the impingement length of a node, the equivalent lumped constant is obtained:

$$k' = \frac{1}{zR} 2\pi Et l_i = k_o l_i$$

This is true only at the line of contact with the frame, where the skin is forced to remain circular. k diminishes gradually, when moving away from the frame. Here k is assumed zero at mid-length of panel, $x = 216.0''$. When x' is measured from node 3: (contact point with a frame)

$$k = k_o (1 - x'/164)$$

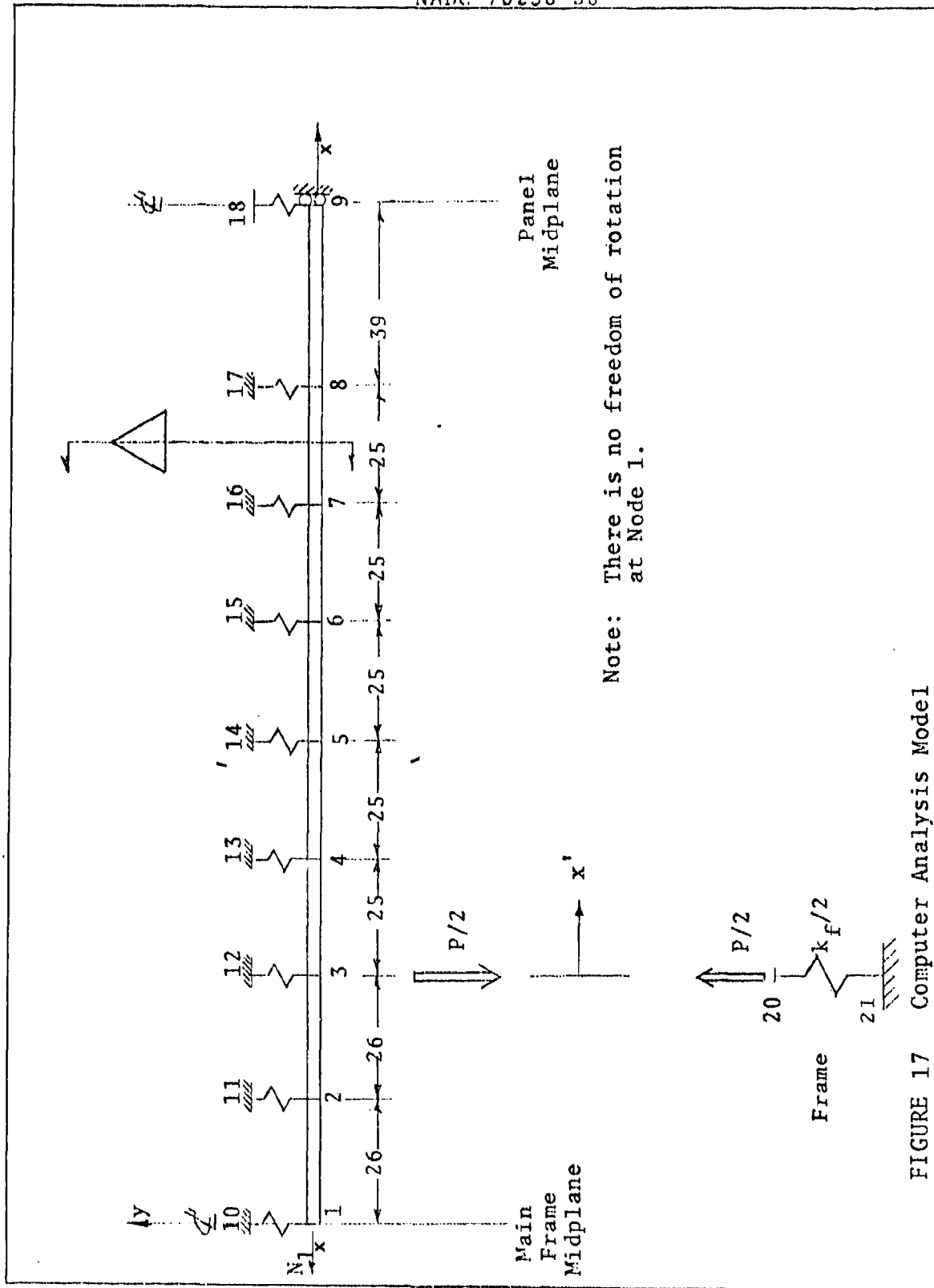
$$k_o = \frac{2\pi \times 10.4 \times 10^6 \times 0.05}{48 \times 1224} = 55.61 \text{ lb/in}^2$$

(Unlike in the rest of this section, skin thickness is assumed to be 0.050" and 48 rather than 24 longerons are used.)

TABLE 4 Stiffness of Foundation Springs

Node	$ x' $ in	k lb/in ²	l_i in	k' lb/in
10	52	37.98	13	493.7
11	26	46.79	26	1216.5
12	0	55.61	25.5	1418.1
13	25	47.13	25	1178.2
14	50	38.66	25	966.5
15	75	30.18	25	754.5
16	100	21.70	25	542.5
17	125	13.22	32	423.0
18	164	0	19.5	0

$$k = 55.61 (1 - x'/164)$$



5.2.2 Applied Forces. Total cross section area for $R = 1224''$:

$$A_T = \pi \times (1224)^2 = 4.7067 \times 10^6 \text{ in}^2$$

Axial force due to pressure $p = 0.976 \text{ psi}$:

$$N = pA = 0.976 \times 4.7067 \times 10^6 = 4.594 \times 10^6 \text{ lb}$$

Metal area for skin of 0.045" and 24 longerons:

$$A_m = 2\pi R t + z A_L = (2\pi) \times (1224) \times (0.045) + (24) \times (5.889) = 487.4 \text{ in}^2$$

Axial stress:

$$\sigma_t = 4.594 \times 10^6 / 487.4 = 9426 \text{ psi}$$

Axial force in a longeron:

$$N_L = 5.889 \times 9426 = 55,507 \text{ lb}$$

This force is applied to the longeron at node 1 and reacted at node 9.

Upon inflating the hull with pressure, there is a gap Δ between the skin and the surface of frame. (This is only at the first stage of solution.) The magnitude of this gap is calculated in the next sub-section. The forces applied to nodes 20 and 3 (equal and opposite) are $P = 20,000 \text{ lb}$ (each).

5.2.3 Representation Of Frame And Initial Gap. The frame subjected to uniform pressure loads is a ring in the state of nearly constant tension. The radial stiffness of such ring is:

$$k_f = \frac{2\pi E A_f}{zR}$$

in which A_f is the frame section area and n is the number of equally spaced radial forces.

$$k_f = \frac{2\pi \times 10.4 \times 10^6 \times 17.0}{24 \times 1224} = 37,815 \text{ lb/in}$$

Only one-half of this value is assigned to the spring 20-21 representing the frame, because node 3 is one of the two contact points of this frame with skin. (see Figure 18)

The initial gap between skin and frame

$$\Delta r = \frac{pR^2}{Et} = \frac{0.976 \times 1224^2}{10.4 \times 10^6 \times 0.045} = 3.124''$$

The interaction force P is then applied at nodes 3 and 20 with the purpose of closing the gap. The magnitude of this force is not known beforehand and whatever is chosen will be too large or too small. In order to avoid that difficulty a nonlinear element is inserted between nodes 3 and 20. This arrangement limits the magnitude of the interaction force imposed on the structure to the value needed to close the gap.

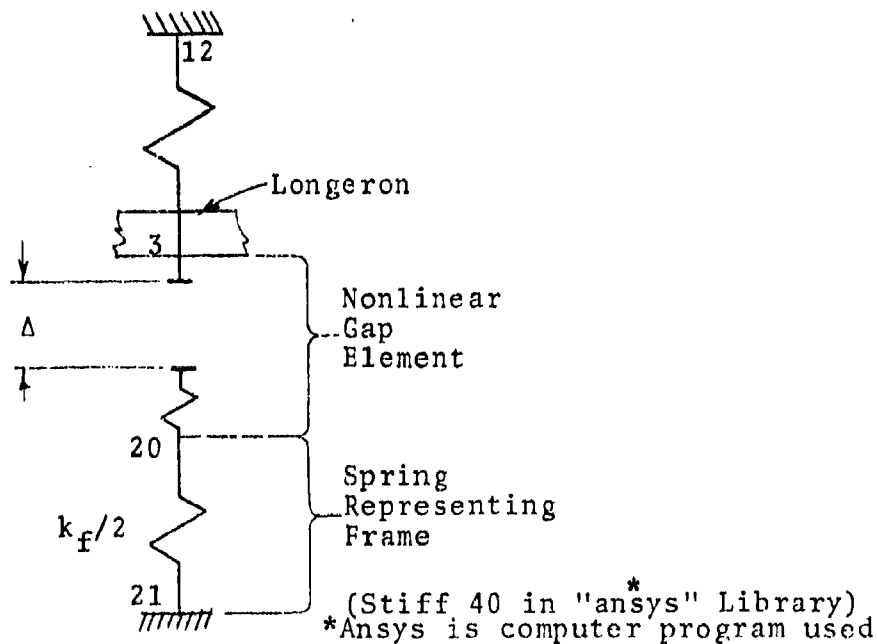


FIGURE 18 Computer Model Of Gap Between Skin and Frames

The gap element consists of a gap of magnitude Δ and a rigid spring, 10×10^6 lb/in is used here. When the interaction force P tries to pull points 3 and 20 together it will have no resistance from the rigid spring until the gap closes and a very large resistance thereafter sets in.

If P_{\min} is the minimum interaction force closing the gap, any $P > P_{\min}$ may be used as input.

5.2.4 Summary Of Computer Run. Determination of the effects of the lateral load when the axial force is present is a nonlinear problem, which requires an iterative solution. Three iterations were carried out and the printout showed that two were sufficient in this particular case.



The interaction force is:

$$P = 2 \times 15,124 = 30,248 \text{ lb}$$

The axial force in the frame is:

$$N_f = \frac{zP}{2\pi} = \frac{24 \times 30,248}{2\pi} = 115,540 \text{ lb}$$

Axial stress is:

$$\sigma_f = N_f/A_f = 115,540/17.0 = 6,796 \text{ psi, (not critical)}$$

The effects of lateral load, i.e., bending moments and stress are shown next.

TABLE 5 Longeron Deflection

Node	-y (in)	σ_t (psi)	$10^3 M$ lb/in)	σ_{oc} (psi)	σ_{ic} (psi)
1	2.394	9,420.1	133.29	2,631.6	12,814.3
2	2.378	9,420.1	164.87	1,023.1	13,618.6
3	2.325	9,407.6	273.79	-4,540.3	16,379.6
4	2.198	9,404.0	86.951	4,975.6	16,376.
5	2.054	9,395.0	-34.177	11,136.	8,524.7
6	1.920	9,387.9	-106.19	14,796.	6,683.7
7	1.811	9,383.6	-143.37	16,685.	5,732.6
8	1.737	9,381.2	-157.79	17,417.	5,363.1
9	1.693	9,380.3	-155.50	17,300.	5,420.5

y = lateral deflection

σ_t = tensile stress, 9,426 lb/in², for undeformed form

M = bending moment

σ_{oc} = resultant stress, outer chord

σ_{ic} = resultant stress, inner chord

The largest tensile stress is 17,417 psi, which is well below the allowable 32,350 psi. No reinforcement is required.

The largest compression, 4,540 psi, is insignificant.

5.3 HULL GEOMETRY, MC 200. The main portion of the hull, which extends between frames No. 5 and No. 26 is described with the set of parameters shown in tables 6 and 7.

Station = distance from the tip of the bow, in feet.

x = station in inches.

R_T = outer radius of hull.

L = length of frame bay.

t = skin thickness.

R_1, R_2 = radius on the left and on the right side of the frame bay. (Bow on left.)

l_1, l_2 = half of the distance between corner nodes of frame, on the left and right ends of bay

A = cross section area of the metal at the left end of a frame bay.

The dimensions of typical longeron sections and the change of depth along the length is shown in Figures 19 and 20.

TABLE 6 Hull Parameters I

Sta. (ft)	x (in)	R (in)	N _f (lb)	M _f (10 ⁶ in/lb)	h (in)	A _{f2} (in ²)	k _f (lb/in)	Frame No.
121.87	1,462	956	116,632	9.068	100.0	10.80	30,759	5
158.38	1,901	1,044	101,894	0.		3.69	9,630	6
192.24	2,307	1,115	108,824	0.		3.94	9,630	7
229.50	2,754	1,173	143,106	11.126	123.0	11.76	27,297	8
265.85	3,190	1,200	117,120	0.		4.24	9,630	9
298.50	3,582	1,221	119,170	0.		4.32	9,630	10
334.50	4,014	1,224	149,328	11.610	128.0	11.98	26,649	11
370.70	4,448	1,221	119,170	0.		4.32	9,630	12
404.06	4,849	1,216	118,682	0.		4.30	9,630	13
438.81	5,266	1,208	147,376	11.458	126.4	11.91	26,844	14
475.16	5,702	1,187	115,851	0.		4.20	9,630	15
508.26	6,099	1,168	113,997	0.		4.13	9,630	16
543.16	6,518	1,146	139,812	10.870	119.9	11.64	27,655	17
578.96	6,948	1,110	108,336	0.		3.93	9,630	18
611.08	7,333	1,080	105,408	0.		3.82	9,630	19

TABLE 6 Continued.

Sta. (ft)	x (in)	R (in)	N _f (lb)	M _f (10 ⁶ in/lb)	h (in)	A _{f2} (in ²)	k _f (lb/in)	Frame No.
646.46	7,758	1,035	126,270	9.817	108.3	11.15	29,332	20
683.21	8,199	978	95,453	0.		3.46	9,630	21
715.09	8,581	926	90,378	0.		3.27	9,630	22
751.64	9,020	858	104,676	8.138	89.7	10.36	32,875	23
787.76	9,453	765	74,664	0.		2.71	9,630	24
820.76	9,849	672	65,587	0.		2.38	9,630	25
853.08	10,237	562	68,564	5.331	58.8	9.05	43,844	26

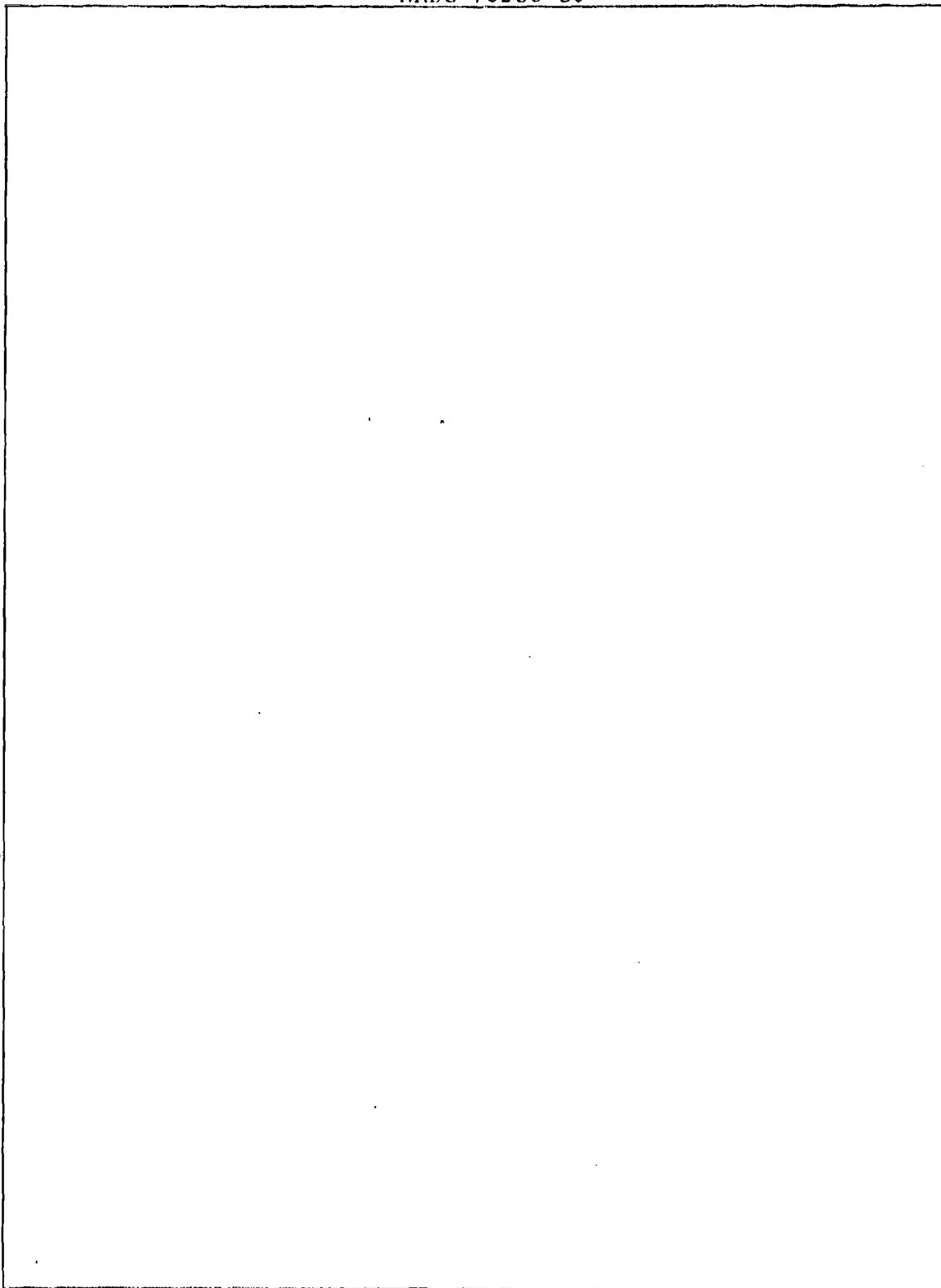


TABLE 7 Hull Parameters II

Frame Bay	L (in)	t (in)	R ₁ (in)	R ₂ (in)	z ₁ (in)	z ₂ (in)	b ₁ (in)	k _{f1} (lb/in)
5-6	439	.038	956	1,044	40.38	7.4	29.85	30,759
6-7	406	.040	1,044	1,115	7.4	7.4	31.37	9,630
7-8	447	.042	1,115	1,173	7.4	49.55	34.78	9,630
8-9	436	.045	1,173	1,200	49.55	7.4	28.08	27,297
9-10	392	.045	1,200	1,221	7.4	7.4	30.20	9,630
10-11	432	.045	1,221	1,224	7.4	51.70	33.53	9,630
11-12	434	.045	1,224	1,221	51.70	7.4	27.55	26,649
12-13	401	.045	1,221	1,216	7.4	7.4	30.95	9,630
13-14	417	.045	1,216	1,208	7.4	51.02	32.28	9,630
14-15	436	.045	1,208	1,187	51.02	7.4	27.83	26,844
15-16	397	.042	1,187	1,168	7.4	7.4	30.62	9,630
16-17	419	.042	1,168	1,146	7.4	48.41	32.45	9,630
17-18	430	.042	1,146	1,110	48.41	7.4	27.76	27,655
18-19	385	.040	1,110	1,080	7.4	7.4	29.62	9,630
19-20	425	.040	1,080	1,035	7.4	43.72	32.95	9,630
20-21	441	.038	1,035	978	43.72	7.4	29.46	29,332
21-22	382	.036	978	926	7.4	7.4	29.37	9,630
22-23	439	.034	926	858	7.4	36.24	34.12	9,630
23-24	433	.032	858	765	36.24	7.4	30.04	32,875
24-25	396	.028	768	672	7.4	7.4	30.53	9,630
25-26	388	.024	672	562	7.4	23.74	29.87	9,630



TABLE 7 Continued.

k_{f2} (lb/in)	b_2 (in)	N (10^6 lb)	A (in ²)	N_1 (lb)	k_{o1} (lb/in)	k_{o2} (lb/in)
9,630	34.12	2.802	268.2	17,370	108.2	99.1
9,630	31.37	3.342	322.2	25,870	104.3	97.7
27,297	28.99	3.812	374.0	33,890	102.6	97.5
9,630	33.87	4.219	411.5	34,090	104.5	102.1
9,630	30.20	4.415	419.1	35,030	102.1	100.3
26,649	27.38	4.571	425.0	35,760	100.3	100.1
9,630	33.70	4.594	425.9	35,870	100.1	100.3
9,630	30.95	4.571	425.0	35,760	100.3	100.8
26,844	26.25	4.534	423.6	35,590	100.8	101.4
9,630	33.87	4.474	421.4	35,300	101.4	103.2
9,630	30.62	4.320	393.0	36,550	96.3	97.9
27,655	26.85	4.183	388.0	35,850	97.9	99.8
9,630	33.37	4.027	382.2	35,030	99.8	103.0
9,630	29.62	3.778	358.8	35,010	98.1	100.8
29,332	28.13	3.576	351.2	33,860	100.8	105.2
9,630	34.28	3.285	326.9	33,410	100.0	105.8
9,630	29.37	2.933	301.0	32,400	100.2	105.8
32,875	30.54	2.629	277.6	31,490	100.0	107.9
9,630	33.62	2.257	252.3	29,740	101.5	113.9
9,630	30.53	1.794	194.4	23,020	99.7	113.4
43,844	28.37	1.385	141.2	16,310	97.2	116.3

Three typical longeron sizes appear in the analysis:

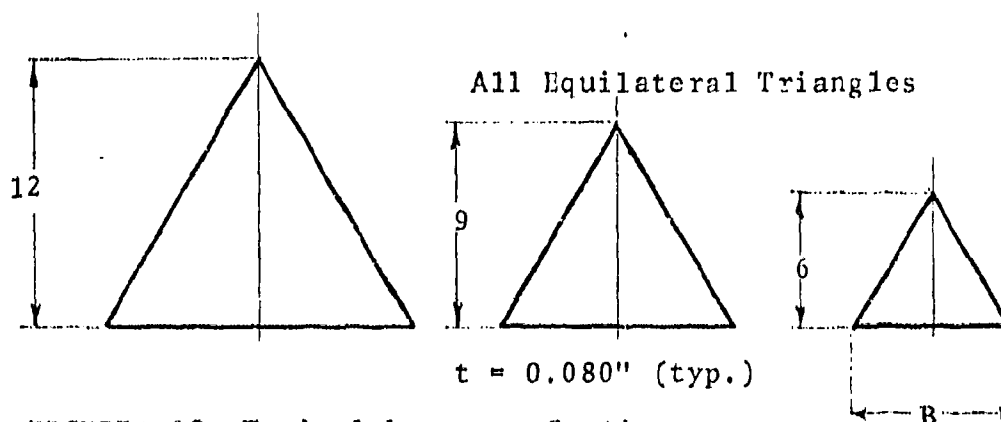


FIGURE 19 Typical Longeron Section

H (in)	A (in ²)	I (in ⁴)	B (in)
12	3.325	53.204	13.856
9	2.494	22.445	10.392
6	1.663	6.650	6.928

$$A = 3Bt; I = \frac{1}{4}B^3t; B = \frac{2}{\sqrt{3}} H$$

The longeron is of constant section (12 in.) between frames 7 and 24:

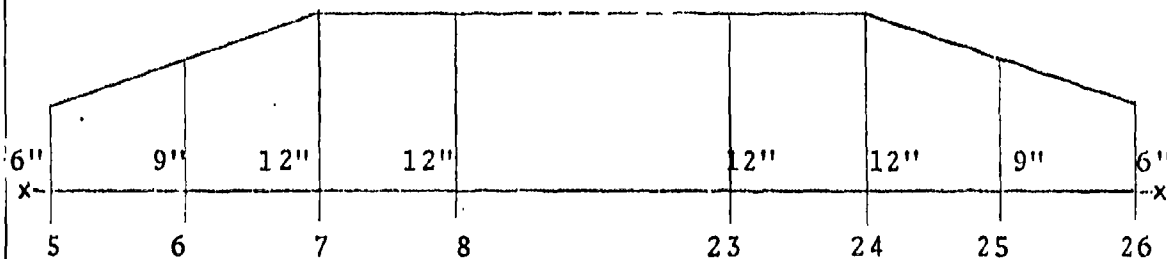


FIGURE 20 Longeron Height Variation

The dimensions of elements shown here are obtained as a result of preliminary calculations based on pressure $p = 0.976$ psi and the allowable, cross area stress in tension of 27,600 psi. In particular, the following simple equations were used to determine the amount of material used.

$$t_{\min} = R/28,279 \quad \text{skin thickness from hoop tension}$$

$$N_f = 122 R, \quad \text{axial force in main frame}$$

$$M_f = 9485 R, \quad \text{bending moment in the main frame}$$

$$h = 0.1046 R, \quad \text{effective depth of main frame}$$

$$\sigma = 27,600 = \frac{N_f}{A_f} + \frac{2M_f}{A_f h}, \quad \text{to determine the area of main frame}$$

$$A_f = R/282.75, \quad \text{section area of secondary frame}$$

$$R = \text{inches}$$

The values of N_f , M_f , h and A_f are shown in Table 6.

5.4 FINITE-ELEMENT MODEL OF LONGERON, PRESSURE CONDITION, MC 200. The model of longeron extending over major portion of hull is essentially a repetition of the model in Fig. 17 over 21 frame bays, or 42 times. Fig. 21 shows a segment of a longeron extending over a bay which has a main frame on the left and a secondary frame on the right. Fig. 22 shows the numbering over the first four bays - only the node numbers located on the longeron are shown. A main frame is always followed by two secondary frames.

The maximum radial stiffness of skin per unit length k is calculated by Eq.(1) and shown in Table 7 as k_{o1} and k_{o2} (left and right end of bay respectively, when the bow is on the left). It is also used in the determination of constants of the springs representing the skin, but in somewhat different manner than was done in Section 5.2. The constant of a discrete spring located in the immediate vicinity of a frame is

$$k'_i = k_{o1i}$$

While for the springs which are farther away than one node space from the frame corner:

$$k'_i = \frac{1}{2}k_{o1i}$$

Table 7 shows the constants of all pertinent springs.

Regardless of the frame type the radial stiffness is determined by

$$k_f = \frac{P}{\Delta_f} = \frac{2\pi EA_f}{zR}$$

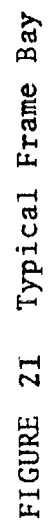
$$k_f = \frac{2\pi \times 10.4}{24} 10^6 \frac{A_f}{R} = 2.7227 \times 10^6 A_f/R$$

The secondary frames are sized according to $A = R/282.75$, therefore

$$k_f = 9,630 \text{ lb/in}$$

The calculated values of k_f are shown in Table 6. When denoted by k_{f1} and k_{f2} in Table 7, these values represent the frame rigidities on the left and right of each bay, respectively.

Quantities b_1 and b_2 appearing in Table 7 are the node spacing according to Fig. 21



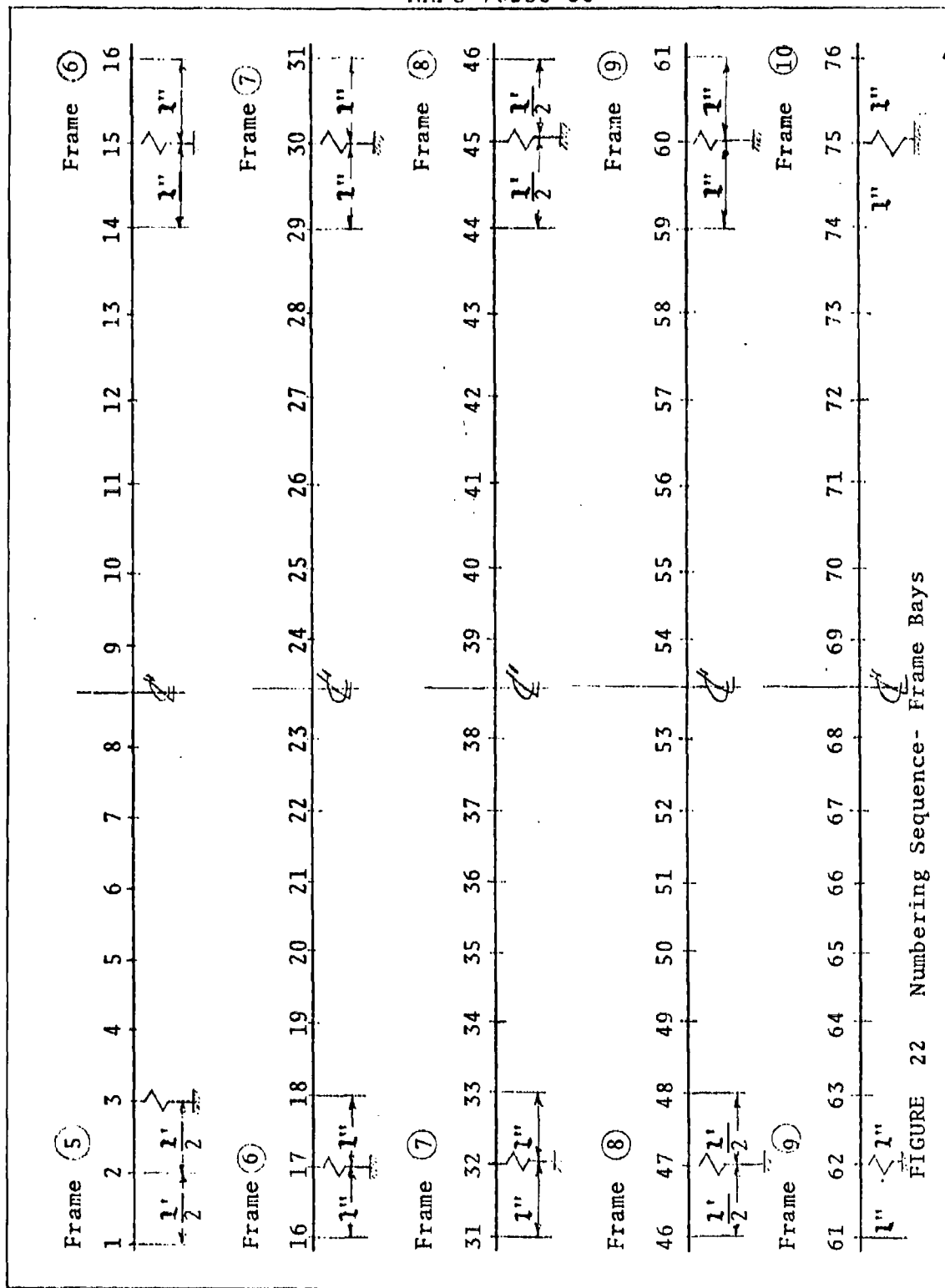


FIGURE 22 Numbering Sequence- Frame Bays

TABLE 8 Spring Constants

Node	l_i (in)	Frame No.	k/k_0	k' (lb/in)
1	10.10	5		1,092
2	20.19			2,185
M3	25.02			2,707
4	29.85			3,230
5	29.85		.5	1,615
6	29.85		.5	1,615
7	29.85		.5	1,615
8	46.91	5	.5	2,538
9	49.04	6	.5	2,430
10	34.12		.5	1,691
11	34.12		.5	1,691
12	34.12		.5	1,691
13	34.12		.5	1,691
14	20.76			2,057
S15	7.40			733
16	7.4			733
S17	7.4			772
18	19.39			2,022
19	31.37		.5	1,636
20	31.37		.5	1,636
21	31.37		.5	1,636
22	31.37		.5	1,636
23	47.05	6	.5	2,454

TABLE 8 continued-

Node	l_i (in)	Frame No.	k/k_o	k' (lb/in)
24	47.05	7	.5	2,298
25	31.37		.5	1,532
26	31.37		.5	1,532
27	31.37		.5	1,532
28	31.37		.5	1,532
29	19.38			1,893
S30	7.4			723
31	7.4			723
S32	7.4			759
33	21.1			2,165
34	34.8		.5	1,785
35	34.8		.5	1,785
36	34.8		.5	1,785
37	34.8		.5	1,785
38	49.3	7	.5	2,529
39	46.4	8	.5	2,262
40	29.0		.5	1,414
41	29.		.5	1,414
42	29.		.5	1,414
43	29.			2,828
M44	26.9			2,623
45	24.8			2,418
46	24.8			2,418

TABLE 8 Continued -

Node	l_i (in)	Frame No.	k/k_o	k' (lb/in)
47	24.8			2,592
M48	26.4			2,759
49	28.1			2,936
50	28.1		.5	1,468
51	28.1		.5	1,468
52	28.1		.5	1,468
53	45.0	8	.5	2,351
54	47.9	9	.5	2,445
55	33.9		.5	1,731
56	33.9		.5	1,731
57	33.9		.5	1,731
58	33.9		.5	1,731
59	20.7			2,113
S60	7.4			756
61	7.4			756
S62	7.4			756
63	18.8			1,919
64	30.2		.5	1,542
65	30.2		.5	1,542
66	30.2		.5	1,542
67	30.2		.5	1,542
68	45.3	9	.5	2,313
69	45.3	10	.5	2,272

TABLE 8 continued

Node	l_i (in)	Frame No.	k/k_0	k' (lb/in)
70	30.2		.5	1,515
71	30.2		.5	1,515
72	30.2		.5	1,515
73	30.2		.5	1,515
74	18.8			1,886
S75	7.4			742
76	7.4			742
S77	7.4			742
78	20.5			2,056
79	33.5		.5	1,680
80	33.5		.5	1,680
81	33.5		.5	1,680
82	33.5		.5	1,680
83	47.2	10	.5	2,367
84	44.1	11	.5	2,207
85	27.4		.5	1,371
86	27.4		.5	1,371
87	27.4		.5	1,371
88	27.4			2,743
M89	26.6			2,663
90	25.8			2,583
91	25.8			2,583

TABLE 8 Continued-

Node	l_i (in)	Frame No.	k/k_o	k' (lb/in)
92	25.8			2,583
M93	26.7			2,673
94	27.6			2,763
95	27.6		.5	1,381
96	27.6		.5	1,381
97	27.6		.5	1,381
98	44.4	11	.5	2,222
99	47.5	12	.5	2,382
100	33.7		.5	1,690
101	33.7		.5	1,690
102	33.7		.5	1,690
103	33.7		.5	1,690
104	20.6			2,066
S105	7.4			742
106	7.4			742
S107	7.4			742
108	19.2			1,926
109	31.0		.5	1,555
110	31.0		.5	1,555
111	31.0		.5	1,555
112	31.0		.5	1,555
113	46.4	12	.5	2,327
114	46.4	13	.5	2,339

TABLE 8 continued

Node	l_i (in)	Frame No.	k/k_o	k' (lb/in)
115	31.0		.5	1,562
116	31.0		.5	1,562
117	31.0		.5	1,562
118	31.0		.5	1,562
119	19.2			1,935
S120	7.4			746
121	7.4			746
S122	7.4			746
123	19.8			1,996
124	32.3		.5	1,628
125	32.3		.5	1,628
126	32.3		.5	1,628
127	32.3		.5	1,628
128	45.4	13	.5	2,288
129	42.4	14	.5	2,150
130	26.3		.5	1,333
131	26.3		.5	1,333
132	26.3		.5	1,333
133	26.3			2,667
M134	25.9			2,626
135	25.5			2,586
136	25.5			2,586
137	25.5			2,586

TABLE 8 Continued-

Node	l_i (in)	Frame No.	k/k_o	k' (lb/in)
M138	26.7			2,707
139	27.8			2,819
140	27.8		.5	1,409
141	27.8		.5	1,409
142	27.8		.5	1,409
143	44.8	14	.5	2,271
144	47.8	15	.5	2,466
145	33.9		.5	1,749
146	33.9		.5	1,749
147	33.9		.5	1,749
148	33.9		.5	1,749
149	20.6			2,126
S150	7.4			764
151	7.4			764
S152	7.4			713
153	19.0			1,830
154	30.6		.5	1,473
155	30.6		.5	1,473
156	30.6		.5	1,473
157	30.6		.5	1,473
158	45.9	15	.5	2,210
159	45.9	16	.5	2,247
160	30.6		.5	1,498

TABLE 8 continued-

Node	l_i (in)	Frame No.	k/k_0	k' (lb/in)
161	30.6		.5	1,498
162	30.6		.5	1,498
163	30.6		.5	1,498
164	19.0			1,860
S165	7.4			724
166	7.4			724
S167	7.4			724
168	19.9			1,948
169	32.5		.5	1,591
170	32.5		.5	1,591
171	32.5		.5	1,591
172	32.5		.5	1,591
173	45.9	16	.5	2,247
174	43.1	17	.5	2,151
175	26.9		.5	1,342
176	26.9		.5	1,342
177	26.9		.5	1,342
178	26.9			2,685
M179	25.5			2,545
180	24.2			2,415
181	24.2			2,415
182	24.2			2,415
M183	26.0			2,595

TABLE 8 Continued-

Node	l_i (in)	Frame No.	k/k_0	k' (lb/in)
184	27.8			2,774
185	27.8		.5	1,387
186	27.8		.5	1,387
187	27.8		.5	1,387
188	44.4	17	.5	2,216
189	47.3	18	.5	2,436
190	33.4		.5	1,720
191	33.4		.5	1,720
192	33.4		.5	1,720
193	33.4		.5	1,720
194	20.4			2,101
S195	7.4			762
196	7.4			762
S197	7.4			726
198	18.5			1,815
199	29.6		.5	1,452
200	29.6		.5	1,452
201	29.6		.5	1,452
202	29.6		.5	1,452
203	44.4	18	.5	2,178
204	44.4	19	.5	2,238
205	29.6		.5	1,492
206	29.6		.5	1,492

TABLE 8 continued-

Node	l_i (in)	Frame No.	k/k_0	k' (lb/in)
207	29.6		.5	1,492
208	29.6		.5	1,492
209	18.5			1,865
S210	7.4			746
211	7.4			746
S212	7.4			746
213	20.2			2,036
214	32.9		.5	1,658
215	32.9		.5	1,658
216	32.9		.5	1,658
217	32.9		.5	1,658
218	47.0	19	.5	2,369
219	44.6	20	.5	2,346
220	28.1		.5	1,478
221	28.1		.5	1,478
222	28.1		.5	1,478
223	28.1			2,956
M224	25.0			2,630
225	21.9			2,304
226	21.9			2,304
227	21.9			2,190
M228	25.7			2,570
229	29.5			2,950

TABLE 8 Continued-

Node	l_i (in)	Frame No.	k/k_0	k' (lb/in)
230	29.5		.5	1,475
231	29.5		.5	1,475
232	29.5		.5	1,475
233	46.6	20	.5	2,330
234	49.0	21	.5	2,592
235	34.3		.5	1,814
236	34.3		.5	1,814
237	34.3		.5	1,814
238	34.3		.5	1,814
239	20.8			2,201
S240	7.4			783
241	7.4			783
S242	7.4			741
243	18.4			1,844
244	29.4		.5	1,473
245	29.4		.5	1,473
246	29.4		.5	1,473
247	29.4		.5	1,473
248	44.1	21	.5	2,209
249	44.1	22	.5	2,333
250	29.4		.5	1,555
251	29.4		.5	1,555
252	29.4		.5	1,555

TABLE 8 continued-

Node	l_j (in)	Frame No.	k/k_0	k_i (lb/in)
253	29.4		.5	1,555
254	18.4			1,947
S255	7.4			783
256	7.4			783
S257	7.4			740
258	20.8			2,080
259	34.1		.5	1,705
260	34.1		.5	1,705
261	34.1		.5	1,705
262	34.1		.5	1,705
263	49.4	22	.5	2,470
264	47.6	23	.5	2,568
265	30.5		.5	1,645
266	30.5		.5	1,645
267	30.5		.5	1,645
268	30.5			3,291
M269	24.3			2,622
270	18.1			1,953
271	18.1			1,953
272	18.1			1,837
M273	24.1			2,446
274	30.0			3,045
275	30.0		.5	1,523

TABLE 8 Continued-

Node	l_i (in)	Frame No.	k/k_0	k' (lb/in)
276	30.0		.5	1,523
277	30.0		.5	1,523
278	46.9	23	.5	2,380
279	48.6	24	.5	2,768
280	33.6		.5	1,914
281	33.6		.5	1,914
282	33.6		.5	1,914
283	33.6		.5	1,914
284	20.5			2,335
S285	7.4			843
286	7.4			843
S287	7.4			738
288	19.0			1,894
289	30.5		.5	1,520
290	30.5		.5	1,520
291	30.5		.5	1,520
292	30.5		.5	1,520
293	45.8	24	.5	2,283
294	45.8	25	.5	2,597
295	30.5		.5	1,729
296	30.5		.5	1,729
297	30.5		.5	1,729
298	30.5		.5	1,729

TABLE 8 continued-

Node	l_i (in)	Frame No.	k/k_o	k' (lb/in)
299	19.0			2,155
S300	7.4			839
301	7.4			839
S302	7.4			719
303	18.6			1,808
304	29.9		.5	1,453
305	29.9		.5	1,453
306	29.9		.5	1,453
307	29.9		.5	1,453
308	44.0	25	.5	2,138
309	43.3	26	.5	2,518
310	28.4		.5	1,651
311	28.4		.5	1,651
312	28.4		.5	1,651
313	28.4			3,303
M314	20.1			2,338
315	11.9			1,384
316	6.0	26		692

Letter "M" preceeding a node number indicates a corner point of a main frame. "S" is for a secondary frame.

5.5 Force and Displacement Input, Pressure Condition, MC 200. The approach is the same as in Section 5.2. The axial forces are calculated by hand, while the lateral interaction forces are generated by "ansys" program.*

Lateral Action. Table 9 shows the initial discontinuity Δr between the skin and the frames. This discontinuity is removed by the interaction forces in the course of program execution.

$$\Delta r = \frac{pR^2}{Et_{av}} = \frac{0.976 R^2}{10.4 \times 10^6 t_{av}} = \frac{(R/1000)^2}{10.66 t_{av}}$$

The average thickness is used whenever there is a jump of thickness at a frame station.

The initial value of $P = 10,000$ lb is used as an interaction force at every secondary frame and $P = 20,000$ lb at every main frame. The nonlinear gap elements described in Section 5.2 prevent the interaction forces from exceeding their true values.

TABLE 9 Gap Discontinuity.

Frame No.	t_{av} (in)	Δr (in)	Center Node No.	ΔN_j (lb)
5	.038	2.256	1	17,370
6	.039	2.622	16	8,500
7	.041	2.845	31	8,020
8	.0435	2.967	46	200
9	.045	3.002	61	940
10	.045	3.108	76	730
11	.045	3.123	91	110
12	.045	3.108	106	-110
13	.045	3.082	121	-170
14	.045	3.042	136	-290
15	.0435	2.937	151	1,250

* "ANSYS Program" - General Purpose Engineering Computer Program.

TABLE 9 continued-

Frame No.	t_{av} (in)	Δr (in)	Center Node No.	ΔN_1 (lb)
16	.042	3.047	166	-700
17	.042	2.933	181	-820
18	.041	2.819	196	-20
19	.040	2.735	211	-1,150
20	.039	2.577	226	-450
21	.037	2.425	241	-1,010
22	.035	2.298	256	-910
23	.033	2.093	271	-1,750
24	.030	1.830	286	-6,720
25	.026	1.629	301	-6,710
26	.024	1.235	316	-11,410

Axial Forces.

In the hull section of radius R:

$$N = \pi R^2 p = \pi R^2 \times 0.976 = 3.0662 R^2$$

Area total:

$$A = 2\pi R t + 24 A_2$$

For typical 12 in. longeron $A_2 = 3.325 \text{ in}^2$:

$$A = 2\pi R t + 79.8$$

Force in longeron:

$$N_2 = \frac{A_2}{A} N$$

For 12 in. longeron:

$$N_2 = 3.325 N/A$$

The quantities A, N, and N_1 are shown in Table 7

The increments of axial longeron load are shown in Table 9
These values are applied to the model at the nodal points.

5.6 Results Of Computer Analysis, Pressure Condition, MC 200. Table 10 shows the results of computer printout after the second (final) iteration, at the stations, where the skin and the frame come in contact. The notation is the same as in Table 5.

Near the ends of the longeron segment under consideration the input values were averages, rather than the actual longeron properties as implied by Figure 20. The stress levels on the bow side (beginning of Table 10) are high and therefore, a closer examination must be made.

To determine the location of nodal points of interest, Table 6 together with Figure 22 must be used.

Node	Frame	x (in)	h (in)	A	I	C_o
1	5	1462	6.0	1.663	6.65	4.0
3	5	1502.4	6.28	1.740	7.626	4.187
15	6	1893.6	8.95	2.480	22.075	5.967
16	6	1901	9.0	2.494	22.445	6.0

The computer analysis assumes $h = 6.0$ at node 3 and $h = 9.0$ at node 15.

TABLE 10 Longerons Stress

Node	-y (in)	σ_t (psi)	M (10^3 lb/in)	σ_{oc} (psi)	σ_{ic} (psi)
3	1.434	11,186.	87.632	-42,334	37,542
15	1.234	6,780.6	116.93	-24,561	22,410
17	1.230	10,174.	115.81	-20,860	25,654
30	0.931	7,473.3	124.49	-11,316	16,833
32	0.953	9,806.9	164.48	-14,928	22,173
44	1.670	9,749.1	217.41	-23,031	26,095
48	1.649	9,648.	215.22	-22,739	25,829

TABLE 10 continued-

Node	-y (in)	σ_t (psi)	$10^3 M$ lb/in	σ_{oc} (psi)	σ_{ic} (psi)
60	1.321	9,517.6	195.11	-19,846	24,186
62	1.322	9,783.3	195.82	-19,677	24,505
75	1.386	9,704.7	201.82	-20,688	24,878
77	1.386	9,908.1	201.04	-20,336	25,023
89	1.731	9,867.5	224.90	-24,015	<u>26,776</u>
93	1.732	9,812.7	224.56	23,984	26,696
105	1.394	9,746.3	199.53	-20,279	24,747
107	1.395	9,706.4	200.15	-20,407	24,754
120	1.384	9,680.7	198.79	-20,231	24,626
122	1.383	9,626.8	198.48	-20,237	24,549
134	1.696	9,644.	218.44	-23,254	26,067
138	1.695	7,924.6	219.39	<u>-25,116</u>	24,419
150	1.324	7,911.8	188.36	-20,435	22,073
152	1.329	8,286.3	190.63	-20,401	22,618
165	1.389	8,308.9	197.69	-21,436	23,171
167	1.387	8,105.0	197.35	-21,593	22,942
179	1.683	8,182.5	211.69	-23,702	24,098
183	1.682	8,005.9	211.55	-23,886	23,911
195	1.260	8,020.7	182.51	-19,445	21,743
197	1.264	8,024.3	184.38	-19,729	21,887
210	1.221	8,088.0	178.95	-18,843	21,542
212	1.220	7,754.5	178.48	-19,114	21,173
224	1.509	7,916.4	190.36	-20,707	22,228

TABLE 10 Continued-

Node	-y (in)	σ_t (psi)	(10^3 lb/in)	σ_{oc} (psi)	σ_{ic} (psi)
228	1.524	7,895.4	191.81	-21,081	22,316
240	1.055	7,906.2	158.42	-15,943	19,817
242	1.058	7,617.7	160.38	-16,536	19,675
255	0.993	7,715.0	151.69	-15,129	19,119
257	0.996	7,447.0	152.24	-15,482	18,893
269	1.298	7,777.1	165.14	-17,251	20,193
273	1.314	7,365.8	167.52	-18,077	19,961
285	0.753	7,296.5	121.81	-11,074	16,455
287	0.760	5,262.3	124.86	-13,555	14,650
300	0.728	7,332.1	74.347	-12,748	17,269
302	0.738	4,532.7	77.011	-16,179	14,826
314	0.917	11,629.	47.256	-21,088	25,841

Take axial forces and bending moments from the printout.

At Node 3:

$$N = 18,603 \text{ lb}$$

$$M = 87,632 \text{ lb/in}$$

$$\sigma_{ic} = 18,603/1.74 + 87,632 \times 2.093/7.626 = 34,742 \text{ psi}$$

$$\sigma_{oc} = 18,603/1.74 - 87,632 \times 4.187/7.626 = -37,422 \text{ psi}$$

At Node 15:

$$N = 16,911 \text{ lb}$$

$$M = 116,930 \text{ lb/in}$$

$$\sigma_{ic} = 16,911/2.48 + 116,930 \times 2.984/22.075 = 22,625 \text{ psi}$$

$$\sigma_{oc} = 16,911/2.48 - 116,930 \times 5.967/22.075 = -24,788 \text{ psi}$$

It may be seen that while at Node 15 the actual and the print-out stress are nearly the same, the magnitude of stress is over estimated by the program at Node 3.

The allowable stress is:

$$F_t = 32,850 \text{ psi}$$

$$F_c = 30,500 \text{ psi}$$

(The outer chord assumed to buckle at $F_{cy} = 61 \text{ ksi}$)

At Node 3:

$$M.S. = \frac{32,850}{34,740} - 1.0 = \frac{-0.054}{(\text{tension})}$$

$$M.S. = \frac{30,500}{37,420} - 1.0 = \frac{-0.185}{(\text{Compression})}$$

The remedies for this location are discussed in Section 5.8 .

Other critical locations:

At Node 89:

$$\sigma_{oc} = 26,776 \text{ psi}$$

$$M.S. = \frac{32,850}{26,776} - 1.0 = \frac{0.23}{(\text{tension})}$$

At Node 138:

$$\sigma_{ic} = -25,116 \text{ psi}$$

$$M.S. = \frac{30,500}{25,116} - 1.0 = \frac{0.21}{(\text{compression})}$$

Table 11 shows the results for the frames. The maximum tension is reached at Frame No. 7: $\sigma_t = 17,940 \text{ psi}$. This hoop tension is not critical by itself, but it is combined with other components.

Note that the hoop stress is smaller in the main than in the secondary frames. This is due to a larger section area of the former.

TABLE 11 Frame Stress

Node	Frame No.	P/2 (lb)	N _f (lb)	σ_f (psi)
903	5	12,843	98,121	9,085
915	6	6,768	51,708	14,013
917	6	6,789	51,868	14,056
930	7	9,252	70,685	<u>17,940</u>
932	7	9,146	69,875	17,735
944	8	17,785	135,877	11,554
948	8	18,135	138,551	11,782
960	9	8,150	62,266	14,685
962	9	8,145	62,228	14,676
975	10	8,339	63,710	14,748
977	10	8,342	63,733	14,753
989	11	18,593	142,051	11,857
993	11	18,581	141,959	11,850
1005	12	8,296	63,381	14,672
1007	12	8,290	63,336	14,661
1020	13	8,219	62,793	14,603
1022	13	8,225	62,839	14,613
1034	14	18,103	138,307	11,613
1038	14	18,105	138,322	11,614
1050	15	7,808	59,653	14,203
1052	15	7,783	59,462	14,158
1065	16	8,024	61,303	14,843
1067	16	8,032	61,364	14,858

TABLE 11 continued-

Node	Frame No.	P/2 (lb)	N _f (lb)	σ_f (psi)
1079	17	17,333	132,424	11,377
1083	17	17,357	132,607	11,392
1095	18	7,555	57,720	14,687
1097	18	7,537	57,583	14,652
1110	19	7,344	56,108	14,688
1112	19	7,348	56,138	14,696
1124	20	15,755	120,368	10,795
1128	20	15,548	118,787	10,654
1140	21	6,666	50,928	14,719
1142	21	6,653	50,829	14,690
1155	22	6,362	48,606	14,864
1157	22	6,350	48,514	14,836
1169	23	13,239	101,146	9,763
1173	23	12,986	99,213	9,577
1185	24	5,277	40,316	14,877
1187	24	5,245	40,072	14,787
1200	25	4,440	33,922	14,253
1202	25	4,397	33,593	14,115
1214	26	7,286	55,665	6,151

5.7 Flight Condition With Deflated Cell, MC 200.

The following situation is assumed after the loss of pressure takes place:

1. The ship is flying with 52 knots, forward velocity (87.766 ft/s).
2. It encounters a gust with the vertical velocity of 55 ft/sec (This assumption is on the conservative side. 35 ft/sec is used as more realistic in Sec 5.11)

This results in the bending moment

$$M_{m200} = 465.90 \times 10^6 \text{ inlb}$$

Frame No. 17 is the smallest radius main frame subject to this maximum moment. ($R_T = 1,146 \text{ in}$).

There are 24 longerons, each with $A = 3.325 \text{ in}^2$. When this is uniformly distributed on the circumference of the cross section, an equivalent thickness \bar{t} is obtained:

$$\bar{t} = \frac{z A_1}{2\pi R} = \frac{24 \times 3.325}{2\pi \times 1146}$$

To simplify the calculation, assume that only the longeron material resists the bending moment. (This is conservative, as no credit is taken for the skin in tension) Stress from bending:

$$\sigma_b = \frac{M_{m200}}{\pi R^2 \bar{t}} = \frac{465.90 \times 10^6}{\pi \times 1146^2 \times 0.011083} = 10,102 \text{ psi}$$

The axial force:

$$N_o = A \sigma_b = 3.325 \times 10,102 = 33,589 \text{ lb}$$

The buckling force for a longeron treated as a beam on an elastic foundation is:

$$N_{cr} = 2(kEI)^{1/2}$$

Maximum value of the foundation modulus in Table 7 is 99.8 lb/in² for this location. No more than one-half of this is the effective value:

$$N_{cr} = 2[(99.8/2) \times 10.4 \times 10^6 \times 53.2]^{1/2} = 332,317 \text{ lb}$$

For a simply supported column:

$$N_{cr} = \frac{\pi^2 EI}{l^2}$$

Equivalent free length:

$$l^2 = \frac{\pi^2 EI}{N_{cr}} = \frac{\pi^2 \times 10.4 \times 10^6 \times 53.2}{332,317}$$

$$l = 128.2 \text{ in.}$$

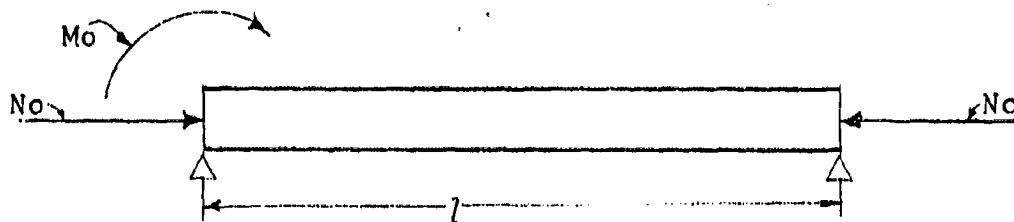


FIGURE 23 Longeron Loading Pattern

Figure 23 shows the loading pattern of a longeron, immediately adjacent to the main frame on its deflated side.

When the hull is fully inflated, the computer analysis shows the bending moment at Frame No. 17 (Node No. 179) is

$$M = 211,690 \text{ inlb}$$

It is estimated that upon deflation this moment will drop to 50% of its initial value. Thus,

$$M_o = 0.5 \times 211,690 = 105,845 \text{ inlb}$$

Resultant compressive stress at the left end:

$$\sigma = \frac{N_o}{A} + \frac{M_o c}{I} = \frac{37,790}{3.325} + \frac{105,845 \times 8}{53.2} = 27,282 \text{ psi}$$

Check if the factor of safety is indeed two, i.e., check on the stress when the loading is doubled.

When the axial force is sufficiently large, the maximum bending moment is not at the support, but at some distance x_1 away from it.

$$x_1 = j \arctan(-\cot U)$$

$$j = (EI/N)^{1/2} = (10.4)(10)^6(53.2)/(2)(33,882)^{1/2} = 90.36$$

$$U = 1/j = 128.2/90.36 = 1.4188$$

Therefore,

$$x_1 = 90.36 \arctan(-\cot 1.4188) = -13.83 \text{ in.}$$

The negative value of x_1 indicates that the maximum moment occurs over the support. (The axial force is too small to give a beam-column effect.)

$$\sigma_{\max} = 2 \times 27,282 = 54,564 \text{ lb/in}^2$$

$$F = F_{cy} = 61,000 \text{ lb/in}^2$$

$$\text{M.S.} = \frac{61,000}{54,564} - 1.0 = 0.12$$

5.8 Local Reinforcements Required, MC 200. The only location where the longeron is shown overstressed, is Node 3. This is the result of an unfortunate combination of structural parameters. The main reason for the overstressing is that the depth of the longeron is too small. The bending stress is inversely proportional to the (depth)² of an idealized constant-thickness section. The necessary minimum depth:

$$h_{\min} = h \left(\frac{\sigma}{F_c} \right)^{1/2} = 6.28 \left(\frac{37,420}{30,500} \right)^{1/2} = 6.96 \text{ in. say } 7 \text{ in.}$$

Of course, an increase in stiffness attracts more load, but that will not be of a great influence here.

The conclusion is that Figure 20 should be suitably modified to show about a 7 in. deep section at Frame No. 5.

5.9 Pressure Condition, MC 100. The analysis will be very similar to what was developed in Sections 5.2 through 5.6 for MC 200.

The hull is uniformly pressurized with $p = 0.6733 \text{ psi}$

Only a segment of the hull between the Frames No. 7 and 10 is analyzed. Figure 24 shows the spacing of the two secondary frames changed slightly to obtain uniform spacing. This has negligible effect on the result, but saves a considerable analysis time.

For the purpose of this calculation the cross-section of a longeron is as in Figure 25. The outer chord is assumed to be of such proportions that it can withstand $\sigma_c = F_{cy}$.

$$A = 3 \times 12.12 \times 0.060 = 2.182 \text{ in.}^2$$

$$I = \frac{1}{4}(12.12)^3 \times 0.060 = 26.71 \text{ in.}^4$$

There are $z = 42$ longerons.

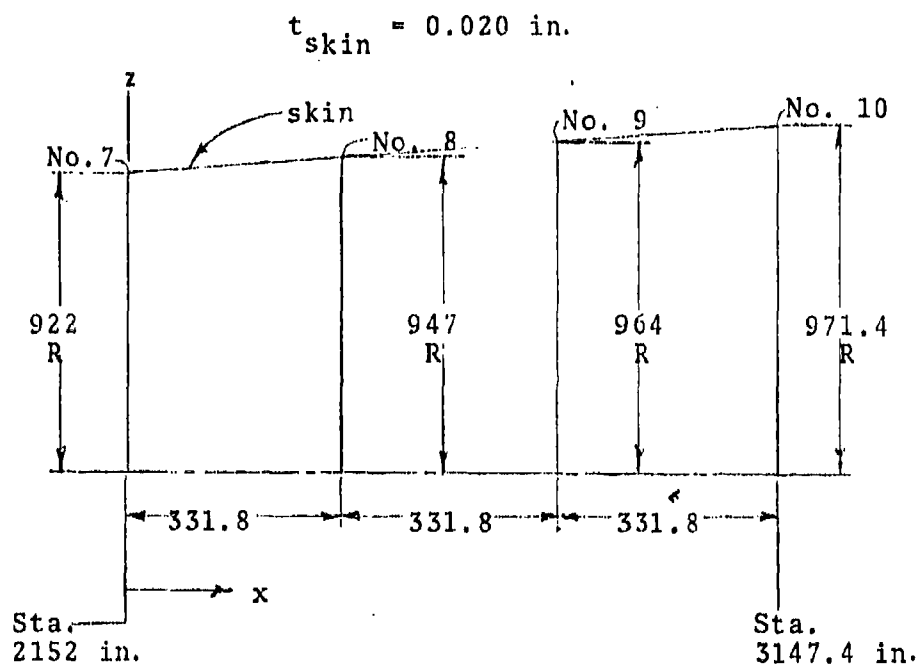


FIGURE 24 Spacing - Secondary Frames

$t = 0.060 \text{ in.}$
(typical)

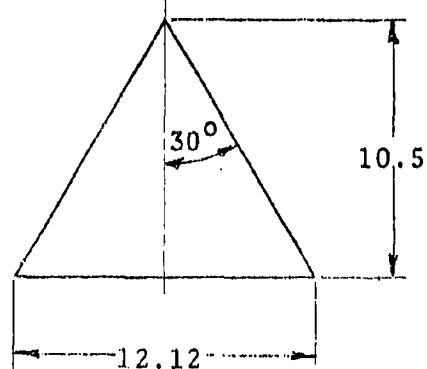


FIGURE 25 Longeron Cross-section

Skin thickness is constant, $t = 0.020$ in.

The effective depth of a main frame is 110 in.

Section area $A_f = 8.2$ in.²

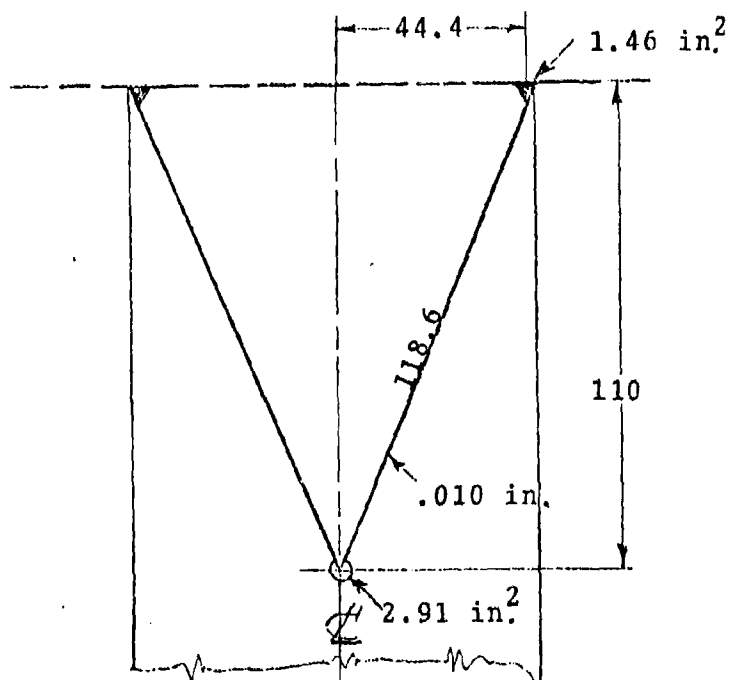


FIGURE 26 Main Frame Cross-section

The effective depth of a secondary frame is 12.8 in. Section area $A_f = 2.9$ in.²

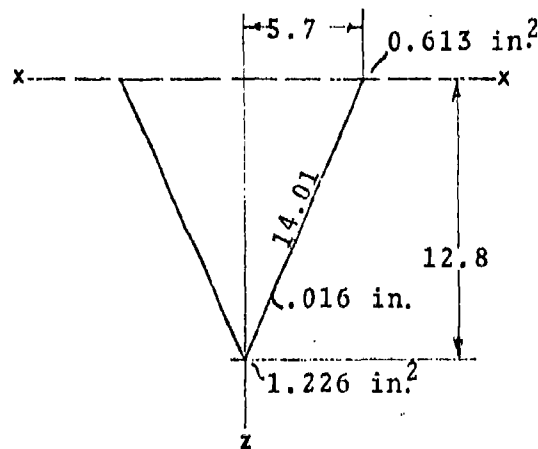


FIGURE 27 Secondary Frame Cross-section

The model of the longeron segment is in Figure 28. The foundation (skin) springs are not shown, but they are placed as was done for the previous model. Numbering of fixed nodes of the foundation springs is consecutive beginning with Node No. 51.

The constants of the skin rings are calculated from Equation:

$$k_o = \frac{2\pi Et}{zR} = \frac{2\pi \times 10.4 \times 10^6 \times 0.020}{42 \times R} = \frac{31.12}{R} \times 1000$$

These constants for various locations are shown in Table 12. Lumping of the continuous foundation into discrete springs is performed in the same manner as in Section 5.4.

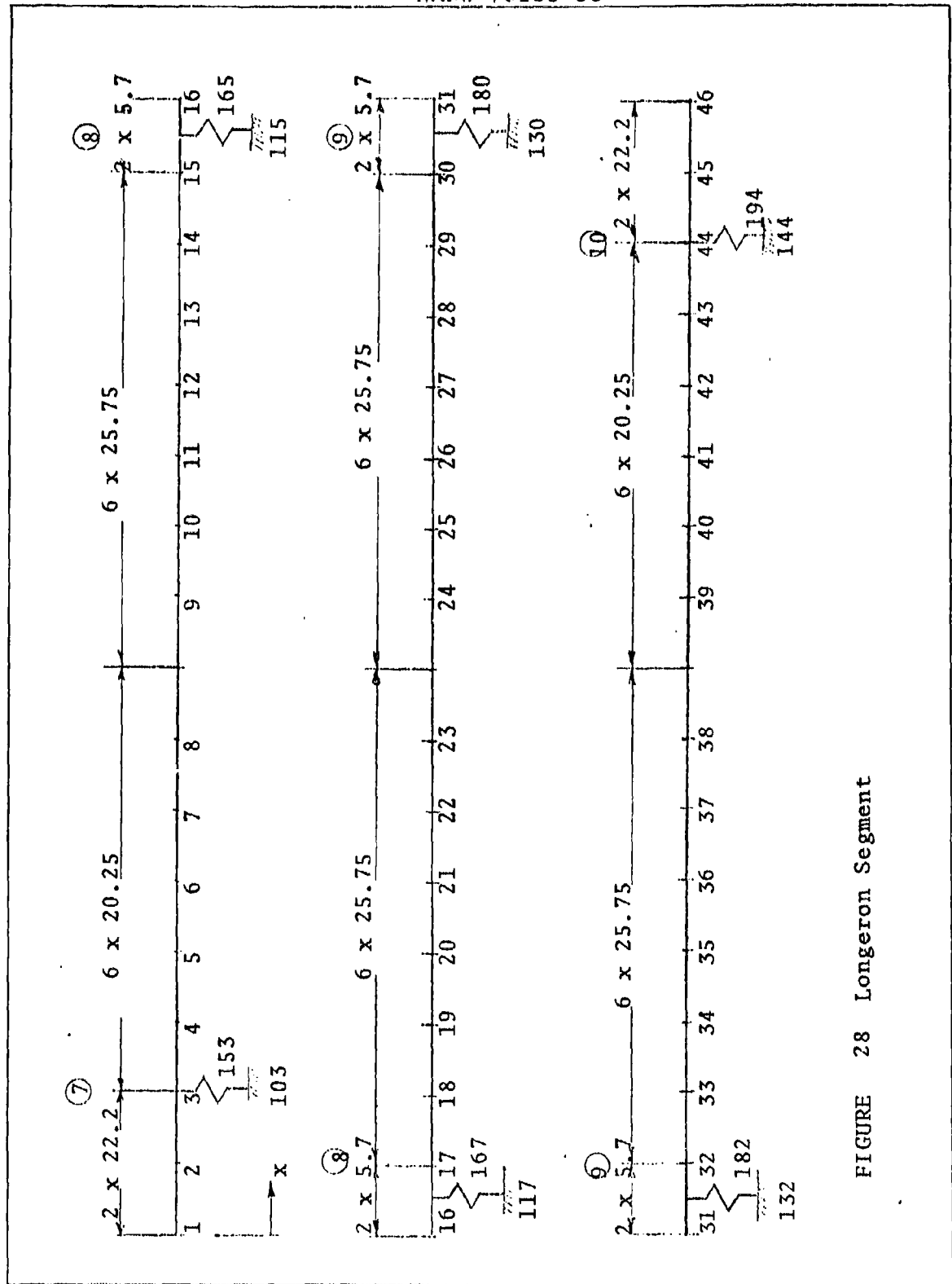


FIGURE 28 Longeron Segment

TABLE 12 Skin Ring Constants

Node No.	Frame No.	k_0 (lb/in)	k/k_0	l_i (in)	k' (lb/in)
1	7	33.75	1.0	11.1	374.6
2			1.0	22.2	749.3
3			1.0	21.23	716.5
4			1.0	20.25	683.4
8	7	33.75	0.5	20.25	341.7
9	8	32.86	0.5	25.75	423.1
13			0.5	25.75	423.1
14			1.0	15.73	516.9
15			1.0	5.7	187.3
17			1.0	5.7	187.3
18			1.0	15.73	516.9
19			0.5	25.75	423.1
23	8	32.86	0.5	25.75	423.1
24	9	32.28	0.5	25.75	415.6
28			0.5	25.75	415.6
29			1.0	15.73	507.8
30			1.0	5.7	184.0
32			1.0	5.7	184.0
33			1.0	15.73	507.8
34			0.5	25.75	415.6
38	9	32.28	0.5	25.75	415.6
39	10	32.04	0.5	20.25	324.4
43			1.0	20.25	648.8

TABLE 12 continued-

Node No.	Frame No.	k_0 (lb/in)	k/k_0	l_i (in)	k' (lb/in)
44			1.0	21.23	680.2
45			1.0	22.2	711.3
46	10	32.04	1.0	11.1	355.6

The initial radial discontinuity is calculated from:

$$\Delta r = \frac{pR^2}{Et} = \frac{0.6733R^2}{10.4 \times 10^6 \times 0.020} = \left(\frac{R}{555.8} \right)^2$$

Frame	R (in)	Δr (in)
7	922	2.752
8	947	2.903
9	964	3.008
10	971.4	3.055

At every spring, representing a half of a main or a secondary frame, there is a lateral force of 20,000 or 10,000 lb respectively, which is attempting to close the discontinuity.

The axial force in a hull section:

$$N = \pi R^2 p = \pi R^2 \times 0.6733 = 2.1152R^2$$

Cross-Section area:

$$A = 2\pi R t + 42A_L$$

Longeron area $A_L = 2.182 \text{ in}^2$

$$A = 0.12566R + 91.644$$

Force in longeron:

$$N_1 = \frac{A_L}{A} N = \frac{2.182}{A} N$$

TABLE 13 Typical Longeron Forces

Frame	R (in)	N (10^6 lb)	A (in^2)	N_L (lb)	ΔN_L (lb)
7	922	1.798	207.5	18,908	
8	947	1.897	210.6	19,650	742
9	964	1.966	212.8	20,157	507
10	971.4	1.996	213.7	20,378	221

The spring constants of the frames are calculated by Equation :

$$k_f = \frac{2\pi E A_f}{z R} = \frac{2\pi \times 10.4 \times 10^6 A_f}{42 R} = 1.556 \times 10^6 \frac{A_f}{R}$$

The calculations are shown in Table 14

TABLE 14 Spring Forces

Frame	A_f (in^2)	R (in)	k_f (lb/in)
7	8.2	922	13,839
8	2.9	947	4,765
9	2.9	964	4,681
10	8.2	971.4	13,135

The results of computer analysis are presented in Table 15
Three iterations were performed.

The largest tension is at Node 32, inner chord:

$$\sigma_t = 21,433 \text{ psi}$$

$$\text{M.S.} = \frac{32,850}{21,433} - 1.0 = \frac{0.53}{(\text{tension})}$$

The largest compression occurs at Node 30, outer chord:

$$\sigma_c = 15,161 \text{ psi}$$

$$\text{M.S.} = \frac{30,500}{15,161} - 1.0 = \frac{1.01}{(\text{compression})}$$

The compressive outer chord stress appears only in the vicinity of frames.

TABLE 15 Computer Analysis Results

Node	y (in)	σ_t (psi)	M (10^3 lb/in)	σ_{oc} (psi)	σ_{ic} (psi)
1	1.942	9,006	16.033	4,804	11,107
2	1.927	9,014	32.261	559	13,241
3	1.850	9,039	81.271	-12,260	19,689
4	1.662	9,050	28.329	1,626	12,762
14	1.551	9,015	74.465	-10,513	18,773
15	1.560	9,003	89.994	-14,588	20,795
16	1.572	9,207	89.292	-14,404	20,908
17	1.566	9,212	90.431	-14,492	21,062
18	1.546	9,219	75.307	-10,524	19,087
29	1.593	9,222	77.538	-11,104	19,383
30	1.613	9,216	93.000	<u>-15,161</u>	21,403
31	1.620	9,315	91.782	-14,841	21,342
32	1.616	9,321	92.432	-14,909	<u>21,433</u>
33	1.598	9,336	76.442	-10,712	19,353
43	1.834	9,382	31.429	1,146	13,501
44	2.044	9,372	88.389	-13,819	20,955
45	2.131	9,345	36.677	-274	14,151
46	2.150	9,339	19.555	4,214	11,901

Table 16 shows the results for the frames. The maximum tension is reached at Frame No. 9: $\sigma_t = 15,050$ psi. This hoop tension is not critical by itself, but it is combined with other components.

TABLE 16 Secondary Frame Results

Node	Frame No.	P/2 (lb)	N _f (lb)	σ_f (psi)
103	7	6,248	83,530	10,190
115	8	3,182	42,540	14,670
117	8	3,187	42,607	14,690
130	9	3,265	43,650	<u>15,050</u>
132	9	3,259	43,570	15,020
144	10	6,648	88,877	10,840

5.10 Flight Condition With Deflated Cell, MC-100.
The approach is exactly the same as in Section 5.7.

When the flight velocity is 52 knots and the gust velocity is 55 ft/s, the maximum bending moment is:

$$M_{m100} = (148.254) \times (10)^6 \text{ in/lb} \quad \text{Ref.: Page 129.}$$

Frame No. 16 is the smallest radius main frame subject to this maximum moment ($R = 911$ in).

There are 42 longerons, each with $A = 2.182 \text{ in}^2$. Equivalent thickness:

$$\bar{t} = \frac{zA_1}{2\pi R} = \frac{42 \times 2.182}{2\pi \times 911.0} = 0.01601 \text{ in.}$$

Compressive stress due to bending:

$$\sigma_b = \frac{M_{m100}}{\pi R^2 \bar{t}} = \frac{(148.254) 10^6}{\pi \times 911^2 \times 0.01601} = 3,552 \text{ psi}$$

The axial force:

$$N_o = A\sigma_b = 2.182 \times 3,552 = 7,750 \text{ lb}$$

Buckling force:

$$N_{cr} = 2(kEI)^{1/2}$$

Skin thickness at this location is .020 in.

Maximum stiffness of the elastic foundation calculated as in Section 5.2.

$$k_o = \frac{2\pi Et}{R} = \frac{2\pi \times 10.4 \times 10^6 \times 0.020}{42 \times 911} = 34.16 \text{ lb/in}$$

Use only one-half of this value, or $k = 17.08 \text{ lb/in}$ as the effective constant.

$$N_{cr} = 2(17.08 \times 10.4 \times 10^6 \times 26.71)^{1/2} = 137,760 \text{ lb}$$

Equivalent free length:

$$l^2 = \frac{\pi^2 EI}{N_{cr}} = \frac{\pi^2 \times 10.4 \times 10^6 \times 26.71}{137,760}$$

$$l = 141.1 \text{ in.}$$

The same loading pattern as in Figure 23

When the hull is fully inflated, the computer printout shows the bending moment in Frame No. 7 (Node No. 3) as:

$$M = 81,271 \text{ inlb}$$

50% drop upon deflation:

$$M_o = 40,636 \text{ inlb}$$

Resultant compressive stress, outer chord, end of column:

$$\sigma = \frac{N_o}{A} + \frac{M_o C}{I} = \frac{13,583}{2.182} + \frac{40,636 \times 7.0}{26.71} = 16,875 \text{ psi}$$

Similarly to Section 5.7, doubling of the load will not cause more than doubling of the resultant stress, because the ratio of N/N_{cr} is relatively small.

$$M.S. = \frac{30,500}{16,875} - 1.0 = \frac{0.81}{(\text{Compression})}$$

In the same beam, without an axial force, the bending moments will be :

$$M_O' = \left(\frac{1}{12}\right)(0.349)(160.2)^2 = 746.4 \text{ inlb}$$

$$M_O'' = \frac{1}{2} M_O' = 373.2 \text{ inlb} \quad \text{The stretching force is :}$$

$$N = (0.628 - 0.349)(1224) = 341.5 \text{ lb}$$

The true moments are :

$$M^1 = (746.4) \left(\frac{3}{\pi}\right) (18.43)(10)^{-3}/341.5)^{1/2} = 5.236 \text{ inlb}$$

$$M'' = \frac{6}{\pi^2} \frac{(18.43)(10)^{-3}}{341.5} (373.2) = 12.24(10)^{-3} \text{ inlb}$$

Corresponding bending stress

$$\sigma_b' = M^1/t^2 = (6)(5.236)(0.024)^2 = 54,542 \text{ lb/in}^2$$

$$\sigma_b'' = 128 \text{ lb/in}^2$$

While the bending stress near the supports (longerons) is excessive, the center bending is negligible. The bending moment stress in the skin at longerons is reduced by extending the thicker-than-skin ($t_{\text{base}} = 2t_{\text{skin}}$) Bases of longerons parallel to their base sides, a measure described in section 5. of this report.

MC-100 at Maximum Diameter.

This calculation follows closely that of MC-200, as much as the data permit.

$$R = 971.4 \text{ in.}$$

$$z = 42 \text{ (Number of longerons)}$$

$$l = 2 R/42 = 145.3 \text{ in.}$$

$$t = 0.020 \text{ in.}$$

Maximum longeron displacement, from computer printout:

$$\Delta r = 2.15 \text{ in.}$$

$$\text{Pressure load } p = 0.6733 \text{ lb/in}^2$$

Section properties of the circumferential strap of skin:

$$A = 0.020 \text{ in}^2 \quad (\approx t)$$

$$I = \frac{1}{12} t^3 = 0.6667(10)^{-6} \text{ in}^4$$

$$EI = 10.4(10)^6(0.6667)(10)^{-6} = 6.933 \text{ lb/in}^2$$

Buckling load:

$$N_{cr} = \frac{4\pi^2}{L^2} EI = \left(\frac{2\pi}{145.3}\right)^2 (6.933) = 12.96(10)^{-3} \text{ lb}$$

Evaluate the bending component of pressure from

$$w = \frac{p}{\frac{12}{8R\Delta r} + 1} = \frac{0.6733}{\frac{145.3^2}{(8)(971.4)(2.15)} + 1} = 0.2974 \text{ lb/in}^2$$

Stretching force

$$N = (0.6733 - 0.2974)971.4 = 365.1 \text{ lb}$$

Bending moments, if no axial force present:

$$M'_0 = \frac{1}{12} w L^2 = \frac{1}{12} (0.2974)(145.3)^2 = 523.2 \text{ inlb}$$

$$M''_0 = \frac{1}{2} M'_0 = 261.6 \text{ inlb}$$

True Moments:

$$M' = M'_0 \frac{3}{\pi} \left(\frac{N_{cr}}{N}\right)^{1/2} = 523.2 \frac{3}{\pi} (12.96)(10)^{-3}/365.1)^{1/2} = 2.977 \text{ inlb}$$

$$M'' = \frac{6}{\pi} \left(\frac{N_{cr}}{N}\right) M''_0 = \frac{6}{\pi} (12.96)(10)^{-3}/365.1) 261.6 = 5.65(10)^{-3} \text{ inlb}$$

Corresponding bending stress:

$$\sigma'_b = 6M'/t^2 = (6)(2.977)/0.020^2 = 44,655 \text{ lb/in}^2$$

$$\sigma''_b = 85 \text{ lb/in}^2$$

Again the bending stress at the center is negligible; while the bending near end-points is excessive.

Effect of Longeron Doubler On Bending of Skin

The theory presented in the previous section is applicable only to the constant - section band of skin. Assume a doubler of the following form. (see Figure 29).

Length "l" is measured between longeron centerlines.

The simplest estimate of the change in bending stress as a result of introduction of doublers is to apply the previously calculated bending moments to the new total skin thickness. This is partially justified by the fact that there is very little bending in the beam-column except the immediate vicinity of ends. Doubling the thickness near the ends would then result in reducing the bending stress four times.

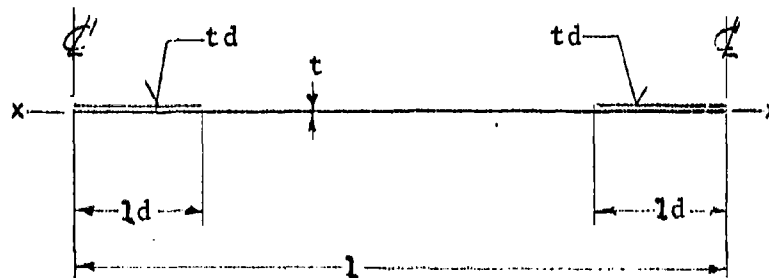


FIGURE 29 Longeron Doubler

The next degree of approximation is to take into account the diminishing effect of the stretching force, when the thickness of beam (or of a part of it) increases. This will be done by means of calculating the new value of the buckling force and then repeating the previous calculations.

MC-200

Assume $t_d = t = 0.024$ in.

$l_d = 20$ in.

To avoid excessive computations, only a gross estimate of new N_{cr} will be made. N_{cr} is proportional to t^3 for a constant thickness beam. Doubling of the whole thickness would mean adding $(7)N_{cr}$ to the present value. Taking length into account:

$$N'_{cr} = N_{cr} + \frac{(2)(20)}{160.2}(7N_{cr}) = 2.748 N_{cr}$$

(2.748) N_{cr} indicates that the end moment will grow by $\sqrt{2.748}$. Bending stress is proportional to the bending moment and inversely proportional to the square of thickness:

$$\sigma'_b = 54542 \left(\frac{0.024}{0.048} \right)^2 \sqrt{2.748} = \underline{22,604 \text{ lb/in}^2}$$

MC-100

Assume $t_d = t = 0.020 \text{ in.}$ $ld = 18 \text{ in.}$

$$N'_{cr} = N_{cr} + \frac{2(18)}{146.3} (7N_{cr}) = 2.734 N_{cr}$$

The end moment will grow by $\sqrt{2.734}$.

New bending stress near supports:

$$\sigma'_b = 44,655 \left(\frac{0.020}{0.040} \right)^2 \sqrt{2.734} = 18,460 \text{ lb/in}^2$$

The calculated bending stress must be superimposed on the hoop stress, which is also diminished because of presence of the doubler.

MC-200

$$p = 0.628 \text{ lb/in}^2$$

$$R = 1224 \text{ in.}$$

$$t = 0.048 \text{ in. (total)}$$

$$\sigma = \frac{pR}{t} + \sigma'_b = \frac{(0.628)(1224)}{0.048} + 22604 = 38618 \text{ lb/in}^2$$

$$\text{M.S.} = \frac{32850}{38618} - 1.0 = \underline{\text{Neg.}} \\ (\text{Bend.} + \text{Tens.})$$

MC-200:

$$p = 0.6733 \text{ lb/in}^2$$

$$R = 971.4 \text{ in.}$$

$$t = 0.040 \text{ in. (total)}$$

$$\sigma = \frac{pR}{t} + \sigma'_b = \frac{(0.6733)(971.4)}{0.040} + 18460 = 34811 \text{ lb/in}^2$$

$$\text{M.S.} = \frac{32850}{34811} - 1.0 = \underline{\text{Neg.}} \\ (\text{Bend.} + \text{Tens.})$$

It is shown above that the skin is overstressed, but this does not necessarily mean so, as the estimate may be inaccurate with respect to skin with a doubler. A step in the right direction is to employ finite-element techniques.

A following model, which is representative of MC-200 configuration was analyzed using "ANSYS" computer program. The loading consists of stretching with the force $N = 341.51b$ and lateral load 0.349 lb/in^2 . The number of elements employed is relatively small, which makes the model coarse, but is sufficient within the scope of this report.

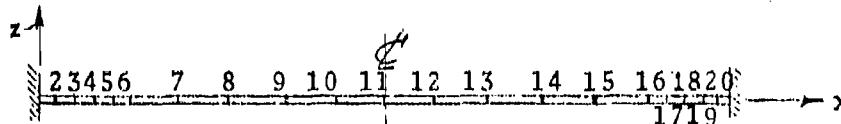


FIGURE 30. Element Model

The results for the unreinforced strap are:

(Computer Calculated)

$$\Delta r = 1.352 \text{ in. (maximum deflection)}$$

$$M' = 7.463 \text{ inlb (moment at end)}$$

$$M'' = 2.139 \text{ inlb (moment at center)}$$

(Hand Calculated)

$$\Delta r = 2.06 \text{ in.}$$

$$M' = 5.236 \text{ inlb}$$

$$M'' = 12.24(10)^{-3} \text{ inlb}$$

Comparing the above values, notice that the computer-calculated deflections are smaller, while the bending moments are larger than those calculated by hand. This may be due to model imperfection or to the inaccuracy inherent in the resolution of pressure prescribed by:

$$w = \frac{p}{\frac{12}{8RAr} + 1}$$



When the doubler is placed, as previously described, one obtains:

$$\Delta r = 1.352 \text{ in.}$$

$$M' = 10.164 \text{ inlb}$$

$$M'' = 2.141 \text{ inlb}$$

The increase of the end moment is 36%, resulting from the estimate compared to the moment without the doubler.

It must be mentioned here that some of the conclusions presented here from the computer work bear a degree of uncertainty. This is not an accident, but a result of unusual slenderness of elements, which creates some numerical difficulties. The iteration process converges very slowly and a number of tests are needed to obtain a reasonable solution.

The next logical step would be to generate a more sophisticated model, which should have:

- a. more elements
- b. two, rather than one contact point of longeron and skin

5.11. DETERMINATION OF THE SIZE OF LONGERONS. The most critical loading of longerons arises in a section of the hull with loss of lifting gas and air pressure. Erection loads in dock are lower than flight loads without pressure, analyzed in 1.8 and 7.1.

Maximum speed with a deflated cell is approximately 52 knots, (Reference, Section 1.8). The conditions of loading are given below, repeated for convenience from section 7.1. The gust moment is more severe than the aerodynamic moment and the gas head moment is zero. It is desired to find the area of section of a longeron to resist the gust moment M_m , as follows:

$$M_m = (.1) \frac{\gamma}{2g} (u)(c)(V)^{2/3} (L)$$

$$\gamma = .076475 \text{ lb/ft}^3$$

$$2g = 64.348 \text{ ft/sec}^2$$

$$u = 52 \text{ knots} = 87.828 \text{ ft/s}$$

$$c = 35 \text{ ft/s, gust velocity}$$

$$V = \text{volume of hull, } 20(10)^6 \text{ ft}^3 \text{ for MC-200}$$

$$L = 917.949 \text{ ft, for MC-200}$$

$$M_m = (.1) \frac{.076475}{64.348} (87.828)(35)(73680.6)(917.949)$$

$$M_m = 24.7091(10)^6 \text{ ftlb}$$

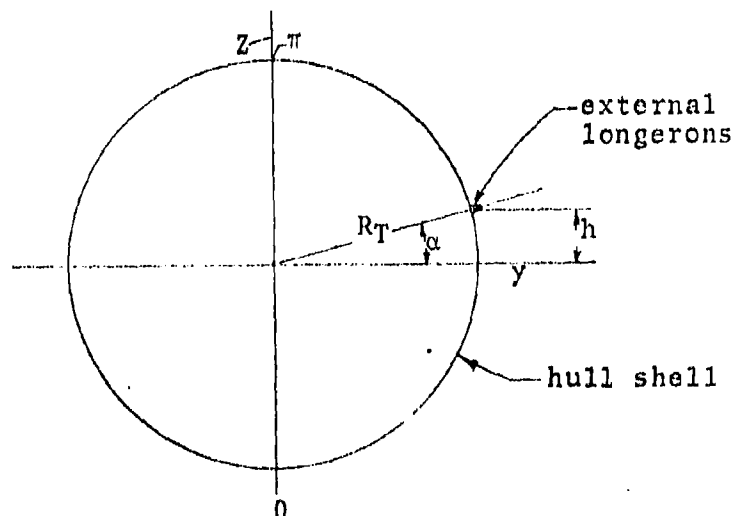


FIGURE 31 Hull Cross-section

Moment Of Inertia Of All Longerons Around The Hull.

$$h = R_T \sin \alpha \quad \text{where } R_T = 101.9945 \text{ ft max. (MC-200)}$$

$$I \text{ (each longeron)} = A(h^2)$$

$$\Sigma I_{\text{hull}} = 4A\pi h^2$$

$$\sigma = \frac{M_m R_T}{A\pi h^2} = \frac{(24.69167)(10)^6(102)}{(.57)(270,474.7)} = 16,336 \text{ lb/in}^2$$

$$\sigma_L = \frac{32850}{2} = 16,425 \text{ lb/in}^2$$

Note: σ_L = Stress in compression on longerons.
It is expected that the allowable load in compression will equal the max. allowable tensile stress in the skin (see Section 7, page 167).

TABLE 17 Longeron Sizes. MC-200

α°	h(ft)	$h^2(\text{ft}^2)$	α°	h(ft)	$h^2(\text{ft}^2)$
7.5	13.313	177.234	82.5	101.122	10,225.644
15.0	26.400	696.860	90.0	101.995	10,402.878
22.5	39.032	1,523.463			
30.0	51.000	2,600.720	Σh^2 one quadrant = 67,618.678		
37.5	62.090	3,855.202			ft ²
45.0	72.121	5,201.442			
52.5	80.918	6,547.665			
60.0	88.330	7,802.151	For full circle:		
67.5	94.231	8,879,401			
75.0	98.519	9,706.021	$\Sigma h^2 = (4)(67,618.678) =$		
					270,474.71 ft ²

MC-200

Now, using

$$\sigma = \frac{M_m R_T}{A \Sigma h^2} = 16,425 \text{ lb/in}^2$$

$$A = \frac{M_m R}{\Sigma h^2 \sigma (144)} \text{ ft}^2 = \frac{(24.7091)(10)^6(101.9945)}{(270474.71)(16425)(144)} = .00397 \text{ ft}^2$$

$$A = 0.567 \text{ in}^2 \approx 0.57 \text{ in}^2 \text{ (MC-200)}$$

With the neutral axis at half the longeron height, the area of the apex cornice equals 0.290 in² and the area of each base equals 1/4 of the total area which equals 0.150 in². (approx)

For MC-100

$$\begin{aligned}
 M_m &= (0.1) \left(\frac{0.076475}{64.348} \right) \left(\frac{(52)(6076.1062)}{3600} \right) (35) (10(10)^6)^{2/3} \\
 &\quad \times (728.576) \\
 &= (0.1) (1.1884596) (10)^{-3} (35) (46415.8) (728.576) \\
 &\quad \times (87.766) \\
 &= 12.3458 (10)^6 \text{ ftlb}
 \end{aligned}$$

M_{des} = Design moment with maximum gas cell deflated.

$$M_m = 12.3458 (10)^6 \text{ ftlb}$$

$$h = R_T \sin \alpha \quad \text{where } R_T = \frac{161.906}{2} = 80.953 \text{ ft}$$

$$I \text{ (each longeron)} = A(h^2)$$

$$EI_{hull} = 4A\sum h^2 \text{ (one quadrant)}$$

$$\sigma = \frac{M_m R_T}{A\sum h^2} = \frac{(12.3458)(80.953)}{(.360)(170,388)} = 16,293 \text{ lb/in}^2$$

$$\sigma_L = \frac{32850}{2} = 16,425 \text{ lb/in}^2$$

TABLE 18 Longerons sizes - MC-100

α°	$h \text{ (ft)}$	$h^2 \text{ (ft}^2\text{)}$	α°	$h \text{ (ft)}$	$h^2 \text{ (ft}^2\text{)}$
7.5	10.5665	111.650	82.5	80.260	6,441.739
15.0	20.952	438.994	90.0	80.953	6,553.388
22.5	30.979	957.719			
30.0	40.477	1,638.347			
37.5	49.281	2,428.620	$\sum h^2, \text{ (one quadrant)} =$		
			42,597.006 ft^2		
45.0	57.242	3,276.696			
52.5	64.224	4,124.761			

TABLE 18 Continued-

α°	h (ft)	h^2 (ft ²)	α°	h (ft)	h^2 (ft ²)
60.0	70.107	4,915.036	For full circle:		
67.5	74.971	5,593.660	$\Sigma h^2 = 4(\Sigma h^2) = 170,388.02 \text{ ft}^2$		
75.0	78.195	6,114.396			

MC-100

Now using:

$$\sigma = \frac{M_m R_T}{A \Sigma h^2} = 16,425 \text{ lb/in}^2$$

$$A = \frac{M_m R_T}{\Sigma h^2 \sigma (144)} \text{ ft}^2$$

$$= \frac{(12.3458)(10)^6(80.953)}{(170388.02)(16425)(144)}$$

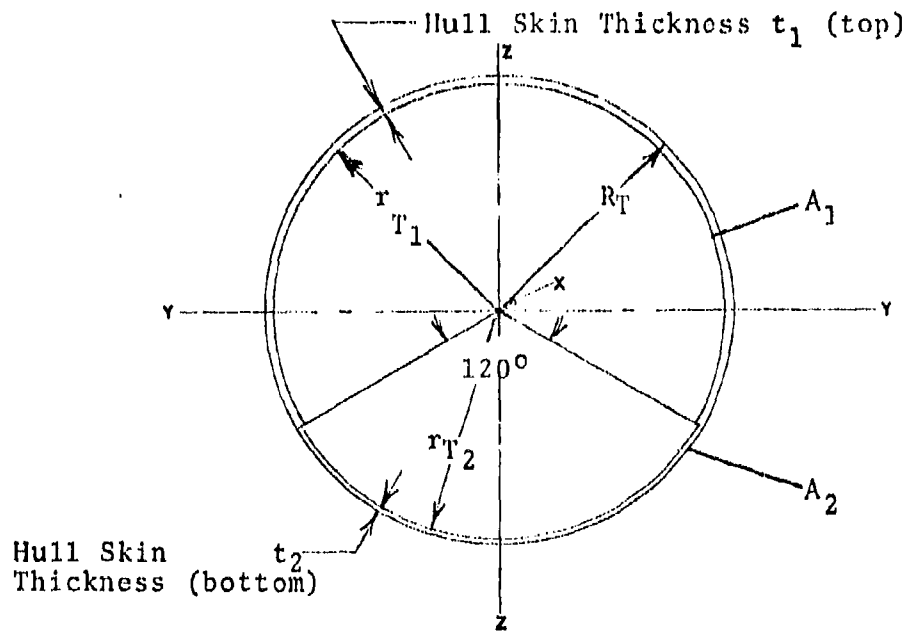
$$= 2.4780 (10)^{-3} \text{ ft}^2$$

$$= .3568 \text{ in}^2$$

$$\approx .360 \text{ in}^2$$

With neutral axis at one-half the height of the longeron,

Area of apex cornice	= .180 in ²	} MC-100
Area of each base cornice	= .090 in ²	



MC-200 FIGURE 32 Hull Skin Cross-Section

Cross-sectional area of skin at central main frame:

$$A_S = A_1 + A_2 = \frac{2\pi}{3}(R_T^2 - r_{T1}^2) + \frac{\pi}{3}(R_T^2 - r_{T2}^2) \text{ in}^2$$

$$A_S = \frac{2\pi}{3} (1223.934)^2 - (1223.91)^2 + \frac{\pi}{3} (1223.934)^2 - (1223.912)^2$$

$$A_S = 123.15042 + 56.443946$$

$$A_S = 179.59436 \text{ in}^2$$

Cross-sectional area 48 longerons:

$$A_L = (48)(0.57)$$

$$A_L = 27.36 \text{ in}^2$$

Ratio of longeron area to skin area:

$$\frac{A_L}{A_S} = \frac{27.36}{179.59436} = 0.15235$$

Euler's equation for long columns:

$$\frac{N_{cr}}{A} = \sigma = \frac{\pi^2 EI}{A \rho^2 \lambda^2}$$

$$\lambda = \frac{l}{\rho}$$

A = Area of column

λ = Slenderness ratio

ρ = Radius of gyration

I = Moment of inertia of the section

For a column of elastic foundation:

$$N_{cr} = 2(kEI)^{1/2}$$

$$k \approx 13.5 \text{ lb/in}$$

$$\sigma_{cr} = \frac{N_{cr}}{A}$$

$$\sigma_{compr_{cr}} = \frac{\pi^2 E}{\lambda^2}$$

$$\lambda^2_{limit} = \frac{2\pi^2 E}{\sigma_y}$$

$$\lambda_{limit} = 58.5 : (\text{slenderness})$$

Below this value of λ : Johnson's parabola:

$$\sigma_{cr} = \left(1 - \frac{\sigma_{yp} \lambda^2}{4E\pi^2}\right) \sigma_{yp}$$

$$\sigma_y = \text{Y.P. compression} = 61,000 \text{ lb/in}^2$$

$$\text{Allowable: } \frac{\sigma_y}{2} = 30,500 \text{ lb/in}^2$$

Deflection of longeron as a beam, MC-200:

$$\begin{aligned} y_{\max} &= \frac{(2.64354)w \times l^4}{384EI} \\ &= \frac{(2.64354)(0.39254198)[(36.2)(12)]^4}{(384)(10.4)(10)^6(16.621)} \\ &= .5565 \text{ in.} \end{aligned}$$

Where w = load, pounds per linear inch:

l = distance between frames and first secondary frame (in inches)

I = moment of inertia of individual longeron

$$= \rho^2 A = (0.57)(5.4)^2 = 16.621 \text{ in}^4$$

E = modulus of elasticity of 7050-T76

$$\text{aluminum alloy} = 10.4(10)^6 \text{ lb/in}^2$$

Slenderness ratio =

$$\lambda = \frac{l}{\rho} = \frac{(36.2)(12)}{5.4} = 80.44$$

Therefore by Euler's equation:

$$\sigma = \frac{\pi^2 E}{\lambda^2} = \frac{\pi^2 (10.4)(10)^6}{(80.44)^2} = 15,863 \text{ lb/in}^2$$

For MC-100, similar to above for MC-200.

Cross-sectional area of skin at central main frame:

$$A_S = A_1 + A_2 = \frac{2\pi}{3}(R_T^2 - r_{T1}^2) + \frac{\pi}{3}(R_T^2 - r_{T2}^2) \text{ in}^2$$

$$A_S = \frac{2\pi}{3} [(971.436)^2 - (971.416)^2] + \frac{\pi}{3} [(971.436)^2 - (971.418)^2]$$

$$A_S = 81.38819 + 36.620496$$

$$A_S = 118.00868 \text{ in}^2$$

Ratio of longeron area to skin area:

$$\frac{A_L}{A_S} = \frac{(42)(0.360)}{118.00868}$$

$$= 0.12813$$

Now, interpolating between the MC-100 and MC-200, we get the following longeron area to skin area ratios:

$$MC-125 = 0.13418$$

$$MC-150 = 0.14024$$

$$MC-175 = 0.14629$$

Deflection of longeron = y , MC-100;

$$y_{\max} = \frac{(2.64354)wl^4}{384 EI}$$

where: w = load in pounds per linear inch

l = distance between main frame and first intermediate frame - inches.

I = moment of inertia individual longeron

$$= \rho^2 A = (4.29)^2 (.360) = 6.6286 \text{ in}^4$$

E = mean modulus of elasticity, aluminum alloy

$$= 10.4(10)^6$$

$$y_{\max} = \frac{(2.64354)(0.3299162)(346.356)^4}{(384)(10.4)(10)^6(6.6286)}$$

$$= .4741 \text{ in.}$$

Slenderness ratio

$$\frac{l}{\rho} = \frac{346.356}{4.4} = 78.717272$$

By Euler's equation:

$$\sigma = \frac{\pi^2 E}{\lambda^2} = \frac{\pi^2 (10.4)(10)^6}{(78.717272)^2} = 16,565.059 \text{ lb/in}^2$$

Parametric determination of section properties of longerons from the sectional areas of longerons for MC-100 and MC-200, can be determined for properties of longerons of intermediate hulls.

The moment of inertia of longeron is approximately expressed by

$$I_1 = (2)\frac{A}{2} \rho^2, \text{ in}^4$$

where A = the area computed for longeron section on preceding pages

$$\rho = \text{radius of gyration } \rho = (.810)(h_1)/2$$

The heights of the longerons for MC-100 and MC-200 are tabulated in Tables 17 and 18 .

It is assumed that the following relation holds:

$$\frac{I_i}{I_{200}} = \frac{M_{mi}}{M_{m200}} \cdot \frac{R_i}{R_{200}}$$

$$I_{100} = \left[\frac{M_{m100}}{M_{m200}} \right] \left[\frac{R_{100}}{R_{200}} \right] I_{200}$$

$$I_{100} = \left[\frac{12.3458}{24.7091} \right] (.7936997)(16.621)$$

$$I_{100} = 6.5914 \text{ in}^4$$

Then, for example:

$$I_{100} = A_{100} \cdot \rho^2 = A_{100} \left[(.45)h_{100} \right]^2$$

$$A_{100} = \frac{I_{100}}{[(.45)(h_{100})]^2} = \frac{6.5914}{[(.45)(9.53)]^2} = \frac{6.5914}{18.39123}$$

$$A_{100} = .3584 \text{ in}^2$$

Section properties of longerons on all hulls are tabulated in Table 19

TABLE 19 Longerons Section Properties

Hull	R_i/R_{200}	$M_{mi}(\text{ftlb})$	M_{mi}/M_{m200}	$I_i(\text{in}^4)$	$A_i(\text{in}^2)$
100	.7937	12.345	.4997	6.5914	.357
125	.855	15.444	.625	8.9355	.4146
150	.908	18.4976	.749	11.2595	.46724
175	.956	21.589	.874	13.8326	.51796
200	1.00	24.7091	1.000	16.621	.570

The gust moments at 52 knots (for major cell deflated) are computed from sea levels values.

$$M_m = (.10) \frac{\gamma}{2g} u c V^{2/3} L$$

$$M_{m100}, (\text{previously computed on page 152}) = 12.3458(10)^6 \text{ftlb}$$

$$M_{m125} = (.36531) \left(12.5(10)^6 \right)^{2/3} (784.835)$$

$$M_{m125} = 15.444(10)^6, \text{ftlb}$$

$$M_{m150} = (.36531) \left(15(10)^6 \right)^{2/3} (834.01875)$$

$$M_{m150} = 18.4976 (10)^6 \text{ftlb}$$

$$M_{m175} = (.36531) \left(17.5(10)^6 \right)^{2/3} (877.987)$$

$$M_{m175} = 21.589 (10)^6 \text{ftlb}$$

All study hulls are strong enough in their respective longerons to support gust bending moments at 52 knots speed with the largest cell deflated. This is the severe condition examined and all hulls should have strength and rigidity to stand up to the lesser stresses during construction without gas and air pressure. During construction, light, removable jury structure will be needed and used to locate the main frames at their exact stations prior and during the installation of longerons and skin. During construction, the jury spacers will be successively removed, as the assembly progresses and serve as incidental structures.

6. BULKHEAD DIAPHRAGMS

6.1 DIAPHRAGMS BETWEEN THE CELLS. The inflation gas is contained by the Metalclad shell above the equator and by transverse fabric bulkheads in the plane of main frames, backed up by a restraining network and semi-cylindrical fabric bottoms of the cells. All fabric parts of cells are called membranes.

The diaphragms acting as fabric bulkheads in the plane of main frames, separate adjacent cells. The bulkhead is only in the upper half of the circular arc of inner radius of a main frame.

In this area, the network (shown in appendix M-5 for the MC-200 hull) is integral with the fabric; one spiral network system (i.e. LH) can be on one side of the diaphragm, the other (RH) side of the spiral network system can be on the other side of the fabric, the network being attached to the fabric by adhesives. At equidistantly spaced peripheral gathering knots, the diaphragm is attached to swivelling anchor joints on the main frames, as shown in the referenced appendix. Below the equatorial plane, the network is independent of the fabric; the LH spiral system is attached to the RH spiral system directly, at all crossing joints. Below the equatorial plane, the diaphragm is double, each half free to float on air below it in the lower part of the hull.

The semi-disc upper half of the diaphragm is joined by a sealing shoe to the apex cornice of the main frame by means of a radially accorded, narrow peripheral curtain, which seals off the gas between adjacent cells. The main frame corrugated sides are sealed off by thin flat sheet, spot welded to corrugations. The inner perimetral corridor within each main frame is gas tight and contains air under hull pressure. The shear sides of the frames are well capable of supporting the gas head, as they are parts of frustum cone envelopes. The floating cylindrical membranes, comprising the lower walls of each cell, are removable and fastened to the shell of the hull above equatorial plane by a sealed, bolted joint which is longitudinally continuous between frames and permits the fabric to be loaded in tension and shear only, with no possibility of re-entry angles appearing anywhere. This joint is shown on the hull layout in Appendix M -5 ; it can be seen that in deflated state, the diaphragm lies tightly against the skin, with no potential air entrapment. When inflated, the fabric wraps on a curved channel without changing the mode of loading and within a short distance again lies on the inner wall or the hull skin when upon full inflation. The joint allows for replacement of the membrane without damage to the hull structure.

The radial network system will be elastic enough to support surging gas loads, and it is expected to be sufficiently self-damping to suppress oscillations. Should further analysis reveal inadequate elasticity, provision is made for hydraulic shock absorbers to be placed between the horns to which the diaphragm is attached and special rockers on which the joint rides, (also shown on layout of hull of MC-200). Damped anchorages are then required only on the top half of the inner network system. At three main frames noted on the hull layouts, the network diaphragm completely occupies the circular area of the inner diameter of main frames. This reduces surging motions of the air in the hull as well as that of the lifting gas. Whether these frames should have sealed corrugated sides along the lower half of the frame structure; requires further analysis, beyond the constraints of this report.

The diaphragm structure for containing lifting gas in separate cells and restraining the movement of air masses, is the simplest solution for Metalclad hulls. It requires the least amount of fabric, permitting complete deflation of cells via suction, and also complete volumetric expansion with gas at altitude or for test purposes in the dock. It will assure inflation with minimal dilution of the lifting gas during inflation an important condition for economical operation of airships never fully attained in the past. It also permits removal and replacement of any cell without disturbing adjacent cells.

With a projected 10,000 ft. ceiling, the cells would be inflated to $(.04828/.06535 = .7388)$ of the maximum theoretical gas volume at sea level except the cells in the bow and stern air sub-volume. These gas cells would be inflated to approximately 50% fullness at sea level, allowing excess air volume at altitude for trimming purposes. The air space below the cells in the bow and stern serve as ballonets. The degree of this inflation will be analyzed separately. In relation to the use of thrusters, it appears possible that the gas inflation can be allowed to a higher volumetric ratio in the bow and stern than in those vehicles without thrusters.

Removable bolt-on and air-sealed gore panels between the longerons and two secondary frames will be provided on the bottom of the hull in each cell section for access into the hull and exchange or insertion of cell diaphragms and membranes in the dock.

In this report all cell diaphragms are projected to be made of ILCI A 105004 fabric as described in Figure 34. Weight calculations, Section 10.5, are also based on this fabric.

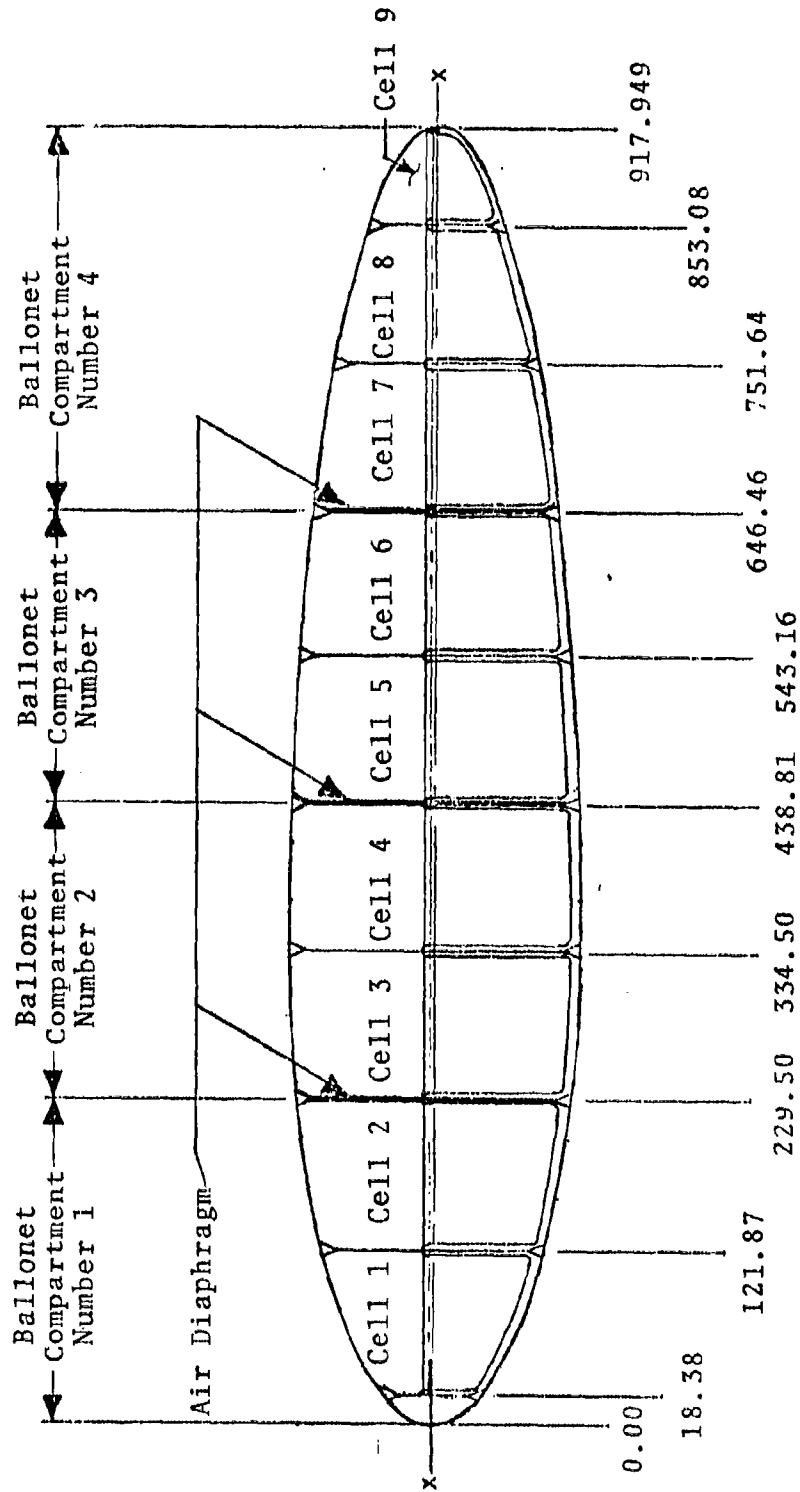
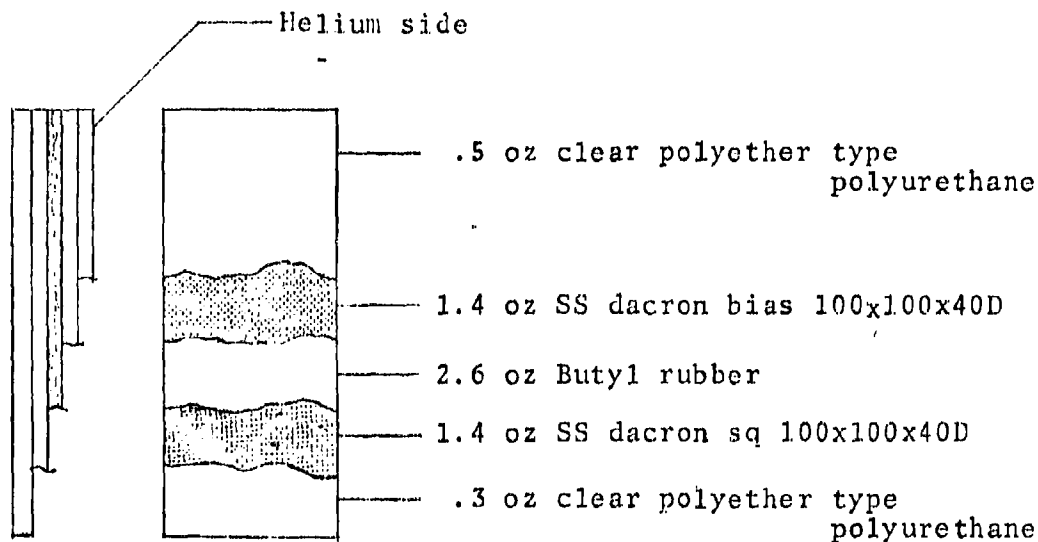


FIGURE 33 Gas Cell And Ballonet Arrangement For MC-200 (Typ. All Hulls)

Fabric: ILCI A 105004

Mfr. : Reeves Bros.

Structure and Composition



Gross Properties: (objective)

Strip Tensile, lb/in

Stress Limits(nominal)

hoop

90 (n)

long

90 (n)

shear

weight : oz/yd²

6.4

permeability : 1/m²/da

>0.5

FIGURE 34 Diaphragm Fabric

7 HULL SHELL SKIN THICKNESS

7.1 SKIN THICKNESS VARIATION, PANEL SIZE PARAMETERS AND THICKNESS DISTRIBUTION OVER THE HULL. There is only one singular process to establish the thickness of skin of a Metalclad hull and that is to determine the skin thickness at the maximum diameter, loading the skin to the maximum allowable stress in transverse (hoop) tension. In the longitudinal direction, the stress due to internal pressure is approximately less than 1/2 of the transverse stress (in a cylinder exactly 1/2). Therefore, the hoop stress is a primary figure and the thickness required for it is basic. The transverse (or hoop) skin stress is defined by

$$\sigma_T = \frac{2kR_T^2 + pR_T}{t_T} \text{ lb/in}^2, \text{ at the top of the hull} \quad (1)$$

The skin thickness in the transverse direction is the same as in the longitudinal direction, $t_T = t_L$.

Equation(1) has two unknowns and t_T has to be expressed, in addition, by some other relation.

Such a relation exists in the form parameter for critical shear stress which is

$$\xi = \frac{t}{b} \sqrt{\frac{t}{R_T}} \quad (2)$$

This parameter is known experimentally from the ZMC-2 hull experience

$$\xi_{ZMC-2} = \frac{.0095}{82.73} \sqrt{\frac{.0095}{316}} = .62878(10)^{-6}$$

Its merit is that nowhere on the ZMC-2 hull was there found a permanent set caused by elastic buckling when the hull was without internal pressure. Furthermore, the skin of the ZMC-2 was oversize and it is probable that the parameter ξ can be actually smaller. In the absence of knowledge in this respect, the above value is used in the determination of maximum skin thickness on all hulls. The manipulation of Eq. (1) and (2) is influenced by the spacing of the longerons, therefore, by their number. In Metalclad hulls another important parameter is κ , the ratio of the total area of longerons and of the transverse skin area. If this ratio is low, the longerons will be few and probably inadequate for support of the hull in flight with a deflated cell and perhaps even to support the skin during erection of the hull; the skin will have to be too thick and heavy



and the overall hull design far off the optimum strength-weight ratio. The optimum value of κ is at this time still an elusive number, depending upon the form of the longerons, spacing of frames, etc.

In Metalclad hulls, κ is a very small ratio, in ZMC-2 its value was $\kappa = .0124$. This is no guidance for larger hulls; analytical studies indicate that the value of κ should be, approximately $\kappa \approx .10$ for large hulls, with a highly refined design of longeron section and two secondary frames between main frames. This is a region for further analytical research before constructing large hulls. In the analysis of this report $\kappa \approx .16$, which is considered conservative. In the initial period of preparation of this report, it appeared attractive to use as few longerons as practicable and the number decided upon was $z = 24$. This led to heavy skin and very low κ and it was understood quickly that this was not the right direction to follow in the design. The number was increased by repeated analysis, to $z = 48$ for MC-200 and $z = 42$ for MC-100. Although the cost of construction increased due to a higher number of longerons, the skin weight was reduced dramatically and also very importantly, the longerons were unloaded from weight during erection (mostly due to skin), as well as the improvement of bending strength of the hull with a deflated cell and loss of supercharge pressure.

For MC-200

$$b \approx R_T = 101.9945 \text{ ft} = 1223.934 \text{ in.}$$

$$L = 917.949 \text{ ft} = 11015.388 \text{ in.}$$

$b = \text{minor axis}$
 $a = .64L$

$$R_L = \frac{a^2}{b} = \frac{(917.949)(.64)^2}{101.9945} (12) = 40,607.008 \text{ in.}$$

With 48 longerons, the maximum peripheral distance(b) between longerons

$$b = \frac{P}{z} = \frac{7690.204}{48} = 160.2126 \text{ in, centerline to centerline}$$

of longeron, a conservative assumption in view of thicker-than-skin base of all Metalclad structures.

$$\xi = (.6287825)(10)^{-6} = \frac{t}{160.2126} \sqrt{\frac{t}{1223.934}}$$

$$t^3 = (.3953674)(31.416032)(10)^{-6}$$

$$t^3 = (12.430874)(10)^{-6}$$

$$t = 2.215885(10)^{-2} = .0233 \text{ in.}$$

The standard sheet gage near this number is $t = .024$ in. maximum skin thickness at maximum hull diameter.

With factor of safety of 2.0 with respect to the ultimate tensile stress in tension:

$$\sigma_{\text{design}} = 36,500 \text{ lb/in}^2$$

$$\sigma_{\text{design}_{yp_t}} = 32,000 \text{ lb/in}^2$$

$$\tau_{\text{design}_{yp_\tau}} = 22,000 \text{ lb/in}^2$$

The skin splicing seams (Refer to Section 8) will be bonded and riveted. Due to this combination, all seam joints will have at least 100% efficiency, but for the purpose of analysis, the maximum allowable design stress of any seam joint is reduced by a factor of (.90), skin = $(.9)(36,500) = 32,850 \text{ lb/in}^2$. Therefore, maximum allowable tensile stress in the skin

$$\sigma_{\text{des}_S} = (.90)(36500) = 32,850 \text{ lb/in}^2 \text{ and in shear,}$$

$$\tau_{\text{des}_S} = (.90)(22000) = 19,800 \text{ lb/in}^2$$

Then, at maximum diameter of MC-200, on top of the hull, the transverse design stress is

$$\sigma_{\text{des}_T} = 32,850 \text{ lb/in}^2$$

and the longitudinal radius of curvature aft of the maximum diameter station is

$$R_{LS} = \frac{a_s^2}{R_T} = \frac{(587.487)^2}{101.9945} = 3383.9174 \text{ ft} = 40607.008 \text{ in.}$$

Hoop stress on top of the hull

$$\sigma_{T_{ST}} = \sigma_{\text{des}_T} = \frac{2kR_T + p}{t} \left(\frac{2R_T R_{LS}}{2R_{LS} + R_T} \right), \text{ and}$$

the hull air pressure is

$$p = t \sigma_{\text{des}_T} \left(\frac{2R_{LS} + R_T}{2R_T R_{LS}} \right) - 2kR_T$$

$$\begin{aligned}
 p &= (.024)(32850) \frac{(2)(40607.008) + 1223.934}{(2)(1223.934)(40607.008)} \\
 &\quad - (2) \frac{.06535}{1728} (1223.934)
 \end{aligned}$$

$$\begin{aligned}
 p &= .65381 - .092574 = .561247 \text{ lb/in}^2 \\
 &\approx .56125 \text{ lb/in}^2
 \end{aligned}$$

Hull air pressure: $p = (12)(2.307)(.561247) = 15.537$ in. of water. This is a reasonable value and with modern pressure control means, there should be no difficulty in controlling it within narrow limits.

Before maximum stresses in the hull can be determined, the acting maximum moments must be computed. These moments are at full speed, with hull inflated:

1. Aerodynamic moment, $M_{ae} = (.02)(\gamma/2g)u^2V^{2/3}L$ ftlb
2. Gas head moment, $M_g = (.20)\pi kR_T^4$ ftlb
3. Gust moment $M_m = (.1)(\gamma/2g)ucV^{1/3}L$ ftlb

The gas head moment can be partially compensated for by distribution of fixed weight loads at the bottom of the hull and in main frames, and only $(.80)M_g$ is taken as effective. M_{ae} and M_m can be either hogging or sagging moments. M_g is a hogging moment.

Aerodynamic moment is determined first (refer to aerodynamic moment, Section 2) at sea level, a conservative assumption;

$$\begin{aligned}
 M_{ae} &= (.02)qV^{2/3}L \quad q = \frac{\gamma}{2g}u^2 \\
 M_{ae} &= (.02)\left(\frac{.076475}{64.348}\right)(168.9)^2 \left(20(10)^6\right)^{2/3}(918) \text{ at 100 knots} \\
 M_{ae} &= 45.863782(10)^6 \text{ ftlb}
 \end{aligned}$$

Gas head moment

$$\begin{aligned}
 M_g &= (.20)\pi kR_T^4 \\
 M_g &= (.20)(3.14159)(101.9945)^4(.06535) \\
 M_g &= 4.443657(10)^6 \text{ ftlb}
 \end{aligned}$$

Gust moment, $c = 35 \text{ ft/s}$

$$M_m = (.10) \frac{\gamma}{2g} u c V^{2/3} L$$

$$M_m = (.10) \frac{.076475}{64.348} (168.9) (35.0) \left(20(10)^6\right)^{2/3} (918)$$

$$M_m = 47.5202(10)^6 \text{ ftlb}$$

M_m and M_g are used in Woodward's envelope, Fig. 6 page 64. Therefore, $M_m = 47.5202(10)^6 \text{ ftlb}$ becomes the design moment for the MC-200 hull.

The hull pressure and the gas head pressure determine the maximum longitudinal skin stress at the top of the hull.

$$\sigma_{LST} = \frac{2kR_T + p}{t} \left(\frac{R_T R_{LS}}{2R_{LS} + R_T} \right)$$

$$\sigma_{LST} = \frac{.092574 + .56125}{.024} \frac{(1223.934)(40607.008)}{2(40607.008) + 1223.934}$$

$$\sigma_{LST} = (27.24267)(602.8813)$$

$$\sigma_{LST} = 16,424 \text{ lb/in}^2$$

at the bottom of the hull, the maximum transverse stress

$$\sigma_{TSB} = \frac{p}{t} \left(\frac{2R_T R_{LS}}{2R_{LS} + R_T} \right)$$

$$\sigma_{TSB} = \frac{.56125}{.024} (1205.778)$$

$$\sigma_{TSB} = 28,198 \text{ lb/in}^2$$

Skin thickness of .024 on top can be reduced to a lower value; to be practical, the skin thickness on bottom was reduced to $t_B = .022 \text{ in.}$

$$\sigma_{TSB} = \frac{(.56125)}{.022} (1205.778) = 30,761 \text{ lb/in}^2$$



The skin thickness of .020 in. is too thin and .022 in. has to be used. A non-standard skin gage would save weight. Skin thicknesses are reduced on the bottom of the MC-200 hull in the ratio of .022/.024 = .9167. This reduction applies to the lower 120° section of the hull, therefore 120° of the hull, 60° on each side from the lowest station is .022 in. thick and the remaining 240° of hull is .024 in. Longitudinal stress in the skin on top of the hull, at maximum diameter section is:

$$\sigma_{LST} = \frac{p}{t_T} \left(\frac{R_T R_{LS}}{2R_{LS} + R_T} \right)$$

$$\sigma_{LST} = \frac{.56125}{.024} \left(\frac{(1223.93)(40607.008)}{2(40607.008) + 1223.934} \right)$$

$$\sigma_{LST} = \frac{.56125}{.024} (602.88)$$

$$\sigma_{LST} = 14,097 \text{ lb/in}^2 \text{ without imposed moments.}$$

Longitudinal stress in the skin on the bottom of the hull, at maximum diameter

$$\sigma_{LSB} = \frac{p}{t_B} \left(\frac{R_T R_{LS}}{2R_{LS} + R_T} \right)$$

$$\sigma_{LSB} = \frac{.56125}{.022} (602.88) = 15,380 \text{ lb/in}^2$$

Maximum longitudinal stress on top of the hull, at maximum speed immediately aft of the maximum diameter section, with an upward gust

$$\sigma_{LSTM} = \sigma_{LST} - \frac{M_m - M_g}{\pi t_T R_T^2}$$

$$\sigma_{LSTM} = 16424 - \frac{(47.5202 - 4.4443657)(10)^6(12)}{(3.14159)(.024)(1223.934)^2}$$

$$\sigma_{LSTM} = 16424 - 4577 = 11,847 \text{ lb/in}^2$$

Maximum longitudinal stress on top of the hull, at maximum speed, immediately aft of the maximum diameter station, with a downward gust:

$$\sigma_{LSTM} = \sigma_{LST} + \frac{M_m + M_g}{\pi t_T R_T^2}$$

$$\sigma_{LSTM} = 16424 + \frac{(51.963767)(10)^6(12)}{(1.129475)(10)^5}$$

$$\sigma_{LSTM} = 16424 + 5521 = 21,945 \text{ lb/in}^2$$

Maximum longitudinal stress on the bottom of the hull, at maximum speed, immediately aft of the maximum diameter station, with an upward gust

$$\sigma_{LSBM} = \sigma_{LSB} + \frac{M_m - M_g}{\pi t_B R_T^2}$$

$$\sigma_{LSBM} = 15380 + \frac{(47.5202 - 4.443657)(10)^6(12)}{(3.14159)(.022)(1223.934)^2}$$

$$\sigma_{LSBM} = 15380 + \frac{(43.07654)(10)^6(12)}{(1.0353524)(10)^5}$$

$$\sigma_{LSBM} = 15380 + 4993 = 20,373 \text{ lb/in}^2$$

Maximum longitudinal stress on the bottom of the hull at maximum speed, immediately aft of the maximum diameter station, with a downward gust

$$\sigma_{LSBM} = \sigma_{LSB} - \frac{M_m + M_g}{\pi t_B R_T^2}$$

$$\sigma_{LSBM} = 15380 - \frac{(51.963767)(10)^6(12)}{(1.0353524)(10)^5}$$

$$\sigma_{LSBM} = 15380 - 6023 = 9,357 \text{ lb/in}^2$$

MC-100

Similar analysis is now carried out for MC-100.

$$R_T = 80.935 \text{ ft} = 971.436 \text{ in.}$$

$$R_{LS} = \frac{a_s^2}{R_T} = \frac{(466.289)^2}{80.953} = 2,685.823 \text{ ft}$$

$$= 32,230 \text{ in.}$$

$$u = 100 \text{ knots}$$

$$t_T = .020 \text{ in.}$$

With 42 longerons, the maximum peripheral distance between longerons

$$b = \frac{p}{Z} = \frac{2\pi R_T}{Z} = \frac{(6.28318)(971.436)}{42} = 145.32 \text{ in.}$$

$$\xi = (.6287825)(10)^{-6} = \frac{t}{145.32} \sqrt{\frac{t}{971.436}}$$

$$(.3953674)(10)^{-12} (2.11179)(10)^4 (971.436) = t^3 = \xi^2 b^2 R_T$$

$$(.811083989)(10)^{-6} = t^3$$

$$2.009(10)^{-2} = t$$

$$t = .020 \text{ in.}$$

Transverse stress (hoop tension) immediately aft of the maximum diameter station, on top of the hull

$$\sigma_T = 32850 = \frac{2kR_T + p}{t} \left(\frac{2R_T R_{LS}}{2R_{LS} + R_T} \right)$$

from this is computed the air pressure in the hull

$$p = .6876088 - .0734761$$

$$\text{maximum hull pressure} = p = .6141327 \text{ lb/in}^2$$

$$p \approx .6143 \text{ lb/in}^2$$

$$p = (.6143)(12)(2.307) = 17.00 \text{ in. of water column}$$

Transverse stress in the skin at the bottom of the hull,
immediately aft of the maximum diameter station

$$\begin{aligned}\sigma_{TSB} &= \frac{p}{t} \left(\frac{2R_T R_{LS}}{2R_{LS} + R_T} \right) \\ \sigma_{TSB} &= \frac{.6143}{.018} \left(\frac{(2)(971.436)(32230)}{2(32230) + 971.436} \right) \\ \sigma_{TSB} &= (34.1278)(957.01345) \\ \sigma_{TSB} &= 32,661 \text{ lb/in}^2\end{aligned}$$

Transverse stress in the skin at the top of the hull, immed-
iately aft of the maximum diameter station

$$\begin{aligned}\sigma_{TST} &= \frac{2kR_T + p}{t} \left(\frac{2R_T R_{LS}}{2R_{LS} + R_T} \right) \\ \sigma_{TST} &= \frac{.0734761 + .6143}{.020} (957.01345) \\ \sigma_{TST} &= (34.38881)(957.01345) \\ \sigma_{TST} &= 32,911 \text{ lb/in}^2\end{aligned}$$

Longitudinal stress in the skin on top of the hull, immediately
aft of the maximum diameter station

$$\begin{aligned}\sigma_{LST} &= \frac{2kR_T + p}{t} \left(\frac{R_T R_{LS}}{2R_{LS} + R_T} \right) \\ \sigma_{LST} &= \frac{.0734761 + .6143}{.020} (477.74257) \\ \sigma_{LST} &= 16,429 \text{ lb/in}^2\end{aligned}$$

Longitudinal stress in the skin on the bottom of the hull,
immediately aft of the maximum diameter station

$$\begin{aligned}\sigma_{LSB} &= \frac{p}{t} \left(\frac{R_T R_{LS}}{2R_{LS} + R_T} \right) \\ \sigma_{LSB} &= \frac{.6143}{.018} (477.74257) \\ \sigma_{LSB} &= 16,304 \text{ lb/in}^2\end{aligned}$$

Maximum aerodynamic moment, at sea level on MC-100

$$M_{ae} = (.02) (\gamma/2g) u^2 V^{2/3} L \text{ ftlb}$$

$$M_{ae} = (.02) \left(\frac{.076475}{64.348} \right) (168.9)^2 \left(10(10)^6 \right)^{2/3} (728.576)$$

$$M_{ae} = 22.9306(10)^6 \text{ ftlb}$$

Maximum gas head moment, at sea level

$$M_g = (.20) \pi k R_T^4$$

$$M_g = (.20) (3.14159) (.06535) (80.953)^4$$

$$M_g = 1.76342(10)^6 \text{ ftlb}$$

Maximum gust moment, at sea level, with 35 ft/s gust and maximum speed

$$M_m = (.10) \frac{\gamma}{2g} u c V^{2/3} L$$

$$M_m = (.10) \left(\frac{.076475}{64.348} \right) (168.9) (35.0) \left(10(10)^6 \right)^{2/3} (728.576)$$

$$M_m = 23.7588(10)^6 \text{ ftlb}$$

Maximum longitudinal stress in the skin on top of the hull, at maximum speed, immediately aft of the maximum diameter station, with upward gust

$$\sigma_{LST_M} = \sigma_{LST} - \frac{M_m - M_g}{\pi t_T R_T^2}$$

$$\sigma_{LST_M} = 16429 - \frac{(23.7588 - 1.76342)(10)^6 (12)}{(3.14159) (.020) (971.436)^2}$$

$$\sigma_{LST_M} = 16429 - \frac{(21.99538)(10)^6 (12)}{59293.6096}$$

$$\sigma_{LST_M} = 16429 - 4451 = 11,978 \text{ lb/in}^2$$

Maximum longitudinal stress in the skin on top of the hull, immediately aft of the maximum diameter station with downward gust (@ max speed):

$$\begin{aligned}\sigma_{LSTM} &= \sigma_{LST} + \frac{M_m + M_g}{\pi t_T R_T^2} \\ \sigma_{LSTM} &= 16429 + \frac{(25.5222)(10)^6(12)}{59293.6096} \\ \sigma_{LSTM} &= 16429 + 5165 = 21,594 \text{ lb/in}^2\end{aligned}$$

Maximum longitudinal stress in the skin on the bottom of the hull, immediately aft of the maximum diameter station with upward gust (@ max speed):

$$\begin{aligned}\sigma_{LSBM} &= \sigma_{LSB} + \frac{M_m - M_g}{t_B R_T^2} \\ \sigma_{LSBM} &= 16304 + \frac{(21.99538)(10)^6(12)}{(3.14159)(.018)(971.436)^2} \\ \sigma_{LSBM} &= 16304 + \frac{263.94456(10)^6}{53364.2487} \\ \sigma_{LSBM} &= 16304 + 4946 = 21,250 \text{ lb/in}^2\end{aligned}$$

Maximum longitudinal stress in the skin on the bottom of the hull, immediately aft of the maximum diameter station, with a downward gust (@ max speed):

$$\begin{aligned}\sigma_{LSBM} &= \sigma_{LSB} - \frac{M_m + M_g}{\pi t_B R_T^2} \\ \sigma_{LSBM} &= 16304 - \frac{(25.2552)(10)^6(12)}{53364.2487} \\ \sigma_{LSBM} &= 16304 - \frac{(303.0624)(10)^6}{53364.2487} \\ \sigma_{LSBM} &= 16304 - 5673 = 10,631 \text{ lb/in}^2\end{aligned}$$

Similar analysis for MC-125

$$R_T = 87.204 \text{ ft} = 1046.45 \text{ in.}$$

$$L = 784.837 \text{ ft} = 9418.00 \text{ in.}$$

$$u = 100 \text{ knots} \quad Z = 42 \text{ longerons}$$

$$R_{LS} = \frac{(L(.64))^2}{R_T} = \frac{((784.837)(.64))^2}{R_T} = 2,893.212 \text{ ft}$$

$$= \frac{a_s^2}{R_T} = 34,718.5 \text{ in.}$$

$$M_{ae} = (.02) \frac{\gamma}{2g} u^2 V^{2/3} L$$

$$M_{ae} = (.02) \left(\frac{.076475}{64.348} \right) (168.9)^2 (12.5(10)^6)^{2/3} (784.835)$$

$$M_{ae} = 28.5448(10)^6 \text{ ftlb}$$

Gas head moment

$$M_g = (.20) \pi k R_T^4$$

$$M_g = (.20) (3.14159) (.06535) (87.204)^4$$

$$M_g = 2.37449(10)^6 \text{ ftlb}$$

Gust moment

$$M_m = (.10) \frac{\gamma}{2g} u c V^{2/3} L$$

$$M_m = (.10) \left(\frac{.076475}{64.348} \right) (168.9) (35.0) (12.5(10)^6)^{2/3} (784.835)$$

$$M_m = 29.5882(10)^6 \text{ ftlb}$$

Determination of maximum skin thickness

$$b = \frac{2\pi R_T}{Z} = \frac{(6.283185)(87.204)}{42} (12) = 156.55 \text{ in.}$$

$$t^3 = \frac{(.395295)(10)^{-12}}{(24507.9)(1046.448)} = (10.137831)(10)^{-6}$$

$$t = .0216 \text{ in. maximum}$$

Nearest standard gage $t = .022 \text{ in.}$

Maximum flight pressure (similarly as for MC-200 and MC-100)

$$\begin{aligned}\sigma_{T_{Max}} &= 32850 = \frac{2kR_T + p}{t} \left(\frac{2R_T R_{LS}}{2R_{LS} + R_T} \right) \\ 32850 &= \frac{(2)(3.7818287)(10)^{-5}(1046.45) + p}{.022} \times \\ &\quad \left(\frac{(2)(1046.45)(34718.5)}{(2)(34718.5) + 1046.45} \right)\end{aligned}$$

$$p = \frac{638.6065}{1062.4618} = .60106 \text{ lb/in}^2$$

$$p = (12)(2.307)(.60106) = 16.6397 \text{ in of water}$$

Transverse stress in the skin at the bottom of the hull, immediately aft of the maximum diameter station

$$\begin{aligned}\sigma_{T_{SB}} &= \frac{p}{t_B} \left(\frac{2R_T R_{LS}}{2R_{LS} + R_T} \right) \\ \sigma_{T_{SB}} &= \frac{.60106}{.022} \left(\frac{(2)(1046.45)(34718.5)}{(2)(34718.5) + 1046.45} \right) \\ \sigma_{T_{SB}} &= (27.321)(1030.9136) = 28,166 \text{ lb/in}^2 \\ \text{with } t_B &= .020 \text{ in,}\end{aligned}$$

The hoop stress at the bottom of the hull will be, with $t_B = .020$ in:

$$\sigma_{T_{SB}} = \frac{.60106}{.020} (1030.9136) = 30,982 \text{ lb/in}$$

This is acceptable.

Longitudinal stress in the skin on top of the hull, immediately aft of the maximum diameter station

$$\begin{aligned}\sigma_{L_{ST}} &= \frac{2kR_T + p}{t_T} \left(\frac{R_T R_{LS}}{2R_{LS} + R_T} \right) \\ \sigma_{L_{ST}} &= \frac{(2)(3.7818287)(10)^{-5}(1046.45) + .60106}{.022} (515.4568) \\ \sigma_{L_{ST}} &= (30.91863)(515.4568) = 15,937 \text{ lb/in}^2\end{aligned}$$



Longitudinal stress in the skin on the bottom of the hull, immediately aft of the maximum diameter station

$$\sigma_{LSB} = \frac{p}{t_B} \left(\frac{R_T R_{LS}}{2R_{LS} + R_T} \right)$$

$$\sigma_{LSB} = \frac{.60106}{.020} (515.4568)$$

$$\sigma_{LSB} = 15,491 \text{ lb/in}^2$$

Maximum longitudinal stress in the skin on top of the hull, at maximum speed, immediately aft of the maximum diameter station, with upward gust

$$\sigma_{LSTM} = \sigma_{LST} - \frac{M_m - M_g}{\pi t_T R_T^2}$$

$$\sigma_{LSTM} = 15937 - \frac{(29.5882 - 2.37449)(10)^6(12)}{(3.14159)(.022)(1045.45)^2}$$

$$\sigma_{LSTM} = 15937 - 4315 = 11,622 \text{ lb/in}^2$$

Maximum longitudinal stress in the skin on top of the hull, immediately aft of the maximum diameter station with downward gust (@ max speed):

$$\sigma_{LSTM} = \sigma_{LST} + \frac{M_m + M_g}{\pi t_T R_T^2}$$

$$\sigma_{LSTM} = 15937 + \frac{(29.5882 + 2.37449)(10)^6(12)}{7.5684885(10)^4}$$

$$\sigma_{LSTM} = 15937 + 5068 = 21,005 \text{ lb/in}^2$$

Maximum longitudinal stress in the skin on the bottom of the hull, immediately aft of the maximum diameter station with upward gust (@max speed):

$$\sigma_{LSBM} = \sigma_{LSB} + \frac{M_m - M_g}{\pi t_B R_T^2}$$

$$\sigma_{LSB_M} = 15491 + \frac{(27.21371)(10)^6(12)}{(3.14159)(.020)(1046.45)^2}$$

$$\sigma_{LSB_M} = 15491 + \frac{(3.265645)(10)^6}{6.880444(10)^4}$$

$$\sigma_{LSB_M} = 15491 + 4740 = 20,237 \text{ lb/in}^2$$

Maximum longitudinal stress in the skin on the bottom of the hull, immediately aft of the maximum diameter station, with downward gust (@ max speed):

$$\sigma_{LSB_M} = \sigma_{LSB} - \frac{M_m + M_g(12)}{\pi t_B R_T^2}$$

$$\sigma_{LSB_M} = 15491 - \frac{3.8355228(10)^8}{6.880444(10)^4}$$

$$\sigma_{LSB_M} = 15491 - 5575 = 9,916 \text{ lb/in}^2$$

MC-150

$$R_T = 92.6688 \text{ ft} = 1,120.3 \text{ in.}$$

$$L = 834.01875 \text{ ft} = 10,008.23 \text{ in.}$$

$$u = 100 \text{ knots} \quad z = 44 \text{ longerons}$$

$$R_{LS} = \frac{a_s^2}{R_T} = \frac{((834.01875)(.64))^2}{92.6688} = 3,074 \text{ ft}$$

$$= 36,894.4 \text{ in.}$$

Aerodynamic moment, at sea level

$$M_{ae} = (.02) q V^{2/3} L \quad q = \frac{\gamma}{2g} u^2$$

$$M_{ae} = (.02)(33.9034) \left(15(10)^6\right)^{2/3} (834.01875)$$

$$M_{ae} = 35.6385(10)^6 \text{ ft lb}$$

Gas head moment, at sea level

$$M_g = (.20) \pi k R_T^4$$

$$M_g = (.20)(3.14159)(.06535)(92.6688)^4$$

$$M_g = 3.02802(10)^6 \text{ ft lb}$$

Gust moment, at sea level, $c = 35 \text{ ft/s}$

$$M_m = (.10) \frac{\gamma}{2g} u c V^{2/3} L$$

$$M_m = (.10) \left(\frac{.076475}{64.348} \right) (168.9) (35.0) \left(15(10)^6 \right)^{2/3} (834.01875)$$

$$M_m = 35.6384(10)^6 \text{ ft lb}$$

Determination of the maximum skin thickness

$$b = \frac{2\pi R_T}{Z} = \frac{(6.283185)(1120.3)}{44} = 159.98 \text{ in.}$$

$$t^3 = \xi^2 b^2 R_T$$

$$t^3 = \left((.62878)(10)^{-6} \right)^2 (159.98)^2 (1120.3)$$

$$t^3 = (11336.0866)(10)^{-9}$$

$$t = .0224 \text{ in.}$$

Nearest standard gage $t = .024 \text{ in.}$

Maximum flight pressure from

$$\sigma_T = \frac{2kR_T + p}{t} \left(\frac{2R_T R_{LS}}{2R_{LS} + R_T} \right)$$

$$32850 = \frac{(2)(3.7818287)(10)^{-5}(1120.3) + p}{.024} \times$$

$$\left(\frac{(2)(1120.3)(36894.4)}{(2)(36894.4 + 1120.3)} \right)$$

$$p = \frac{694.69}{1103.5454} = .62968 \text{ lb/in}^2$$

$$p = (12)(2.307)(.62968) = 17.432 \text{ in. of water}$$

Transverse stress in the skin at the bottom of the hull,
immediately aft of the maximum diameter station

$$\sigma_{TSB} = \frac{p}{t} \left(\frac{2R_T R_{LS}}{2R_{LS} + R_T} \right)$$

$$\sigma_{TSB} = \frac{.62968}{.024} \left(\frac{(2)(1120.3)(36894.4)}{2(36894.4) + 1120.3} \right)$$

$$\sigma_{TSB} = (26.2367)(1103.545)$$

$$\sigma_{TSB} = 28,953 \text{ lb/in}^2$$

The hoop stress at the bottom of the hull will be ($t_B = .022$)

$$\sigma_{TSB} = \frac{.62968}{.022} (1103.545) = 31,585 \text{ lb/in}^2$$

The skin on the bottom of the hull at maximum diameter

$$t_B = .022 \text{ in}$$

Longitudinal stress in the skin on top of the hull immediately
aft of the maximum diameter station

$$\sigma_{LST} = \frac{2kR_T + p}{t_T} \left(\frac{R_T R_{LS}}{2R_{LS} + R_T} \right)$$

$$\sigma_{LST} = \frac{(2)(3.7818287)(10)^{-5}(1120.3) + .62968}{.024} (551.773)$$

$$\sigma_{LST} = \frac{.714416}{.024} (551.773)$$

$$\sigma_{LST} = 16,425 \text{ lb/in}^2$$

Longitudinal stress in the skin on the bottom of the hull,
immediately aft of the maximum diameter station

$$\sigma_{LSB} = \frac{p}{t_B} \left(\frac{R_T R_{LS}}{2R_{LS} + R_T} \right)$$

$$\sigma_{LSB} = \frac{.62968}{.022} (551.773)$$

$$\sigma_{LSB} = 15,793, \text{ lb/in}^2$$

Longitudinal stress in the skin on top of the hull, immediately aft of the maximum diameter station, with upward gust (@ max speed):

$$\sigma_{LSTM} = \sigma_{LST} - \frac{M_m - M_g}{\pi t_T R_T^2}$$

$$\sigma_{LSTM} = 16425 - \frac{(35.6385 - 3.02802)(10)^6(12)}{3.14159(.024)(1120.3)^2}$$

$$\sigma_{LSTM} = 16425 - \frac{3.913258(10)^8}{9.463013(10)^4}$$

$$\sigma_{LSTM} = 16425 - 4135 = 12,290 \text{ lb/in}^2$$

Maximum longitudinal stress in the skin on top of the hull, immediately aft of the maximum diameter station, with downward gust (@ max speed):

$$\sigma_{LSTM} = \sigma_{LST} + \frac{M_m + M_g}{\pi t_T R_T^2}$$

$$\sigma_{LSTM} = 16425 + \frac{(38.66652)(10)^6(12)}{9.463013(10)^4}$$

$$\sigma_{LSTM} = 16425 + 4903 = 21,328 \text{ lb/in}^2$$

Maximum longitudinal stress in the skin on the bottom of the hull, immediately aft of the maximum diameter station, with upward gust (@ max speed):

$$\sigma_{LSBM} = \sigma_{LSB} + \frac{M_m - M_g}{\pi t_B R_T^2}$$

$$\sigma_{LSBM} = 15793 + \frac{(3.913258)(10)^8}{8.6744282(10)^4}$$

$$\sigma_{LSBM} = 15793 + 4511 = 20,304 \text{ lb/in}^2$$

Maximum longitudinal stress in the skin on the bottom of the hull, immediately aft of the maximum diameter station, with downward gust (@ max speed):

$$\begin{aligned}\sigma_{LSBM} &= \sigma_{LSB} - \frac{M_m + M_g}{\pi t_B R_T^2} \\ \sigma_{LSBM} &= 15793 - \frac{38.66652(10)^6(12)}{(3.14159)(.022)(1120.3)^2} \\ \sigma_{LSBM} &= 15793 - \frac{4.6399824(10)^8}{8.6744282(10)^4} \\ \sigma_{LSBM} &= 15793 - 5349 = 10,444 \text{ lb/in}^2\end{aligned}$$

MC-175

$$R_T = 97.554 \text{ ft} = 1170.65 \text{ in.}$$

$$L = 877.987 \text{ ft} = 1053.584 \text{ in.}$$

$$u = 100 \text{ knots} \quad Z = 46 \text{ longerons}$$

$$\begin{aligned}R_{LS} &= \frac{a_s^2}{R_T} = \frac{((877.987)(.64))^2}{97.554} = 3236.515 \text{ ft} \\ &= 38839.4 \text{ in.}\end{aligned}$$

Aerodynamic moment at sea level

$$\begin{aligned}M_{ae} &= (.02)qV^{2/3}L \\ q &= \frac{\gamma}{2g}u^2 = 33.9034 \text{ lb/ft}^2 \text{ @ } 100 \text{ knots.} \\ M_{ae} &= (.02)(33.9034) \left(17.5(10)^6\right)^{2/3} (877.987) \\ M_{ae} &= 40.1286(10)^6 \text{ ftlb}\end{aligned}$$

Gas head moment at sea level

$$\begin{aligned}M_g &= (.20)\pi k R^4 \\ M_g &= (.20)(3.14159)(.06535)(97.554)^4 \\ M_g &= 3.71882(10)^6 \text{ ftlb}\end{aligned}$$

Gust moment, $c = 35.0 \text{ ft/s}$ at full speed, at sea level

$$M_m = (.10)\frac{\gamma}{2g}cuV^{2/3}L$$

$$M_m = (.10) \left(\frac{.076475}{64.348} \right) (168.9) (35.0) \left(17.6(10)^6 \right)^{2/3} (877.987)$$

$$M_m = 41.5775(10)^6 \text{ ftlb}$$

Determination of maximum thickness of skin at maximum hull section

$$b = \frac{2\pi R_T}{46} = \frac{(6.28318)(1170.65)}{46} = 159.90 \text{ in.}$$

$$\xi^2 = (.395295)(10)^{-12} = \frac{t^3}{(159.9)^2 (1170.65)} = \frac{t^3}{b^2 P_T}$$

$$t^3 = 11.83165(10)^{-6}$$

$$t = .0228 \text{ in.}$$

Nearest standard gage $t = .024 \text{ in.}$

Maximum flight pressure, for $\sigma_T = 32,850 \text{ lb/in}^2$

Hoop stress on top of the hull

$$\sigma_T = \frac{2kR_T + p}{t} \left(\frac{2R_T R_{LS}}{2R_{LS} + R_T} \right)$$

$$32850 = \frac{(2)(3.7818287)(10)^{-5}(1170.65) + p}{.024} \times \left(\frac{(2)(1170.65)(38839.4)}{(2)(38839.4) + 1170.65} \right)$$

$$p = \frac{686.22}{1154.0} = .59464 \text{ lb/in}^2$$

$$p = (12)(2.307)(.59464) = 16.47 \text{ in. of water}$$

Transverse stress in the skin at the bottom of the hull, immediately aft of the maximum diameter station

$$\sigma_{TSB} = \frac{p}{t} \left(\frac{2R_T R_{LS}}{2R_{LS} + R_T} \right)$$

$$\sigma_{TSB} = \frac{.59464}{.024} \left(\frac{(2)(1170.65)(38839.4)}{(2)(38839.4) + 1170.65} \right)$$

$$\sigma_{TSB} = (24.7767)(1153.2698)$$

$$\sigma_{TSB} = 28,574 \text{ lb/in}^2$$

The hoop stress at the bottom of the hull will be: ($t_B = .022$)

$$\sigma_{TSB} = \frac{.59464}{.022} (1153.2698) = 31,172 \text{ lb/in}^2$$

The skin on the bottom of the hull at maximum diameter is

$$t_B = .022 \text{ in.}$$

Longitudinal stress in the skin on top of the hull, immediately aft of the maximum diameter station

$$\begin{aligned} \sigma_{LST} &= \frac{2kR_T + p}{t_T} \left(\frac{R_T R_{LS}}{2R_{LS} R_T + R_T} \right) \\ \sigma_{LST} &= \frac{(2)(3.7818287)(10)^{-5}(1170.65) + .59464}{.024} (576.6349) \\ \sigma_{LST} &= \frac{.683184}{.024} (516.6349) = 14,707 \text{ lb/in}^2 \end{aligned}$$

Longitudinal stress in the skin on the bottom of the hull, immediately aft of the maximum diameter station

$$\begin{aligned} \sigma_{LSB} &= \frac{p}{t_B} \left(\frac{R_T R_{LS}}{2R_{LS} + R_T} \right) \\ \sigma_{LSB} &= \frac{.59464}{.022} (576.6349) = 15,586 \text{ lb/in}^2 \end{aligned}$$

Longitudinal stress in the skin on top of the hull, immediately aft of the maximum diameter station, with upward gust (@ max speed):

$$\begin{aligned} \sigma_{LSTM} &= \sigma_{LST} - \frac{M_m - M_g}{\pi t_T R_T^2} \\ \sigma_{LSTM} &= 14707 - \frac{(41.5775 - 3.71882)(10)^6(12)}{(3.14159)(.024)(1170.65)^2} \\ \sigma_{LSTM} &= 14707 - \frac{4.543042(10)^8}{10.3327254(10)^4} \\ \sigma_{LSTM} &= 14707 - 4397 = 10,310 \text{ lb/in}^2 \end{aligned}$$

Maximum longitudinal stress in the skin on top of the hull, immediately aft of the maximum diameter station, with downward gust (@ max speed):

$$\begin{aligned}\sigma_{LST_M} &= \sigma_{LST} + \frac{M_m + M_g}{\pi t_T R_T^2} \\ \sigma_{LST_M} &= 14707 + \frac{(41.5775 + 3.71882)(10)^6(12)}{10.3327254(10)^4} \\ \sigma_{LST_M} &= 14707 + \frac{45.29632(10)^6(12)}{10.3327254(10)^4} \\ \sigma_{LST_M} &= 14707 + 5261 = 19,968 \text{ lb/in}^2\end{aligned}$$

Maximum longitudinal stress in the skin on the bottom of the hull, immediately aft of the maximum diameter station, with upward gust (@max speed):

$$\begin{aligned}\sigma_{LSB_M} &= \sigma_{LSB} + \frac{M_m - M_g}{\pi t_B R_T^2} \\ \sigma_{LSB_M} &= 15586 + \frac{4.542816(10)^8}{(3.14159)(.022)(1170.65)^2} \\ \sigma_{LSB_M} &= 15586 + \frac{4.542816(10)^8}{9.4716649(10)^4} \\ \sigma_{LSB_M} &= 15586 + 4796 = 20,382 \text{ lb/in}^2\end{aligned}$$

Maximum longitudinal stress in the skin on the bottom of the hull, immediately aft of the maximum diameter station, with downward gust(@ max speed):

$$\begin{aligned}\sigma_{LSB_M} &= \sigma_{LSB} - \frac{M_m + M_g}{\pi t_B R_T^2} \\ \sigma_{LSB_M} &= 15586 - \frac{(45.29632)(10)^6(12)}{9.4716649(10)^4} \\ \sigma_{LSB_M} &= 15586 - 5739 = 9,847 \text{ lb/in}^2\end{aligned}$$

The hull skin is loaded by a transverse (or hoop) stress, a longitudinal stress and shear stress, everywhere on the surface of the hull; the preceeding analysis took up only the stress state at the maximum hull diameter with maximum loading.

The highest principal stress in the hull skin arises in the region above and below its equator

The principal stress in tension is:

$$\sigma_o = \frac{\sigma_T + \sigma_L}{2} \pm \sqrt{\tau^2 + \left(\frac{\sigma_T - \sigma_L}{2}\right)^2}$$

and in shear:

$$\tau_o = \sqrt{\left(\frac{\sigma_T - \sigma_L}{2}\right)^2 + \tau^2}$$

The shear load on the skin is the lift load forward or aft of each main frame, up to one half of the distance between adjacent main frames.

The lift load is reduced by the weight of skin, fabric diaphragm, one secondary frame and longerons; all these weights can be assumed to be lifted directly by the gas. The weight of the main frame has to be supported by skin shear as well as the weight loads acting on the main frame.

In MC-200, at maximum hull diameter, the total lift on the hull section one half the distance between main frames forward and aft is 164,098 lb.* (Refer to 1.8). One half of this lift acts forward and one half acts aft of the frame. The lift acting forward or aft of the frame is also divided, one half acting on the port side and one half acting on the starboard side of the hull; therefore, the maximum lift on each side of the hull forward or aft of frame station 334.50 is:

$$L = 1/4 (164098) = 41,024 \text{ lb}$$

The weight of skin on port or starboard side of the hull, forward or aft of the maximum diameter main frame is:

$$\begin{aligned} W_{\text{skin}} &= 1/4 \gamma \cdot P \cdot 2 \left((120/360)t_B + (240/360)t_T \right) \\ W_S &= (.25)(.102)(2\pi)(1223.934)(12)(104) \left((.333)(.022) \right. \\ &\quad \left. + (.667)(.024) \right) \end{aligned}$$

* @ 10,000 ft

$$W_s = (244733) (.00735 + .01601)$$

$$W_s = 5,711.6 \text{ lb}$$

Weight of longerons (approximately):

$$\text{Area of longeron } A_L = .57 \text{ in}^2$$

$$\text{Adjustment for weight } (1.25)(.57) = .7125 \text{ in}^2$$

$$\text{Volume per 1 ft } V = (12)(.7125) = 8.55 \text{ in}^3$$

$$\text{Weight per 1 ft } W_L = (.102)(8.55) = .872 \text{ lb}$$

In the hull section considered:

$$W_L = (52)(24)(.872) = 1,088 \text{ lb}$$

Weight of one half of secondary frame (approximately):

$$W_f = 2.02 \text{ lb/ft}$$

$$P = 2\pi R = 7690.2 \text{ in}$$

$$P/2 = 3845.1 \text{ in} = 320.425 \text{ ft}$$

$$W_f = (2.02)(320.425) = 647.26 \text{ lb}$$

One half of cell membrane weight lifted directly either forward or aft of the main frame:

$$W_{\text{diaphragm}} = 1/2 \pi R Y \left(\frac{l}{2} + R \right)$$

$$W_{\text{diaphragm}} = 1/2 \pi (102) \left(\frac{6.4}{16} (9) \right) (52+102) \text{ lb}$$

$$W_{\text{diaphragm}} = 1,095.5 \text{ lb}$$

Structural weights of one half of the hull lifted directly by gas either forward or aft of the maximum diameter main frame are:

Weight of skin	5712 lb
Weight of longerons	1088 "
Weight of one half of secondary frame	647 "
Weight of one half diaphragm	1097 "
	<hr/>
	8,544 lb

The lift shear load acting on either the forward or aft side of the maximum diameter main frame is:

$$Q = 41024 - 8544 = 32,480 \text{ lb}$$

The unit shear forward or aft of the maximum diameter main frame is:

$$V = \frac{QR}{\pi R^2} \frac{\sin \theta}{\cos \theta} \text{ lb/in.}$$

Q = total transverse shear

The highest shear is at $\theta = 0^\circ$ (at equator)

$$V = \frac{QR \cdot \sin \theta \tan \theta}{\pi R^2} \cos \theta \text{ lb/in}$$

$$V = \frac{QR}{\pi R^2} \text{ at equator (on each side of the main frame)}$$

Principal stress:

$$\sigma_{o_{\max \min}} = \frac{\sigma_T + \sigma_L}{2} \pm \frac{1}{2} \sqrt{4\tau^2 + (\sigma_T - \sigma_L)^2}$$

$$\sigma_{LST} = \text{longitudinal tension, } 14,097 \text{ lb/in}^2$$

$$\sigma_{TST} = \text{transverse tension, } 32,850 \text{ lb/in}^2$$

Shear per unit length of perimeter at equator,

$$V = \frac{Q}{\pi R} = \frac{32,480}{(3.14159)(1223.934)} = 8.4471, \text{ lb/in.}$$

Shear stress at equator,

$$\tau = \frac{V}{t} = \frac{8.4471}{.024} = 351.96 \text{ lb/in}^2$$

$$\sigma_{TST} = 32,850 \text{ lb/in}^2$$

$$\sigma_{LST} = 14,097 \text{ lb/in}^2$$

Principal stress in the skin at equator,

$$\sigma_o = \frac{32850 + 14097}{2} \pm \frac{1}{2} \sqrt{(352.0)^2(4) + (32850 - 14097)^2}$$

$$\sigma_o = 23474 + \frac{1}{2} \sqrt{495616 + (351.675)(10)^6}$$

$$\sigma_o = 23474 + 9383$$

$\sigma_o = 32,857 \text{ lb/in}^2$ (maximum) This still can be considered within factor of safety of 2.

At 45° with respect to the planes of σ_{\max} . and σ_{\min} are the planes of the maximum shear stress

The principal shear stress is:

$$\tau_o = \sqrt{\left(\frac{\sigma_{TST} - \sigma_{LST}}{2}\right)^2 + \tau^2}$$

$$\tau_o = \sqrt{(9372)^2 + (352.0)^2} = \sqrt{87.9383(10)^6}$$

$$\tau_o = 9,376 \text{ lb/in}^2$$

All stresses are without the contributing effect of areas of longerons and therefore, conservative.

Cross-section area of skin at maximum diameter,

$$A_s = \frac{240}{360} (2\pi R_T) t_T + \frac{(120)}{360} (2\pi R_T) t_B$$

$$A_s = (.667)(6.28318)(1223.934)(.024) + (.333)(6.28318) \times (1223.934)(.022)$$

$$A_s = (1.23105)(10)^2 + (.563384)(10)^2 = 179.44 \text{ in}^2$$

Area of 48 longerons,

$$A_L = (48)(.57) = 27.36 \text{ in}^2$$

Ratio: $\frac{A_L}{A_s} = \frac{27.36}{174.32} = .15695$ This ratio is high and further analysis should reduce it.

When the maximum volume cell is deflated and the air pressure is also lost, the skin cannot contribute to the strength of the hull significantly; this is described in Section 1.8 and also in later Sections of this report. At this time it is useful to determine the maximum moments that may arise at $u = 52$ knots (the maximum speed with deflated cell) and 35 ft/sec maximum gust velocity.

MC-200

Case of deflated maximum volume cell.

Aerodynamic moment at 52 knots is: $(M_{ac} = (.02) \frac{\gamma}{2g} u^2 V^{2/3} L)$

$$M_{ae} = (.020) \left(\frac{.076475}{64.348} \right) (87.78)^2 \left(20(10)^6 \right)^{2/3} (918)$$

$$M_{ae} = 12.38732 (10)^6 \text{ftlb}$$

Gas moment $M_g = 0.0$ (zero) at the deflated cell

$$\text{Gust moment: } M_m = (.1) \left(\frac{.076475}{64.348} \right) (87.77600) (35) \left(20(10)^6 \right)^{2/3} \times (918)$$

$$M_m = 24.694485 (10)^6 \text{ftlb}$$

This moment has to be resisted by the longerons of the hull with the small contribution from the skin on the tension side of the hull; this contribution is disregarded.

A similar analysis is now described for MC-100 with the purpose of interpolating the skin thicknesses for other intermediate size hulls, between MC-100 and MC-200 values.

The shear load on the skin is the lift load forward or aft of each main frame, up to one half of the distance between adjacent main frames.

The lift load is reduced by the weight of skin, fabric diaphragm, one secondary frame and longerons; all these weights can be assumed to be lifted directly by gas. The weight of the main frame has to be supported by skin shear as well as the weight loads acting on the main frame.

Analysis similar to MC-200 is repeated here for the MC-100 hull, with analysis for MC-125, MC-150 and MC-175, not shown in this report because of similarity. The maximum lift on each side of the MC-100 hull, forward and aft of the maximum diameter main frame No. 262.287, (Section 1.8, page 56) is:

$$L = 1/4 (82500)^* = 20,625 \text{ lb} \quad * \text{at } 10,000 \text{ ft}$$

The weight of skin on port or starboard side of the hull, forward or aft of the maximum diameter main frame is:

$$W_{\text{skin}} = \frac{1}{4} \cdot \gamma \cdot P \cdot L (120/360 t_B + 240/360 t_T)$$

$$W_{\text{skin}} = (.25) (.102) (2\pi) (971.44) (83) (12) \left((.3333) (.018) + (.6667) (.020) \right)$$

$$W_{\text{skin}} = (155023) \left((.006) + .0133 \right)$$

$$W_{\text{skin}} = 2,992 \text{ lb}$$

Weight of longerons (approximately):

$$\text{Weight per 1 ft} = .62 \text{ lb}$$

In the hull section considered:

$$W_L = (41.5)(21)(.62) = 540.3 \text{ lb}$$

Weight of one half of the secondary frame (approximately):

$$W_f = 1.3 \text{ lb/ft}$$

In the hull section considered:

$$W_f = (1.3)(\pi r) = (1.3)(\pi)(80.953) = 371.5 \text{ lb}$$

One half of the cell diaphragm weight lifted directly either forward or aft of the main frame is:

$$W_{\text{diaphragm}} = \frac{1}{2} \pi R_Y \cdot \left(\frac{1}{2} + R\right)$$

$$W_{\text{diaphragm}} = (.5)(3.14159)(80.953)(.04444)(41.5 + 80.953)$$

$$W_{\text{diaphragm}} = 691.98 \approx 692 \text{ lb}$$

Structure weights of one half hull, lifted directly by gas either forward or aft of the maximum diameter main frame are:

Weight of skin	2992 lb
Weight of longerons	540 "
Weight of one half secondary frame	372 "
Weight of diaphragm	692 "
	<hr/> 4596 lb

Lift shear load acting on either forward or aft side of the maximum diameter main frame is:

$$Q = \frac{82500}{4} - 4596 = 16,029 \text{ lb}$$

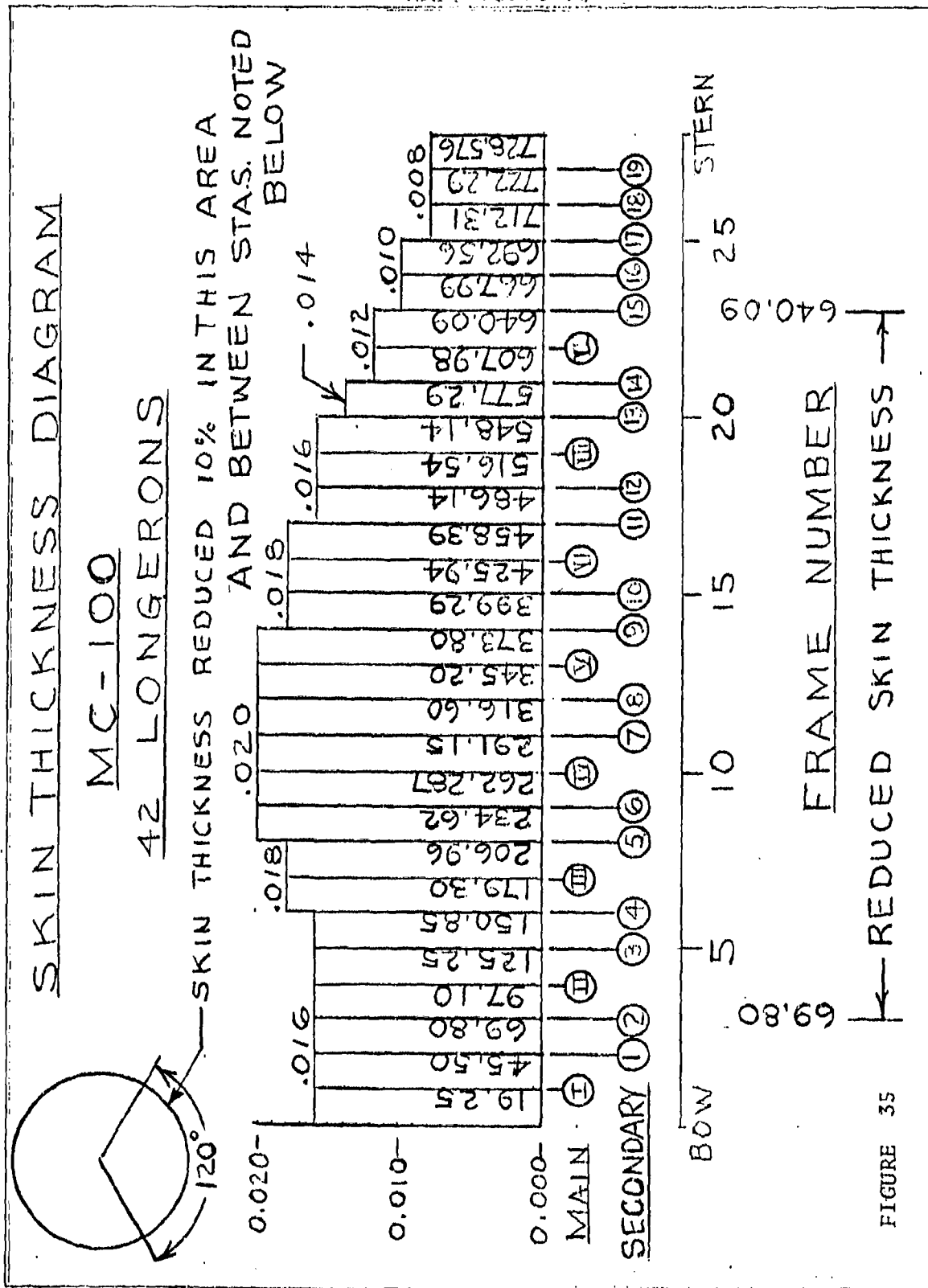
$$V = \frac{Q}{\pi R} = \frac{16029}{(971.44)} = 5.2522 \text{ lb/in (=shear/unit length of perimeter at the equator).}$$

Shear stress at equator:

$$\tau = \frac{V}{t} = \frac{5.2522}{.020} = 262.6 \text{ lb/in}^2$$

$$\sigma_{TST} = 32,850 \text{ lb/in}^2$$

$$\sigma_{LST} = 16,425 \text{ lb/in}^2$$



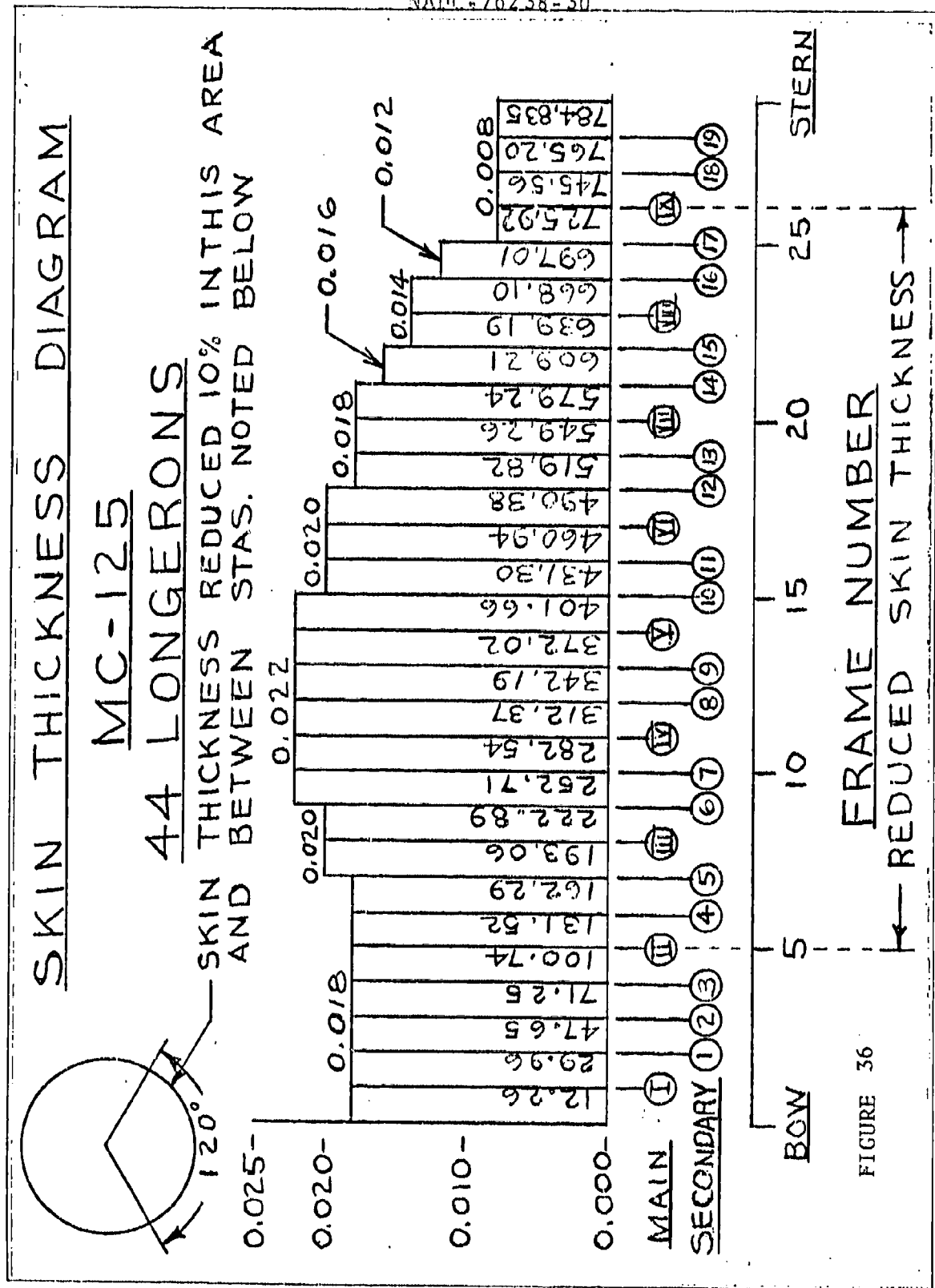
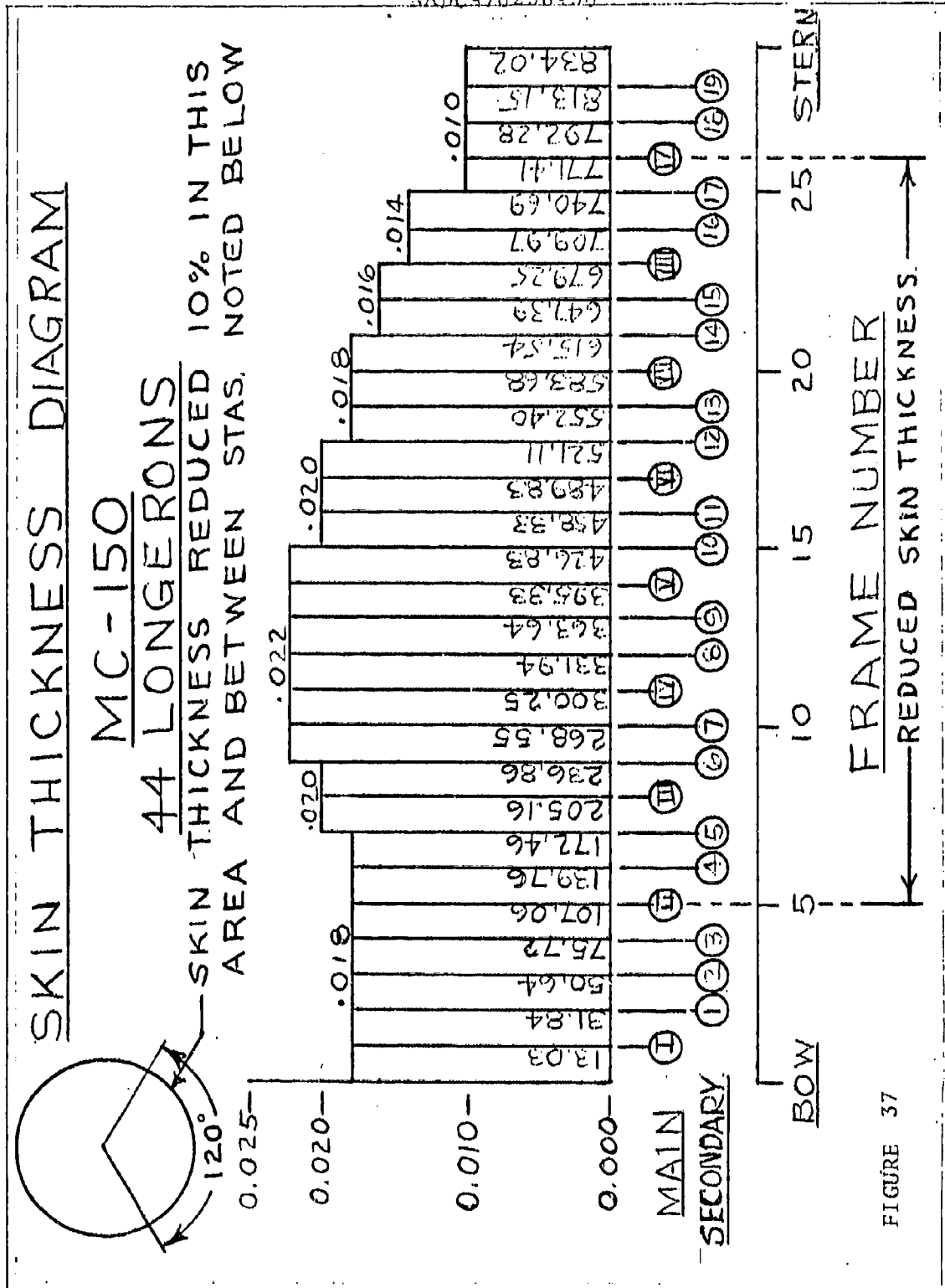


FIGURE 36



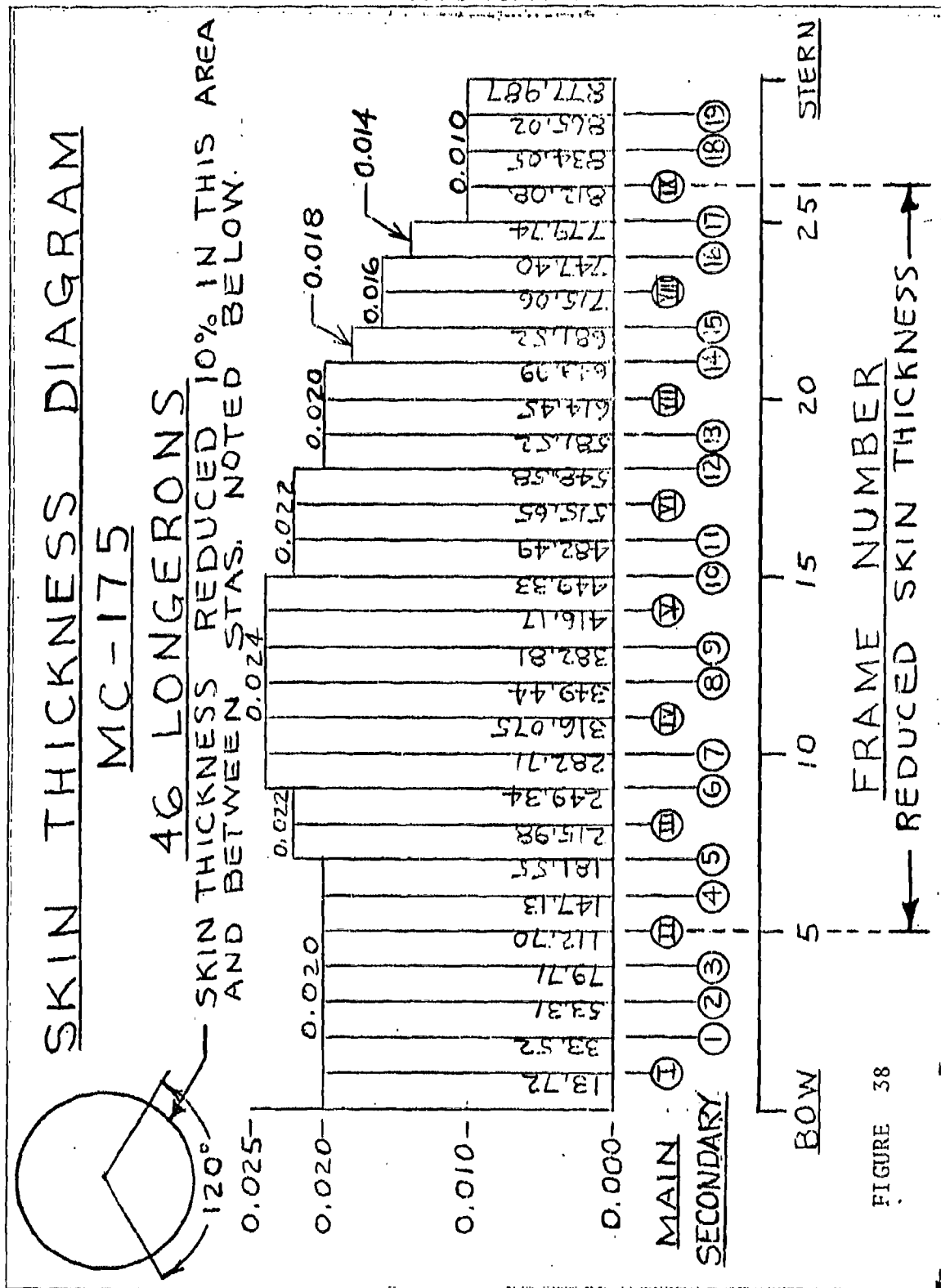


FIGURE 38

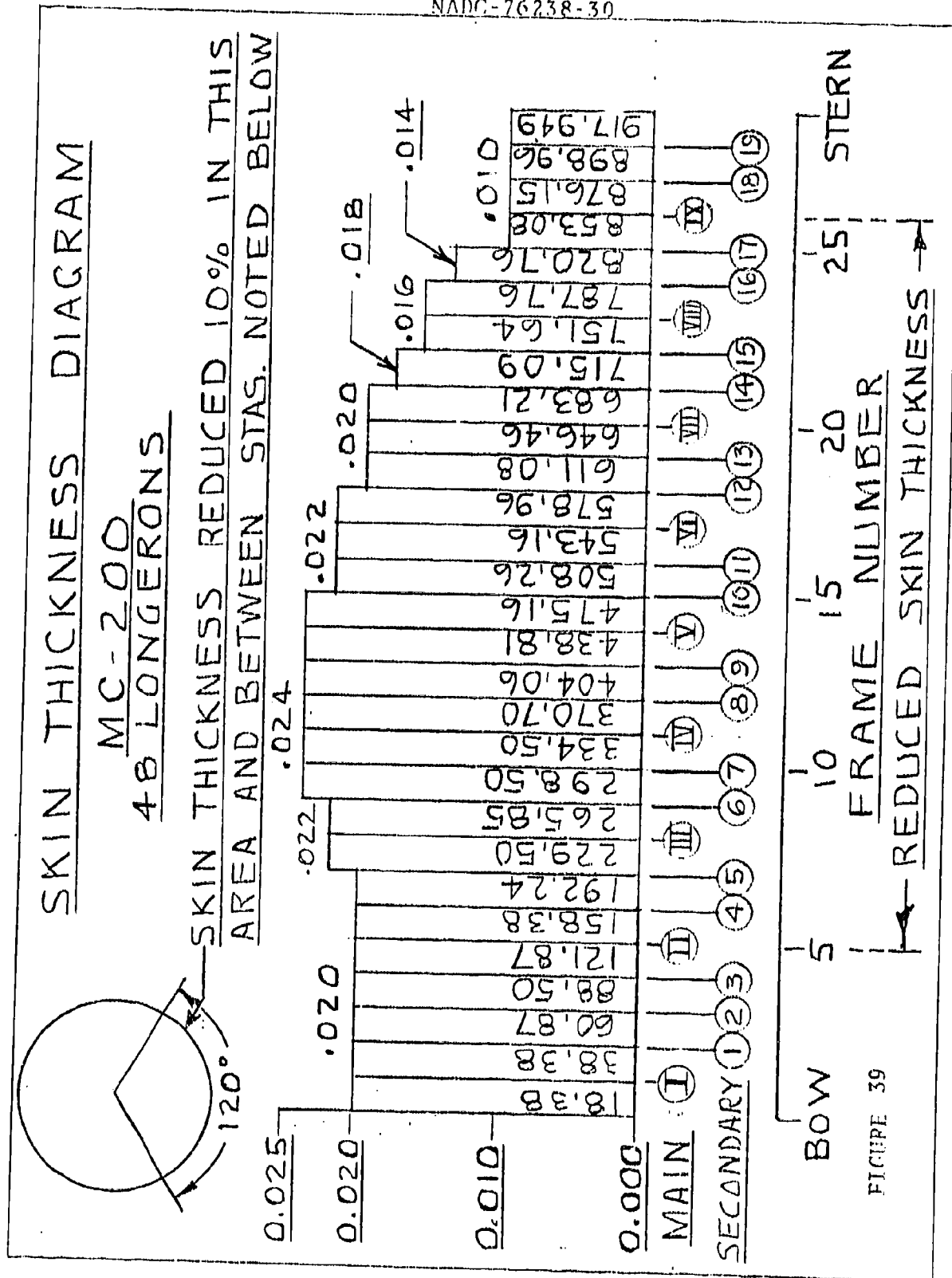


FIGURE 39

Principal stress in the skin @ equator:

$$\sigma_o = 24639 + \frac{1}{2} \sqrt{(262.6)^2(4) + (32850 - 16429)^2}$$

$$\sigma_o = 24639 + \frac{1}{2} \sqrt{269925086} = 24639 + 8215$$

$$\sigma_o = 32,854 \text{ lb/in}^2 \text{ (max.)}$$

All stresses are without contributing effect of areas of longerons and therefore, conservative.

The (.018) skin at the bottom of the hull is applied from an angle of $\alpha = 0^\circ$ to 60° upward on each side of the hull at maximum section and is proportioned with other thicknesses along the length between frame stations 69.80 and 640.09.

7.2 RELATIVE ELASTICITY OF SKIN AND STRUCTURE. The highest stress used in all hulls is the hoop stress when the hull is under maximum allowable gas and air pressure and designed to a factor of safety of two, with a maximum allowable stress of $\sigma_T = 32,850 \text{ lb/in}^2$. In the instance of MC-200, at maximum diameter, this stress would produce a radial elastic deformation of the hull shell equal to:

$$\epsilon = \Delta R_T = R_T \frac{\sigma_T}{E} = (1223.934) \frac{32850}{(10.2)(10)^6}$$

$$\Delta R_T = 3.94179 \text{ in., radially}$$

However, the longitudinal stress at the same station is, $\sigma_L = 1/2 \sigma_T = 16,425 \text{ lb/in}^2$, normal to the stress σ_T . This stress will reduce the radial deformation due to the effect of Poisson's Ratio ν , as follows:

$$-\Delta R_V = -\nu R_T \frac{\sigma_L}{E} = -\nu R_T \frac{\sigma_T}{2E}$$

The actual radial deformation will be:

$$\Delta R_{To} = \Delta R_T - \Delta R_V = R_T \left(1 - \frac{\nu}{2}\right) \frac{\sigma_T}{E}$$

$$\Delta R_{To} = (1223.934) \left(1 - \frac{.33}{2}\right) \frac{32850}{(10.2)(10)^6}$$

$$\Delta R_{To} = 3.29139 \text{ in., actual radial deformation}$$

$$\frac{\Delta R_{To}}{\Delta R_T} = \frac{3.29139}{3.94179} = .83499 \approx .835$$

This alleviates considerably, the elastic strain between the shell skin and the structure attached to it.

Poisson's Ratio has an influential effect on all Metalclad structures due to the large dimensions of Metalclad shells. For instance, it reduces the radial deformation of the skin, due to the presence of longitudinal skin stresses, while at the same time the effect of Poisson's Ratio on the radial growth of the frames, main as well as secondary, is almost zero. Therefore the strain between the transverse structure and skin is inherently reduced. In addition, further alleviation of this interaction strain is accomplished by means of elastic "springs" between the structure and the skin, mentioned in section 5, and other sections of this report. A similar effect exists also in the longitudinal direction caused by transverse stress, which tends to unload the longerons from tension. Therefore, the longitudinal tension in the shell skin will be normally higher than the tension in the longerons.

The preceding analysis was for the maximum diameter station of the hulls. The maximum moment is assumed to prevail from a station (.4615)(L) to a station (.650)(L). The following will review the conditions at both of these stations on the MC-200 and MC-100 hulls.

MC-200

The (.4615)(L) station is at (.4615)(917949) or 423.6335 ft. from the bow and called station "a" in this analysis. This station is aft of the maximum hull diameter station.

The hull radius is(station "a")

$$R_{Ta} = R_T \sqrt{1 - \frac{(423.6335 - a_B)^2}{a_S^2}} \quad \begin{array}{l} a_B = 330.4616 \text{ ft} \\ a_S = 587.4874 \text{ ft} \end{array}$$

$$R_{Ta} = (101.9945)(.987361) = 100.7054 \text{ ft}$$

The thickness of skin on top of the hull of the MC-200 is

$$t_T = .024 \text{ in.}$$

The longitudinal radius of curvature of the hull at station "a" is:

$$R_{La} = \frac{(R_T^4 x^2 + a_S^4 y^2)^{3/2}}{a_S^4 R_T^4}$$

$$R_{La} = \frac{((101.9945)^4 (93.1715)^2 + (587.487)^4 (100.7054)^2)^{3/2}}{(587.487)^4 (101.9945)^4}$$

$$R_{La} = 3.256656(10)^3 \text{ ft} = 999,079.87 \text{ in.}$$

The hoop stress on top of the hull at station "a" is:

$$\sigma_{T_{Ta}} = \frac{2kR_{Ta} + p}{t} \left(\frac{2R_{Ta}R_{La}}{2R_{La} + R_{Ta}} \right)$$

$$\sigma_{T_{STa}} = \frac{(2)(.06535)(1/1728)(100.7054)(12) + .56125}{.024} \times$$

$$\left(\frac{(2)(39080.0)(1208.46)}{(2)(39080.0) + 1208.46} \right)$$

$$\sigma_{T_{STa}} = \frac{.091404 + .56125}{.024} \times \frac{(9.4453234)(10)^7}{78160 + 1208.46}$$

$$\sigma_{T_{STa}} = (27.1939)(1190) = 32,362 \text{ lb/in}^2$$

Longitudinal stress at station "a"

$$\sigma_{La} = \frac{2kR_{Ta} + p}{t} \left(\frac{R_{Ta}R_{La}}{2R_{La} + R_{Ta}} \right)$$

$$\sigma_{La} = (27.1939)(595) = 16,181 \text{ lb/in}^2$$

This stress is only slightly lower than at the maximum diameter station and therefore, it is obvious all other stresses, as computed for the MC-200 at maximum diameter, will be insignificantly lower at station "a".

Station "b"

Station "b" is $(.650)(L) = (.650)(917.34)$ or 596.661 ft. from the bow.

$$596.661 - 330.462 = 266.199 = x \text{ distance}$$

from the maximum diameter station.

Radius of hull at station "b" is:

$$R_{Tb} = R_T \sqrt{1 - \frac{(266.199)^2}{a_s^2}}$$



$$R_{Tb} = (101.9945) \sqrt{1 - \frac{(266.199)^2}{(587.487)^2}}$$

$$R_{Tb} = (101.9945)(691452) = 90.92322 \text{ ft} = 1091.08 \text{ in.}$$

Longitudinal radius of curvature of hull at station "b" is:

$$R_{Lb} = \frac{(R_T^4 x^2 + a_s^4 y^2)^{3/2}}{a_s^4 R_T^4}$$

$$R_{Lb} = \frac{((101.9945)^4 (266.199)^2 + (587.487)^4 (90.92322)^2)^{3/2}}{(587.487)^4 (101.9945)^4}$$

$$R_{Lb} = \frac{31265.6309}{12.092289} = 2423.2625 \text{ ft} = 29079.15 \text{ in.}$$

The hoop stress on top of the hull, at station "b" is:

$$\sigma_{Tb} = \frac{2kR_{Tb} + p}{t} \left(\frac{2R_{Tb}R_{Lb}}{2R_{Lb} + R_{Ta}} \right)$$

$$\sigma_{Tb} = \frac{(2)(3.7818287)(10)^{-5}(1091.08) + .56125}{.024} \times$$

$$\left(\frac{(2)(1091.08)(29079.15)}{(2)(29079.15) + 1091.08} \right)$$

$$\sigma_{Tb} = \frac{.0825255 + .56.125}{.024} \left(\frac{(6.3455358)(10)^7}{59249.38} \right)$$

$$\sigma_{Tb} = (26.82398)(1070.99) = 28,728 \text{ lb/in}^2$$

The stress $\sigma_{Tb} = 28,728 \text{ lb/in}^2$ is lower than was computed for the maximum diameter station of the hull ($\sigma_{TS} = 32,850 \text{ lb/in}^2$). Therefore, the maximum diameter station has the highest stress in the hull shell skin in any of the five hulls investigated.

In the case of the MC-200, the maximum moment,

$M_m + M_g = 51.963767(10)^6 \text{ ftlb}$, declines toward the bow at the rate of:

$$\frac{51.963767(10)^6 \text{ ftlb}}{423.6335 \text{ ft}} = 122,662 \frac{\text{ftlb}}{\text{ft}}$$



At the maximum diameter station, 330.462 ft from the bow, the maximum moment is:

$$(330.462)(122662) = 40.535130(10)^6 \text{ ftlb}$$

This compares with $51.963767(10)^6 \text{ ftlb}$, used in preceding analysis. This difference is too large and the maximum diameter station is re-computed, to allow for it. The influence of the lower than maximum moment at the maximum diameter station will result in higher residual tensile stresses in the skin on the compression side of the hull shell and lower tensile stresses on the tension side of the hull. This points to a broader range of admissible hull pressure variation than at first appeared from the preceding analysis.

Recomputed longitudinal stress on top of the MC-200 hull, at maximum speed, immediately aft of the maximum diameter station, with an upward gust (Refer to page 170):

$$\sigma_{LSTM} = \sigma_{LST} - \frac{M_m - M_g}{\pi t_T R_T^2}$$

$$\sigma_{LSTM} = 16424 = \frac{(37.040 - 3.463542)(10)^6(12)}{(1.129475)(10)^5}$$

$$\sigma_{LSTM} = 16424 - 3567 = 12,851 \text{ lb/in}^2 \text{ residual tension stress.}$$

Compared to previous:

$$\sigma_{LSTM} = 11,847 \text{ lb/in}^2$$

Maximum longitudinal stress on top of the hull, at maximum speed, immediately aft of the maximum diameter station, with a downward gust (Refer to page 170):

$$\sigma_{LSTM} = \sigma_{LST} + \frac{M_m + M_g}{\pi t_T R_T^2}$$

$$\sigma_{LSTM} = 16424 + \frac{(37.040 + 3.463542)(10)^6(12)}{(1.129475)(10)^5}$$

$$\sigma_{LSTM} = 16424 + \frac{(40.503542)(10)^6(12)}{(1.129475)(10)^5}$$

$$\sigma_{LST_M} = 16424 + 4303 = 20,727 \text{ lb/in}^2$$

Compared to previous (page 171)

$$\sigma_{LST_M} = 21,945 \text{ lb/in}^2$$

Maximum longitudinal stress on the bottom of the MC-200 hull, at maximum speed, immediately aft of the maximum diameter station, with an upward gust:

$$\sigma_{LSB_M} = \sigma_{LSB} = \frac{M_m - M_g}{\pi t_B R_T^2}$$

$$\sigma_{LSB_M} = 15300 + \frac{(33.57646)(10)^6(12)}{(1.0353524)(10)^5}$$

$$\sigma_{LSB_M} = 15300 + 3892 = 19,192 \text{ lb/in}^2$$

Compare to previous (page 171)

$$\sigma_{LSB_M} = 20,373 \text{ lb/in}$$

Maximum longitudinal stress on the bottom of the hull at maximum speed, immediately aft of the maximum diameter station, with a downward gust:

$$\sigma_{LSB_M} = \sigma_{LSB} - \frac{M_m + M_g}{\pi t_B R_T^2}$$

$$\sigma_{LSB_M} = 15380 - \frac{(40.503542)(10)^6(12)}{(1.0353524)(10)^5}$$

$$\sigma_{LSB_M} = 15380 - 4694 = 10,686 \text{ lb/in}^2 \text{ (Residual)}$$

stress in the skin at the bottom of the hull.)

Compare to previous (page 171)

$$\sigma_{LSB_M} = 9,357 \text{ lb/in}^2$$

This is the lowest residual stress at the maximum diameter station, due to the sum of moments at that station.

The computed hull air pressures are at sea level. With altitude, as the ambient pressure decreases, the relative

hull air pressure stays constant while the absolute hull air pressure decreases in a constant ratio with the ambient air pressure p_o . Therefore, absolute hull pressure :

$$p_{\text{hull}} = p_o + \Delta p_{\text{hull}}$$

Relative hull pressure =

$$p_{\text{gage}} = \Delta p_{\text{hull}} = \text{constant}$$

At 10,000 ft ceiling altitude the ambient pressure is

$$p_{10} = 10.1078 \text{ lb/in}^2$$

In the case of MC-200:

$$\Delta p_{\text{hull}} = .56125 \text{ lb/in}^2;$$

$$p_{\text{hull}}_{10} = 10.1078 + .56125 = 10.66905 \text{ lb/in}^2 \text{ absolute.}$$

Although the absolute hull air pressure varies with change of altitude, the gage air pressure is constant at all altitudes.

The stresses in the hull shell skin are very nearly constant at any identical location in all hulls. This originates by making the maximum hoop stress in all hulls equal to one half of the ultimate tensile strength of the metal skin, a rational basis of comparison.

For MC-200

$$\sigma_{LST} = 16,424 \text{ lb/in}^2$$

Longitudinal stresses in the skin without any moment

$$\sigma_{LSB} = 15,380 \text{ lb/in}^2$$

$$\sigma_{LSTM} = 11,847 \text{ lb/in}^2$$

Minimum residual stresses in the hull with maximum bending

$$\sigma_{LSBM} = 9,357 \text{ lb/in}^2$$

Minimum margin in skin stress at the top of the hull:

$$1 - \frac{\sigma_{LSTM}}{\sigma_{LST}} = 1 - \frac{11847}{16424} = 1 - .7213 = .2787$$

Minimum margin in the skin stress at the bottom of the hull:

$$1 - \frac{\sigma_{LSBM}}{\sigma_{LSB}} = 1 - \frac{9357}{15380} = 1 - .60839 = .3916$$

Similar minimum margins also exist in other hulls of this report.

It is appropriate to point out the duality of the shell stress Equation

$$\frac{\sigma_T}{R_T} + \frac{\sigma_L}{R_L} = \frac{p}{t}$$

used in this section. It is a close assumption for the purpose at this time, that

$$\sigma_L = 1/2\sigma_T$$

The above shell Equation can be solved in two ways, set here side-by-side:

I

$$\frac{\sigma_T}{R_T} + \frac{\sigma_L}{R_L} = \frac{p}{t}$$

$$\frac{\sigma_T}{R_T} + \frac{\sigma_T}{2R_L} = \frac{p}{t}$$

$$\sigma_T' \left(\frac{1}{R_T} + \frac{1}{2R_L} \right) = \frac{p}{t}$$

$$\sigma_T' \left(\frac{2R_L + R_T}{2R_L R_T} \right) = \frac{p}{t}$$

$$\sigma_T' = \frac{p}{t} \left(\frac{2R_L R_T}{2R_L + R_T} \right)$$

II^v

$$\frac{\sigma_T}{R_T} + \frac{\sigma_L}{R_L} = \frac{p}{t}$$

$$\frac{\sigma_T}{R_T} + \frac{p R_T}{2R_L t} = \frac{p}{t}$$

$$\frac{\sigma_T''}{R_T} = \frac{p}{t} \left(1 - \frac{R_T}{2R_L} \right)$$

$$\sigma_T'' = \frac{p}{t} \left(R_T - \frac{R_T^2}{2R_L} \right)$$

$$\sigma_T'' = \frac{p}{t} \left(\frac{2R_L R_T - R_T^2}{2R_L} \right)$$

$$\frac{2R_L R_T}{2R_L + R_T} \neq \frac{2R_L R_T - R_T^2}{2R_L}$$

The σ_L' satisfies $\sigma_L' = 1/2\sigma_T$, while $\sigma_L'' > 1/2\sigma_T$; or, pressure p , computed by method I is lower, by method II, higher. Method I is used in the analysis of this section, because its results check with the basic Equation. On the other hand, Method II is rational, e.g., when $R_L \rightarrow \infty$, expression for σ_T reduces to:

$$\sigma_T'' = \frac{p}{t} R_T, \text{ while under the same condition,}$$

$$\sigma_T' \text{ becomes indefinite.}$$

^v Engineering Design, J.H. Faupel, John Wiley & Sons, 1964 .

8. SKIN SEAMS

8.1 TYPE, STRENGTH, AND WEIGHT.

8.1.1 Type. There are two types of seams used on Metalclad airship hulls. One consists of the butt splice seam between two skin panels and the other is a lap joint seam between skin panels and the thicker base skin under all structural elements attached to the skin of the hull, e.g., under the main frames, secondary frames, and the longerons. Both seam joints are shown on the MC-200 hull layout, Appendix M-5 and on Figure 39. All rivets will be installed in "dimpled" recesses which is the standard practice for 100° rivets, although, for simplicity, they are shown as being recessed by machined countersinking. Altogether five types of seam joints are used on the hulls to join skin to skin and skin to thicker skin forming the bases of all structure. These seams are shown in Figure 40 and Tables No. 20 through No. 31. They are:

Type I, Lap seam joint that connects pieces or panels of skin which form the bases of main frames. This seam joins the same thicknesses of sheets and its external side is smooth.

Type II, Lap seam joint connects pieces of skin under the longerons, and secondary frames. In addition, this joint is used to connect pieces of the transition strip which is used between the main frames base skin and the local skin panel, as well as the seam between the transition panel and the longeron base skin. (Same thickness of skin at joint.)

Type III, Lap seam joint that connects skin panel with heavier base skin under all structural frame work; (different thicknesses of skin at joint).

Type IV, Lap seam joint that connects base skin of main frames to transition strip from main frame to skin panels; (different thicknesses of skin at joint.)

Butt joint, that connects pieces of skin to make a layer size unit panel for mounting on the hull between two longerons and two frames; back-up strip is used; (same thickness of skin).

8.1.2 Strength. The construction of the seams, both butt and lap joints, is such that the joint strength is at least equivalent to the strength of the unbroken metal or better; therefore, the seam efficiency is higher than 100%. This is accomplished by using compound riveted and bonded joints. These joints have one inch width of lapped or faying area that is bonded and riveted together by a double row of .094 diameter rivets spaced at 1.50 inch intervals in a

staggered pattern. The rivets are to be driven during the curing time interval for the bonding material and force the faying surfaces of the skin together with a force such that the final cured thickness of the bond will be approximately .004 in. maximum. The strength of the joint is developed by the bonding material shear and the rivets assure a tight bond without voids and other imperfections in the joints, as well as providing security against prying forces on the bonded interface. Fatigue endurance of "dimpled" flush rivets is known to be high already and bonding will raise it even higher. The bonding substance functions also as a sealant for containing lifting gas or air.

The technology of bonding and sealing is now well developed and has been used for many years in aircraft construction. TI has researched several chemical corporations and their respective bonding-sealing products. Most products are adaptable to thin aluminum sheet bonding with strengths depending on method and time for curing. Metalclad construction will require room temperature application and curing, however local supplementary heat in the form of controlled infra-red can be used on structure seams, after riveting in place. Particular environmental parameters to satisfy, and still maintain strength, will be conditions of humidity and high or low temperatures encountered in airship operations. Several references have been analyzed including the Airforce "PABST" study conducted by McDonald Douglas Corp. on adhesive bonding of aircraft structures. Bonded and riveted seams of high strength and efficiency as required by Metalclad construction are easily obtainable with present state of technology.

8.1.3 Weight. The weight per unit length of the seams varies according to type of seam and its location on the hull. The unit weights of seams are tabulated in Tables No. 20 through No. 24.

8.2 Length Of Seams In The Hulls. The lengths of various types of seams in the MC-200 hull are tabulated in Tables No. 25 through No. 31 and are shown below:

<u>Type</u>	<u>Length, ft</u>
I	1,976.9
II	325.0
III	1,035.7

<u>Type</u>	<u>Length, ft</u>
IV	10,890.0
Butt	<u>8,931.6</u>
	23,159.2 ft

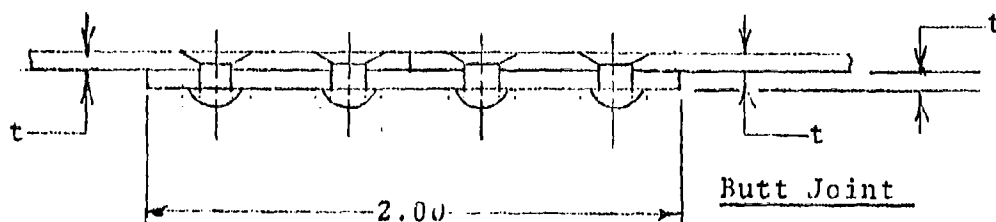
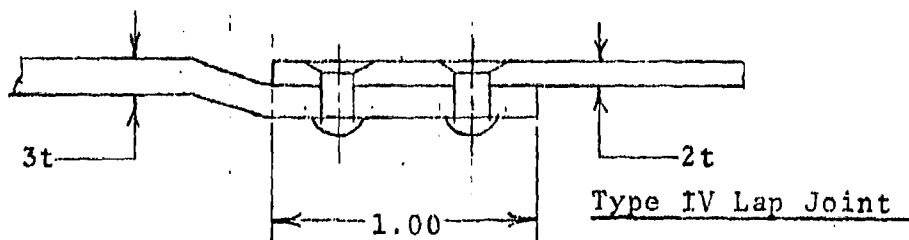
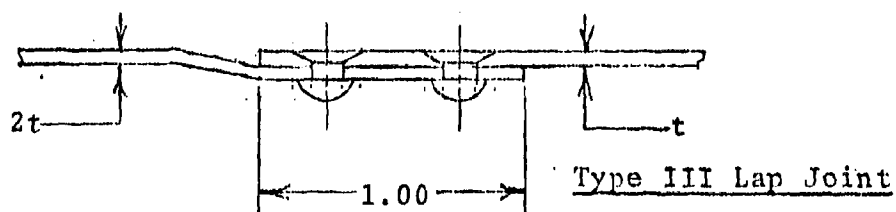
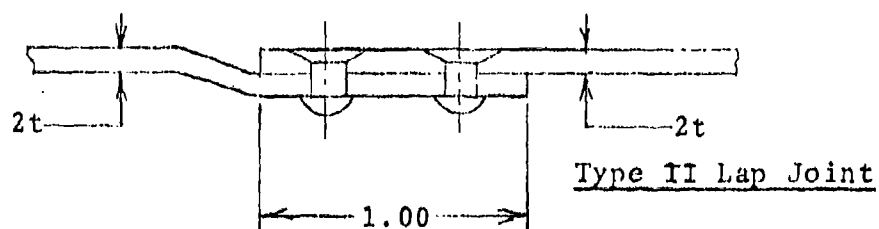
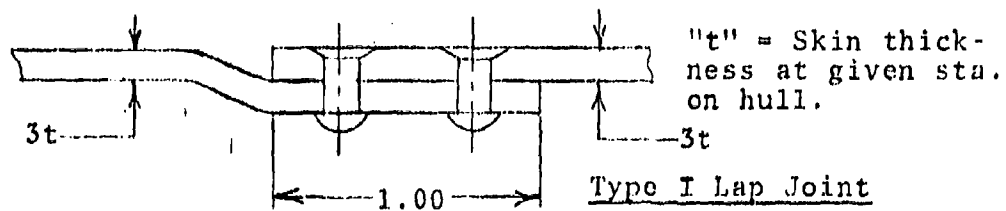


FIGURE 40 Types Of Seam Joints

TABLE 20 MC-100: Seams- Weight Per Foot (Pounds)

<u>Hull Station</u>	<u>Type I</u>	<u>Type II</u>	<u>Type III</u>	<u>Type IV</u>	<u>Butt Joint</u>
0.00 T	0.120769	0.081601	0.062017	0.101185	0.084866
to					
150.85 B	0.106082	0.071809	0.054673	0.088945	0.075074
150.85 T	0.135457	0.091393	0.069361	0.113425	0.094658
to					
206.96 B	0.120769	0.081601	0.062017	0.101185	0.084866
206.96 T	0.150145	0.101185	0.076705	0.125665	0.104450
to					
373.80 B	0.135457	0.091393	0.069361	0.113425	0.094658
373.80 T	0.135457	0.091393	0.069361	0.113425	0.094658
to					
458.39 B	0.120769	0.081601	0.062017	0.101185	0.084866
458.39 T	0.120769	0.081601	0.062017	0.101185	0.084866
to					
548.14 B	0.106082	0.071809	0.054673	0.088945	0.075074
548.14 T		0.071809	0.054673		0.075074
to					
577.29 B		0.062017	0.047329		0.065282
577.29 T	0.091393	0.062017	0.047329	0.076705	0.065282
to					
640.09 B	0.084049	0.057121	0.043657	0.070585	0.060386
640.09 T		0.052225	0.039985		0.055490
to					
692.56 B					
692.56 T		0.042433	0.032641		0.045698
to					
728.576B					

TABLE 21 MC-125: Seams- Weight Per Foot (Pounds)

<u>Hull Station</u>	<u>Type I</u>	<u>Type II</u>	<u>Type III</u>	<u>Type IV</u>	<u>Butt Joint</u>
0.00 T	0.135454	0.091393	0.069361	0.113425	0.094658
to					
162.29 B	0.120769	0.081601	0.062017	0.101185	0.084866
162.29 T	0.150145	0.101185	0.076705	0.125665	0.104450
to					
222.89 B	0.135457	0.091393	0.069361	0.113425	0.094658
222.89 T	0.164833	0.100977	0.084049	0.137905	0.114242
to					
401.66 B	0.150145	0.101185	0.076705	0.125665	0.104450
401.66 T	0.150145	0.101185	0.076705	0.125665	0.104450
to					
490.38 B	0.135457	0.091393	0.069361	0.113425	0.094658
490.38 T	0.135457	0.091393	0.069361	0.113425	0.094658
to					
579.24 B	0.120769	0.081601	0.062017	0.101185	0.084866
579.24 T		0.081601	0.062017		0.084866
to					
609.21 B		0.071809	0.054673		0.075074
609.21 T	0.106081	0.071809	0.054673	0.088945	0.075074
to					
668.10 B	0.091393	0.062017	0.047329	0.076705	0.065282
668.10 T		0.062017	0.047329		0.065282
to					
697.01 B		0.057121	0.043657		0.060386
697.01 T	0.062017	0.042433	0.032641	0.052225	0.045698
to					
784.835B	0.054673	0.037537	0.028969	0.046105	0.040802

TABLE 22 MC-150: Seams- Weight Per Foot (Pounds)

<u>Hull Station</u>	<u>Type I</u>	<u>Type II</u>	<u>Type III</u>	<u>Type IV</u>	<u>Butt Joint</u>
0.00 T	0.135457	0.091393	0.069361	0.113425	0.094658
to					
172.46 B	0.120769	0.081601	0.062017	0.101185	0.084866
172.46 T	0.150145	0.101185	0.076705	0.125665	0.104450
to					
236.86 B	0.135457	0.091393	0.069361	0.113425	0.094658
236.86 T	0.164833	0.110977	0.084049	0.137905	0.114242
to					
426.83 B	0.150145	0.101185	0.076705	0.125665	0.104450
426.83 T	0.150145	0.101185	0.076705	0.125665	0.104450
to					
521.11 B	0.135457	0.091393	0.069361	0.113425	0.094658
521.11 T	0.135457	0.091393	0.069361	0.113425	0.094658
to					
615.54 B	0.120769	0.081601	0.062017	0.101185	0.084866
615.54 T		0.081601	0.062017		0.084866
to					
679.25 B		0.071809	0.054673		0.075074
679.25 T	0.106081	0.071809	0.054673	0.088945	0.075074
to					
740.69 B	0.091393	0.062017	0.047329	0.076705	0.065282
740.69 T	0.076705	0.052225	0.039985	0.064465	0.055490
to					
834.02 B	0.069361	0.047329	0.036313	0.058345	0.050594

TABLE 23 MC-175: Seams- Weight Per Foot (Pounds)

<u>Hull Station</u>	<u>Type I</u>	<u>Type II</u>	<u>Type III</u>	<u>Type IV</u>	<u>Butt Joint</u>
0.00 T	0.150145	0.101185	0.076705	0.125665	0.104450
to					
181.55 B	0.135457	0.091393	0.069361	0.113425	0.094658
181.55 T	0.164833	0.110977	0.084049	0.137905	0.114242
to					
249.34 B	0.150145	0.101185	0.076705	0.125665	0.104450
249.34 T	0.179521	0.120769	0.091393	0.150145	0.124034
to					
449.33 B	0.164833	0.110977	0.084049	0.137905	0.114242
449.33 T	0.164833	0.110977	0.084049	0.137905	0.114242
to					
548.58 B	0.150145	0.101185	0.076705	0.125665	0.104450
548.58 T	0.150145	0.101185	0.076705	0.125665	0.104450
to					
649.99 B	0.135457	0.091393	0.069361	0.113425	0.094658
649.99 T		0.091393	0.069361		0.094658
to					
681.52 B		0.081601	0.062017		0.084866
681.52 T	0.120769	0.081601	0.062017	0.101185	0.084866
to					
747.40 B	0.106082	0.071809	0.054673	0.088945	0.075074
747.40 T		0.071809	0.054673		0.075074
to					
779.74 B		0.062017	0.047329		0.065282
779.74 T	0.076705	0.052225	0.039985	0.064465	0.055490
to					
877.987B	0.069361	0.047329	0.036313	0.058345	0.050594

TABLE 24 MC-200: Seams- Weight Per Foot (Pounds)

<u>Hull Station</u>	<u>Type I</u>	<u>Type II</u>	<u>Type III</u>	<u>Type IV</u>	<u>Butt Joint</u>
0.00 T	0.150145	0.101185	0.076705	0.125665	0.104450
to					
192.24 B	0.135457	0.091393	0.069361	0.113425	0.094658
192.24 T	0.164833	0.110977	0.084049	0.137905	0.114242
to					
265.85 B	0.150145	0.101185	0.076705	0.125665	0.104450
265.85 T	0.179521	0.120769	0.091393	0.150145	0.124034
to					
475.16 B	0.164833	0.110977	0.084049	0.137905	0.114242
475.16 T	0.164833	0.110977	0.084049	0.137905	0.114242
to					
578.96 B	0.150145	0.101185	0.076705	0.125665	0.104450
578.96 T	0.150145	0.101185	0.076705	0.125665	0.104450
to					
683.21 B	0.135457	0.091393	0.069361	0.113425	0.094658
683.21 T		0.091393	0.069361		0.094658
to					
715.09 B		0.081601	0.062017		0.084866
715.09 T	0.120769	0.081601	0.062017	0.101185	0.084866
to					
787.76 B	0.106082	0.071809	0.054673	0.088945	0.075074
787.76 T		0.071809	0.054673		0.075074
to					
820.76 B		0.062017	0.047329		0.065282
820.76 T	0.076705	0.052225	0.039985	0.064465	0.055490
to					
917.949B	0.069361	0.047329	0.036313	0.058345	0.050594

TABLE 25 MC-200: Type I Lap Joint

Station	Diameter ft	Circumference ft	Width of Base ft	Total Width of Base Material (Basic + .7)ft	Number of Seams	Total Length of Seams ft
18.38	67.083	210.74603	9.25	9.9583	11	109.54166
121.87	158.216	497.04949	6.904	9.6120	25	190.30119
229.50	194.235	610.20896	8.475	9.1837	31	284.69666
334.50	203.984	640.83519	8.901	9.6091	33	317.1017
438.81	200.499	629.85739	8.748	9.4566	32	302.61338
543.16	190.1503	597.3749	8.297	9.0055	30	270.16517
646.46	171.967	540.25022	7.504	8.2120	28	229.93822
751.64	142.213	446.77584	6.46	7.1727	23	164.97323
853.08	93.1771	292.72446	6.464	7.1727	15	107.59123

Total Length = 1976.9222 ft

TABLE 26 MC-200 Type II Lap Joint - Transition Panel

<u>Station</u>	<u>Diameter ft</u>	<u>Circumference ft</u>	<u>Number of Seams</u>	<u>Total Length of Seams ft</u>
18.38	67.083	210.746	22	18.333
121.87	158.216	497.049	50	41.667
229.50	194.236	610.209	62	51.667
334.5	203.984	640.835	66	55.000
438.81	200.400	629.857	64	53.333
543.16	190.150	597.37	60	50.000
646.46	171.967	540.250	56	46.667
751.64	142.213	446.776	46	38.333
853.08	93.177	292.724	30	25.00

Total = 325.0

TABLE 27 MC-200 Type II Lap Joint - Secondary Frames

Station	Diameter ft	Circumference ft	Width of Base ft	Total Width of Base Skin ft (Base + 1.21)	Number of Seams	Total Length of Seams ft
38.38	95.416	299.759	0.481	1.690	16	27.043
60.87	117.973	370.623	0.596	1.804	16	28.866
88.50	138.936	436.481	0.7017	1.910	24	45.840
158.38	174.150	547.107	0.880	2.088	24	50.108
192.24	185.288	582.099	0.936	2.144	36	77.187
265.85	200.052	628.482	1.010	2.219	36	79.872
298.50	203.033	637.846	1.025	2.234	36	80.414
370.70	203.510	639.345	1.028	2.236	36	80.500
404.06	202.382	635.802	1.022	2.230	36	80.295
475.16	197.705	621.108	0.998	2.20	36	79.445
508.26	194.423	610.797	0.982	2.190	36	78.841
578.96	184.842	580.698	0.934	2.4	36	77.106
611.08	179.212	563.016	0.905	2.113	24	50.722
683.21	163.12	512.471	0.824	2.032	24	48.772
715.09	154.198	484.411	0.779	1.987	24	47.689

TABLE 27 -Continued

Station	Diameter ft	Circumference ft	Width of Base ft	Total Width of Base Skin ft (Base + 1.21)	Number of Seams	Total Length of Seams ft
787.76	128.059	402.308	0.647	1.855	24	44.522
820.76	112.378	353.047	0.566	1.776	16	28.414
876.15	75.568	237.405	0.382	1.590	12	19.079
898.96	51.444	161.617	0.260	1.468	8	11.745
Total						1,035.7 ft

TABLE 28 MC-200 Type II Lap Joint - Longeron

Type of Frame	Station	Circumference ft	Width of Base ft	Total Width of Base ft	Number of Seams	Total Length of Seams ft
M	18.38	210.746	0.295	1.504		
S	38.38	299.759	0.420	1.629		
S	60.87	370.623	0.519	1.728		
S	88.50	436.481	0.6119	1.820		
M	121.87	497.049	0.697	1.905		
S	158.38	547.107	0.767	1.975	79 Seams	
S	192.24	582.099	0.816	2.024	Per	*
M	229.50	610.209	0.855	2.064	Longeron	
S	265.85	628.482	0.881	2.089		
S	298.50	637.846	0.894	2.102		
M	334.50	640.835	0.898	2.107		
S	370.70	639.345	0.896	2.105		
S	404.06	635.802	0.891	2.100		
M	438.81	629.857	0.888	2.091		
S	475.16	621.108	0.871	2.079		

TABLE 28 Continued-

Type of Frame	Station	Circumference ft	Width of Base ft	Total Width of Base ft	Number of Seam	Total Length of Seams ft
S	508.26	610.797	0.857	2.065		
M	543.16	597.37	0.837	2.046		
S	578.96	580.698	0.814	2.022		
S	611.08	563.016	0.789	1.998		
M	646.46	540.250	0.757	1.966		
S	683.21	512.471	0.718	1.927	79 Seams	
S	715.09	484.411	0.679	1.887	Per	*
M	751.64	446.776	0.626	1.835	Longeron	
S	787.76	402.308	0.564	1.772		
S	820.76	353.047	0.495	1.703		
M	853.08	292.724	0.410	1.619		
S	876.15	237.405	0.333	1.541		
S	898.96	161.617	0.227	1.435		

* Per one longeron = (79)(1.897731) = 149.92071 ft

Longeron seams per hull = (48)(149.92071) = 7,196.194 ft

TABLE 29 MC-200: Type III Lap Joint - Skin Panels

Mid Point of Arc Between Frames	Radius at Mid Point Station	Length of Arc From Layout	1-Frame Base Skin = $l - (1.625)$ or (1.125)
<u>Station</u>	<u>R ft</u>	<u>l ft</u>	<u>l' ft</u>
29.95	42.429	15.95	14.325
49.75	53.819	22.35	21.225
74.40	64.474	27.35	26.225
103.90	74.250	30.0	28.375
141.95	83.771	32.225	30.6005
175.29	90.050	32.10	30.975
209.05	94.861	31.85	30.225
249.70	98.902	30.65	29.025
282.05	100.894	30.45	29.325
314.15	101.870	30.00	28.375
354.262	101.911	30.00	28.375
386.962	101.521	32.9	31.775
421.162	100.771	35.25	33.625
456.912	99.604	36.15	34.525
491.212	98.102	32.25	31.125
525.112	96.233	35.75	34.125
560.762	93.831	35.85	34.225
594.962	91.073	32.00	30.875
629.082	87.836	35.70	34.075
664.862	83.859	36.80	35.175
697.312	79.665	32.2	31.075

See page 226 for continuation of stations.

TABLE 29 Continued-

0.0109 R _T	ϕ to ϵ of Longeron	Base Skin $s' = 2 - (2)(h \tan 22^\circ + \frac{6.75}{12})$	Seam Length Per Panel $= (2)L' + (2)s'$
<u>h ft</u>	<u>s ft</u>	<u>s' ft</u>	<u>L ft</u>
0.462	5.554	4.0552	36.760
0.587	7.045	5.446	53.342
0.703	8.440	6.747	65.943
0.809	9.719	1.940	72.631
0.913	10.966	9.103	79.407
0.982	11.788	9.869	81.689
1.034	12.417	10.457	81.364
1.078	12.946	10.950	79.950
1.100	13.207	11.193	81.037
1.110	13.335	11.313	79.375
1.111	13.340	11.317	79.385
1.107	13.289	11.270	86.090
1.098	13.191	11.178	89.607
1.086	13.038	11.036	91.122
1.069	12.842	10.852	83.955
1.049	12.600	10.624	89.499
1.023	12.282	10.331	89.112
0.993	11.921	9.994	81.738
0.957	11.498	9.599	87.348
0.914	10.977	9.115	88.577
0.868	10.428	8.60	79.353

See page 227 for continuation of stations.



TABLE 29 continued

<u>Mid Point of Arc Between Frames</u>	<u>Seam Length For 48 Panels = (48)L</u>
<u>Station</u>	<u>Total ft</u>
.29.95	1,764.499
49.75	2,560.401
74.40	3,165.288
103.90	3,486.278
141.95	3,811.518
175.29	3,921.072
209.05	3,905.453
249.70	3,837.609
282.05	3,889.762
314.15	3,810.002
354.262	3,810.478
386.962	4,132.318
421.162	4,301.127
456.912	4,373.840
491.212	4,029.837
525.112	4,295.936
560.762	4,277.377
594.962	3,923.445
629.082	4,192.706
664.862	4,251.703
697.312	3,808.942

See page 228 for continuation of stations.

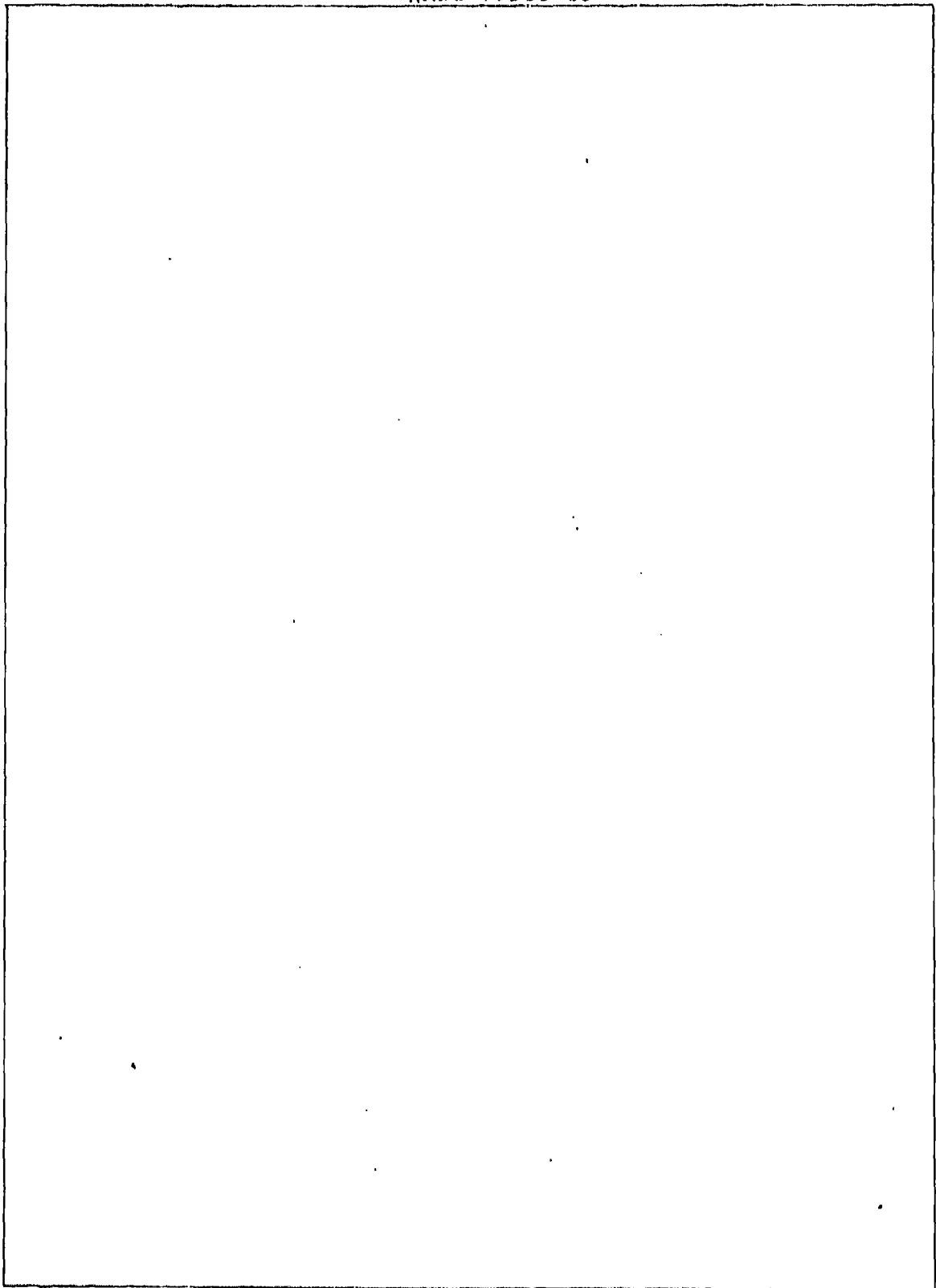


TABLE 29 Continued

Mid Point of Arc Between Frames	Radius at Mid Point Station	Length of Arc From Layout	↓ Frame Base Skin = $l - (1.625)$ or (1.125)
<u>Station</u>	<u>R ft</u>	<u>l ft</u>	<u>l' ft</u>
733.362	74.230	37.0	35.375
769.712	67.731	36.75	35.125
804.262	60.305	33.70	32.575
836.962	51.676	33.50	31.875
865.212	42.236	26.20	24.575
888.612	31.828	25.50	24.375

TABLE 29 Continued

0.0109 R_T	top of Longeron	Base Skin $s' = 2 - (2)(h \tan 22^\circ + \frac{6.75}{12})$	Seam Length Per Panel $= (2)l' + (2)s'$
<u>h ft</u>	<u>s ft</u>	<u>s' ft</u>	<u>L ft</u>
0.809	9.717	7.938	86.626
0.738	8.866	7.144	84.539
0.657	7.894	6.238	77.625
0.563	6.764	5.184	74.119
0.460	5.529	4.0316	57.213
0.347	4.166	2.761	54.272

TABLE 29 continued

Mid Point of Arc Between Frames	Seam Length For 48 Panels = (48)L
<u>Station</u>	<u>Total ft</u>
733.362	4,158.041
769.712	4,057.861
804.262	8,726.019
836.962	3,557.69
865.212	2,746.236
888.612	<u>2,605.051</u>
	96,842.785

TABLE 30 MC-200: Type IV Lap Joint

<u>Station</u>	<u>Diameter ft</u>	<u>Circumference ft</u>	<u>Number of Seams</u>	<u>Total Length of Seams ft</u>
18.38	67.082548	210.74603	2	421.49206
121.87	158.21577	497.04949	2	994.09898
229.50	194.23555	610.20896	2	1,220.4179
334.50	203.98418	640.83519	2	1,281.6703
438.81	200.48984	629.84739	2	1,259.7147
543.16	190.15034	597.3749	2	1,194.7498
646.46	171.96699	540.25022	2	1,080.5004
751.64	142.21317	446.77584	2	893.55168
853.08	93.177094	292.72446	2	<u>585.44892</u>

Σ 8,931.6446 ft

TABLE 31 MC-200: Butt Joint

	Length of Splice Per 1 Panel = s ft + 1.0 in.	Total Length For 48 Panels = y(48)
<u>Station</u>	<u>y ft</u>	<u>Total ft</u>
29.95		
49.75		
74.40	6.830	327.844
103.90	8.024	385.139
141.95	9.186	440.935
175.29	9.953	477.736
209.05	10.540	505.926
249.70	11.033	529.605
282.05	11.277	541.281
314.15	11.396	547.001
354.262	11.401	547.239
386.962	11.353	544.959
421.162	11.262	540.563
456.912	11.119	533.720
491.212	10.936	524.919
525.112	10.708	513.968
560.762	10.414	499.888
594.962	10.078	483.723
629.082	9.682	464.753
664.862	9.197	441.451
697.312	8.685	416.871

See next page for continuation of stations.

TABLE 31 Continued

<u>Station</u>	Length of Splice Per 1 Panel = s ft + 1.0 in.	Total Length For 48 Panels = y(48)
	<u>y ft</u>	<u>Total ft</u>
733.362	8.021	385.020
769.712	7.228	346.931
804.262	6.321	303.410
836.962	5.268	252.845
865.212	4.115	197.518
888.612	2.844	<u>136.525</u>
		$\Sigma 10,889.767$

9. HULL OPENINGS & REINFORCEMENT OF BOW

9.1 DESCRIPTION Metalclad hulls will be provided with openings for a number of purposes:

1. Permanently framed openings with unstressed covers or devices. Among them are circular openings for gas and air valves. Terminals on top of the hull for cell evaluation and inflation; air entries for blowers; human entry from spaces external to the hull; and thrusters, etc. It is improbable that emergency air entry openings will be needed, as was the case with ZMC-2.

It is expected that the study hulls will be provided with power driven blowers with standby capacity for each air sub-volume and will not require emergency suction air entries.

2. Openings on the bottom of the hull with replacable stress carrying covers, (i.e., for introducing cell diaphragms into air sub-volumes). The covers would be attached with screw fasteners along two longerons and two secondary frames, providing air-tight seam joints and thus restoring the hull. Layouts (appendix M) show typical views and Sections of both types of hull openings.

9.2 OPENING REINFORCEMENT All permanently framed openings would be defined by a rigid, light-weight ring, with a skin doubler at the innermost flange. Between the skin and the doubler would be aluminum alloy honeycomb, with the doubler sloping toward the skin with increasing radial distance from the ring until it meets the skin. The doubler-honeycomb structure restores the strength of the cut-out skin as well as reduces stress concentrations around the openings.

9.3 BOW STRUCTURE A similar construction is considered for the reinforcement of the bow to support the skin against the locally high dynamic pressure, and also, to distribute the loads from the mooring cone spindle. Sketch Figure 41 shows a typical Metalclad hull bow, with an internal skin attached to honeycomb structure and forming a hollow, rigid, bow dome principally for distributing cone anchor loads into the skin and longerons. The dome supports the bow flight pressure, as well. This structure concept is used in estimating the bow weight.

The structure indicated in Figure 41, is exclusively for flight purposes, excluding cone spindle structure, which is not part of the lift structure.

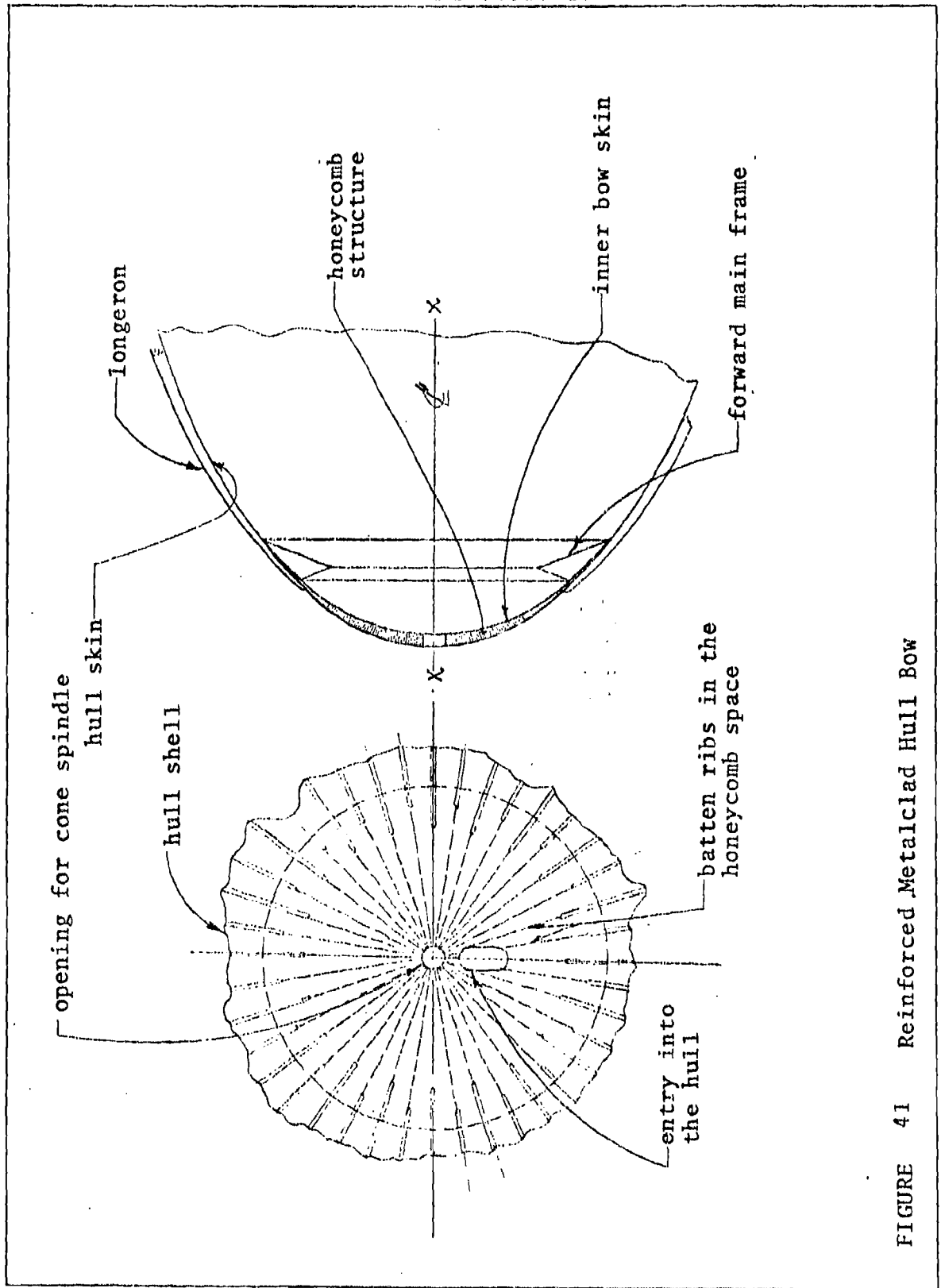


FIGURE 41 Reinforced Metalclad Hull Bow

10 HULL STRUCTURE WEIGHT

10.1 WEIGHTS OF HULL COMPONENTS. All the structures of metalclad hulls are of the same architecture; main frames, secondary frames, and longerons, as described in Section 1. In Figures 2, 3 and 4, are shown relative dimensional values of the structure for all hulls.

The weights of main frames were determined for MC-100 and MC-200 and extrapolated for the remaining hulls. In Section 3 is described the analysis of a main frame for MC-200, with the comment that this analysis is, at this time, still imperfect and results in an overweight conclusion. The main frames of MC-200 are computed on this basic analysis and subsequently these weights are reduced to 80% of computed value as noted under the heading of "Adjusted Total Frame Weight" in the last column of table for frames. These adjusted weights are considered to be close to weights that will be determined by a more thorough analysis.

The secondary frames are loaded by weight loads during construction and in case of loss of pressure in a cell. Determination of loads on them is considered in Section 1.8 and Section 4. The principal function of secondary frames is to maintain circularity of hull in deflated state and to provide a stabilizing support to the longerons. Their weights are tabulated in Table 33 for MC-200, Table 36 for MC-100 and extrapolated for intermediate hulls. The analysis of secondary frames also needs further study, including the interaction of longerons with these frames on an analytical scale model as well as with actual structural parameters. The objective of this study is to determine whether the frames as now designed, are not too rigid.

The longerons were given much analytical attention, especially in Section 5 and by computer programs. Their principal function is the support of hull during construction and in case of loss of pressure. The sections arrived at are capable of supporting all these loads. The interaction of longerons (as well as of frames) was given much time and effort and the conditions for it are satisfied in all structures including the longerons. The weights of longerons are tabulated in Table 34 for MC-200, Table 37 for MC-100 and extrapolated for intermediate hulls.

NOTE: Columns showing "adjusted weights" of main frames and "total weights" of secondary frames, diaphragms and membranes were factored, after extrapolation, using MC-150 as a base to provide a more realistic and accurate weight calculation.

10.2 WEIGHT DETERMINATION OF THE MAIN FRAMES, SECONDARY FRAMES AND LONGERONS. The weights of structure are determined for MC-200 and MC-100 and interpolated for other, intermediate volumes of hulls.

The basic parameters of all structure are noted below as frame construction constants.

1. Geometrical height of main frame from base to apex
 $= (0.108)(\text{Radius of hull at given station})$
(except minimum height of 8 ft)
2. Height of main frame with cap
 $= (0.9)(\text{Value determined in 1.})$
3. Geometrical height of secondary frame apex
 $= (0.0125)(\text{Radius of hull at given station})$
4. Height of secondary frame with cap
 $= (0.9)(\text{Value determined in 3.})$
5. Geometrical height of longeron apex
 $= (0.0109)(\text{Radius of hull at given station})$
6. Height of longeron with cap
 $= (0.9)(\text{Value determined in 5.})$

The weights of structure are tabulated below in this section.

10.2.1 Main Frames

TABLE 32 MC-200, Main Frame Weights

<u>Main Frame Station</u>	<u>X-Section Area (in²) Cap and Feet</u>	<u>X-Section Area (in²) Corrugations</u>	<u>X-Section Area (in²) Skin</u>	<u>Weight for (lb) Anchors Ea.</u>
18.38	4.6045694	5.1408492	0.9550487	20.0
121.87	4.9174797	5.4902033	1.0199504	20.0
229.50	6.0370048	6.7401159	1.2521547	20.0
334.5	6.34	7.0784	1.315	20.0
438.8	6.2313931	6.957144	1.2924734	20.0
543.16	5.910066	6.598393	1.225826	20.0
646.46	5.3448763	5.9673773	1.1085981	20.0
751.64	4.6045694	5.1408492	0.9550487	20.0
853.08	4.6045694	5.1408492	0.9550487	20.0

10.2.1 continued

TABLE 32 MC-200, Main Frame Weights

<u>Total Weight (lb) Anchors</u>	<u>Radius at Station Feet</u>	<u>Height of Apex (ft) Geometrical</u>	<u>Height of Apex Cap (ft)</u>
960	33.541274	8.000	7.600
960	79.107889	8.543652	8.1164694
960	97.117778	10.48872	9.964284
960	101.99209	11.015145	10.464387
960	100.24492	10.826451	10.285128
960	95.075712	10.268176	9.7547672
960	85.983498	9.2862177	8.8219068
960	71.106589	8.000	7.600
960	46.588547	8.000	7.600

10.2.1 continued

TABLE 32 MC-200, Main Frame Weights

<u>Main Frame Station</u>	<u>Height of Centroid (ft) From Skin</u>	<u>Radius of Revolution (ft)</u>	<u>Total X-Section Area (in²)</u>
18.38	3.800	29.741274	10.700467
121.87	4.058234	75.049655	11.427633
229.50	4.982142	92.135636	14.029274
334.5	5.2321935	96.7599	14.7334
438.8	5.142564	95.10236	14.48101
543.16	4.8773836	90.198329	13.734285
646.46	4.4109534	81.572545	12.420851
751.64	3.800	67.306589	10.700467
853.08	3.800	42.788547	10.700467

10.2.1 continued

TABLE 32 MC-200, Main Frame Weights

<u>Volume (in³)</u>	<u>Weight of Frame (Less Anchors)</u>	<u>Total Weight of Frame Structure + Anchor</u>
22,835.09	2,329.1793	3,289.1793
61,538.295	6,276.9060	7,236.9060
97,459.44	9,940.8628	10,900.862
102,291.33	10,433.715	11,393.715
103,836.78	10,591.351	11,551.351
88,888.384	9,066.6151	10,026.615
76,393.504	7,792.1374	8,752.1374
51,677.415	5,271.0963	6,231.0963
32,852.67	3,350.9723	<u>4,310.9723</u>
		73,692.833 lb (36.846416 tons)

10.2.1 continued

TABLE 32 MC-200, Main Frame Weights

<u>Main Frame Station</u>	<u>Caps*</u>	<u>Cornices*</u>	<u>Skin*</u>
18.38	50.723935	61.995921	11.689795
121.87	138.43687	150.47487	27.465223
229.50	206.90022	229.0681	88.892966
334.5	225.04464	256.08528	45.06768
438.8	221.18952	244.07119	94.919245
543.16	195.31585	217.01762	39.010686
646.46	163.5532	183.17959	70.560051
751.64	112.71985	129.62783	23.379591
853.08	73.267905	84.539889	16.365714

*Additional weight (lb) due to splices in these items.

10.2.1 continued

TABLE 32 MC-200, Main Frame Weights

<u>Total Weight Of Splices</u>	<u>Adjusted Total Frame Weight (1b)</u>
124.40964	2,687.11
316.37696	5,945.80
524.86128	8,994.12
526.1976	9,383.13
560.17995	9,533.97
451.34415	8,248.05
417.29284	7,218.00
265.72727	5,114.18
174.1735	<u>3,530.62</u>
	60,654.98

10.2.2 Secondary Frames

TABLE 33 Secondary Frame Weights MC-200

<u>Secondary Frame Station</u>	<u>X-Section Area (in²) Cap and Feet</u>	<u>X-Section Area (in²) Corrugations</u>	<u>Radius at Station Feet</u>
38.38	0.34695153	0.40568039	47.708171
60.87	0.4289712	0.50158362	58.986427
88.50	0.50519826	0.59071371	69.46816
158.38	0.63324023	0.74073948	87.074795
192.24	0.67374135	0.78778627	92.643973
265.85	0.72742599	0.85055817	100.02597
298.50	0.73826439	0.86323119	101.51632
370.70	0.7400	0.86526058	101.75498
404.06	0.73589836	0.86046467	101.19098
475.16	0.71889155	0.84057909	98.852424
508.26	0.70695747	0.82662492	97.211411
578.96	0.67211961	0.78589002	92.420974
611.08	0.65165417	0.76196037	89.606837
683.21	0.59315114	0.69355447	81.562278
715.09	0.56067414	0.65558005	77.096467
787.76	0.46564526	0.54446553	64.029356
820.76	0.40862902	0.4777981	56.18924
876.15	0.2747806	0.32129301	37.784178
898.96	0.18706047	0.2187244	25.722074

10.2.2 continued

TABLE 33 continued

<u>Height of Apex (ft) Geometrical</u>	<u>Height of Apex Cap (ft)</u>	<u>Height of Centroid (ft) From Skin</u>	<u>Radius of Revolution (ft)</u>
0.596315213	0.53671691	0.26835845	47.439813
0.73733033	0.66359729	0.33179864	58.654629
0.868352	0.7815168	0.3907584	69.077402
1.0884349	0.97959141	0.4897957	86.585
1.1580496	1.0422446	0.5211223	92.122851
1.2503246	1.1252921	0.56264605	99.46333
1.268954	1.1420586	0.5710293	100.9453
1.2719372	1.1447434	0.5723717	101.18261
1.2648872	1.1383984	0.5691992	100.62179
1.2356553	1.1120897	0.55604485	98.29638
1.2151426	1.0936283	0.54681415	96.664597
1.1552671	1.0397358	0.5198679	91.901107
1.1200854	1.0080768	0.5040384	89.102799
1.0195284	0.91757556	0.45878778	81.103491
0.96370583	0.86733524	0.43366762	76.6628
0.80036695	0.72033025	0.36016512	63.669191
0.7023655	0.63212895	0.31606447	55.873176
0.47230222	0.42507199	0.21253599	37.571643
0.32152592	0.28937332	0.14468666	25.577388

10.2.2 continued

TABLE 33 Secondary Frame Weights MC-200

Secondary Frame Station	Total X-Section Area (in ²)	Volume (in ³)	Total Weight of Frame Structures
38.38	0.75263192	2,692.0721	274.59135
60.87	0.93055482	4,115.3364	419.76431
88.50	1.0949199	5,707.8524	582.20094
158.38	1.3739697	8,969.7618	914.9151
192.24	1.4615276	10,151.623	1,035.4655
265.85	1.5779841	11,833.867	1,207.0544
298.50	1.6014955	12,189.134	1,243.2916
370.70	1.6052605	12,246.514	1,249.1444
404.06	1.596363	12,111.132	1,235.3314
475.16	1.5594706	11,557.817	1,178.8973
508.26	1.5335823	11,177.266	1,140.0811
578.96	1.4580096	10,102.81	1,030.4866
611.08	1.4136145	9,496.9345	968.68731
683.21	1.2867056	7,868.2806	802.56462
715.09	1.2162541	7,030.2391	717.08438
787.76	1.0101107	4,849.0806	494.60622
820.76	0.88642712	3,734.2852	380.89709
876.15	0.5960736	1,688.5781	172.23496
898.96	0.40578487	782.55184	79.820287
			15,127.12 lbs (7.56356 tons)

10.2.2 continued

TABLE 33 Secondary Frame Weights MC-200

<u>Cans*</u>	<u>Cornices*</u>	<u>Total Weight of Splices</u>	<u>Total Frame Weight (lb)</u>
6.37003	6.37003	12.74006	286.05
9.9761538	9.9761538	19.952307	437.75
13.603978	13.603978	27.207956	606.68
21.702408	21.702408	43.404816	954.03
23.915121	23.915121	47.830242	1,078.45
28.491821	28.491821	56.983642	1,258.38
28.916339	28.916339	57.832678	1,295.30
28.98432	28.98432	57.96864	1,301.26
28.823666	28.823666	57.647332	1,287.19
27.27762	27.27762	54.55524	1,227.93
26.824793	26.824793	53.649586	1,188.39
23.857557	23.857557	47.715114	1,073.38
22.333491	22.333491	44.666982	1,008.82
18.876441	18.876441	37.752882	836.56
17.156628	17.156628	34.313256	748.03
11.398995	11.398995	22.79799	515.09
9.0029145	9.0029145	18.005829	397.12
4.0359774	4.0359774	8.0719548	179.50
1.8316961	1.8316961	<u>3.6633922</u>	<u>83.11</u>
		706.75984	15,763.02

*Additional weight (lb) due to splices in these items.

10.2.3 Longerons

TABLE 34 MC-200, Longerons Weights
Apex Height At Maximum Radius = 1.11174 ft

<u>Station to Station</u>	<u>Mid Station</u>	<u>Radius ft Mid Station</u>	<u>Apex Height ft Mid Station</u>
18.38/38.38	28.38	41.352989	0.45074758
38.38/60.87	49.625	53.756674	0.58594774
60.87/88.50	74.685	64.581673	0.70394023
88.50/121.87	105.185	74.622119	0.81338109
121.87/158.38	140.125	83.3377356	0.90881318
158.38/192.24	175.31	90.054241	0.98159122
192.24/229.50	210.87	95.081266	1.0363857
229.50/265.85	247.675	98.742069	1.0762885
265.85/298.50	282.175	100.89978	1.0998076
298.50/334.50	316.50	101.90342	1.1107472
334.50/370.70	352.60	101.92206	1.1109504
370.70/404.06	387.38	101.51469	1.1065101
404.06/438.81	421.435	100.76422	1.0983299
438.81/475.16	456.985	99.601104	1.085652
475.16/508.26	491.710	98.077451	1.0690442
508.26/543.16	525.710	96.196943	1.0485466
543.16/578.96	561.060	93.808954	1.0225175
578.96/611.08	595.020	91.067472	0.99263544
611.08/646.46	628.770	87.867547	0.95775626
646.46/683.21	664.835	83.862747	0.91410394
683.21/715.09	699.150	79.409028	0.8655584

(For continuation see page 248)

10.2.3 continued

TABLE 34 MC-200, Longeron Weights

Cap Height ft Mid Station	X-Section Area in ² Mid Station	Longeron Length Between Stations in	Longeron Volume Between Stations in ³
0.40567282	.49139	330.0	162.16
0.52735296	.63877	300.0	191.63
0.6335462	.76738	349.8	268.43
0.73204298	.88670	413.40	366.56
0.81793186	.99073	443.4	439.29
0.88343209	1.0701	405.0	433.38
0.93274713	1.1298	439.2	496.21
0.96865965	1.1733	437.7	513.56
0.98982684	1.1989	388.8	466.15
0.99967248	1.2109	426.0	515.83
0.99985536	1.21109	427.2	517.38
0.99585909	1.2063	391.2	471.89
0.98849691	1.1973	420.0	502.88
0.9770868	1.1835	428.4	507.02
0.96213978	1.1654	383.4	446.82
0.94369194	1.1431	426.6	487.63
0.92026575	1.1147	427.8	476.86
0.89337189	1.0821	382.8	414.23
0.86198063	1.0441	424.2	442.90
0.82269354	.99651	438.0	436.47
0.77900256	.94357	382.8	361.20

(For continuation see page 249)

10.2.3 continued
TABLE 34 continued-

Apex Height At Maximum Radius = 1.11174 ft

<u>Station to Station</u>	<u>Mid Station</u>	<u>Radius ft Mid Station</u>	<u>Apex Height ft Mid Station</u>
715.09/751.64	733.365	74.229863	0.8091055
751.64/787.76	769.700	67.733179	0.73829165
787.76/820.76	804.260	60.305062	0.65732517
820.76/853.08	836.92	51.688805	0.56340797
853.08/876.15	864.615	42.462675	0.46284315
876.15/898.96	887.555	32.381398	0.35295723

10.2.3 continued

TABLE 34 continued

Cap Height ft Mid Station	X-Section Area in ² Mid Station	Longeron Length Between Stations in.	Longeron Volume Between Stations in ³
0.72819495	.88204	426.0	375.75
0.66446248	.80484	454.2	365.56
0.59159265	.71657	402.0	288.06
0.50706717	.61418	399.0	245.06
0.41655883	.50458	310.2	156.52
0.3176615	.38478	303.6	116.82

Total 10,466.21 in³

For 48 502,377.85 in³

Weight 51,242.54 lb
25.62 tons

Added Splice Weight:

Length of longeron = 909.28929
 Total number of splices = 2,208
 Total length of splices = 52,992 in.
 Total Volume of splices = 52,992 x average area
 = 50,543.48 in³

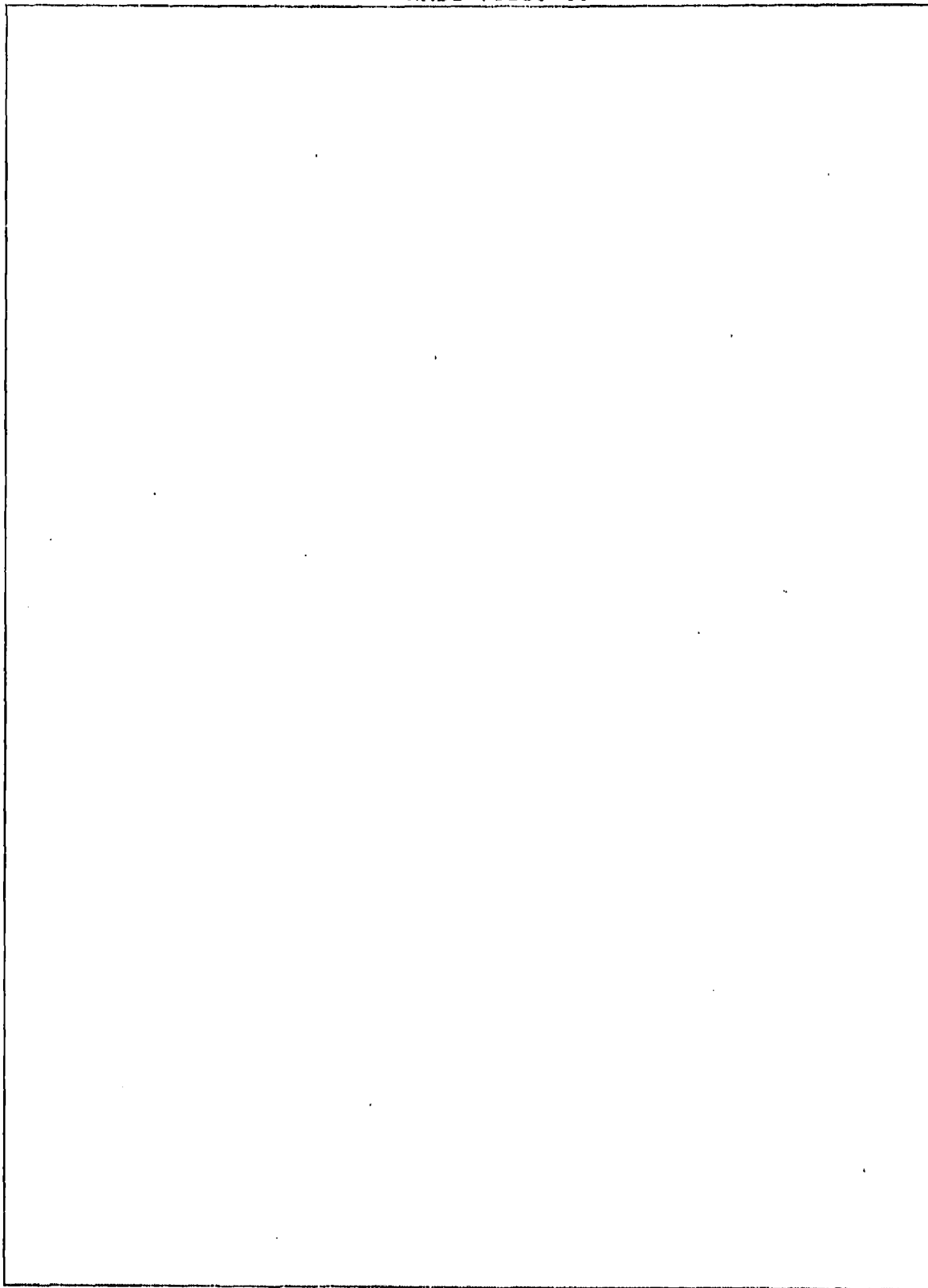
Weight of splices (50,543.48)(.102) = 5,155.44 lb

Total weight - 56,398.00 lb
28.199 tons

10.2.1 continued
10.2.2 continued
10.2.3 continued

Total Weight of Hull Structure: MC-200

Main Frames	60,655.00 lb = 30.33 tons
Secondary Frames	15,763.00 lb = 7.88 tons
Longerons	56,398.00 lb = 28.20 tons
Total	132,816.00 lb = 66.41 tons



10.2.1

TABLE 35 MC-100, Main Frame Weight Calculations

<u>Main Frame Station</u>	<u>X-Section Area Cap & Feet (in²)</u>	<u>X-Section Area Corrugations (in²)</u>	<u>X-Section Area Skin in²</u>
19.25	2.9006906	3.2385249	0.60164166
97.10	3.0978113	3.4586038	0.64252708
179.30	3.8030664	4.2459976	0.78880631
262.287	3.993941	4.4591028	4.4591028
345.20	3.9255231	4.3827165	0.81420544
425.94	3.7231001	4.156718	0.722203
516.54	3.3670537	3.7592039	0.69837151
607.98	2.9006906	3.2385249	0.60164166

10.2.1

TABLE 35 MC-100, Main Frame Weight Calculations
(Continued)

<u>Main Frame Station</u>	<u>Weight For Anchors Each (lb)</u>	<u>Total Weight Anchors (lb)</u>	<u>Total X-Section Area (in²)</u>	<u>Volume (in³)</u>
19.25	12.6	529.2	6.7408571	11,417.51
97.10	12.6	529.2	7.1989421	30,769.053
179.30	12.6	529.2	8.8378703	48,729.571
262.287	12.6	529.2	9.4133652	51,145.509
345.20	12.6	529.2	9.122445	51,918.232
425.94	12.6	529.2	8.6020211	44,444.056
516.54	12.6	529.2	7.8246291	38,196.635
607.98	12.6	529.2	6.7408571	25,838.628

10.2.1

TABLE 35 MC-100, Main Frame Weight Calculations
(Continued)

Main Frame Station	Weight Of Frame (Less Anchors) (lb)	Total Weight Of Frame (Structure + Anchor) (lb)	Caps* (lb)
19.25	1,164.5861	1,693.7861	25.36189
97.10	3,138.4434	3,667.6434	69.218224
179.30	4,970.4162	5,499.6162	103.44979
262.287	5,216.8416	5,746.0416	112.52197
345.20	5,295.6594	5,824.8594	110.59442
425.94	4,533.2937	5,062.4937	97.657628
516.54	3,896.0568	4,425.2568	81.776351
607.98	2,635.5401	3,164.7401	56.359753

*Additional weight (lbs) due to splices.

10.2.1

TABLE 35

MC-100, Main Frame Weight Calculations
(Continued)

Main Frame Station	Cornicos* (lb)	Skin* (lb)	Total Weight Of Splice (lb)	Adjusted Total Weight Of Frame (lb)
19.25	30.997866	5.8448797	62.204635	1,452.00
97.10	75.237206	13.732569	158.18799	3,163.50
179.30	114.5337	44.446347	262.42983	4,764.52
262.287	128.04225	22.533771	263.09799	4,968.84
345.20	122.03522	47.459478	280.08911	5,048.06
425.94	108.50848	19.505283	225.67138	4,372.68
516.54	91.589516	35.279918	208.64577	3,831.68
607.98	64.813717	11.689759	132.8632	2,726.72
Total				30,328 lb

*Additional weight (lbs) due to splices.

10.2.2

TABLE 36 MC-100, Secondary Frame Weight Calculations

Secondary Frame Station	X-Section Area Cap & Feet (in ²)	X-Section Area Corrugations (in ²)	Total X-Section Area (in ²)
45.50	0.270234	0.315977	0.586211
69.80	0.318254	0.377126	0.690380
125.25	0.398915	0.466629	0.865544
150.85	0.424430	0.496273	0.920703
206.96	0.458249	0.535817	0.994066
234.62	0.465076	0.543800	1.008876
291.15	0.466170	0.545079	1.011249
316.60	0.463586	0.542058	1.005644
373.80	0.452872	0.529530	0.982402
399.29	0.445354	0.520740	0.966094
458.39	0.423408	0.495079	0.918487
486.14	0.410516	0.480004	0.890520
548.14	0.373661	0.436911	0.810572
577.29	0.353202	0.412989	0.766191
640.09	0.293337	0.342991	0.636328
667.99	0.257420	0.269495	0.526915
692.56	0.173101	0.202401	0.375502
712.31	0.117840	0.137787	0.255627
722.29	0.090209	0.106480	0.196689

10.2.2

TABLE 36 MC-100, Secondary Frame Weight Calculations
(Continued)

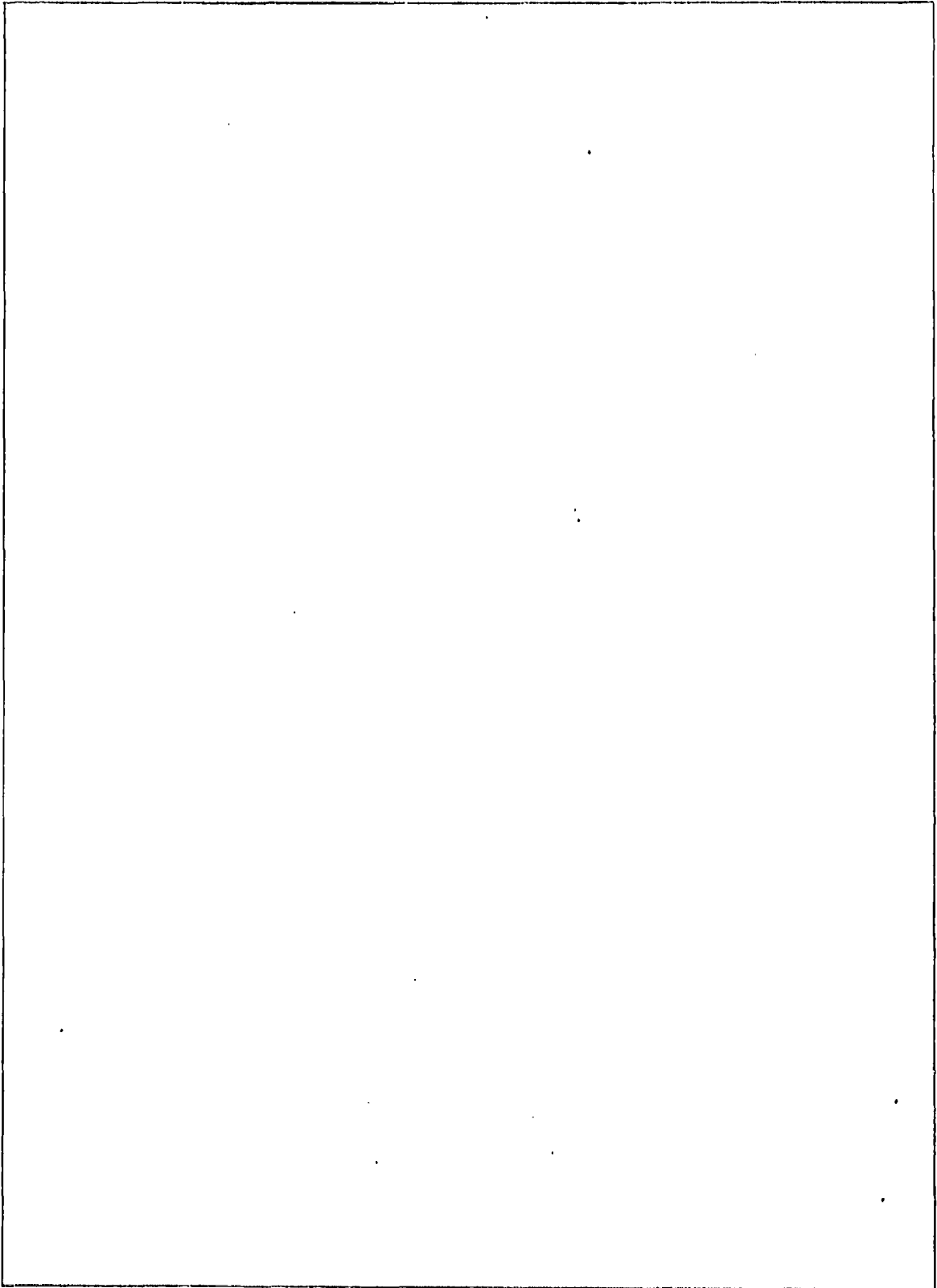
<u>Secondary Frame Station</u>	<u>Volume (in³)</u>	<u>Total Weight Of Frame Structure (lb)</u>	<u>Caps* (lb)</u>
45.50	2,057.6619	209.88151	3.1850053
69.80	2,853.9175	291.09958	4.9880617
125.25	4,484.8672	457.45645	6.8019683
150.85	5,075.796	517.73119	10.851171
206.96	5,916.9155	603.52538	11.957524
234.62	6,094.5484	621.64393	14.245867
291.15	6,123.2383	624.5703	14.458125
316.60	6,055.5475	617.66584	14.492115
373.80	5,778.8909	589.44687	14.411789
399.29	5,588.616	570.03883	13.638768
458.39	5,051.3896	575.24173	13.412355
486.14	4,748.4528	484.34218	11.928742
548.14	3,934.1283	401.28108	11.166711
577.29	3,515.1088	358.54109	9.4381918
640.09	2,424.5329	247.30235	8.5782879
667.99	1,867.1369	190.44796	5.6994801
692.56	844.28648	86.11722	4.5014435
712.31	391.27473	39.910022	2.0179825
722.29	301.06145	30.708267	0.915845

*Additional Weight (lbs) due to splices.

10.2.2 continued
TABLE 36 MC-100, Secondary Frame Weight Calculations

Secondary Frame Station	Cornices* (lb)	Total Weight Of Splice (lb)	Total Weight Of Frame (lb)
45.50	3.1850053	6.3700106	218.21
69.80	4.9880617	9.9761234	303.80
125.25	6.8019683	13.603936	475.32
150.85	10.851171	21.702342	544.31
206.96	11.957524	23.915048	633.12
234.62	14.245867	28.491734	656.02
291.15	14.458125	28.916250	659.40
316.60	14.492115	28.98423	652.50
373.80	14.411789	28.823578	623.86
399.29	13.638768	27.277536	602.72
458.39	13.412355	26.824710	546.97
486.14	11.928742	23.857484	512.80
548.14	11.166711	22.333422	427.45
577.29	9.4381918	18.876383	380.83
640.09	8.5782879	17.156575	266.85
667.99	5.6994801	11.398960	203.67
692.56	4.5014435	9.002887	95.98
712.31	2.0179825	4.035965	44.34
722.29	0.915845	1.831690	32.83
			7,880.98

*Additional weight (lbs) due to splices.



10.2.3

TABLE 37 MC-100, Longerons Calculations

Apex height at maximum radius = 0.8823877 ft.

Station to Station	Mid- Station	Radius At Mid-Station (ft)	Volume Of Longerons Between Stations (in ³)	Volume For 42 Longerons (in ³)	Weight For 42 Longerons (lb)
19.25/45.50	32.375	38.961123	184.65	7,755.39	791.05
45.50/69.80	57.65	50.638284	222.17	9,330.98	951.76
69.80/97.10	83.45	59.217453	291.88	12,259.02	1,250.42
97.10/125.25	111.175	66.167463	316.52	13,293.92	1,355.98
125.25/150.85	138.05	71.295583	329.53	13,840.29	1,411.71
150.85/179.30	165.075	75.187505	386.21	16,220.78	1,654.52
179.30/206.96	193.13	78.08833	389.97	16,378.82	1,670.64
206.96/234.62	220.79	79.932952	399.18	16,765.69	1,710.10
234.62/262.287	248.4535	80.840322	403.82	16,960.29	1,729.95
262.287/291.15	276.7185	80.914221	421.66	17,709.71	1,806.39
291.15/316.60	303.875	80.630378	370.49	15,560.78	1,587.20
316.60/345.20	330.900	80.071798	413.47	17,365.59	1,771.29
345.20/373.80	359.500	79.174152	408.83	17,170.88	1,751.43
373.80/399.29	386.545	78.025716	359.09	15,081.76	1,538.34

TABLE 37 continued

399.29/425.94	412.615	76.630606	368.72	15,486.18	1,579.59
425.94/458.39	442.165	74.654288	437.39	18,370.20	1,873.76
458.39/486.14	472.265	72.280394	362.14	15,209.90	1,551.41
486.15/516.54	501.34	69.50503	381.49	16,022.65	1,634.31
516.54/548.14	532.34	65.994372	376.52	15,813.82	1,613.01
548.14/577.29	562.715	61.910952	325.84	13,685.20	1,395.89
577.29/607.98	592.635	57.132506	316.58	13,296.47	1,356.25
607.98/640.09	624.035	51.079424	296.13	12,437.45	1,268.62
640.09/667.99	654.040	43.905118	221.16	9,288.92	947.47
667.99/692.56	680.275	35.879808	159.17	6,685.00	681.87
692.56/712.31	702.435	26.724386	95.29	4,002.35	408.24
712.31/722.29	717.300	17.695240	31.88	1,339.12	136.59
				Total =	35,427.78 lbs

Number of splices per longeron = 26
 Total for 42 longerons = 1,092
 Volume of splices per longeron = 21.209 in³
 Volume of splices for 42 longerons = 890.76 in³
 Weight of splices for 42 longerons = 100.25 lb
 Therefore, total weight of longerons = 35,428 lb

10.2.1, 10.2.2, 10.2.3 continued

SUMMARY

Total Structure Weight For MC-100:

Main Frames	30,328.00 lb
Secondary Frames	7,881.00 lb
Longerons	<u>35,428.00 lb</u>
Total	73,737.00 lb
	36.87 tons

10.3 HULL SKIN WEIGHT SUMMARY

10.3.1 Description. The weight summary as shown in the following tables is the summation of the total hull shell skin weight. This hull skin consists of the complete metal hull shell minus main and secondary frame and longeron, side structure. This shell, therefore, includes main frame base and transition skin, secondary frame base skin, longeron base skin and all adjoining skin panels. For this weight analysis the hull was divided into ellipsoidal segments labeled A, B, C and etc. These segments are located between frames. Their widths contain the skin panels and are the lengths of the tapered longeron base skins. Segment A (bow to main frame No.1) and Segment B-B (MC-100) or D-D (MC-200) which are segments from last frame to stern are treated as spheroidal segments for surface area calculations. All other segments were a ratio of ellipsoidal and trapezoidal areas. Main and secondary base and transition skin surface areas were treated as cone segments due to their small angles and minimal width compared to the total hull perimeter. Longeron base skin surface areas were treated as trapezoids with a factor for curvature included for their true lengths. All joggles and their inherent overlap of skin were accounted for on this weight analysis due to skin thickness differences at the joggles. See Figure 42 for graphical description.

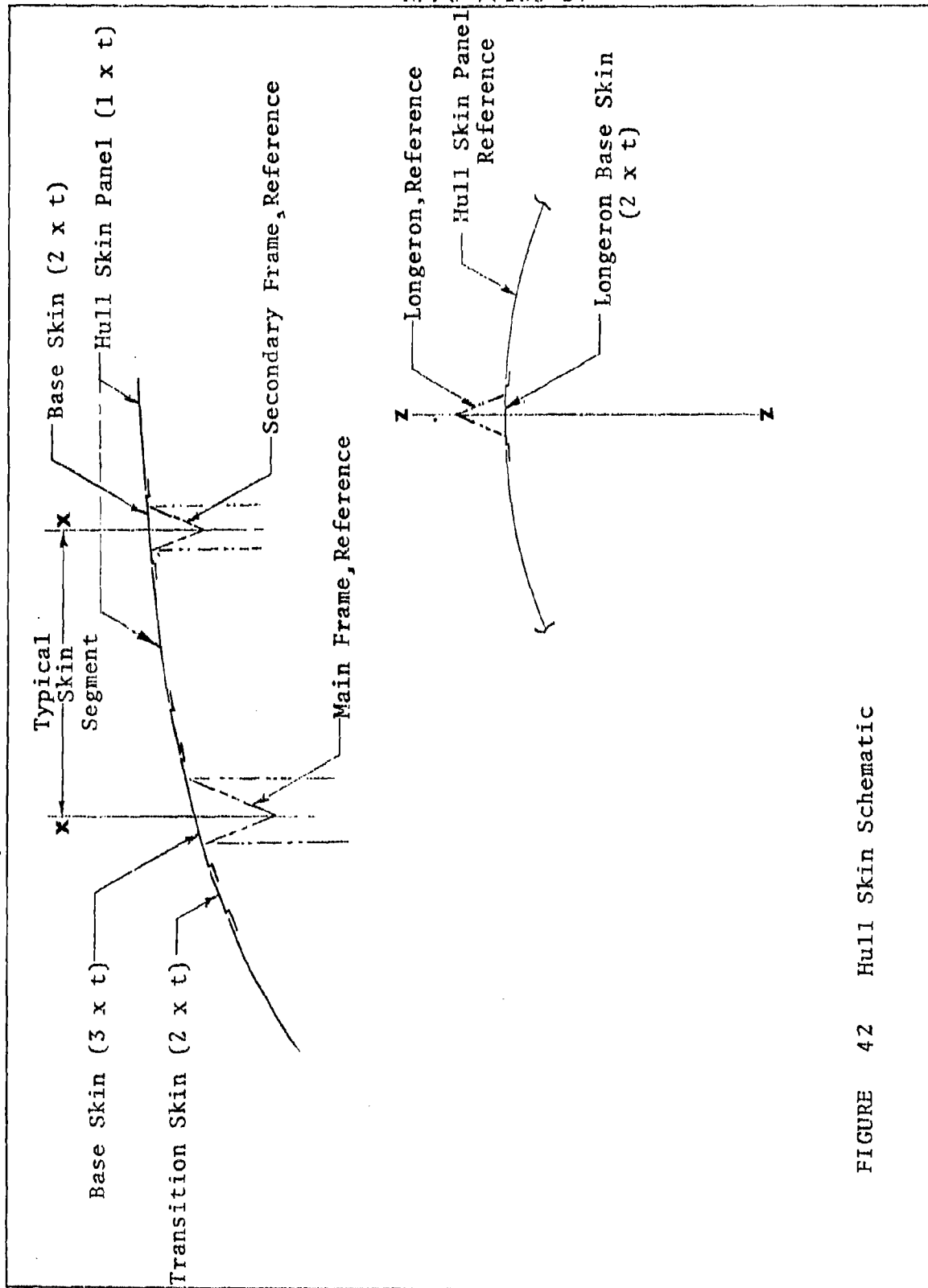


FIGURE 42 Hull Skin Schematic

TABLE 38 Weight Summary - All Hull Skin MC-100

Frame No. And Hull Segment	Frame Stations	<div style="text-align: center;">1</div> Frame Base Skin Weight lbs	Longeron Base Skin Weight lbs	Hull Skin Weight lbs
Bow	0			
I A				710
1 B	19.25	1,434		
2 C	45.50	234	738	1,077
3 D	69.80	293	816	1,494
II E	97.10	2,276	824	1,721
4 F	125.25	376	779	1,844
5 G	150.85	459	848	2,065
III H	179.30	3,157	946	2,398
6 I	206.96	567	913	2,388
7 J	234.62	580	1,182	3,145
IV K	262.287	3,840	1,018	2,732
8 L	291.15	583	1,073	2,881
9 M	316.60	579	1,081	2,898
V N	345.20	3,736	1,058	2,825
10 O	373.80	562	1,059	2,798
11 P	399.29	493	963	2,519
VI Q	425.94	3,072	865	2,231
12 R	458.39	458	1,097	2,773
13 S	486.14	387	916	2,258
VII T	516.54	2,401	877	2,102
14 U	548.14	338	916	2,097
			811	1,764

TABLE 38 Weight Summary, All Hull Skin MC-100
continued-

Frame No. And Hull Segment	Frame Stations	Frame Base Skin Weight lbs	Longeron Base Skin Weight lbs	Hull Skin Weight lbs
14	577.29	255		
V			626	1,279
VIII	607.98	1,438		
W			659	1,207
15	640.09	170		
X			550	883
16	667.99	121		
Y			477	623
17	692.56	91		
Z			312	288
18	712.31	47		
A-A			164	84
19	722.29	29		
B-B				66
Stern	728.576			
Sub Total		27,975	21,566	51,149
Total = 100,690 lbs				


 Includes base transition skin on main frames.

TABLE 39 Weight Summary, Hull Skin MC-200

Frame No. And Hull Segment	Frame Stations	<div style="display: inline-block; border: 1px solid black; padding: 2px;">1</div>		Hull Skin Weight lbs
		Frame Base Skin Weight lbs	Longeron Base Skin Weight lbs	
Bow	0			
I A				1,100
I B	18.38	2,120	796	1,045
1 C	38.38	327		
2 C	60.87	421	1,181	1,926
3 D	88.50	519	1,463	2,805
II E	121.87	4,052	1,620	3,476
4 F	158.38	675	1,733	4,091
5 G	192.24	735	1,826	4,544
III H	229.50	6,086	1,993	5,141
6 I	265.85	901	1,936	5,142
7 J	298.50	1,006	2,175	5,852
IV K	334.50	7,263	2,101	5,690
8 L	370.70	1,009	2,116	5,735
9 M	404.06	1,001	2,226	6,019
V N	438.81	7,033	2,007	5,401
10 O	475.16	968	2,120	5,654
11 P	508.26	865	1,996	5,274
VI Q	543.16	5,861	1,827	4,767
12 R	578.96	804	1,880	4,813
13 S	611.08	698	1,710	4,295
T			1,654	4,054


 Includes base transition skin on main frames.

TABLE 39 Weight Summary, Hull Skin MC-200
continued-

Frame No. And Hull Segment	Frame Stations	1		
		Frame Base Skin Weight lbs	Longeron Base Skin Weight lbs	Hull Skin Weight lbs
VII		646.46	4,444	
U			1,722	4,064
14		683.21	612	
V			1,463	3,322
15		715.09	508	
W			1,319	2,855
VIII		751.64	2,616	
X			1,289	2,574
16		787.76	350	
Y			1,099	1,999
17		820.76	257	
Z			690	1,098
IX		853.08	1,127	
A-A			467	599
18		876.15	118	
B-B			556	531
19		898.96	76	
C-C			154	234
20		910.462		127
D-D				
Stern		917.949		
Sub Total		52,453	43,116	104,226

Total = 199,794 lbs

Skin Weight Summary For All Hulls:

	Displacement ft ³	Weight lb	Specific Weight lb/ft ³
MC-100	10(10) ⁶	100,690	.010069
MC-200	20(10) ⁶	199,794	.009990

Volume Ratio = 2:1

Weight Ratio = 1.984249:1

By extrapolation of specific weights the following hull weights were determined:

MC-125	12.5(10) ⁶	124,143	.009931
MC-150	15(10) ⁶	148,434	.009896
MC-175	17.5(10) ⁶	173,638	.009922

2 Station only

10.4 Seams

TABLE 40 Weight Of Seams

	MC-100 (1b)	MC-125 (1b)	MC-150 (1b)	MC-175 (1b)	MC-200 (1b)
Type I Lap Joint	170.67	197.76	224.85	246.52	270.90
Type II Lap Joint	452.16	523.93	595.70	653.12	717.71
Type III Lap Joint	4,119.77	4,773.70	5,427.63	5,950.77	6,539.31
Type IV Lap Joint	721.07	762.52	866.98	950.54	1,044.55
Butt Joint	<u>539.51</u>	<u>625.14</u>	<u>710.78</u>	<u>779.29</u>	<u>856.36</u>
Total Weight	6,003.16	6,883.05	7,825.94	8,580.24	9,428.83

10.5 Diaphragm And Cell Membrane Weights

TABLE 41 MC-100, Diaphragms

<u>Main Frame Station</u>	<u>Radius - Hull At Station ft</u>	<u>Radius - Less Main Frame Height, ft</u>	<u>Length Of Cord in Net in</u>	<u>Volume Of Cord in³</u>
19.25	30.440835	22.440835	27,608.86	762.3262
97.10	62.881176	54.881176	67,520.069	1,864.3406
179.30	76.794176	68.500405	84,275.746	2,326.9925
262.287	80.953	72.210076	88,839.745	2,453.0121
345.20	79.667934	71.059338	87,423.99	2,413.9207
425.94	75.803344	67.616583	83,188.384	2,296.9687
516.54	67.859746	59.859746	73,645.182	2,033.4651
607.98	54.327218	46.327218	56,996.172	1,573.7584

Weight of Membrane: .045072 lb/ft²

TABLE 42 MC-100, Gas Cell Membranes

<u>Station to Station</u>	<u>Length Between Stations</u>	<u>Mid- Station</u>	<u>Radius At Mid-Station ft</u>	<u>Area Of Ends ft²</u>
19.25/97.10	77.85	58.175	50.839727	8,893.3376
97.10/179.30	82.2	138.20	71.320465	17,501.96
179.30/262.287	82.987	220.7935	79.933583	21,984.516
262.287/345.20	82.913	303.7435	80.632418	22,370.606
345.20/425.94	80.74	385.57	78.072316	20,972.61
425.94/516.54	90.60	471.24	72.369867	18,020.793
516.54/607.98	91.44	562.26	61.977411	13,216.766
607.98/728.576	120.596	668.278	39.815965	5,454.7247



TABLE 41 MC-100, Diaphragms (continued)

<u>Weight of Net lb</u>	<u>Diaphragm "A" (Air) Area ft²</u>	<u>Diaphragm "A" Weight lb</u>	<u>Diaphragm "B" Area ft²</u>
39.79664	-	-	715.70193
97.326424	-	-	4,280.564
121.4788	14,741.311	655.16937	-
128.05755	-	-	7,410.5386
126.01681	15,863.25	705.03332	-
119.91143	-	-	6,497.7143
106.15543	11,256.92	500.30755	-
82.15681	-	-	3,050.1881

TABLE 42 MC-100, Gas Cell Membranes (continued)

<u>Area Of Sides ft²</u>	<u>Total Area ft²</u>	<u>Weight lb</u>
13,618.214	22,511.551	1,014.64
20,171.785	37,673.745	1,698.04
22,824.312	44,808.828	2,019.63
23,003.327	45,373.933	2,045.10
21,689.231	42,661.841	1,922.86
22,560.272	40,581.065	1,829.08
19,499.703	32,716.469	1,474.60
16,521.462	21,976.186	<u>990.51</u>

Total = 12,994.46

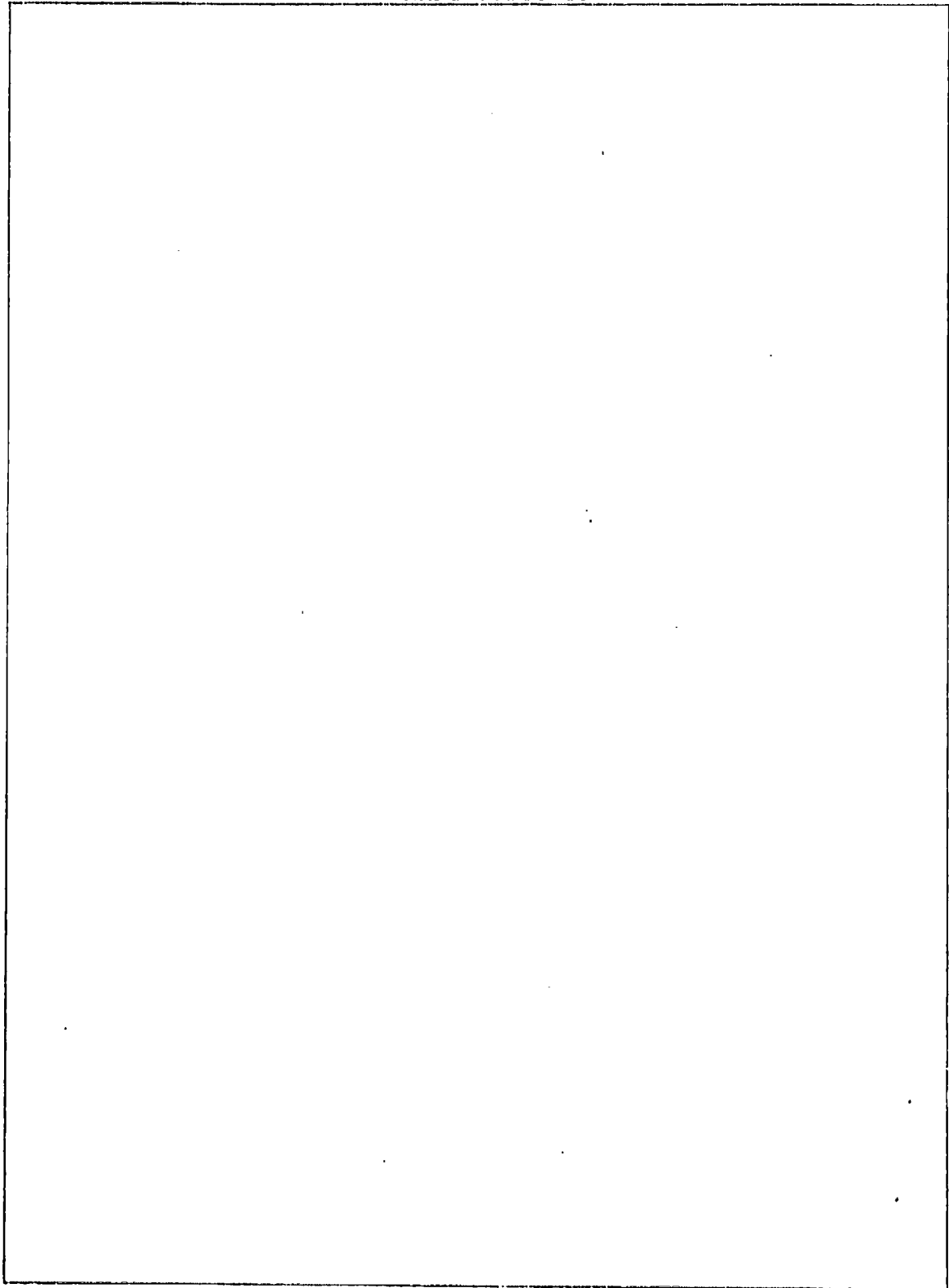
TABLE 41 MC-100, Diaphragms (continued)

<u>Main Frame Station</u>	<u>Diaphragm "B" Weight lb</u>	<u>Total Weight lb</u>
19.25	31.808974	72.62
97.10	190.24728	291.64
179.30	-	787.19
262.287	329.35726	463.87
345.20	-	842.79
425.94	288.78729	414.47
516.54	-	615.03
607.98	135.56391	<u>220.80</u>
Total =		3,708.40 lb

Total weight of membranes: 16,702.857 lb

Plus allowance for seams, adhesives, etc. = 5% = 835.1429 lb

total weight: 17,538 lb



10.5 Diaphragm and Cell Membrane Weights

TABLE 43 MC-125, Diaphragms

<u>Main Frame Station</u>	<u>Radius - Hull At Station ft</u>	<u>Radius - Loss Main Frame Height, ft</u>	<u>Length Of Cord in Net in</u>
12.26	25.411296	17.411296	21,421.04
100.74	66.754863	56.754863	69,825.258
193.06	85.809187	76.541795	94,169.033
282.54	87.204	77.785968	95,699.741
372.02	82.715436	73.782169	90,773.877
460.94	81.518334	72.714354	89,460.149
549.26	73.893825	65.893825	81,068.882
639.19	61.405617	53.405617	65,704.695
725.92	40.979023	32.979023	40,573.946

TABLE 44 MC-125, Cell Membranes

<u>Station to Station</u>	<u>Length Between Stations ft</u>	<u>Mid- Station</u>	<u>Radius At Mid-Station ft</u>
12.26/100.74	88.48	56.5	52.319063
100.74/193.06	92.32	146.9	76.497757
193.06/282.54	89.48	237.8	86.103738
282.54/372.02	89.48	327.28	86.857398
372.02/460.94	88.92	416.48	84.046521
460.94/549.26	88.32	505.10	78.176583
549.26/639.19	89.93	594.225	68.384468
639.19/725.92	86.73	682.555	52.741328
725.92/784.835	58.915	755.3775	29.424405

TABLE 43 MC-125, Diaphragms (continued)

<u>Volume Of Cord in³</u>	<u>Weight of Net lb</u>	<u>Diaphragm "A" (Air) Area ft²</u>	<u>Diaphragm "A" Weight lb</u>
591.4703	30.877238	-	-
1,927.9907	100.64922	-	-
2,600.1625	135.73942	18,405.479	818.02128
2,642.4279	137.94585	-	-
2,506.4167	130.84549	17,120.228	760.09901
2,470.1425	128.95183	-	-
2,238.4457	116.85628	13,640.782	606.25697
1,814.2151	94.709662	-	-
1,120.3136	58.485084	-	-

TABLE 44 MC-125, Cell Membranes (continued)

<u>Area Of Ends ft²</u>	<u>Area Of Sides ft²</u>	<u>Total Area ft²</u>	<u>Weight lb</u>
9,381.1976	15,865.123	25,246.320	1,121.18
20,055.605	24,203.762	44,259.367	1,965.54
25,408.696	26,405.011	51,813.707	2,301.02
25,855.444	26,636.132	52,491.576	2,331.13
24,209.056	25,612.83	49,821.886	2,212.57
20,945.549	23,663.059	44,608.608	1,981.05
16,027.040	21,076.594	37,103.634	1,647.75
9,533.2392	15,676.849	25,210.088	1,119.58
2,967.2474	5,941.1694	8,908.4168	395.62

TABLE 43 MC-125, Diaphragms (continued)

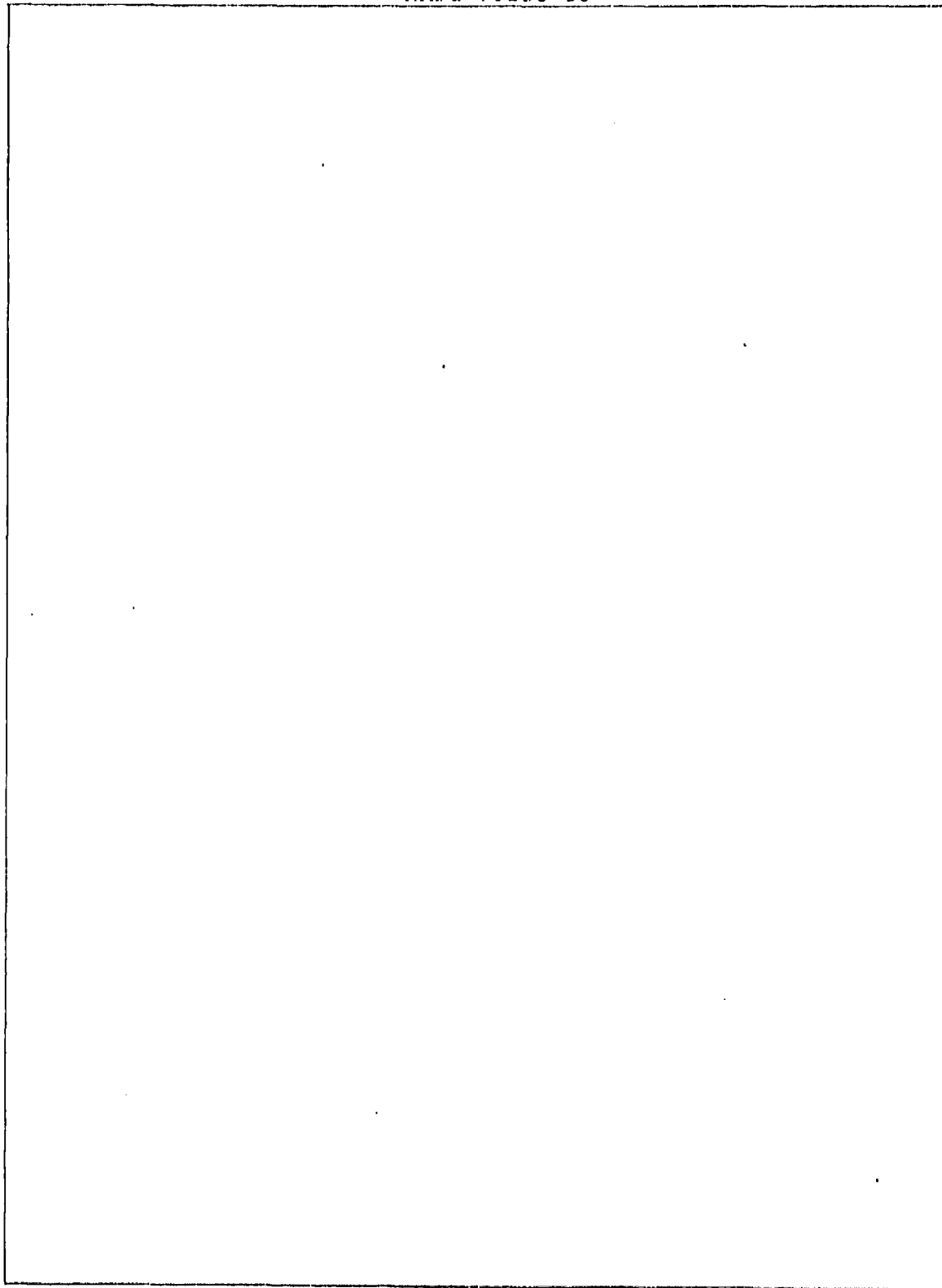
<u>Main Frame Station</u>	<u>Diaphragm "B" Area ft²</u>	<u>Diaphragm "B" Weight lb</u>	<u>Total Weight lb</u>
12.26	432.90176	19.240078	50.08
100.74	4,599.7404	204.4329	304.84
193.06	-	-	953.01
282.54	8,640.3173	384.01409	521.55
372.02	-	-	890.24
460.94	7,550.3566	335.5714	464.16
549.26	-	-	722.54
639.19	4,072.8746	181.01664	275.51
725.92	1,553.1118	69.02719	<u>127.41</u>

Total = 4,309.35 lb

Amended total weight of membranes: 19,384.76 lb

Plus allowance for seams, adhesives, etc. = 5% = 969.24 lb

total weight: 20,354 lb



10.5 Diaphragm And Cell Membrane Weights

TABLE 45 MC-150, Diaphragms

<u>Main Frame Station</u>	<u>Radius - Hull At Station ft</u>	<u>Radius - Less Main Frame Height, ft</u>	<u>Length Of Cord in Net in</u>
13.03	27.003727	19.003727	23,380.199
107.06	70.938142	62.938142	77,432.512
205.16	87.898905	78.405824	96,462.332
300.25	92.66875	82.660525	101,696.88
395.33	91.18653	81.338385	100,070.24
489.83	86.610496	77.256563	95,048.401
583.68	78.524476	70.043833	86,174.612
679.25	65.253678	57.253678	70,438.942
771.41	43.547025	35.547025	43,733.344

TABLE 46 MC-150, Cell Membranes

<u>Station to Station</u>	<u>Length Between Stations ft</u>	<u>Mid- Station</u>	<u>Radius At Mid-Station ft</u>
13.03/107.06	94.03	60.045	55.599465
107.06/205.16	98.10	156.11	81.292283
205.16/300.25	95.09	252.705	91.49967
300.25/395.33	95.08	347.79	92.300424
395.33/489.83	94.50	442.58	89.313393
489.83/583.68	94.35	536.505	83.09692
583.68/679.25	95.57	631.465	72.669684
679.25/771.41	92.16	725.33	56.046224
771.41/834.02	62.61	802.715	31.268432

TABLE 45 MC-150, Diaphragms (continued)

<u>Volume Of Cord in³</u>	<u>Weight of Net lb</u>	<u>Diaphragm "A" (Air) Area ft²</u>	<u>Diaphragm "A" Weight lb</u>
645.56591	33.701257	-	-
2,138.0395	111.61465	-	-
2,663.4843	139.04508	19,312.856	858.34914
2,808.0188	146.59039	-	-
2,736.1046	144.24568	20,784.565	923.75843
2,624.4433	137.00698	-	-
2,379.4233	124.2159	15,413.088	685.02612
1,944.9355	101.53381	-	-
1,207.5498	63.03918	-	-

TABLE 46 MC-150, Cell Membranes (continued)

<u>Area Of Ends ft²</u>	<u>Area Of Sides ft²</u>	<u>Total Area ft²</u>	<u>Weight lb</u>
10,594.479	17,917.417	28,511.896	1,267.1953
22,648.373	27,331.073	49,979.446	2,221.3086
28,693.097	29,818.978	58,512.075	2,600.5366
29,197.507	30.076.773	59.274.28	2,634.4124
27,338.303	28,925.893	56,264.196	2,500.6309
23,665.094	26,869.847	50,534.941	2,245.9973
18,098.597	23,801.988	41,900.585	1,862.2482
10,765.422	17,702.197	28,467.619	1,265.2274
3,350.816	6,709.4691	10,060.285	<u>447.12377</u>
Total =			17,044.678 lb

TABLE 45 MC-150, Diaphragms (continued)

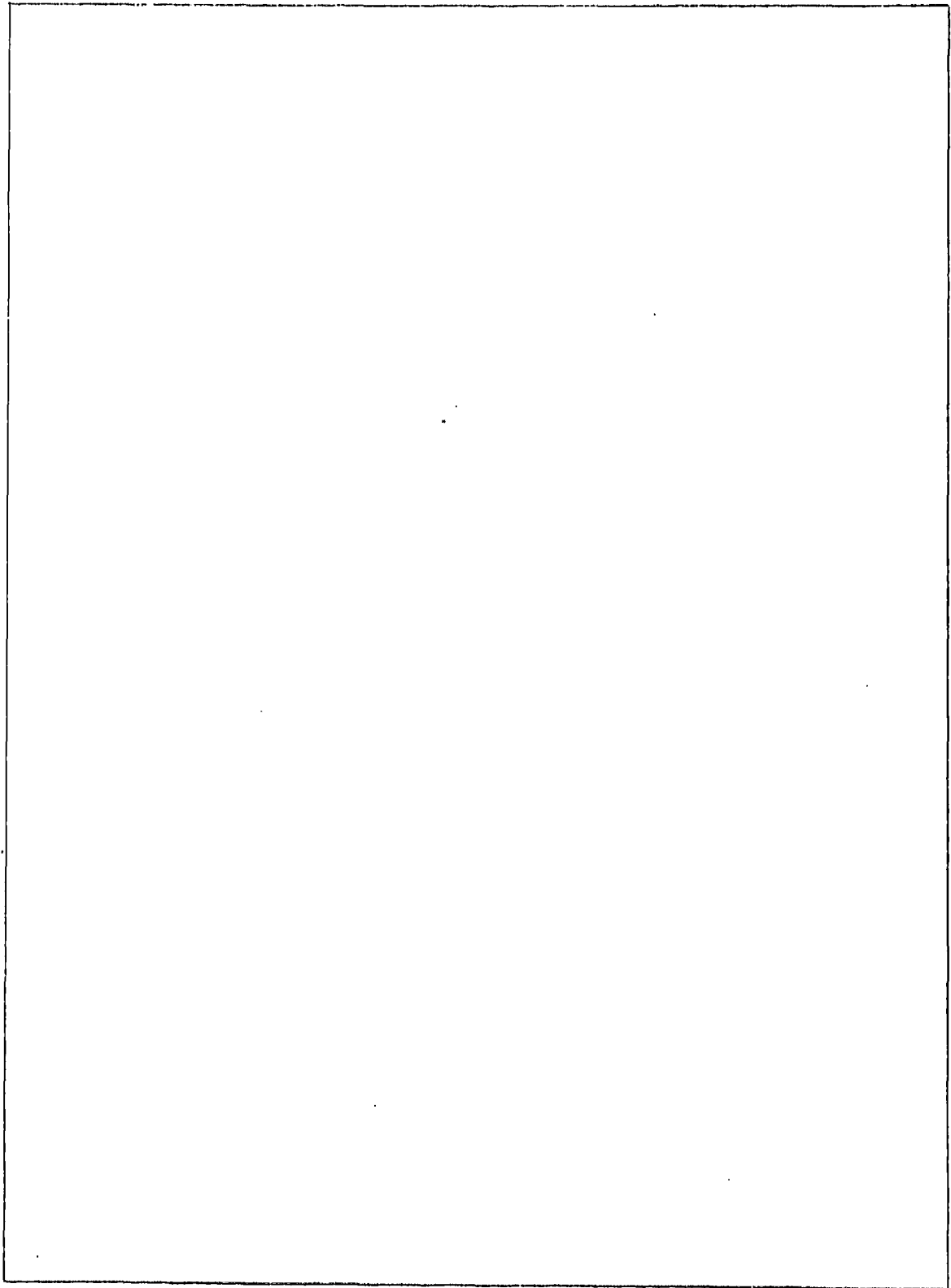
<u>Main Frame Station</u>	<u>Diaphragm "B" Area ft²</u>	<u>Diaphragm "B" Weight lb</u>	<u>Total Weight lb</u>
13.03	515.70901	22.92040	56.621661
107.06	5,656.5939	251.40417	363.01882
205.16	-	-	997.39422
300.25	8,757.1613	433.6516	580.24199
395.33	-	-	1,068.0041
489.83	8,523.1069	378.80474	515.81172
583.68	-	-	809.24202
679.25	4,680.9494	208.04219	309.576
771.41	1,804.4035	80.19571	<u>143.23489</u>

Total = 4,843.1452 lb

Total weight of membranes: 21,887.823 lb

Plus allowance for seams, adhesives, etc. = 5% = 1,094.3911 lb

Total weight: 22,982.214 lb



10.5 Diaphragm And Cell Membrane Weights

TABLE 47 MC-175, Diaphragms

<u>Main Frame Station</u>	<u>Radius - Hull At Station ft</u>	<u>Radius - Less Main Frame Height, ft</u>	<u>Length Of Cord in Net in</u>
13.72	28.43002	20.43002	25,134.875
112.70	74.677303	66.612155	81,952.354
215.98	92.533072	82.539501	101,547.62
316.075	97.554	87.018168	107,058.07
416.17	95.993774	85.626447	105,345.47
515.65	91.193518	81.344619	100,077.57
614.45	82.664078	73.736358	90,717.199
715.06	68.693679	60.93679	74,670.905
812.08	45.842709	33.842709	41,636.390

TABLE 48 MC-175, Cell Membranes

<u>Station to Station</u>	<u>Length Between Stations ft</u>	<u>Mid- Station</u>	<u>Radius At Mid-Station ft</u>
13.72/112.70	98.98	63.21	58.530318
112.70/215.98	103.28	164.34	85.577813
215.98/216.075	100.095	266.0275	96.323299
316.075/416.17	100.095	366.1225	97.166296
416.17/515.65	99.48	465.91	94.021859
515.65/614.45	98.8	565.05	87.455171
614.45/715.06	100.61	664.755	76.500624
715.06/812.08	97.02	763.57	59.000454
812.08/877.987	65.907	845.0335	32.916560

TABLE 47 MC-175, Diaphragms (continued)

<u>Volume Of Cord in³</u>	<u>Weight Of Net lb</u>	<u>Diaphragm "A" (Air) Area ft²</u>	<u>Diaphragm "A" Weight lb</u>
694.01542	36.230525		
2,262.8398	118.12975		
2,803.8975	146.37524	21,402.945	951.24199
2,956.0501	154.31825		
2,908.7624	151.84963	23,033.806	1,023.7247
2,763.3070	144.25625		
2,504.8517	130.76379	17,080.997	759.15541
2,061.787	107.63395		
1,149.6495	60.016541		

TABLE 48 MC-175, Cell Membranes (continued)

<u>Area Of Ends ft²</u>	<u>Area Of Sides ft²</u>	<u>Total Area ft²</u>	<u>Weight lb</u>
11,698.326	19,782.914	31,481.24	1,472.47
25,008.309	30,181.402	55,189.711	2,588.40
31,682.88	32,923.48	64,606.36	3,030.04
32,239.868	33,211.619	65,451.487	3,069.67
30,186.977	31,939.39	62,126.367	2,913.73
26,117.581	29,505.599	55,623.18	2,608.73
19,984.436	26,282.588	46,267.024	2,169.92
11,887.01	19,546.932	31,433.942	1,474.25
3,699.9072	7,408.1194	11,108.026	520.97
Total =			19,852.17 lb



TABLE 47 MC-175, Diaphragms (continued)

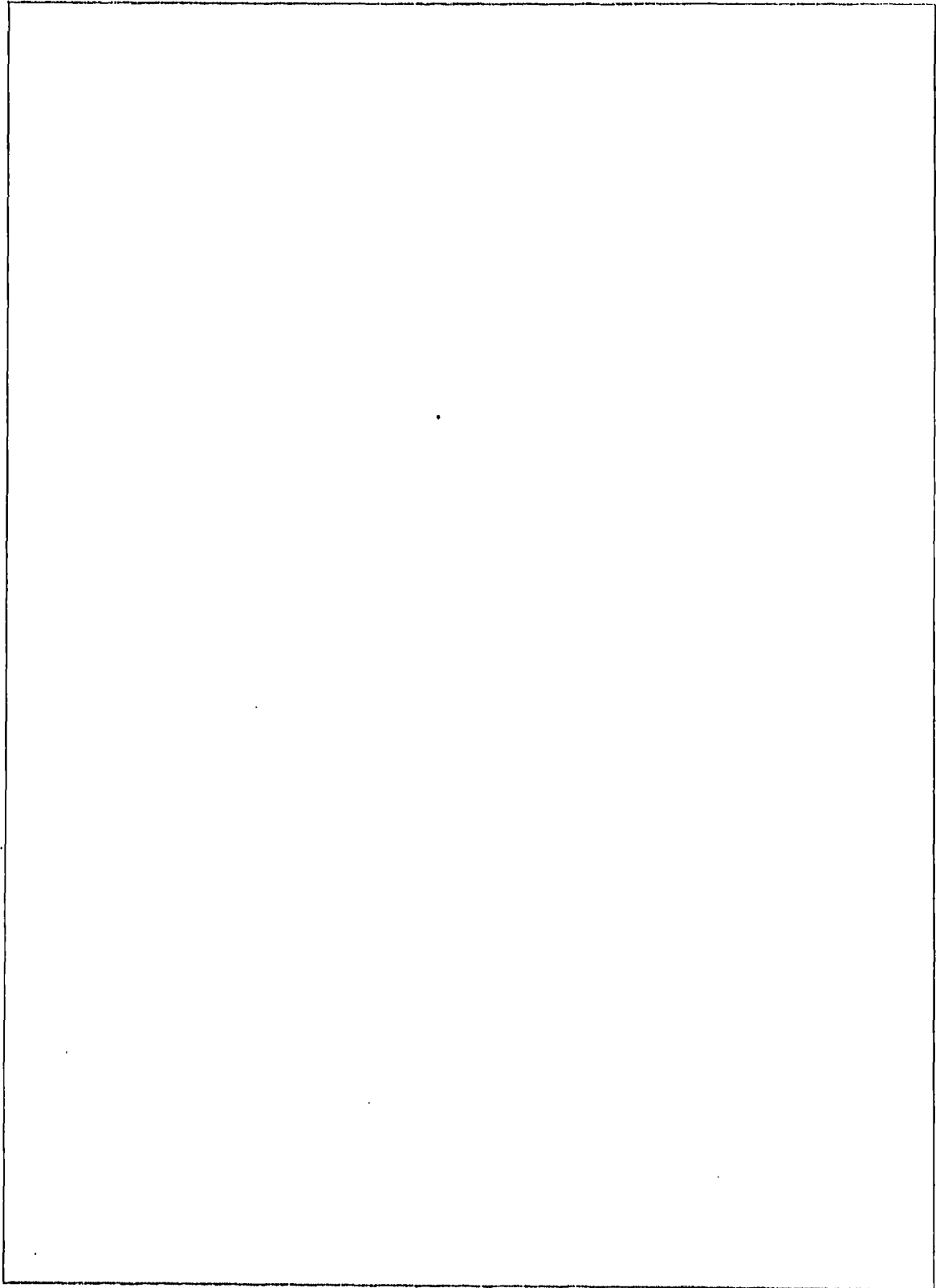
<u>Main Frame Station</u>	<u>Diaphragm "B" Area ft²</u>	<u>Diaphragm "B" Weight lb</u>	<u>Total Weight lb</u>
13.72	598.61679	26.60519	66.31
112.70	6,363.8259	282.8367	423.12
215.98	-	-	1,158.26
316.075	10,860.034	482.66817	672.18
416.17	-	-	1,240.52
515.65	9,487.7271	421.67675	597.20
614.45	-	-	939.09
715.06	5,283.2143	234.80952	361.36
812.08	1,642.6367	73.006074	<u>140.37</u>

Total = 4,404.01 lb

Amended total weight of membranes: 24,256.19 lb

Plus allowance for seams, adhesives, etc. = 5% = 1,212.81 lb

total weight: 25,469 lb



10.5 Diaphragm And Cell Membrane Weights

TABLE 49 MC-200, Diaphragms

<u>Main Frame Station</u>	<u>Radius - Hull At Station ft</u>	<u>Radius - Less Main Frame Height, ft</u>	<u>Length Of Cord in Net in</u>
18.38	33.541274	25.541274	31,423.317
121.87	79.107889	70.564237	86,814.870
229.50	97.117778	86.629058	106,579.34
334.50	101.99209	90.976950	111,928.55
438.81	100.24492	89.418470	110,011.15
543.16	95.075712	84.807536	104,338.33
646.46	85.983498	76.697281	94,360.327
751.64	71.106589	63.106589	77,639.758
853.08	46.588547	38.588547	47,475.319

TABLE 50 MC-200, Cell Membranes

<u>Station to Station</u>	<u>Length Between Stations ft</u>	<u>Mid- Station</u>	<u>Radius At Mid-Station ft</u>
18.38/121.87	103.49	70.1250	62.821971
121.87/229.50	107.63	175.6850	90.115693
229.50/334.50	105.00	282.0000	100.89179
334.50/438.81	104.31	386.6550	101.52686
438.81/543.16	104.35	490.9850	98.113291
543.16/646.46	103.30	594.8100	91.085856
646.46/751.64	105.18	699.0500	79.423019
751.64/853.08	101.44	802.3600	60.75243
853.08/917.949	64.869	885.5145	33.420875

TABLE 49 MC-200, Diaphragms (continued)

<u>Volume Of Cord in³</u>	<u>Weight Of Net lb</u>	<u>Diaphragm "A" (Air) Area ft²</u>	<u>Diaphragm "A" Weight lb</u>
867.64969	45.294964	-	-
2,397.1019	125.1388	-	-
2,942.8314	153.62818	23,576.375	1,047.8388
3,090.5321	161.33878	-	-
3,037.5895	158.57495	25,119.114	1,116.405
2,880.9536	150.3979	-	-
2,605.4445	136.01516	18,480.333	821.3481
2,143.7619	111.91339	-	-
1,310.8719	68.433029	-	-

TABLE 50 MC-200, Cell Membranes (continued)

<u>Area Of Ends ft²</u>	<u>Area Of Sides ft²</u>	<u>Total Area ft²</u>	<u>Weight lb</u>
13,431.826	22,126.967	35,558.793	1,595.47
27,638.394	33,010.013	60,648.407	2,721.21
34,643.644	36,054.301	70,697.945	3,172.12
35,081.152	36,056.649	71,137.801	3,201.95
32,761.791	34.844.34	67,606.131	3,033.39
28,236.691	32,023.088	60,259.779	2,703.77
21,468.650	28,430.958	49,899.608	2,238.93
12,561.435	20,974.172	33,535.607	1,504.70
3,801.4347	7,378.4809	11,179.915	<u>501.63</u>
Total =			20,663.08 lb



TABLE 49 MC-200, Diaphragms (continued)

<u>Main Frame Station</u>	<u>Diaphragm "B" Area ft²</u>	<u>Diaphragm "B" Weight lb</u>	<u>Total Weight lb</u>
18.38	939.32611	41.747825	87.88
121.87	7,169.6936	318.65303	448.03
229.50	-	-	1,212.93
334.50	11,917.743	529.67744	697.61
438.81	-	-	1,287.15
543.16	10,356.194	460.27527	616.50
646.46	-	-	966.50
751.64	5,734.3036	254.85792	370.27
853.08	2,144.1153	95.29401	<u>165.29</u>

Total = 5,852.16 lb

Amended total weight of membranes: 26,515.24 lb

Plus allowance for seams, adhesives, etc. = 5% = 1,325.76 lb

total weight: 27,841 lb

10.6 Corrugations. To properly determine the weight of the corrugations used in the main frames, secondary frames, and the longerons, we need to determine the equivalent cross-sectional area for the corrugation. A typical set of calculations to determine the equivalent thickness for the longerons is delineated below. This same method is used for determining the equivalent cross-sectional areas of the main frame corrugations and the secondary frame corrugations.

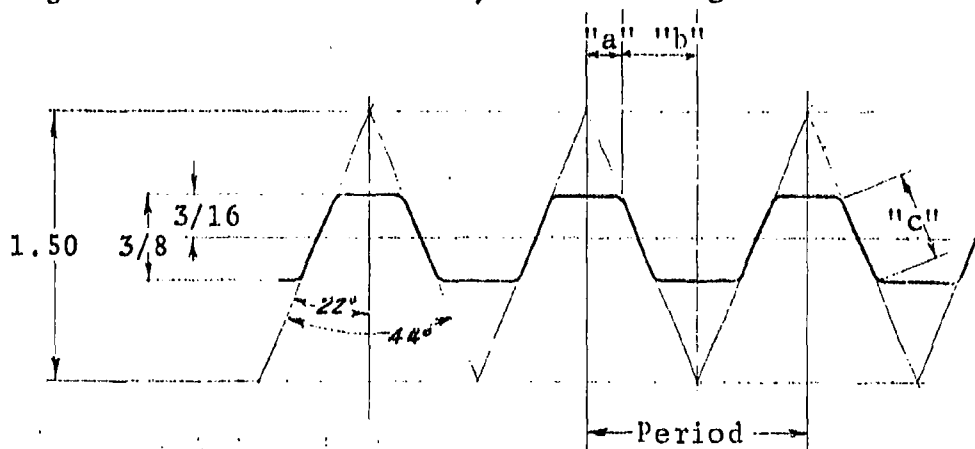


FIGURE 43 Longeron Corrugation

Longeron corrugation development, refer to above figure.

$$\text{Dimension "a": } 0.5625 \times \tan 22^\circ \\ (2.2726462)(10)^{-1} \text{ in.}$$

$$2 \text{ "a": } (4.5452924)(10)^{-1} \text{ in.}$$

$$\text{Dimension "b": } 0.9375 \times \tan 22^\circ \\ (3.7877437)(10)^{-1} \text{ in.}$$

$$2 \text{ "b": } \text{Distance between tops of corrugations} \\ (7.5754874)(10)^{-1} \text{ in.}$$

$$\text{Dimension "c": } \frac{0.375}{\cos 22^\circ} = (4.0445046)(10)^{-1} \text{ in.}$$

$$2 \text{ "c": } (8.0890092)(10)^{-1} \text{ in.}$$

$$\text{Period: } 2a + 2b \\ (4.5452924)(10)^{-1} + (7.5754874)(10)^{-1} \text{ in.} =$$

$$1.2120779 \text{ in.}$$

Total length of corrugation which covers period:

$$\frac{4a + 2c}{4(2.2726462)(10)^{-1} + 2(4.0445046)(10)^{-1}} \text{ in} = 1.7179594 \text{ in.}$$

Corrugation material thickness: 0.018 in.

$$\text{Area: } (1.7179594)(0.018) = (3.0923269)(10)^{-2} \text{ in}^2$$

Now this area must fit within the same distance as the period, $(2a + 2b)$.

Equivalent material thickness is:

$$\frac{(3.0923269)(10)^{-2}}{1.2120779} \text{ in} = (2.5512608)(10)^{-2} \text{ in} = 0.026 \text{ in.}$$

10.7 Paint And Primer Weight Calculations

TABLE 51 Paint and Primer Weights

	<u>MC-100</u>	<u>MC-125</u>	<u>MC-150</u>	<u>MC-175</u>	<u>MC-200</u>
Area of outside and inside of main and secondary frames	137,024.7 ft ²	157,410.96 ft ²	177,792.22 ft ²	198,183.48 ft ²	218,569.74 ft ²
Area of hull skin - inside	297,467.25 ft ²	341,150.66 ft ²	384,834.08 ft ²	428,517.5 ft ²	472,200.92 ft ²
Area of hull skin - outside	297,467.25 ft ²	341,150.66 ft ²	384,834.08 ft ²	428,517.5 ft ²	472,200.92 ft ²
Area of longerons - inside	47,175.519 ft ²	56,637.435 ft ²	66,099.351 ft ²	75,561.267 ft ²	85,023.184 ft ²
Area of longerons - outside	47,175.514 ft ²	56,637.435 ft ²	66,099.351 ft ²	75,561.267 ft ²	85,023.184 ft ²
Total area	826,310.22 ft ²	952,987.14 ft ²	1,079,659.0 ft ²	1,206,340.9 ft ²	1,333,017.8 ft ²
Area paint and primer	344,642.76 ft ² lb (10,236.889)	397,788.09 ft ² lb (11,814.306)	450,933.43 ft ² lb (13,392.722)	504,078.76 ft ² lb (14,971.139)	557,224.1 ft ² lb (16,549.555)
Area - primer only	481,667.46 ft ²	555,199.05 ft ²	628,725.6 ft ²	702,262.2 ft ²	775,793.7 ft ²
Weight - primer only on total area	6,135.3533 lb	7,075.9295 lb	8,016.468 lb	8,957.0811 lb	9,897.6571 lb

(Continued on next page)

TABLE 51 continued

	<u>MC-100</u>	<u>MC-125</u>	<u>MC-150</u>	<u>MC-175</u>	<u>MC-200</u>
Weight - primer on inside and primer and paint on outside	13,812.269 lb	15,936.658 lb	18,061.009 lb	20,185.435 lb	22,309.823 lb

10.8 Structure Weight

TABLE 52 Summary- Weight

<u>Hull</u>	<u>Main Frame</u>	<u>Secondary Frame</u>	<u>Longeron</u>	<u>Total</u>
MC-200	60,655	15,763	56,398	132,816
MC-175	53,073	13,792	51,594	118,459
MC-150	45,492	11,822	46,556	103,871
MC-125	37,910	9,852	41,227	88,989
MC-100	30,328	7,881	35,528	73,737

10.8 Structure Weight (Skin not included)

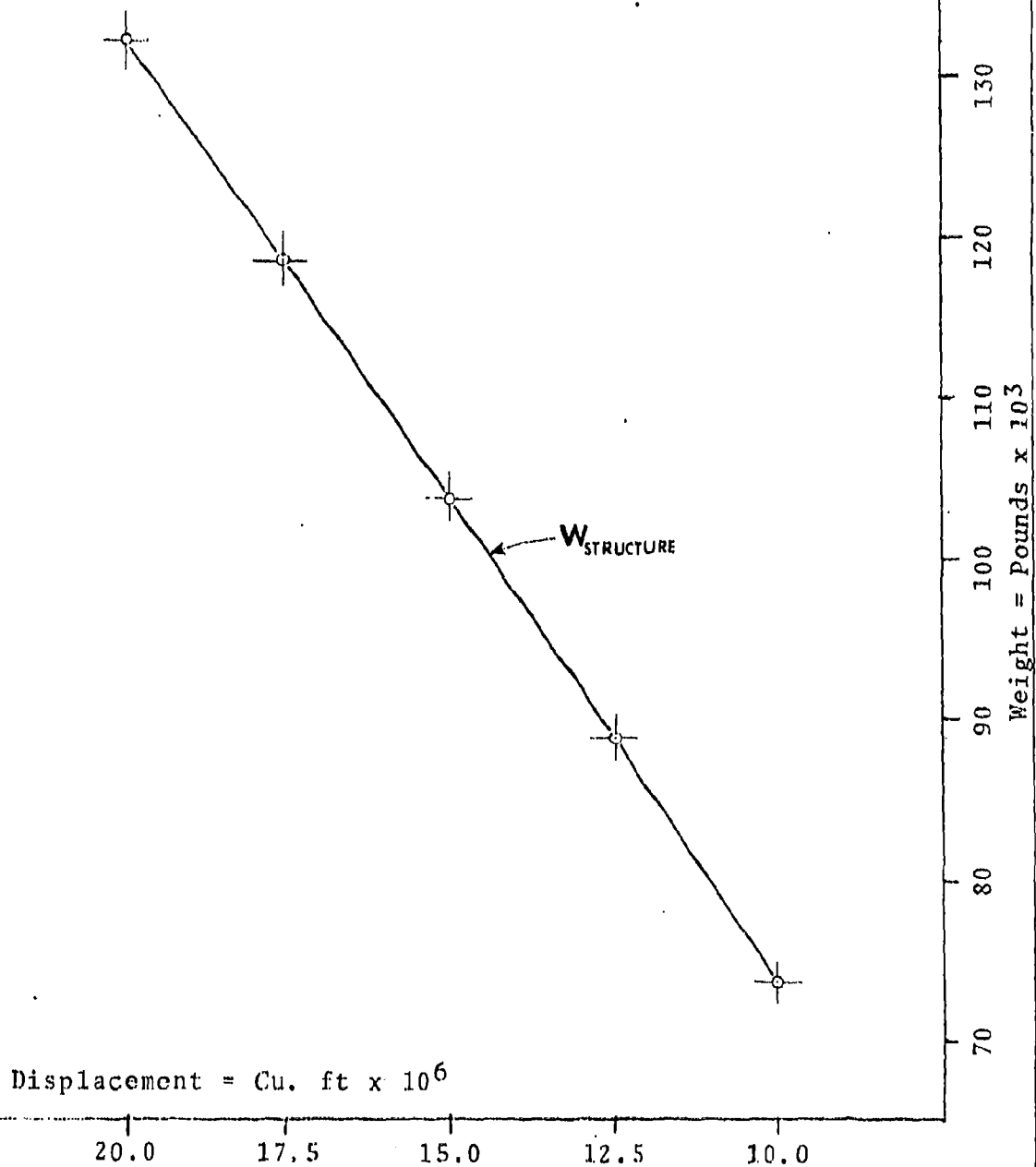


FIGURE 44 Weight to Displacement Chart

10.9 Graphite Fibre Epoxy Composites. This material has been developed by the aerospace industry and is being used on a large scale in the space shuttle vehicle for making 1,500 sq. ft. cargo compartment doors. Weight saving of 25% over an equivalent structure made of aluminum alloy is obtained. This is the most extensive application of a composite material yet undertaken in the industry.

The technology of design, fabrication and available facilities for large unit structures are developed for immediate usefulness.

The prospects for using this material and technology are good. To start with: in the weight load supporting and gathering structures, floors, containers, doors, tanks, thruster enclosures, etc., all of them outside the scope of this study. It may be possible to consider the graphite composites also in primary structures, particularly the main frames, with high prospective weight reductions. The metal-clad cellular structures are suitable for such a conversion; however, design and experimental work needs to be done before such an important commitment could be made with confidence. It deserves to be considered.

The possibility of the use of graphite composites for hull skin is not clear at this time. The graphite composites are need to be experimentally investigated for use as skin for Metalclad hull structures, subject to deep, elastic type of local buckling, if the material is a thin sheet. The strength/weight ratio of graphite composites with respect to high strength aluminum alloys are approximately 2 to 1. To take advantage of this, the skin gages would be thinner than metal sheets; the metal skin is already thin and further reduction of gage would not be desirable with a material that is more brittle than metal. These comments are not conclusive and point out the need to learn more about the use of graphite composites for primary structures in metal-clad hulls.

11. METHOD OF CONSTRUCTION

11.1 DESCRIPTION

The Metalclad hull construction is a departure from the erection methods used in skeletal rigid hulls. This is the inevitable consequence of general advances of technology, experience with the ZMC-2 airship fabrication and principally it is inevitable due to the nature of Metalclad hull structure; the latter can be stated concisely as follows:

1. The Metalclad hull is an integrated structure, as a whole and also locally; all girders, internal as well as external, are directly attached to the skin and follow everywhere the transverse as well as longitudinal curvature of the hull.
2. Metalclad girders, all frames and longerons, are continuous shear web cellular structures, without explicit joints and are attached to the skin by seams and joined by seam splices.
3. The Metalclad structure is relatively simple to construct and is suitable for rapid assembly during subassembly as well as into a hull structure.

The time required for constructing a Metalclad hull is expected to be shortened with respect to past experiences.

The method of assembly of hulls is illustrated by two artists' sketches (see Appendix N). The frames are to be assembled in horizontal position, braced by radial cables between network joints (nesting inside the frames) for the maintenance of circularity and positioned in a vertical attitude of assembly on rig belts with air cushions. Two main frames will be connected by light jury structure into exact mutual positions, ready for the installation of longerons and secondary frames. During this installation, the hull section can be rotated to convenient positions, with air cushions monitored for pressure to adjust for adequate support.

With a few longerons and segments of secondary frames installed, the skin panels will be brought into place on suction platens and held to the base skin of the main and secondary frames and longerons for setting of the seam bond material and riveting.

Progressively, all skin panels will be installed around the hull perimeter, working on both sides of the hull on elevated platforms, providing the most convenient approach to the work. As the circumference is clad with more skin panels, the jury structure can be successively removed, because the hull is

becoming increasingly self-supporting on the belts.

At some time during this progressive assembly, additional main frames may be set up on their own cushioned belts and assembly of adjacent bays initiated, at least with jury structure. The bow and stern will be constructed in vertical attitude, and when structurally complete, brought onto the assembly rig and spliced onto the rest of the hull.

This in brief is the erection process for the primary structure. Many details, for instance the installation of controls and electrical systems, etc., can commence at some early period of the erection. This method of construction is convenient and promises to be a rapid assembly system. Belt rigs are required; approximately four adjustable for different hull diameters. All rigs will traverse on assembly line rails. The hull, once erected in a given section, is self-supporting and will only require a belt rig at every other main frame. The belt rig assembly should result in Metalclad hulls of high precision, local as well as overall. The surface of Metalclad hulls will be held to nearly exact curvatures everywhere, and the drag coefficients of these hulls should be nearly the same as obtained in wind tunnel testing.

The capital cost of the belted rigs would be amortized by indefinite use for constructing other hulls and hulls of different sizes.

12. EVALUATION OF STUDY & COMMENTS

The study described in this report has confirmed the soundness of the structural concepts used in Metalclad airships. Metalclad principles have never been in doubt, but there have been some uncertainties regarding the technology to make them realistically feasible. These uncertainties have now been evaluated again and indicate a capability of construction which is very reasonable in its approach.

The value of this report is perhaps enhanced by the inclusion of material as it was being prepared; in the Appendices the evolution of thinking is recorded through this process as it has developed, searching for a deeper understanding of Metalclad structures in large hulls than existed before. A firmer base of knowledge has been established for continuing this work into deeper detail and perfection which undoubtedly can still be attained.

The required technology has now been either developed to the state of dependable application or is approaching the end of complete development and will be available when needed. For example, hull shell structures can now be constructed from high-strength light alloys with means for joining them as thin sheets by efficient, strong seam joints. The seam joint emerges as one of the most determining and basic elements of Metalclad construction. A riveted seam with a sealant alone, of the ZMC-2 vintage, successful as it was, is no longer adequate.

Structural continuity and a high degree of redundancy is inherent to Metalclad hulls; every element of the shell structure works with the skin as well as the skin working with the structure; there is no separation of duties. The redundancy includes an insensitivity to local damage from human contact; Metalclad structures are highly invulnerable to incidental damage and will continue to function dependably even if locally damaged.

A study of the interaction of the skin and structure in Metalclad hulls was given considerable effort and much knowledge was gained together with a better understanding of the subject matter. The problem was analyzed by computer and reassuring results were obtained after initial problems of getting the computer to respond constructively. More work is required on this subject, although it is now completely understood. At this time, it has been determined that the skin and the structure always work together without overstressing. Where tendencies to higher local stresses arise, especially in longerons at main frame intersections, cornice doublers will be used to control local stress levels.



In view of the above items, the Poisson's ratio has an important function in Metalclad hulls due to large dimensions of the hull shells; this effect has not been recognized until now; its influence on reducing the radial elastic deformations of the skin is significant. Poisson's ratio was not included in the computer programs, thus making the results conservative. The structure, such as frames and longerons, is not significantly affected by Poisson's ratio, and this fact is notable in bringing all radial elastic deformations of the skin and of the structure closer together, in addition to the elastic means provided for this purpose at all skin-structure interfaces, as described in this report.

Furthermore, Metalclad structures, as proposed in this report, are inherently responsive to forces from the skin, thus still further reducing all relative deformations of the skin-structure assembly. The work already accomplished and reported in this volume, assures that this is not a design problem but rather a design condition that can be always satisfactorily resolved and provided for without weight increase, because the thicker skin base of all Metalclad structures is actually a necessary part of the weight of the structure itself.

Closely related to skin seam strength and to interface deformations of structures and skin, is the hull air supercharge pressure. In all past projects of large Metalclad hulls, the maximum allowable pressure had to be, and always was, low. The state of Metalclad technology of 45 years ago was then a cause for concern in large Metalclad airships of the future. It was brought about not only because the air pressure had to be low due to low values of attainable hoop stresses and therefore sensitive to control, but also because it was not possible to provide sufficient tension in the longitudinal direction of the skin to resist imposed hull moments without relying on longerons to prevent the appearance of wrinkles in the skin while in flight. This problem is now completely resolved and this study report shows that the hull pressure can always be comfortably high within the factor of safety of two with respect to the ultimate strength of metal, and the range of pressure variation can be broad without losing tension in the skin, even under the most severe imposed moments on the hull. The supercharge air pressure in all studied hulls is substantially a constant value.

Although air pressure control will be inherently sensitive, thanks to modern instrumentation, there is no specific condition that must be held steady within narrow limits. The reason for this must be credited once more to the high efficiency of skin seam joints which permit high hoop stresses and therefore relatively high air pressure, and to higher specific

strengths of modern light alloy metals, such as the Alclad 7050-T76.

The Metalclad cellular structures, main and secondary frames as well as longerons, are capable of supporting high compressive stresses in their cornices and have a pragmatic quality of being easy to fabricate due to their simplicity and absence of complex skeletal joints. They are composed of few basic components, which themselves are also simple, the frames being continuous circular beams and the longerons continuous columns, all derivatives of the Wagner-Timoshenko^(W) shear web structural principles. All structures are of uniform architecture which will result in only a small amount of waste during fabrication.

Metalclad hull structures occupy a relatively small irreducible volume of air space not available for lifting gas. In completed airship hull, most of the air space needed for load carrying structure and for habitation, will be at the bottom of the hull and will, therefore, not reduce lift of the hulls, but rather lower their maximum ceiling altitude. The Metalclad hulls studied in this report have the least known air volume displaced by lifting structure within a hull, as compared with all historical rigid airships. This is a valuable asset for the economy of airship operation, and the study shows that this can be attained in Metalclad hulls without effort.

Metalclad hulls can be constructed on a "production" basis as described in the report. This is as important a consideration as the validity of Metalclad construction itself. Economical and rapid construction of Metalclad hulls must be attained if they are to be considered for military and civilian transport purposes. This study reveals and illustrates that this can be achieved and that the cost of the Metalclad hulls of this report will be favorable to their prospects of assuming an important role in national air power.

The purpose of this report was to reliably determine the Lambda (λ) coefficient (λ = dead weight of a hull/gross displacement lift). In the course of preparatory work, the study had to also enter into:

1. The exploration of the strength of skin seams.
2. The interaction of structure and hull shell skin.
3. The analysis of hull air pressure.
4. The concept of Metalclad cellular, continuous structures.

W. See Reference page 308.

5. The methods of fabrication and assembly of Metalclad hulls.

The weight of hulls and the parameter λ is still the most important fundamental value of merit and it is discussed last to accent its dominance. The dead weight of a hull is the summation of all weights that are needed for a hull to be capable of lifting equilibrium weight loads, including its own weight, in flight at 100-knot air speed, with adequate strength to withstand the most severe bending moments at this speed.

Each hull weight is itemized as the sum of:

1. Total weight of skin.
2. Total weight of seams.
3. Total weight of main frames.
4. Total weight of secondary frames.
5. Total weight of longerons.
6. Total weight of cell membrames and frame diaphragms.
7. Total weight of paint and primer.

The summation of these component weights is the total hull weight for containment of lifting gas, of air space for dilation and of structure strong enough to resist maximum flight forces and moments. Not included in the total hull weight are:

1. Weight of air and gas valves.
2. Weight of controls and instrumentation relating to pressure, lift, strain, etc.
3. Weight of terminals for mooring, handling near ground, etc.
4. Weight of bow mooring structure, winch, cone anchor and equipment.

All these latter weights are excluded for reasons of having no direct relation to the weight of the lifting structure, all being in the category of equipment. Similarly no weight supporting structure is considered between the main frames, although main frames are included as capable of supporting weight loads equal to the local net lift of the hull.

Two secondary frames are used between any two adjacent main frames, principally to stabilize the longerons in deflated hulls by holding the hull to circular transverse curvature. This design concept was used 50 years ago in proposals of large Metalclad hulls. In preparatory work for this report, it was noted time and again how much stability the skin and the hull longitudinal curvature impart to the longerons when the hull is deflated. Experience with the ZMC-2 airship confirms this. Before the final design of a hull is set, it would be valuable to carry out an analytical and experimental model investigation with only one secondary frame between two main frames. Even if the single secondary frame would have to be deeper, the reduction of the cost of construction and weight would be noticeable.

The stability of skin shear panels between two longerons and two adjacent frames, on either a deflated or an inflated hull, is almost completely unaffected by the distance between frames with constant longeron spacing; therefore, lengthening the frame spacing would be of little adverse influence.

There is no structure in the studied hulls not directly required for the containment of gas and air. In actual airship hulls, weight load supporting structure will be necessary longitudinally along peripheral station number 0°; this structure will contribute significantly to the strength of deflated hulls with the prospect of eliminating at least three longerons along the bottom of the hulls, the skin to be supported (in deflated state) by local internal structure.

The hulls have large diameters at the fineness ratio of 4.5, and it is desirable to provide an internal inverted triangular section corridor on top and inside the hull between main frames to reduce the distance of travel for the crew on inspection missions as well as to provide space for inflation ducts to the cells, for valves, etc. Such a corridor would reduce by its presence, the need for at least one, possibly two longerons at the top, while significantly relieving the longerons from loads during deflated flight, if that condition should arise. The analysis shows that the longerons are stable and strong enough to support all loads during construction and during flight without pressure in the hull. The analysis for the complete loss of air as well as gas pressure during flight has been explored and found satisfactory, without dumping of fuel to compensate for the loss of lift, under the assumption that lifting thrustors would be used (partially) in such an emergency.

In addition to promising potential weight reductions of complete hull lift structures, two useful contributions to the lift of Metalclad hulls are pointed out in the report.

One is the very small volume of air contained in the internal (main frame) structures as noted already, only one percent of the gross displacement volume in MC-200, increasing to almost two percent in MC-100; this is the lowest nonlifting volume in rigid airships, disregarding the volume for habitation and convenience. The second is the means for inflation of cells with high purity gas and with minimal air contamination by evacuation of cell volumes which will draw the membranes tightly against the inner top wall of the hulls with only small volumes of air possibly trapped in incidental folds of membranes against the metal surface of the hulls.

The hulls were evaluated for two ceiling altitudes, 5,000 ft. and 10,000 ft., respectively. These are limit ceilings, the former expected to be the limit for transoceanic trips and the latter for overland flights; the hulls will weigh the same for both altitudes and generally will be flown at lower levels.

The nonavailability of light weight membrane materials with high impermeability is a problem, although through fifty years the progress in this technology has been impressive; the present specific weights are three times better than they were for nonrigid hulls, but for rigid airships, these fabrics are too heavy and not adequate. Materials for this purpose are available, but the art of making light membranes from them is being developed. The membrane fabric used in the weight statement of this report is for envelopes of fabric hulls. For Metalclad hulls there is needed a light membrane material, preferably synthetic.

It appears logical that the impervious material should be impregnated into the structural fabric base, instead of laminating it as an additional layer. Perhaps for Metalclad hulls, the basic fabric could be a closely-woven mesh with small spacing of threads and the impervious material made to function also structurally. Metalclad hulls are protective of membranes in at least two respects; one is shielding against ultraviolet radiation (inside the gas and air volumes of Metalclad hulls is absolute darkness), and the second is the internal smoothness of the Metalclad hull structure, protecting membranes from abrasion and scuffing.

Membranes of Metalclad hull cells are not loaded by high stresses, compared to the strength requirements of envelope fabrics for nonrigid hulls. With this in mind, the cell membranes will have to be specifically developed for this purpose, resulting in low weight (not more than 4.32 oz./yd²)* impervious membranes with long-time durability under the conditions of use in Metalclad hulls. This inadequacy has motivated the group responsible for this report to be aware of this need and give attention to it, because it should be resolved before actual Metalclad hulls are constructed.

* Weight shown is for type of Polyurethane Butyl

Dimensions, weights, significant parameters and characteristics of all hulls are noted in the report and tabulated in Section 1.3, with selected values plotted on graphs.

All calculated weights are tabulated in Section 10. Main frame total weights have been "adjusted" to reflect a 20% reduction in weight to coincide with the conclusion outlined in Section 3, that the frame analysis was too conservative and therefore, the frames were overweight. The adjusted weights on the main frames, as well as total weights on secondary frames, membranes and diaphragms, have also been factored to reflect a smoothing out of weight calculation extrapolation curves using MC-150 as a base.

Lambda (λ) coefficients for all hulls are shown in Section 1.3. The curves show, as they are expected, that Lambda decreases with hull size, however, this decrease is relatively small in the range of hull sizes studied (.294 for MC-100 verses .276 for MC-200). A small effect due to a detail design assumption can influence the result in as close a relationship as Lambda is, in this hull size range.

Throughout the report, there are noted instances of conservative detail assumptions in methods of analysis; in consequence the hull weights, as computed are also conservative. The skin is overweight due to the use of the next higher standard sheet thickness gages. It can be confidently stated that in the course of final design, more weight will be taken out of the hulls as specified in this report than will have to be added to them. At this time, it is not possible to certify a specific figure expressing the conservatism of this weight study; it is expected that approximately four percent of the weight of skin in all hulls is overweight and approximately five percent of the weight of the structure, specifically of the main frames can be saved due to more precise frame analysis in all hulls.

With respect to the skin, it is pointed out in Section 7 that only standard sheet gages are used in the hull skin analysis. Considerable excess weight is built into the skin by this limitation, due to the standard gages progressing in thickness in steps of 0.002 in. within the whole range of used gages, from 0.024 in. to 0.012 in. below this latter thickness, the standard gages decline in steps of 0.001 in. The thickness tolerance is + 0.0003 in. for all above gages. It would be beneficial to Metalclad hull construction to make all gages, from 0.026 in. down to 0.012 in. also decline in steps of 0.001 in. with the current tolerance.

Taking for granted that at least four percent of the weight of skin can be reduced by closer differentiation of skin gages as noted above and five percent saved on the structure by more rational and detailed analysis, and a membrane weight of 4.32 oz/yd², the weight parameter Lambda can be expected to be equal to .2687, for the MC-200 hull.

During the review period of the final report, an important fact was found in the examination of old pictures of the ZMC-2 deflated hull. It is evident that elastic buckles in the hull skin are approximately uniform all over the almost full length of the hull regardless of the spacing of longerons. Apparently, where the appearance of the critical buckling stress is earlier at midsection than toward either the bow or stern, due to the wider spacing of longerons, the severity of buckling is approximately uniform almost everywhere on the hull surface.

The maximum hull pressures in this report were found to be unnecessarily high, approximately 15 - 16 inches of water. The ratio of the maximum-minimum pressure came out to be over six. New computations were carried out for MC-200 and are typical also for other hulls, based on maximum skin thickness of $t = .015$ in place of $.024$ (a reduction of 37.5% in MC-200 and less in smaller hull sizes). The new corresponding hull pressure would be 8.75 inches of water in place of 15.54 inches. The minimum hull pressure, before the skin would commence to buckle under the severest gust moment, is approximately the same, viz., 2.19 - 2.43 inches of water. The ratio of maximum-minimum hull pressure would be 3.5, compared to 6.3 as noted in the report. The possible weight reduction of the skin is approximately 37.5%, resulting in a Lambda factor of $\lambda = .244$, compared to the previously calculated $\lambda = .276$ before.

This is a notable improvement of the structural merit of Metalclad hulls and deserves attention in the future determination of hull design parameters, with the back-up support of structural testing. This gain will be progressively less in smaller hulls, but it will always be significant. Final analysis concluded that the hull pressures derived in this report were unnecessarily over designed and that the new lower pressures will give the hull equivalent strength without requiring pressure controls that are too sensitive.

For the sake of interest, thrust power was also determined for all hulls and tabulated in Section 1.3. Thrust powers, even at 100 knots, are low as is to be expected with energy-conserving airships. If propelled by compound gas-steam turbine power plants of variable air density in the cyclic circuit, constant power output could be maintained to maximum ceiling due to the nature of these power plants. The speed then would

rise from 100 knots at sea level, to 135 knots at 10,000 ft. altitude and to 116 knots at 5,000 ft. altitude. At these speeds and altitudes, the hulls would not be subjected to higher loads than when traveling at 100 knots at sea level.

The work on this report has led to a deep conviction, by all participating in its preparation, that Metalclad airship hulls have structural merits beyond original hopes and expectations, in their strength and rigidity with a high degree of redundancy typical of all shell structures, and the evidence that these structures can be light in weight, reliable under adverse conditions in distress and tolerant of mishandling.

REFERENCES

- L. Bairstow: Applied Aerodynamics. Logmans, Second Edition, 1939.
- C. B. Biezeno:^g Das Durchschlagen eines schwach gekrümmten Stabes, Z. Angew. Mathematics, Mechanics, 18 (1938) P. 21.
- Über eine Stabilitätsfrage ein-Gelenkig Gelagerten, schwache Krümmten Stabe, Proc. Acad. Sci. Amsterdam, 32 (1929) P. 990.
- E. F. Bruhn:^x Design and Analysis of Flight Vehicle Structures. Tri-State Offset Co., 1965.
- C. P. Burgess:^t U. S. Navy Design Memorandum No. 35.
- J. H. Faupel:^v Engineering Design, John Wiley & Sons, Inc. New York, 1964.
- H. B. Freeman: NACA TR430, 1932, "Measurements of Flow in the BL of Model of USA Akron."
- M. Hetenyi:^y Beams on Elastic Foundation. University of Michigan Press, 1946.
- W. H. Klikoff: ASME Aeronautic Transactions Oct. - Dec. 1931, "Pressure in Airships."
- C. J. Mazza:^j Proceedings of the Interagency Workshop on LTA Vehicles, MIT, 1975, P. 133, FTL Report R75-2.
- F. A. Pake & S. J. Pipitone:^l Boundary Layer Control for Airships, Proceedings of the Interagency Workshop on LTA Vehicles, MIT, 1975, P. 147, FTL Report R75-2.

- R. L. Patrick: Structural Adhesives,
Paul Marcel Decker
New York, 1976.
- R. E. Peterson: Stress Concentration Factors
John Wiley & Sons, New York, 1974.
- Pfenniger:^P Schlichting: Boundary Layer
Theory, McGraw-Hill, 1955, P. 239,
Figure 13.14.
- Rizink: Tables of Integral, Sums, Series
and Products. (In Russian)
Moscow 1951.
- R. J. Roark:^U Formulas for Stress and Strain,
Fourth Edition. McGraw-Hill, 1965.
- Schlichting:^k Boundary Layer Theory, McGraw-Hill,
1955.
- S. Timoshenko:^W Theory of Elastic Stability,
Second Edition, McGraw-Hill 1961.
- R. H. Upson:^a Report on Airship Forum.
July 1935.
- D. E. Woodward:^h Proceedings of the Interagency
Workshop on LTA Vehicles, MIT,
1975, P. 169, FTL Report R75-2.
- Alcoa Green Letter, April 1976, Aluminum Company of
America.ⁿ
- General Calculations and Formulas For Metalclad Airship
Design. Aircraft Development Corp. Technical
Report No. 29, 1929.^s
- NASA Technical Report No. 394, 1931.^o
- NASA Technical Report No. 824, 1945.ⁱ
- NASA Technical Report No. 1235, Standard Atmosphere,
1955.^r
- Naval Air Systems Command Report No. N00019-74-C-0065,
January, 1976.^m

GLOSSARY OF TERMS

Sagging moment	A moment making the middle portion of a hull deflect downward.
Hogging moment	A moment making the middle portion of a hull deflect upward.
Cornice	The edge of a girder, usually made of thicker material than the sides of the girder.
Splice	A long joint connecting by seams either two cornices in a longitudinal extension or sheets of metal.
Membrane	Thin, soft material for gas cells, highly impervious to helium.
Diaphragm	A dividing membrane, in the plane of the main frames, separating gas cells, or air sub-volumes. Also used in place of membrane.
Dilation	Expansion of gas with change of thermodynamic state, either due to pressure or temperature or both.
Ballonet	A contained space of air controllable in volume, to increase or decrease the amount of air, thus displacing gas to other locations in the hull.
Skin	Thin metal which forms the shell of the hull of Metalclad airships.
Gore	A part of hull shell skin defined as a segment between two longerons.
Longeron	Fore and aft structural member of a Metalclad hull.
Honeycomb	Cellular structure between two sheet metal bodies, attached to them into a light and rigid assembly.

Metalclad	A verbal composite defining an airship hull assembled from thin metal sheets and pressurized for local elastic stability as well as to induce tensile stresses in the metal skin to sustain all compressive stresses from external loads without buckling.
Supercharge	To maintain a higher than ambient pressure inside an airship hull envelope.
Hoop Stress	A circumferential skin stress in a hull transverse cross section due to a supercharge pressure.
ANSYS	"ANSYS Program" - General Purpose Engineering Computer Program.

APPENDIX A

Model For Pressure Loading Of Main Frame.

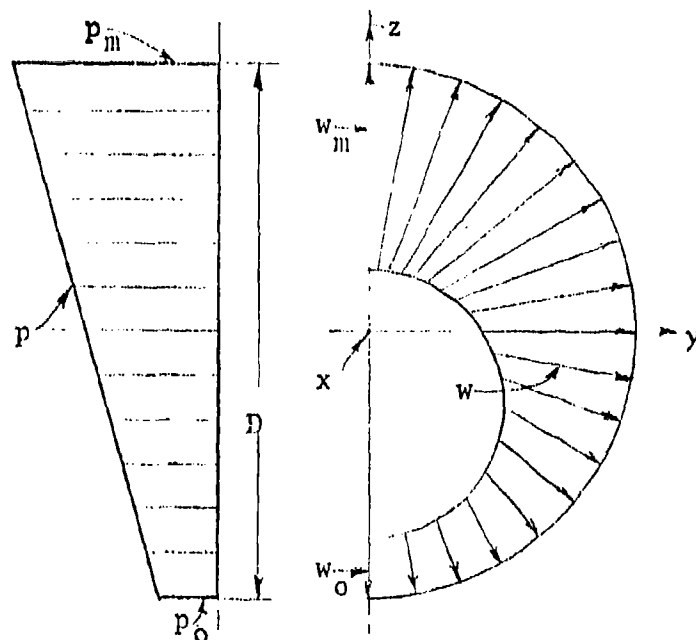


FIGURE A 1 Pressure Forces On A Frame Model

These sketches show pressure distribution along the diameter of the hull and the resulting distributed load w , acting on the main frame.

$$p_o = 0.8833 \text{ lb/in}^2, \text{ Gage}$$

$$p_m = p_o + \Delta p$$

$$k = 0.0654 \text{ lb/ft}^3 \text{ (95\% Helium)}$$

$$D = 204 \text{ ft}$$

$$\Delta p = 204 \times 0.0654 = 13.3416 \text{ lb/ft}^2 = 0.09265 \text{ lb/in}^2$$

$$p_m = 0.8833 + 0.09265 = 0.976 \text{ lb/in}^2 \text{ Gage}$$

Frame loading w is a simple multiple of pressure,

$$w = pl$$

in which l is the spacing of main frames, or more generally, impingement length of a main frame.

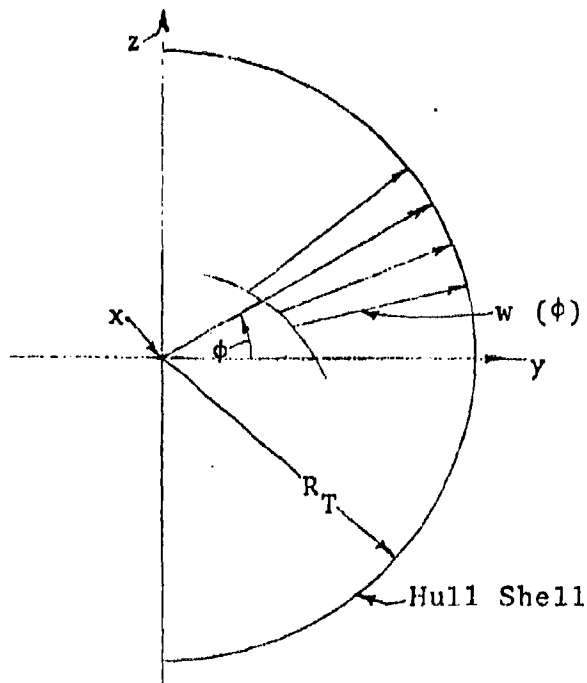


FIGURE A 2 Notation For A Hull Section

$$w = w_0 + \frac{1}{2}(\sin \phi + 1)(w_m - w_0)$$

The average distributed load w_{av}

$$w_{av} = \frac{1}{\pi R} \int_{-\pi/2}^{\pi/2} w R d\phi$$

$$w_{av} = \frac{R}{\pi R} \int_{-\pi/2}^{\pi/2} \left[w_0 + \frac{1}{2} \sin \phi (w_m - w_0) + \frac{1}{2} (w_m - w_0) \right] d\phi$$

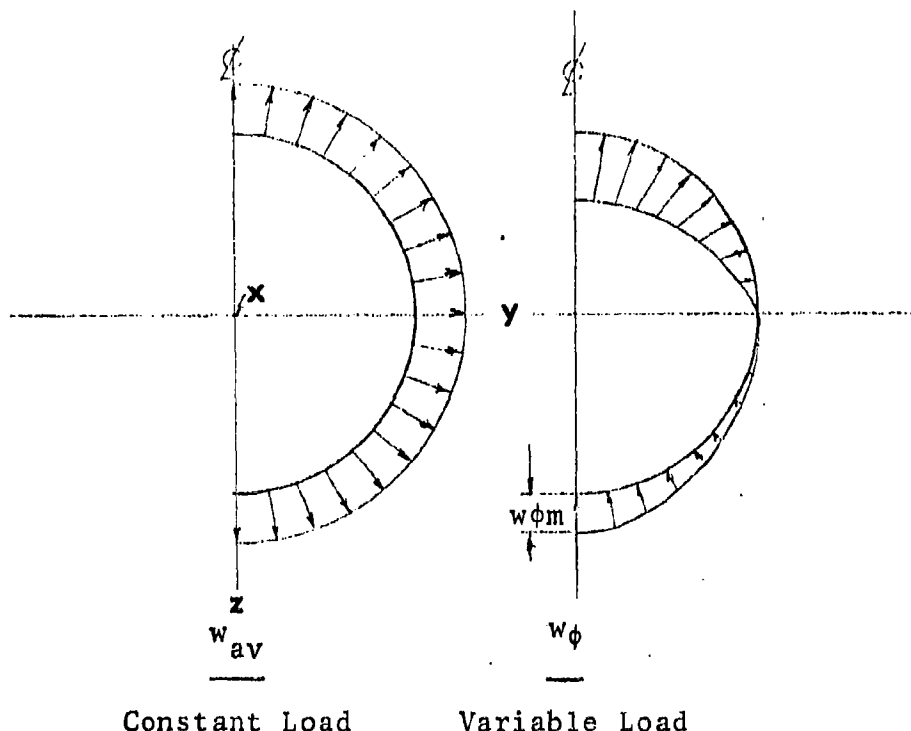
$$\int_{-\pi/2}^{\pi/2} \sin \phi d\phi = 0$$

$$w_{av} = \frac{1}{\pi} \int_{-\pi/2}^{\pi/2} \frac{1}{2} (w_m + w_0) d\phi = \frac{1}{\pi} \times \frac{1}{2} (w_m + w_0) \pi$$

$$w_{av} = \frac{1}{2} (w_m + w_0)$$

The pressure load is resolved into two components: constant w_{av} and variable w_ϕ

$$w = w_{av} + w_\phi \quad \text{and} \quad w_\phi = \frac{1}{2} (w_m - w_0) \sin \phi$$



Constant Load Variable Load

FIGURE A 3 Identification Of Distributed Loads From Pressure

Only the variable loading component gives a resultant in z - direction:

$$dP_z = (w_\phi R d\phi) \sin\phi$$

$$P_z = 2 \int_{-\pi/2}^{\pi/2} \frac{1}{2} (w_m - w_o) \sin^2\phi R d\phi = R (w_m - w_o) \int_{-\pi/2}^{\pi/2} \sin^2\phi d\phi =$$

$$= \frac{\pi R}{2} (w_m - w_o)$$



P_z is the lifting force acting on the frame. It will be made equal in magnitude to the load w assigned to this frame.

Internal Forces In Main Frame. The lifting component of pressure forces is shown on the right sketch of Figure A 4. For simplicity it is assumed that the distribution of the weight balancing the lift is the same as the pressure loading in the lower half. As a result the following frame loading is obtained.

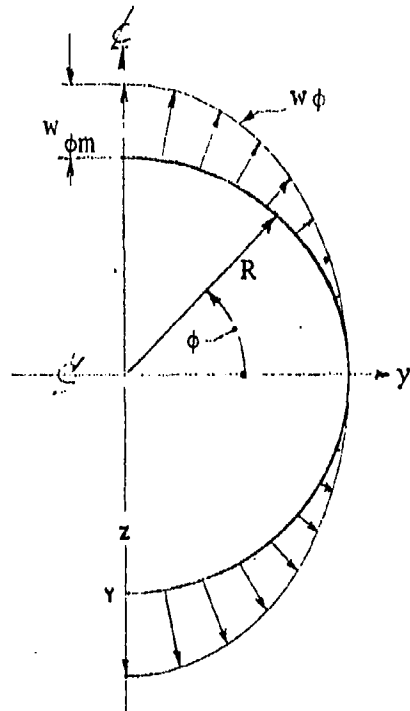


FIGURE A 4 Distribution Of Lift And Weight Forces

$$w_{\phi m} = \frac{1}{2}(w_m - w_o)$$

$$w_{\phi} = w_{\phi m} \sin \phi$$

The distribution of axial force may be found from equilibrium alone by projecting the loading shown in Figure A5 (above) on y - axis.

$$\text{Axial Forces: } N_o = \int_0^{\pi/2} w_{\phi} \cos \phi R d\phi = \int_0^{\pi/2} w_{m\phi} \sin \phi \cos \phi R d\phi$$

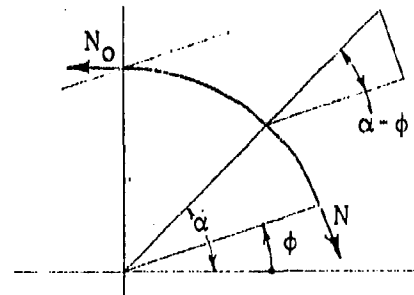


FIGURE A 5
Notation For Axial Forces

$$\int \sin \phi \cos \phi d\phi = \frac{1}{2} \sin^2 \phi$$

$$N_0 = R w_{m\phi} \left(\frac{1}{2} \sin^2 \frac{\pi}{2} \right) = \frac{1}{2} R w_{m\phi}$$

This is the axial force at centerline of the hull for an arbitrary section as shown in Figure A 6

$$N_0 \sin \phi + \int_{\alpha=\phi}^{\alpha=\pi/2} R(d\alpha) w_{\alpha} \sin(\alpha - \phi) = N$$

$$w_{\alpha} = w_{\phi m} \sin \alpha$$

$$N = N_0 \sin \phi + R w_{m\phi} \int_{\phi}^{\pi/2} \sin \alpha \sin(\alpha - \phi) d\alpha$$

$$\begin{aligned} &= \frac{1}{2} \sin \left[\alpha \right]_{\phi}^{\pi/2} - \frac{1}{4} \sin [\sin 2\alpha]_{\phi}^{\pi/2} - \frac{1}{4} \cos [\cos 2\alpha]_{\phi}^{\pi/2} = \\ &= \frac{1}{2} \left(\frac{\pi}{2} - \phi \right) \sin \phi - \frac{1}{4} \sin \phi (0 - \sin 2\phi) - \frac{1}{4} \cos \phi (-1 - \cos 2\phi) \end{aligned}$$

$$1 + \cos 2\phi = 2 \cos^2 \phi$$

$$\begin{aligned} &= \frac{1}{2} \left(\frac{\pi}{2} - \phi \right) \sin \phi + \frac{1}{2} \sin^2 \phi \cos \phi + \frac{1}{2} \cos^3 \phi = \\ &= \frac{1}{2} \left(\frac{\pi}{2} - \phi \right) \sin \phi + \frac{1}{2} \cos \phi \underbrace{(\sin^2 \phi + \cos^2 \phi)}_{1} \end{aligned}$$

$$N = N_0 \sin \phi + \frac{1}{2} R w_{\phi m} \left[\left(\frac{\pi}{2} - \phi \right) \sin \phi + \cos \phi \right]$$

$$\text{For } \phi = 0, N = \frac{1}{2} R w_{\phi m}$$

This result can be verified indirectly by integrating the vertical components along one-quarter of the hull section.

$$N_1 = \int_0^{\pi/2} w_{\phi} \sin^2 \phi R d\phi = w_{\phi m} R \int_0^{\pi/2} \sin^2 \phi d\phi = \frac{\pi}{4} R w_{\phi m}$$

The resultant distribution of axial force:

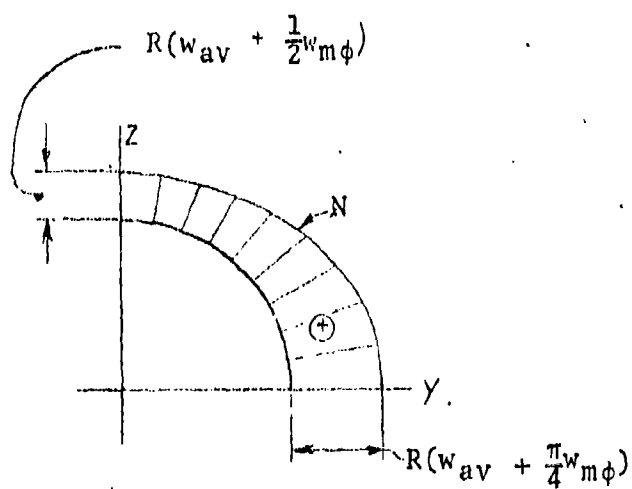


FIGURE A 6 Distribution Of Axial Force Along The Hull Perimeter

APPENDIX B

Model Sizing Of Main Frame, Stress Criterion.

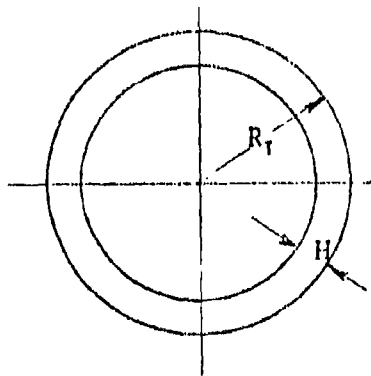


FIGURE B 1 Main Frame

For MC-200:

$$R_f = 1,224'' (102') \text{ and } H = 144'' (12')$$

The required cross section is calculated as a function of frame spacing l .

Maximum axial force:

$$N_{\max} = (w_{av} + \frac{\pi}{4} w_{\phi m}) R \text{ (Appendix A)}$$

$$w_{\phi m} = \frac{1}{2} (w_m - w_o)$$

$$w_{av} = \frac{1}{2} (w_m + w_o)$$

$$N_{\max} = \frac{R}{2} \left[(w_m + w_o) + \frac{\pi}{4} (w_m - w_o) \right]$$

$$\text{But } w = pl$$

$$N_{\max} = \frac{Rl}{2} \left[p_m + p_o + \frac{\pi}{4} (p_m - p_o) \right]$$

$$p_m = 0.976, p_o = 0.8833 \text{ lb/in}^2$$

$$N_{\max} = \frac{1}{4}(1224) l [0.976 + 0.8833 + \frac{\pi}{4}(0.976 - 0.8833)] = 1182 \cdot l$$

Largest bending moment:

$$M = 0.25 w_l R^2$$

$$w_l = \frac{2}{3} w_{\phi m} = \frac{2}{3} \times \frac{1}{2} (w_m - w_o) = \frac{1}{3} (w_m - w_o)$$

$$w_l = \frac{1}{3} (p_m - p_o)$$

$$M = \frac{1}{4} \cdot \frac{1}{3} (p_m - p_o) R^2 = \frac{1}{12} (p_m - p_o) R^2$$

(Positive at horizontal diameter, negative at vertical diameter)

$$M = \frac{1}{12} (0.976 - 0.8833) (1224)^2 = (11,573) l$$

A series of l values is used in Table B-1, spanning the range from $l = 0.25D$ to $l = 1.0 D$.

Allowable stress of 30,000 lb/in² is used, both in tension and compression.

TABLE B I Bending Moment

l (in)	$10^6 N$ lb	$10^6 M$ lb.in	A'
612	0.7234	7.083	27.5
1,224	1.4468	14.165	55.0
1,836	2.1702	21.248	82.5
2,448	2.8935	28.331	110.0

Assume the effective depth of frame to be $h = 140$ in.

The last column in the table above shows the initial total area according to:

$$A' = \frac{l}{30,000} (N + \frac{M}{70})$$

By the method of successive approximations, are determined the actual areas, A_1 and A_2 .

At $z = 612''$

$$A_1 = A_2 = 13.75 \text{ in}^2; \sigma_1 = 30,000; \sigma_2 = 22,630 \text{ lb/in}^2$$

$$A_1 = 24.0; A_2 = 1.0; A_f = 25.0 \text{ in}^2$$

$$\sigma_1 = 31,040 \text{ lb/in}^2; \sigma_2 = -21,660 \text{ lb/in}^2 \text{ (close enough)}$$

At $z = 2448''$

$$A_1 = A_2 = 55.0 \text{ in}^2; \sigma_1 = 30,000; \sigma_2 = 22,630 \text{ lb/in}^2$$

$$A_1 = 101.0; A_2 = 4.0; A_f = 105 \text{ in}^2$$

$$\sigma_1 = 29,560; \sigma_2 = -23,030 \text{ lb/in}^2 \text{ (close enough)}$$

The section areas obtained here are the effective chord areas.

The above calculation is valid for cross-sections on the vertical axis, where the largest negative moment occurs. The largest axial force, which corresponds to the horizontal axis is used.

APPENDIX C

Model of Main Frame Selection, Modified Data.

Factor of safety = 2.31

$$\sigma_{tu} = 69,000 \text{ lb/in}^2; \sigma_{ty} = 60,000 \text{ lb/in}^2$$

$$\sigma_t = 69/2.31 = 29.87, \text{ use } \sigma_t = 30,000 \text{ lb/in}^2$$

$$\sigma_c = 0.95\sigma_t = 28,500 \text{ lb/in}^2$$

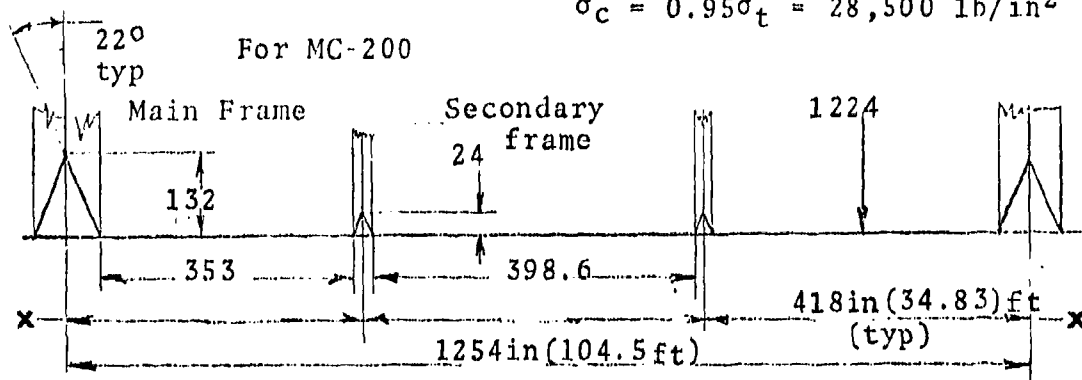


FIGURE C 1 Spacing of Frames

with $l = 1254$ ", the internal frame forces are, Ref.: Appendix B

$$N_{\max} = (1182)(1254) = (1.482)(10)^6 \text{ lb}$$

$$M_{\max} = (11573)(1254) = (14.513)(10)^6 \text{ inlb}$$

Constant frame section has been chosen over a variable section. Two practical alternatives are possible.

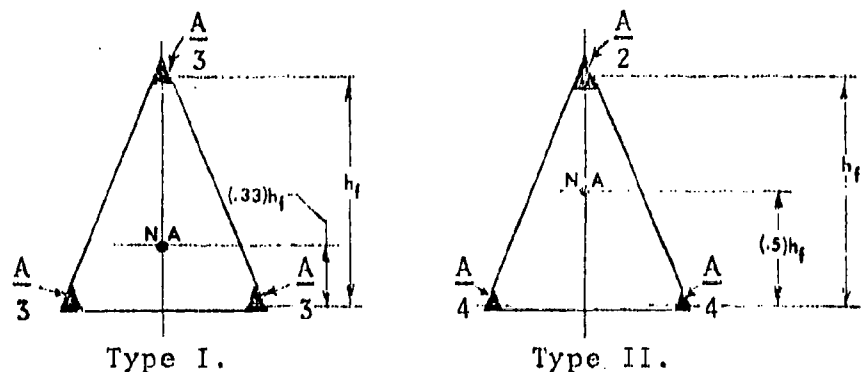


FIGURE C 2 Area Distribution in a Main Frame.

To determine the required area for both types, two locations on the hull should be considered: Vertical plane with negative moment and horizontal plane with positive moment.

Type I Section.

$$A_1 = \frac{2A}{3} ; A_2 = \frac{A}{3} \text{ in vertical section:}$$

$$\sigma_1 = \frac{(1.482)}{A}(10)^6 + (3/2)\frac{14.513}{128A} = \frac{1.652}{A}(10)^6$$

$$\sigma_2 = (1.142)(10)^6/A$$

In horizontal section:

$$\sigma_1 = \frac{(1.482)}{A}(10)^6 - (3/2)\frac{(14.513)(10)^6}{(128)A} = \frac{(1.312)}{A}(10)^6$$

$$\sigma_2 = (1.822)(10)^6/A$$

$$A_{\min} = (1.822)(10)^6/34500 = 52.81 \text{ in}^2$$

Type II section.

$$A_1 = \frac{A}{2} ; A_2 = \frac{A}{2}$$

Maximum stress in either section:

$$\sigma = \frac{(1.482)}{A}(10)^6 + (2)\frac{(14.518)(10)^6}{(128)A} = (1.709)(10)^6/A$$

$$A_{\min} = (1.709)(10)^6/34500 = 49.54 \text{ in}^2$$

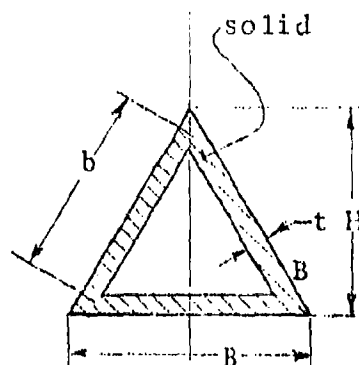
with $A = 49.6 \text{ in}^2$:

$$I = 1/4 Ah^2 = (1/4)(49.6)(128)^2 = 203,162 \text{ in}^4$$

APPENDIX D Model Of Longeron Sizing

Section properties of thin-wall triangle.

Assume equilateral triangle first.



$$H = \frac{\sqrt{3}}{2} B$$

FIGURE D 1 Model of a Girder

Outside triangle: $I_1 = \frac{1}{36} BH^3 = \frac{\sqrt{3}}{96} B^4$

Inside triangle: $I_2 = \frac{\sqrt{3}}{96} b^4$

in which $b = B - 2 \left(\frac{t}{\cos 30^\circ} + t \cdot \tan 30^\circ \right) = B - (3.4641) t$

The thin-wall triangle obtained by subtraction:

$$I = I_1 - I_2 = \frac{\sqrt{3}}{96} (B^4 - b^4)$$

For $t \ll B$: $b^4 \approx B^4 - 4B^3 \times (3.4641) t$

$$I \approx \frac{\sqrt{3}}{96} \left[(4) \times (3.4641) B^3 t \right]$$

$$I = \frac{1}{4} B^3 t$$

Sensible accuracy for $t < B/25$.

Longeron sizing, center section.

Consider the frame spacing shown in Appendix C ; the intermediate frames provide same degree of fixity, both rotational lateral & stiffness is large enough to be considered perfect. (This is to be verified later). The angular constraint is ignored but the support spacing is diminished from 418 398.6 in.

Buckling stress is determined, using a thin-wall, triangular section as shown in Figure D-2.

$$l = 398.6 \text{ in}$$

$$\rho^2 = B^2/12$$

$$B = \frac{2}{\sqrt{3}} H = 2 \times 20/\sqrt{3}$$

$$\rho^2 = 44.44 ; \lambda^2 = (398.6)^2/44.44; \lambda = 59.8 > 58.5$$

$$\sigma_{cr} = \pi^2 E / \lambda^2 = \pi^2 (10.4) (10)^6 / (58.5)^2 = 29,990 \text{ lb/in}^2$$

λ = Slenderness Ratio

The cross-section of a longeron is assumed to be the equilateral triangle with a very thin wall.

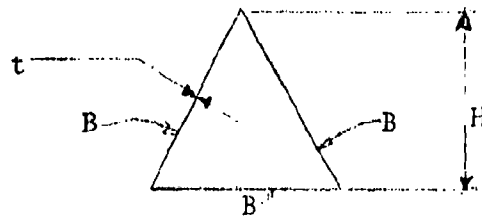


FIGURE D 2 Model of Longeron

For this section $A = 3Bt$, while the formula for I is:

$$I = 1/4 B^3 t \text{ and } \rho^2 = \frac{I}{A} = \frac{B^2}{12}$$

For $H = 20$ in as the total height (for MC-200), the thickness can be computed from the prescribed load acting on the section. (Resultant bending).

The allowable compressive stress in longerons is:

$$\sigma_{cr}/2 = 29940/2 = 15,000 \text{ lb/in}^2$$

The aerodynamic bending moment is:

$$M = (212.043)(10)^6 \text{ inlb}$$

The material which carries the bending stress is distributed as a uniform, equivalent thickness t .

$$\sigma = \frac{M}{\pi R^2 t}$$

$$\text{SET } \sigma_b = \sigma_c = 15,000 \text{ lb/in}^2$$

$$t = \frac{(2.5445)(10)^9}{\pi(1224)^2(15000)} = 0.03604 \text{ in}$$

In this preliminary stage two conservative assumptions are made:

- (1) On the compressive side, the idealized longeron of Figure D2 is the only material which resists the bending moment.
- (2) The same holds true on the tension side and the permissible stress level is the same.

There are 48 longerons, each with the area

$$A_s = 2\pi Rt/48 = 2(1224)(0.03604)/48 = 5.774 \text{ in}^2$$

for the shape of Figure D2, $A_s = 3Bt$;

$$B = \frac{2}{\sqrt{3}} H = \frac{2}{\sqrt{3}} 20 = 23.094 \text{ in}$$

$$5.774 = (3 \times 23.094)t \text{ and } t = 0.08334 \text{ in}$$

use $t = 0.085 \text{ in}$

Compressive force in the longeron

$$N_c = (5.774)(15000) = 86,610 \text{ lb}$$

Buckling force

$$N_{cr} = 3Bt\sigma_{cr} = (3)(23.094)(0.085)(29990) = 176,610 \text{ lb.}$$

Buckling stress of longerons ($z = 24$)

The second area moment for the secondary frame cross-section is:

$$I = 2589.4 \text{ in}^4$$

The stiffness of a frame, when treated as a support for longerons is:

$$k = \frac{bEI}{k_{\Delta} R^4}$$

$$b = 320.4 \text{ in}$$

$$k_{\Delta} = 0.0305$$

$$R = 1224 \text{ in}$$

$$k = \frac{(320.4)(10.4)(10)^6(2589.4)}{(0.0305)(1224)^4} = 126.04 \text{ lb/in}$$

The spacing of main frames is 1254". The secondary frames are treated as elastic supports according to the sketch on Figure C1 of Appendix C. The buckling load will be determined from :

$$P_e = \left(\frac{\pi}{L}\right)^2 EI = \left(\frac{\pi}{1254}\right)^2 (10.4)(10)^6 (261.73) = 17,084 \text{ lb}$$

(This is the Euler force for a column with no intermediate supports.)

$$\frac{kL}{P_e} = \frac{(126.04)(1254)}{17084} = 9.252$$

This value of kL/P_e is small, because of little stiffness of secondary frames, that P_{cr} is only

$$P_{cr} = 3.9 P_e = 66,628 \text{ lb}$$

$$A = 5.889 \text{ in}^2 \text{ and } \sigma_{cr} = 66628/5.889 = 11,310 \text{ lb/in}^2$$

The beneficial effect of skin was not taken into account.

Longeron Bending Due To Pressure.

The interaction of structural elements of the hull under uniform pressure is described in Section 5 which illustrates a hypothetical situation of a hull with only intermediate frames, uniformly spaced. It turns out to be quite a meaningful example, however, because the influence

of one frame does not reach the adjacent one, at least from a practical viewpoint.

It also holds true with respect to a case of a hull with main frames only, spaced at the same distance. To obtain the interaction forces P, Example I* is reworked here with

$$A_f = 49.6 \text{ in}^2$$

$$P = \left[\frac{48 \times 0.05}{(2)(1224)(49.6)} + (6.979)(10)^6 \right]^{-1} (0.976)$$

Maximum bending at $x = 0$

$$M_{\max} = \frac{P}{4\Delta} = \frac{73544}{(4)(12.103)(10)^3} = (1.519)(10)^6 \text{ inlb}$$

Check bending stress due to this moment with 24 longerons:

$$I = 1/4 B^3 t = 1/4 (23.094)^3 (0.085) = 261.7 \text{ in}^4$$

$$c_1 = (2/3)H = 2/3(20) = 13.33 \text{ in}$$

$$c_2 = 20.0 - 13.33 = 6.67 \text{ in}$$

$$\sigma_b = (1.519)(10)^6 \times 13.33 / 261.7 = 77,372 \text{ lb/in}^2$$

compression, outside fiber.

$$\sigma_{b2} = 38,686 \text{ lb/in}^2 \text{ tension.}$$

There is a tensile stress in longeron section

$$\sigma_l = 6,885 \text{ lb/in}^2$$

Resultant longeron stress:

$$\sigma_1 = 77372 - 6885 = 70,487 \text{ lb/in}^2$$

$$\sigma_2 = 38686 + 6885 = 45,571 \text{ lb/in}^2$$

$$\sigma_{1all} = 15,000 \text{ lb/in}^2$$

$$\sigma_{2all} = 34,500 \text{ lb/in}^2$$

Overstressed, needs reinforcing locally.

*Page 339

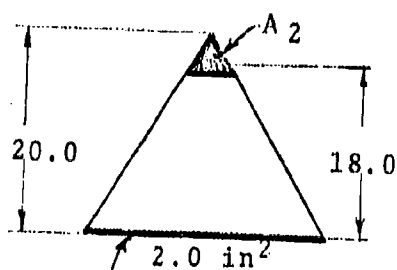
Assume 20% reduction of longeron bending due local skin reinforcement. New Moment:

$$M'_{\max} = (0.8)(1.519)(10)^6 = (1.215)(10)^6 \text{ in lb}$$

Place two additional areas, A_1 and A_2 on the basic area A_0 shown in Figure D 1.

Combined Section Data:

No.	A_i (in ²)	z_i (in)	$A_i z_i$ (in ³)	$A_i z_i^2$ (in ⁴)	I (in ⁴)
0	5.89	6.67	39.29	262.04	261.7
1	2.0	0.1	0.2	0.02	0
2	3.5	18.0	63.0	1134.0	0



$$A_1 = 2.0 \text{ in}^2; A_2 = 3.5 \text{ in}^2$$

FIGURE D 3 Longeron Area Distribution

$$A = \sum A_i = 11.39 \text{ in}^2$$

$$\sum A_i z_i = 102.49 \text{ in}^3$$

$$z_c = 102.49/11.39 = 8.998 \text{ in}; c_1 = 8.998 \text{ in}; c_2 = 11.002 \text{ in.}$$

$$\sum A_i z_i^2 = 1396.06 \text{ in}^4$$

$$I = 261.7 + 1396.06 - (11.39)(8.998)^2 = 735.58 \text{ in}^4$$

$$\sigma_b = \frac{M}{I} \begin{bmatrix} c_1 \\ c_2 \end{bmatrix} = \frac{(1.215)(10)^6}{735.58} \begin{bmatrix} 8.998 \\ 11.002 \end{bmatrix} = \begin{bmatrix} 14,863 \text{ lb/in}^2 \text{ (tens.)} \\ 18,202 \text{ lb/in}^2 \text{ (comp.)} \end{bmatrix}$$

Resultant stress:

$$\sigma_i = 14,863 + 6,885 = 21,748 \text{ lb/in}^2 \quad (\text{inside})$$

$$\sigma_o = -18,202 + 6,885 = -11,317 \text{ lb/in}^2 \quad (\text{outside})$$

This is well within the allowables. The added areas may be reduced.

Longeron bending due to pressure. ($z = 24$)

As the first step determine the interaction force P between the main frame and longeron. Rework the Example using $A_f = 49.6 \text{ in}^2$ and $z = 24$.

$$A = 2\pi R t + n A_c = 2\pi(1224)(0.05) + (24)(5.889) = 525.9 \text{ in}^2$$

$$\sigma = N/A = (4.594)(10)^6 / 525.9 = 8,736 \text{ lb/in}^2$$

The ratio of applied axial stress to the buckling stress determines the stiffening effect of axial forces. The most probable value of σ_{cr} , calculated before in this Appendix is $11,310 \text{ lb/in}^2$. (Using σ_{cr} of larger value, based on frame spacing of $432''$, would be unnecessarily conservative.) Use a stiffening factor given by

$$m = 1/(1 + \sigma/\sigma_{cr})^{1/2}$$

$$T_c = I_c/m = (261.7)(1 + 8736/11310)^{1/2} = 348.4 \text{ in}^4$$

$$K = k(1 + \sigma/\sigma_{cr})^{1/2} = (55.6) [1 + 8736/245.3]^{1/2} = 336.5 \text{ lb/in}^2$$

$$\Delta^4 = \frac{K}{4EI_c} = \frac{336.5}{(4 \times 10.4)(10)^6(348.4)}, \text{ and}$$

$$\Delta = 12.344(10)^{-3}$$

$$\Delta l = 5.3326$$

$$f(\Delta l) \approx 0.996$$

$$P = \left[\frac{(24)(0.05)}{(2\pi)(1224)(49.6)} + \frac{(12.344)(10)^{-3}(10.4)(10)^6(0.05)}{(2)(336.5)(1224)} \right] (0.996)^{-1} \times (0.976)$$

$$P = [(3.146)(10)^{-6} + (6.341)(10)^{-6}]^{-1} (0.976)$$

$$P = 102,880 \text{ lb}$$

This is a larger force than the one obtained for $z = 48$.

$$M_{\max} = \frac{P}{4\lambda} = \frac{102880}{(4)(12.344)(10)^{-3}} = (2.084)(10)^6 \text{ inlb}$$

Bending of skin along longeron.

Description of the problem is given further on in this appendix. Interaction force P between the main frames and longerons is calculated above in this Appendix,

$$P = 73,544 \text{ lb}$$

Inward loading w from:

$$w = p - \frac{t}{R} \cdot \frac{zP}{2\pi A_F}$$

All data the same as in Example I, except $A_F = 49.6 \text{ in}^2$

$$w = 0.976 - \frac{(0.05)(48)(73544)}{(1224)(2\pi)(49.6)} = 0.5133 \text{ lb/in}^2$$

$$p - w = 0.4627 \text{ lb/in}^2$$

Stretching force

$$N = (p-w)R = (0.4627) \times (1224) = 566.3 \text{ lb}$$

Length of a beam - column per sketch of Figure

$$b = 2\pi R/z = 2\pi(1224)/48 = 160.2 \text{ in}$$

Solving for moments and the deflection at the center of panel:

$$j^2 = \frac{EI}{N} = \frac{Et^3}{12N} = \frac{(10.4)(10)^6(0.05)^3}{(12)(566.3)} = 0.1913$$

$$l = 160.2 \text{ in}$$

$$U^2 = l^2/j^2 = 134156$$

$$U = 366.27$$

The Euler force for this 1" strap is only

$$N_e = \left(\frac{\pi}{z}\right)^2 EI = \left(\frac{\pi}{1}\right)^2 \times \frac{Et^3}{12} = \left(\frac{\pi}{160.2}\right)^2 \frac{(10.4)(10)^6(0.05)^3}{12} \\ = 0.04166 \text{ lb}$$

For so large values of U , $\tan h(U/2) \approx 1.0$ and for bending moments at ends:

$$M_1 = M_2 = (1/2)wj^2U = (1/2)(0.5133)(0.1913)(366.27) = 1798 \text{ inlb}$$

Moment at the center

$$M = wj^2 = (0.5133) \times (0.1913) = 0.0982 \text{ inlb (not critical)}$$

For large values of U , the maximum deflection

$$\begin{aligned} y_m &= \frac{wj^2}{8N} (U^2 - 4U) = \frac{0.0982}{(8)(566.3)} (134156 - 4) \times (366.27) \\ &= 2.876 \text{ in (with respect to the supports,} \\ &\quad \text{i.e., to longerons)} \end{aligned}$$

Bending stress in skin:

$$\sigma_b = \frac{6M_1}{t^2} = \frac{6}{(0.05)^2} (17.98) = 43,152 \text{ lb/in}^2$$

This is superimposed on hoop tension:

$$\sigma_h = N/t = 566.3/0.05 = 11,326 \text{ lb/in}^2$$

Resultants, circumferential

$$11,326 - 43,152 = -31,826 \text{ lb/in}^2 \text{ (external)}$$

$$11,326 + 43,152 = 54,478 \text{ lb/in}^2 \text{ (internal) of the skin.}$$

Without thickening of skin along the sides of longerons. The benefit of longeron shape (two, rather than one contact points with skin) was not taken advantage of in the above mode analysis. However, a local doubler may still be necessary, as a resultant inside stress is much larger than the allowable of 34,500 lb/in².

Also it is to be noticed that the assumption of non-deflecting longeron artificially increases skin bending.

Bending of skin along frame.

Bending along the main frame, is more severe than along secondary frame and is analyzed next.

Equation for bending of skin along a frame:

$$M_{\max} = \frac{t^2}{\sqrt{12}} \left(\frac{pR}{t} - \frac{zP}{2\pi A_f} \right)$$

$$M_{\max} = \frac{0.05^2}{\sqrt{12}} \left(\frac{(0.976)(1224)}{0.05} - \frac{(48)(73544)}{(2\pi)(49.6)} \right)$$

$$M_{\max} = 9.068 \text{ inlb}$$

$$\sigma_b = 6M/t^2 = (6)(9.068)(0.05)^2 = 21,763 \text{ lb/in}^2$$

along a secondary frame.

The result shows that by comparison with a longeron, the bending stress along the frame is only about half of bending stress along a longeron. This is thought to be indicative of the true situation, although some of the difference may be ascribed to overly conservative assumptions used in the longeron analysis.

General instability

General instability is the mode of buckling in which the frames, due to insufficient stiffness, deflect under the buckling longerons. There are several criteria of general instability, the one considered below is taken from Bruhn, "Design and Analysis"^x

The minimum frame stiffness to prevent a general instability is

$$EI_f = \frac{MD^2}{(16000)l} \quad (1)$$

M = bending moment

$$D = 2R = (2)(1224) = 2,448 \text{ in}$$

l = frame spacing, in

Assume first typical secondary frame spacing

$$l = 432 \text{ in}$$

With aerodynamic moment $M = (2.5445)(10)^9 \text{ inlb}$

$$\text{with } E = (10.4)(10)^6; \quad I_f = 212 \text{ in}^4$$

^x. See references page 307

$$EI_f = \frac{(2.5445)(10)^9(2.448)^2(10)^6}{(16)(10)^3(0.432)(10)^3} = (2.206)(10)^9 \text{ lbin}^2$$

This is considerably less than the former calculations gave. One has to keep in mind, however, that Equation 1 is semi-empirical and that the test pieces on which it is based may not have been of appropriate diameters.

Method of solution.

The connection or attachment between the frames and the rest of the assembly is considered removed and the hull is pressurized. This makes the radial gap Δ an open distance between the skin and the frame. The effect of Poisson's Ratio is disregarded, a conservative assumption at this time, because Poisson's Ratio reduces the radial skin deformation due to the presence of longitudinal skin stress σ_L .

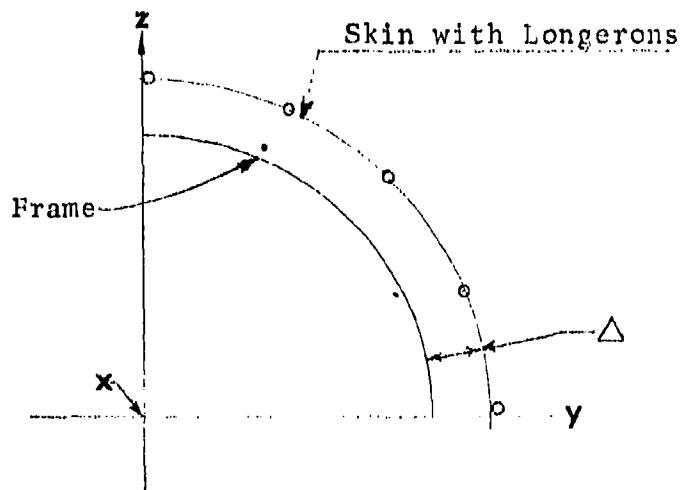


FIGURE D 4

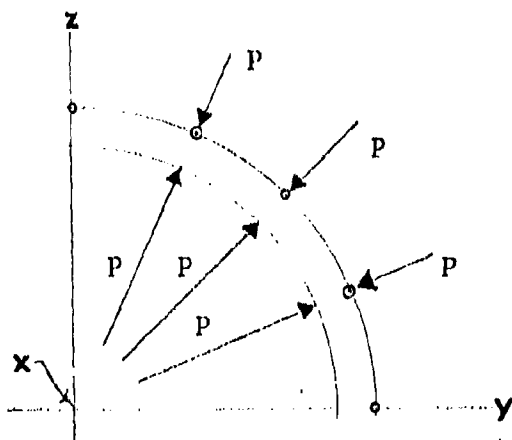
Skin deflection relative to a frame

In the next step the inward directed loads are applied to longerons and the outward directed loads to frame.

These loads are applied simultaneously at a plane of every frame.

The skin longeron deflections are denoted by Δ_f . Forces P are found from the condition

$$\Delta_s + \Delta_f = \Delta \quad (1)$$



Forces Between Skin and Frame

FIGURE D 5

Frame flexibility.

A ring loaded with z concentric forces P is equivalent to a ring loaded uniformly with an intensity w :

$$w = \frac{zP}{2\pi R}$$

Radial displacement:

$$\Delta_f = \frac{wR^2}{EA_f} = \frac{zPR}{2\pi EA_f} \quad (2)$$

A_f = frame cross-section area.

Apart from the above radial component of displacement, there also is one due to bending and shear. However, with z fairly large, say $z \gg 36$, the radial component strongly predominates.



Skin flexibility

When skin is treated as an elastic foundation for longerons, it is divided into rings, each of them one unit wide. The section properties of such ring are:

$$A = t$$

$$I = t^3/12$$

Applying a set of z evenly spaced forces Q gives a radial deflection, which may be expressed by a formula analogous to Equation 2.

$$\delta = \frac{zQR}{2Et}$$

The foundation modulus is defined as $k = Q:$

$$k = \frac{2\pi Et}{zR} \quad (3)$$

It is to be noted that bending flexibility of skin can not be developed, because a frame is continuously attached to it. This is, of course true only in the frame plane. In the classical theory one has a uniform circumferential load intensity w :

$$zQ = 2\pi R w \text{ and } k = w/\delta = Et/R^2$$

Influence of axial stretching.

When skin and longerons are subjected to axial tension, it is more difficult to bend them in lateral (radial) direction, than if the tension did not exist. This effect is considered separately for skin and for longerons.

In case of a longeron subjected to an axial load N , a simple approximation is made; the effective second area moment I_c is assumed to be

$$I_c = \left(1 + \frac{N}{N_{cr}}\right) I_c \quad (4)$$

In which N_{cr} is the elastic buckling force for a longeron supported by the frames.

The stiffening factor for a thin-wall cylinder will be determined from the deflections of a longitudinal strip of skin, which is treated as a beam on an elastic foundation. From Hetenyi's Equations follows that the deflection under a single force P at the origin is $y_0 = \frac{P}{2k}$

When no axial force is acting, according to Hetenyi's work, gives the deflection with the axial force present:

$$y_1 = \frac{P}{2k} \frac{\Delta}{\alpha}$$

The stiffening factor is defined as

$$m = \frac{y_1}{y_0} = \frac{\Delta}{\alpha}$$

In which $\alpha = \left[\Delta^2 + \left(\frac{N}{4EI} \right)^2 \right]^{1/2}$

$$m = \frac{1}{\left(1 + \frac{N}{4EI\Delta^2} \right)^{1/2}} \quad (5)$$

The definition of Δ , is given by : $\Delta^4 = \frac{k}{4EI_c}$ (6)

$$k = \frac{t^3}{12} \frac{Et}{R^2} = \frac{Et^4}{12R^2}$$

$$4EI\Delta^2 = \left[4E \frac{Et^4}{12R^2} \right]^{1/2} = \frac{Et^2}{\sqrt{3} R}$$

In considering skin stiffness, the Poisson's Ratio is assumed equal to zero; setting $\nu = 0$ in the expression for buckling stress of a cylinder, as shown in Roark's "Formulas for Stress and Strain" (See references, page 308).

$$N_{cr} = t\sigma_{cr} = \frac{1}{\sqrt{3}} \frac{Et^2}{R}$$

But this is the same value as previously derived value of $4EI\Delta^2$. Substituting in the expression for m :

$$m = \left[\frac{1}{(1 + \sigma/\sigma_{cr})} \right]^{1/2} \quad (7)$$

in which σ_{cr} is the theoretical value of the cylinder buckling stress.

$$\sigma_{cr} = Et/(\sqrt{3} R), \sigma \text{ is positive, when in tension.}$$

Y. M. Hetenyi, Beams on Elastic Foundation, University of Michigan Press, 1946.

Instead of saying that the deflections of skin decreased m times, one can say that the foundation modulus was changed to \bar{k} :

$$\bar{k} = \frac{k}{m} = k \left(1 + \sigma/\sigma_{cr} \right)^{1/2} \quad (8)$$

The inclusion of the effect of the axial force has the following effect on the previously derived expressions:

1. In Eq. 6, k and I_c are replaced by \bar{k} and T_c .

$$\Lambda^4 = \frac{\bar{k}}{4EI_c}$$

2. In Eq. $\Delta_s = \frac{PA}{2k} \frac{\sinh \Lambda l + \sin \Lambda l}{\cosh \Lambda l - \cos \Lambda l}$, k and Λ are replaced by \bar{k} and $\bar{\Lambda}$, respectively.

General solution.

In accordance with the definition of Δ in Equation 1,

$$\Delta = \frac{pR^2}{Et}, \text{ where } p = \text{internal pressure, uniform.} \quad (10)$$

Substituting Equations 2, 9 in Equation 1.

$$\frac{zPR}{2\pi EA_f} + \frac{P\Lambda}{2\bar{k}} f(\Lambda l) = \frac{pR^2}{Et}$$

$$\text{in which } f(\Lambda l) = \frac{\sinh \Lambda l + \sin \Lambda l}{\cosh \Lambda l - \cos \Lambda l} \quad (11)$$

$$P \left[\frac{zR}{2\pi EA_f} + \frac{\Lambda}{2\bar{k}} f(\Lambda l) \right] \frac{Et}{R^2} = p$$

$$P = \left[\frac{zt}{2\pi RA_f} + \frac{\Lambda Et}{2\bar{k}R^2} f(\Lambda l) \right]^{-1} \cdot p \quad (12)$$

Example I.

To calculate the interaction forces P for a hull with the following data:

$R = 1224 \text{ in}$ $l = 432 \text{ in}$ $t = 0.05 \text{ in}$ $A_f = 21.4 \text{ in}^2$	$I_c = 261.7 \text{ in}^4; A_c = 5.889 \text{ in}^2$ $z_c = 48$ $p = 0.976 \text{ lb/in}^2$ $E = 10.4 \times 10^6 \text{ lb/in}^2$
---	---

Stretching force in hull:

$$N = \pi R^2 p = (\pi)(1224)^2 (0.976) = (4.594)(10)^6 \text{ lb}$$

Total section area:

$$A = 2\pi R t + z A_c = (2\pi)(1224)(0.05) + (48)(5.889) = 667.2 \text{ in}^2$$

Axial stress:

$$\sigma = (4.594)(10)^6 / 667.2 = 6,885 \text{ lb/in}^2$$

Longeron buckling stress σ_{cr} :

$$\rho = (I_c / A_c)^{1/2} = (261.7 / 5.889)^{1/2} = 6.666$$

$$\lambda = 1/\rho = 432/6.666$$

$$\sigma_{cr} = \frac{\pi^2 E}{\lambda^2} = 24,440 \text{ lb/in}^2$$

Modified 2nd area moment, Equation 4:

$$\bar{I}_c = \left(1 + \frac{6885}{24440}\right)(261.7) = 335.5 \text{ in}^4$$

Skin buckling stress:

$$\sigma_{cr} = \frac{E t}{\sqrt{3} R} = \frac{(10.4)(10)^6 (0.05)}{\sqrt{3} (1224)} = 245.3 \text{ lb/in}^2$$

Foundation modulus, Equation 3:

$$k = \frac{2\pi E t}{z R} = \frac{(2\pi)(10.4)(10)^6 (0.05)}{(48)(1224)} = 55.61$$

From Equation B:

$$\bar{K} = k \left(1 + \sigma/\sigma_{cr}\right)^{1/2} = (55.61) \left(1 + 6885/245.3\right)^{1/2} = 299.82 \text{ lb/in}^2$$

The effect of longitudinal stretching is very strongly marked, as far as the skin stiffness is concerned.

$$\Delta^4 = \frac{\bar{K}}{4 E \bar{I}_c} = \frac{299.82}{(4)(10.4)(10)^6 (335.5)}$$

$$\bar{\Delta} = 12.107(10)^{-3} \text{ 1/in}$$

$$\Lambda l = 5.2302$$

From Equation 11:

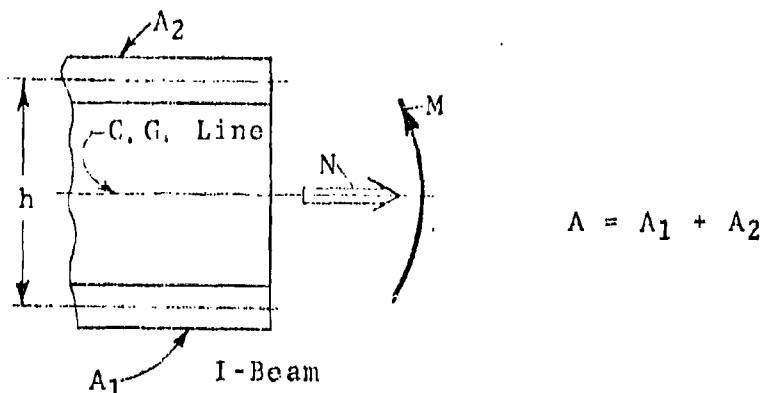
$$f(\Lambda l) = \frac{93.412 + 0.867}{93.418 - 0.495} = 0.9959$$

From Equation 12:

$$P = \left[\frac{(48)(0.05)}{(2\pi)(1224)(21.4)} + \frac{(12.107)(10)^{-3}(10.4)(10)^6(0.05)}{(2)(299.82)(1224)^2} \right]^{-1}$$

$$P = \left[(14.58)(10)^{-6} + (6.979)(10)^{-6} \right]^{-1} \times (0.9959)^{-1} (0.976) = 45,270 \text{ lb}$$

APPENDIX E Sizing of I-Beam with Thin Web.



$$A = A_1 + A_2$$

FIGURE E 1, I-Beam Schematic

The I Beam consists of the lower chord A_1 , the upper chord A_2 and the connecting shear web. The Axial force N is applied at C G of A_1 and A_2 .

The objective is to determine A_1 and A_2 so that the stress levels are σ_1 and σ_2 in the lower and the upper chord, respectively:

$$\sigma_1 = \frac{N}{A} + \frac{M}{A_1 h} \quad (1)$$

$$\sigma_2 = \frac{N}{A} - \frac{M}{A_2 h}$$

When $M = 0$, the loading becomes a pure axial load case. The real need to use Equations 1 is when there is a sizable moment present. The equations will be solved approximately for the case when the effect of the bending moment is of the same order of magnitude as the axial load.

In the first approximation, obtain A'_1 and A'_2 assuming $A'_1 = A'_2 = 0.5A$. From the first of Equations (1)

$$A' = \frac{1}{\sigma_1} \left(N + \frac{2M}{h} \right) \quad (2)$$

1 C.G. Location is not known until A_1 and A_2 are determined.

When the approximate values of A'_1 and A'_2 are inserted in Equations 1, the values for σ'_1 and σ'_2 are obtained. $\sigma'_1 = \sigma_1$; Equation 1 says in effect that the applied stress in the lower chord must be equal to the target stress. However, σ'_2 and σ_2 and as a rule a large difference is to be expected.

In the next step is chosen new A_1 without changing A , so that the target value of stress σ_2 is obtained.

$$\sigma_2 = \frac{N}{A_1} - \frac{M}{A_2 h}$$

$$\sigma_2 - \frac{N}{A_1} = - \frac{M}{A_2 h} \quad (3)$$

$$\frac{1}{A_2} = \left(\frac{N}{A_1} - \sigma_2 \right) \frac{h}{M}$$

The total area will be preserved, if

$$A''_1 = A'_1 + (A'_2 - A''_2) = A' - A''_2 \quad (4)$$

No weight saving, which is the ultimate objective, has been achieved thus far. Small changes of both areas should bring that result.

The areas appear in the denominators of Equations (1). If A , changes to $A + \Delta A$, where $\Delta A \ll A$, one can write

$$\frac{1}{A + \Delta A} = \frac{1}{A} \frac{1}{1 + \Delta A/A} \approx \frac{1}{A} \left(1 - \frac{\Delta A}{A} \right) \quad (5)$$

In the third step the index of stress and areas is changed to ('') notation

$$\sigma''_1 = \frac{N}{A''_1 + \Delta A_1} + \frac{M}{h} \frac{1}{A''_1 + \Delta A_1}$$

$$\sigma''_2 = \frac{N}{A''_2 + \Delta A_2} - \frac{M}{h} \frac{1}{A''_2 + \Delta A_2}$$

The change of A_1 and A_2 thus considered independently.

After using Equation (5):

$$\sigma_1''' = \frac{N}{A''} \left(1 - \frac{\Delta A_1}{A''} \right) + \frac{M}{hA_1''} \left(1 - \frac{\Delta A_1}{A_1''} \right)$$

$$\sigma_2''' = \frac{N}{A''} \left(1 - \frac{\Delta A_2}{A''} \right) - \frac{M}{hA_2''} \left(1 - \frac{\Delta A_2}{A_2''} \right)$$

When one assumes $\Delta A_1 = \Delta A_2 = 0$, the equations for σ_1'' and σ_2'' are obtained. Subtracting the sides of the appropriate expressions:

$$\left. \begin{aligned} \sigma_1'' - \sigma_1''' &= \frac{N}{A''} \cdot \frac{\Delta A_1}{A''} + \frac{M}{hA_1''} \cdot \frac{\Delta A_1}{A_1''} \\ \sigma_2'' - \sigma_2''' &= \frac{N}{A''} \cdot \frac{\Delta A_2}{A''} - \frac{M}{hA_2''} \cdot \frac{\Delta A_2}{A_2''} \end{aligned} \right\}$$

Isolating the unknowns, which are ΔA_1 and ΔA_2 :

$$\left. \begin{aligned} \sigma_1'' - \sigma_1''' &= \left(\frac{N}{A''} + \frac{M}{hA_1''} \cdot \frac{A_1''}{A_1''} \right) \frac{\Delta A_1}{A''} \\ \sigma_2'' - \sigma_2''' &= \left(\frac{N}{A''} - \frac{M}{hA_2''} \cdot \frac{A_2''}{A_2''} \right) \frac{\Delta A_2}{A''} \end{aligned} \right\}$$

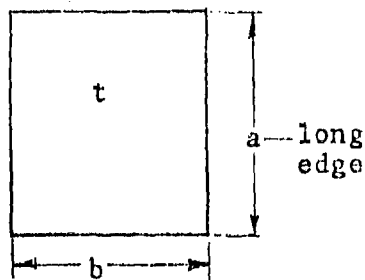
Finally:

$$\left. \begin{aligned} \Delta A_1/A'' &= (\sigma_1'' - \sigma_1''') / \left(\frac{N}{A''} + \frac{M}{hA_1''} \cdot \frac{A_1''}{A_1''} \right) \\ \Delta A_2/A'' &= (\sigma_2'' - \sigma_2''') / \left(\frac{N}{A''} - \frac{M}{hA_2''} \cdot \frac{A_2''}{A_2''} \right) \end{aligned} \right\} \quad (6)$$

APPENDIX F

Fixity of Long Edges in Membrane-Plates.

A membrane-plate is understood to be a plate, which has so sizable a deflection that the membrane component of the internal forces must be accounted for.



Edges are free to rotate.



Edges are fixed rotationally.

Model of a Membrane

FIGURE F 1

The objective is to make some conclusions regarding the behavior of panels between longerons and secondary frames, as their boundary conditions are between the two extremes shown above. The panels are slightly curved, but are treated here as flat for the sake of model convenience.

The following figures are quoted from Roark: (See References)

$$\frac{wb^4}{Et^4} = \text{Non-dimensional pressure load.}$$

$$y/t = \text{ " " deflection.}$$

$$\frac{Sdb^2}{Et^2} = \text{ " " diaphragm stress.}$$

$$\frac{sb^2}{Et^2} = \text{ " " total (diaphragm + bend.) stress}$$

TABLE FI Membrane Pressures And Stresses

	$\frac{wb^4}{Et^4}$	25	125	250
Cond. I	y/t	0.946	1.72	2.20
	$s_d b^2/Et^2$	2.40	8.10	13.20
	s_b^2/Et^2	7.16	16.40	23.60
Cond. II	y/t	0.51	1.40	1.86
	$s_d b^2/Et^2$	0.66	5.40	10.30
	s_b^2/Et^2	11.12	41.0	67.00

Note: Stress is measured at center for boundary cond. I and at the center of the long edge for boundary cond. II.

The following observations can be made.

1. Deflections are smaller in Condition II, but the difference tends to null as the load increases.
2. The same is true for membrane stress.
3. Plate bending stress is much larger in condition II and the difference grows with the load.

The last factor is very undesirable and all means possible should be used to make the panel approach condition I. This can be achieved by removing, as much as possible, the angular restraint from the edges of the panel.

Note: The figures shown above are for long plates, $a/b \geq 1.5$.

APPENDIX G Theory Of Local Skin Bending Near Longerons.

In this Appendix, the magnitude of bending moments on the skin near supports (Longerons) is evaluated. A circumferential strap of skin is treated as a beam-column with a large stretching force. The maximum radial deflection is also calculated.

The Equation for bending moment near supports is:

$$M' = wj^2 \left(\frac{U/2 - \tanh U/2}{\tanh U/2} \right), \text{ from Roark P.152, case 18,}$$

$$U = l/j; \quad j = (EI/N)^{1/2}$$

The order of magnitude of U is a few hundred for pressurized skin; when U is so large: $\tanh U/2 \approx 1.0$ and:

$$\begin{aligned} M' &\approx wj^2 \left(\frac{U}{2} - 1 \right) \approx 1/2 wj^2 U \\ M' &\approx (1/2) w l j = (1/2) w l \sqrt{EI/N} \end{aligned} \quad (1)$$

N is the tangential stretching force ; N = pr.

$$I = t^3/12.$$

It is interesting to note that the maximum bending moment is approximately proportional to the support spacing. This is different in comparison with an ordinary beam, for which the maximum moment would grow in proportion to the square of length.

Equation(1) can be presented in a more general form noting that with the absence of stretching the maximum moment is:

$$M'_0 = \frac{wl^2}{12} \quad (\text{near supports}), \text{ which means that}$$

$$M' = M'_0 \frac{6}{l} \sqrt{\frac{EI}{N}}$$

The magnitude of the buckling force for a beam with both ends fixed:

$$N_{cr} = 4 \left(\frac{\pi}{l} \right)^2 EI$$

$$\frac{EI}{N} = \frac{4\pi^2 EI}{N l^2} \frac{l^2}{4\pi^2} = \frac{N_{cr}}{N} \frac{l^2}{4\pi^2}$$

$$M' = M'_0 \frac{6}{l} \frac{l}{2\pi} \sqrt{\frac{N_{cr}}{N}}$$

$$M' = M'_0 \frac{3}{\pi} \sqrt{\frac{N_{cr}}{N}} \quad (2)$$

This is valid only for $N \gg N_{cr}$.

Maximum deflection, according to the same reference:

$$y_m = \frac{wj^2}{8N} \left(U^2 + 4U \frac{1 - \cosh U/2}{\sinh U/2} \right)$$

For large values of U:

$$y_m \approx \frac{wj^2}{8N} (U^2 - 4U) \quad (3)$$

This can be rewritten to

$$y_m = \frac{wj^2 U^2}{8N} \left(1 - \frac{4}{U} \right) \quad \text{But} \quad j^2 U^2 = l^2 \quad \text{and,} \quad y_m = \frac{wl^2}{8N} \left(1 - \frac{4}{U} \right) \quad (4)$$

This is valid for $N \gg N_{cr}$. Usually the second term in parenthesis is much smaller than unity. Note that for an ordinary beam the deflection is proportional to the fourth power of the support spacing.

The largest bending moment at midpoint of the beam column is:

$$M'' = wj^2 \left(1 - \frac{U/2}{\sinh U/2} \right) \quad \text{When } U \text{ is large:} \quad (5)$$

$$M'' \approx wj^2 \quad \text{or } M'' = w \left(\frac{EI}{N} \right) \quad \text{This may be transformed to:}$$

$$M'' = \frac{wl^2}{4\pi^2} \left(\frac{N_{cr}}{N} \right) \quad \text{When no axial force is present:}$$

$$M''_0 = \frac{wl^2}{24} \quad (\text{at center}) \quad \text{The new form of Equation(5) is:}$$

$$M'' = \frac{6}{\pi^2} \frac{N_{cr}}{N} M''_0$$

For MC-200 At Maximum Diameter.

$$R = 1224 \text{ in.}$$

$$z = 48 \text{ (Number of longerons)}$$

$$l = 2\pi R/48 = 160.2 \text{ in.}$$

$$t = 0.024 \text{ in. (Basic skin thickness)}$$

The computer printout of longeron analysis shows that the maximum radial displacement of the longerons is:

$$\Delta_s = 2.06 \text{ in.}$$

This displacement is first defined by Equation (10), Appendix D and it is the same as deflection y_m defined in this section by Equation 4; it is the relative radial deflection of skin with respect to longerons viewed in a cross-section of the hull, which is of interest.

$$\text{Pressure } p = 0.628 \text{ lb/in}^2$$

Section properties of the circumferential strap of skin:

$$A = 0.024 \text{ in}^2$$

$$I = \frac{1}{12} t^3 = (1.152)(10)^{-6} \text{ in}^4$$

$$EI = (10.4)(10)^6 (1.152)(10)^{-6} = 11.981 \text{ lb in}^2$$

Buckling load:

$$N_{cr} = \frac{4\pi^2}{l^2} EI = \left(\frac{2\pi}{160.2} \right)^2 (11.981) = 18.43(10)^{-3} \text{ lb}$$

The skin loading may be viewed as simultaneous tangential stretching with the magnitude

$$N = (p-w)R$$

And pure bending with the uniformly distributed load "w". Assuming that, Equation 4 may be written

$$\Delta_s \approx \frac{wl^2}{8N}$$

Evaluating the magnitude of w by combining the last two Equations:

$$\Delta_s = \frac{wl^2}{8(p-w)R} \quad (7)$$

$$w = \frac{p}{\frac{l^2}{8R\Delta_s} + 1} = \frac{0.628}{\frac{(160.2)^2}{(8)(1224)(206)} + 1} = 0.349 \text{ lb/in}^2$$

In the same beam, without axial force, the bending moments should be:

$$M'_0 = \frac{1}{12} (.349) (160.2)^2 = 746.4 \text{ inlb}$$

$$M''_0 = \frac{1}{2} M'_0 = 373.2 \text{ inlb}$$

As the stretching force is $N = (.628 - .349)(224) = 341.5 \text{ lb.}$, the true moments are:

$$M' = (746.4) \frac{3}{\pi} \left(\frac{(18.43)(10)^{-3}}{341.5} \right)^{1/2} = 5.236 \text{ inlb}$$

$$M'' = \frac{6}{\pi^2} \frac{18.43(10)^{-3}}{341.5} (373.2) = 12.24(10)^{-3} \text{ inlb}$$

Corresponding bending stress:

$$\sigma'_b = 6M'(1/t)^2 = (6)(5.236)/(.024)^2 = 54,542 \text{ lb/in}^2$$

$$\sigma''_b = 128 \text{ lb/in}^2$$

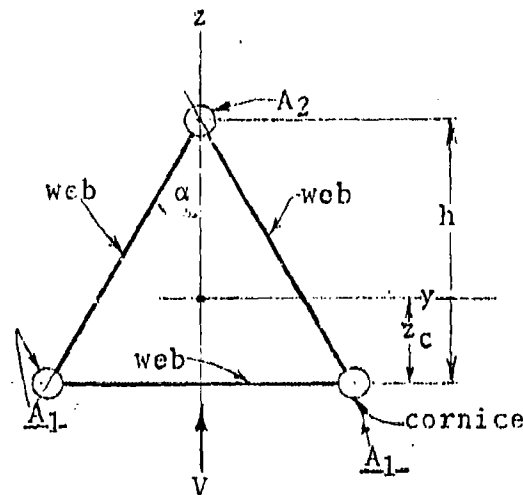
While the bending stress near the supports is excessive, the bending in mid-length is negligible.

APPENDIX H Geometrical Properties of Triangular Sections.

This type of cross-section is used for longerons as well as frames. Because of frequent need to calculate section properties, the necessary formulas are derived in this Appendix.

A general type of section in the form of isosceles triangle of Figure 1 is described first. The properties of an equilateral triangle of constant thickness are defined next.

The isosceles triangle form was selected for all structure sections of Metalclad hulls, principally to favor a radial form deformation caused by loading from the skin deformation due to hull pressure. The angle α will decrease on internal frames and increase in external longerons; this deformation will be very small in the latter case.



Typical Structural Section, with $\alpha < 30^\circ$

FIGURE H-1

$$A = A_1 + A_2$$

$$z_c = hA_2/A \quad (1)$$

$$I = A_2 (h - z_c)^2 + A_1 z_c^2 \quad (2)$$

Shear flow, each side - wall:

$$q = \frac{VS}{I} = \frac{V \left(\frac{A_2}{2} \right) (h - y_c)}{I} = \frac{VA_2 (h - y_c)}{2I}, \text{ lb/in} \quad (3)$$

No shear flow in the bottom wall because of plane of symmetry.

Note that the webs joining the chords are assumed to be pure shear webs and that their tensile and compressive properties are included in the chords.

Consider a special case: $A_1 = A_2$ from Equation (1):

$$z_c = h/2 \quad \text{from Equation (1)} \quad (4)$$

$$I = \frac{1}{4} Ah^2 \quad \text{from Equation (2)} \quad (5)$$

$$q = \frac{V}{2h} \quad (6)$$

Shear flow in each inclined wall is such as if the wall were vertical with the height h .

There is more than one way of including into the chords the axial capacity of the webs. If no buckling is involved and the stress due to axial force predominates over bending stress, almost the whole web area may be included. In case of large bending stress only one-sixth of a wall may be added to each adjoining chord, rather than one-half as in tension case. When buckling is present, an effective stiffness must be calculated.

APPENDIX I. Bending of Longerons

If a beam on an elastic foundation is loaded with a single force P , the bending moment is

$$M = \frac{P}{4} e^{-\Lambda x} (\cos \Lambda x - \sin \Lambda x) \quad (1)$$

when there is an axial load, Λ is replaced by $\bar{\Lambda}$; this is only an approximation; an exact equation, with the effect of axial load, should be used.

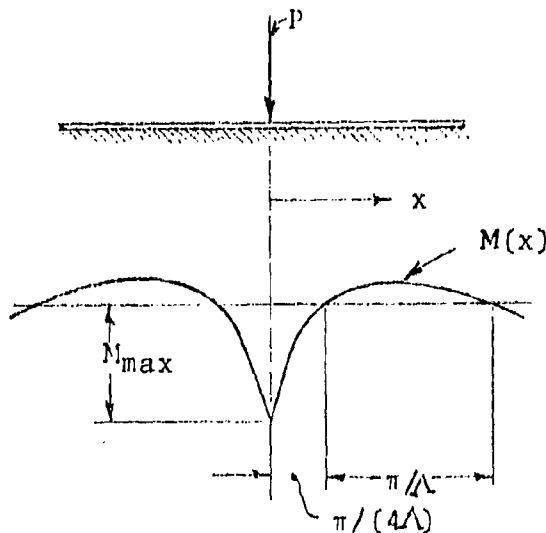


FIGURE I 1 Loading of a Beam on Elastic Foundation

According to Eq. (1), $M_{\max} = P/(4\Lambda)$.

Beyond $x = \pi/(4\Lambda)$, the magnitude of M is quite small.

In Example I, of Appendix D,* there was

$$P = 45270 \text{ lb}$$

$$\bar{\Lambda} = (12,801)(10)^{-3} \text{ 1/in}$$

$$M_{\max} = \frac{44380}{(4)(12,801)(10)^{-3}} = 884,111 \text{ inlb}$$

$$x_1 = \frac{\pi}{4\bar{\Lambda}} = \frac{\pi}{(4)(12,107)(10)^{-3}} = 64.87 \text{ in}$$

* Page 339

The first inflection point is therefore, only $64.87/432 = 0.150$ of the frame spacing away. Hetenyi shows that the first zero for deflections is 3x as large, but this is still much less than frame spacing. This means that in the example considered the effect of loading in one frame plane has negligible influence on the deflection of an adjacent frame.

Calculate bending stress due to that bending moment, using the figures of Example I.

$$I_c = 261.7 \text{ in}^2$$

$$c = 13.33 \text{ in}$$

$$\sigma_b = \frac{Mc}{I} = (866,730)(13.33)/(261.7) = 44,150 \text{ lb/in}^2$$

(Compression. Tension is 1/2 of this value.)

Y. M. Hetenyi, Beams on Elastic Foundation. University of Michigan Press, 1946.

Bending of Skin Along Longerons.

At some distance away from a frame, there will be a following deformed skin pattern:

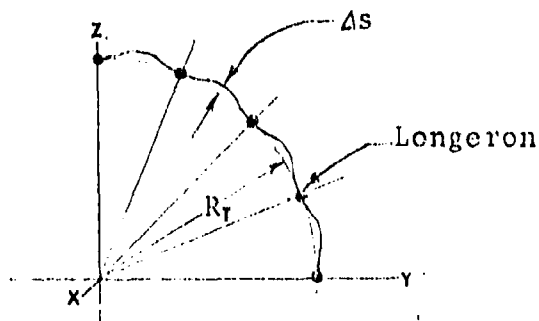


FIGURE I 2 Skin Deflection Between Longerons

This shows that longerons are restraining the skin in radial direction.

To evaluate the effect of this restraint use the procedure similar to the one described in Appendix D; first, cut the connection between frames and the rest of cylinder and let the skin be stressed to

$$\sigma_h = pR/t.$$

The outer radius grows by

$$\Delta = \frac{pR^2}{Et} \quad (2)$$

The interacting forces P cause this radius to shrink by Δ_s .
From equation

$$\Delta_s = \Delta - \Delta_f. \quad (3)$$

Once the general solution giving force

$$p = \left[\frac{2t}{2\pi R \Delta_f} + \frac{\bar{A} E t}{2 \bar{K} R^2} F(\bar{A}) \right]^{-1}$$

is performed, the frame displacement Δ_f , may be calculated from

$$\Delta_f = \frac{w R^2}{E A_f} = \frac{z P R}{2 \pi E A_f}$$

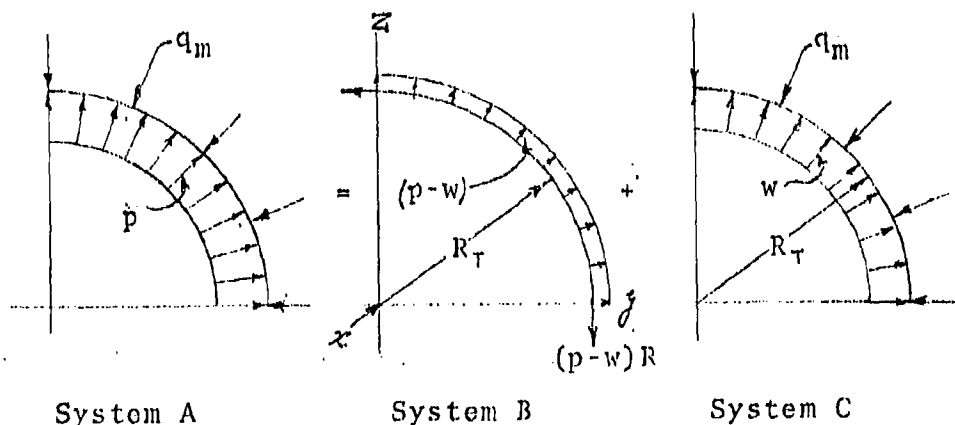


FIGURE I 3 Loading on Skin

$$A = B + C$$

(1 in. wide strap of skin is shown)

It is the shrinking by Δ_s , which gives rise to skin bending. The critical cross section is the one in which the relative skin-longeron displacement is maximum. For the sake of simplification assume skin to be separated from a frame (but not from a longeron, which is now attached to frame).

The interaction load is q (lb/in) between skin and longerons. The maximum value is q_m , applied to the skin at the frame section. The task is separated into two subproblems.

The original system "A" of radial forces q accompanied by pressure p is resolved into pure tension system "B", which causes the skin to stretch and a predominantly bending system "C". Note that this resolution is performed merely to visualize the two major load components. The bending system "C" must be analyzed in the presence of tension system "B".

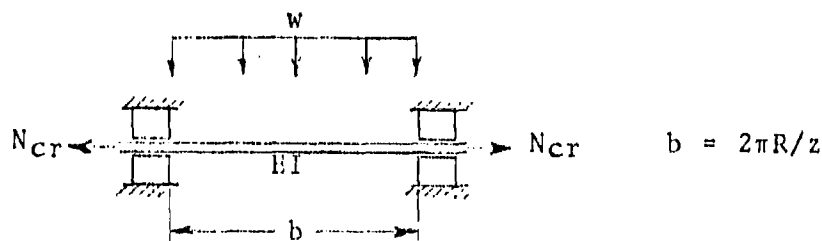


FIGURE I 4 Skin Between Longerons

One of the ways to determine the magnitude of the distributed load w is to say that it induces the relative skin displacement Δ_s . (i.e. the displacement of mid-point of skin segment with respect to the adjacent longerons)

When the magnitude of w is known, the solution of system "C" is reduced to the problem of a single-span beam column, as shown in Figure L4. Keeping in mind that system "B" acts concurrently with system "C", we have the stretching force

$$N = (p-w)R \quad (4)$$

As the bending stiffness of skin is quite small, any axial load encountered is likely to be bigger than the compressive buckling load N_{cr} . This necessitates the use of exact equations for beam-columns.

Bending of Skin Along the Frame.

Figure 5L shows the longeron with a set of frame reactions p . The magnitude of deflection under each force P is denoted by Δ_s and defined by equation

$$\Delta_s = \frac{p}{2k} \frac{\sinh \lambda l + \sin \lambda l}{\cosh \lambda l - \cos \lambda l}$$

The longitudinal bending moment in skin reaches the largest value at where force P is applied.

The equation for deflection y due to P in general case is according to Hetenti,⁷

$$y = \frac{PA}{2K} \frac{1}{\alpha\beta} e^{-\alpha x} (\beta \cosh \beta x + \alpha \sinh \beta x) \quad (4)$$

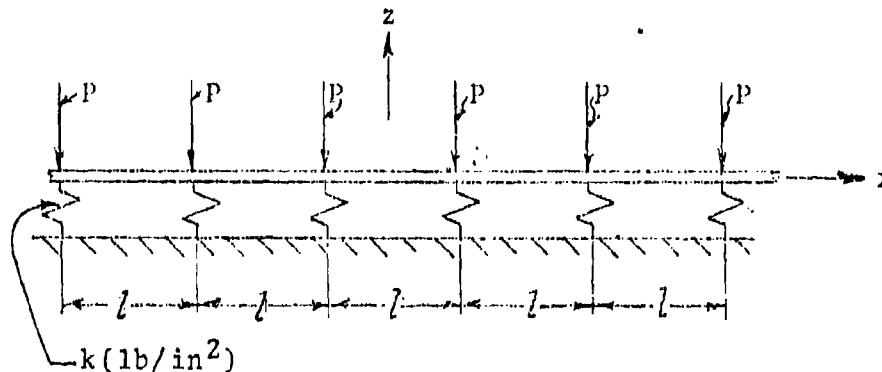


FIGURE 1 5 Skin Bending Along a Frame

Briefly:

$$y = Ge^{-\alpha x} f(x), \quad \text{Bending moment is:} \quad (5)$$

$$M = EI y'' = EIG \frac{d}{dx} [-\alpha e^{-\alpha x} f(x) + e^{-\alpha x} f'(x)]$$

$$M = EIG [\alpha^2 e^{-\alpha x} f(x) - \alpha e^{-\alpha x} f'(x) - \alpha e^{-\alpha x} f'(x) + e^{-\alpha x} f''(x)] =$$

$$= EIG [\alpha^2 e^{-\alpha x} f(x) - 2\alpha e^{-\alpha x} f'(x) + e^{-\alpha x} f''(x)]$$

$$f(x) = \beta \cosh \beta x + \sinh \beta x$$

$$f'(x) = \beta^2 \sinh \beta x + \alpha \beta \cosh \beta x$$

$$f''(x) = \beta^3 \cosh \beta x + \alpha \beta^2 \sinh \beta x = \beta^2 f(x)$$

$$M = EIG [(\alpha^2 + \beta^2) e^{-\alpha x} f(x) - 2\alpha e^{-\alpha x} f'(x)]$$

$$M(0) = EIG [(\alpha^2 + \beta^2) \beta - 2\alpha \alpha \beta] = EIG [\beta^3 - \alpha^2 \beta]$$

Rewrite G according to equations 4 and 5:

$$M = EI \frac{PA}{2K} \frac{A}{\alpha B} [\bar{\beta}^2 - \alpha^2]$$

After Hetenyi:

$$\bar{\beta}^2 - \alpha^2 = \frac{N}{4EI} - \Delta^2 - \left(\Delta^2 + \frac{N}{4EI} \right) = -2\Delta^2$$

$$M = EI \frac{PA}{2K} \frac{A}{\alpha} (-2\Delta^2)$$

Minus sign may be omitted, as it is due only to the convention. Also, from equation

$$\Delta^4 = \frac{k}{4EI_c}$$

$$k = 4EI\Delta^4$$

(I was used instead of I_c , as the skin, rather than the longeron, is of interest.)

$$M_{\max} = \frac{P}{4\alpha} \quad (6)$$

According to equation (1), or by setting $N = 0$ in equation:

$$\alpha^2 = \Delta^2 + \frac{N}{4EI}$$

The moment when the axial force N is absent is:

$$M'_{\max} = \frac{P}{4\Delta}$$

Comparing this with equation (6):

$$M'_{\max} = M_{\max} \left(\frac{\Delta}{\alpha} \right)$$

This result is analogous to one obtained for maximum deflection. The moment may be calculated with no axial force present and then multiplied by factor m given by equation:

$$m'' = \frac{1}{[1 + \sigma/\sigma_{cr}]^{1/2}}$$

If the radial skin displacement is Δ_s , the equivalent, continuous radial loading is

$$w = \frac{Et}{R^2} \Delta_s$$

It is assumed here that the correction for the effect of axial forces had already been made. By comparing equation

$$z = \frac{p\Delta}{2k} e^{-\Delta x} (\cos \Delta x + \sin \Delta x) \text{ with equation (1), for } x=0:$$

$$\frac{M_{\max}}{z_{\max}} = \frac{p}{4\Delta} \frac{2k}{p\Delta} = \frac{k}{2\Delta^2}$$

In this case:

$$M_{\max} = \frac{k}{2\Delta^2} \Delta_s$$

By definition,

$$\frac{k}{2} \frac{1}{\Delta^2} = \frac{k}{2} \left(\frac{4EI}{k} \right)^{1/2} = (EI k)^{1/2}$$

$$I = \frac{t^3}{12} ; k = \frac{Et}{R^2} ; EI k = E \frac{Et^4}{12R^2}$$

$$M_{\max} = \frac{Et^2}{\sqrt{12}R} \Delta_s \quad (7)$$

The bending stress is

$$\sigma_b = \frac{6M}{t^2}$$

which gives, from equation (7):

$$\sigma_b = \frac{\sqrt{3}E}{R} \Delta_s$$

This bending stress is additive with the longitudinal stress due to pressure.

The considerations in this appendix are valid at a reasonable distance away from longerons. As we approach a longeron, its own curvature determines the skin stress. In the vicinity of a frame it is usually tension.

Longeron as Beam on Elastic Foundation.

The skin is the elastic foundation with stiffness k (lb/in²). At each frame station there are concentric forces P applied, which represent the interaction with the frame. Consider one longeron, as shown in Figure 5L. Bending stiffness of a longeron (including a piece of effective skin) is EI_c ; introduce a relative stiffness constant :

$$\Lambda^4 = \frac{K}{4EI_c} \quad (9)$$

If only the force at the origin is applied, the deflected line is

$$z = \frac{P\Lambda}{2k} e^{-\Lambda x} (\cos \Lambda x + \sin \Lambda x), \quad (\text{Hetenyi}) \quad (10)$$

To preserve symmetry about z -axis, the force at the origin is treated as two halves of P . Every other pair of forces P , which is placed symmetrically about z -axis, at a distance λl from it, will give

$$\frac{P\Lambda}{k} e^{-\Lambda z l} (\cos \Lambda z l + \sin \Lambda z l)$$

so that the total displacement is

$$\Delta_s = \frac{P\Lambda}{2k} + \frac{P\Lambda}{k} \sum_{n=1}^{\infty} e^{-\Lambda z l} (\cos \Lambda z l + \sin \Lambda z l) \quad (11)$$

This results from the following identities:

$$\sum_{k=0}^{\infty} e^{-kt} \sin kx = \frac{1}{2} \frac{\sin x}{\cosh t - \cos x}; \quad 1 + 2 \sum_{k=1}^{\infty} e^{-kt} \cos kx = \frac{\sinh t}{\cosh t - \cos x}$$

But $\frac{1}{2} + \sum_{n=1}^{\infty} e^{-\Lambda z l} (\cos \Lambda z l + \sin \Lambda z l) = \frac{1}{2} \frac{\sinh \Lambda l + \sin \Lambda l}{\cosh \Lambda l - \cos \Lambda l}$

$$\Delta_s = \frac{P\Lambda}{2k} \frac{\sinh \Lambda l + \sin \Lambda l}{\cosh \Lambda l - \cos \Lambda l} \quad (12)$$

Influence of Axial Stretching

When skin and longerons are subjected to axial tension, it is more difficult to bend them in lateral (radial) direction, than if the tension did not exist. This effect is considered separately for skin and for longerons.

In case of a longeron subjected to an axial load N , a simple approximation is made; the effective second area moment I_c is assumed to be

$$\bar{I}_c = \left(1 + \frac{N}{N_{cr}}\right) I_c \quad (12)$$

In which N_{cr} is the elastic buckling force for a longeron supported by the frames.

The stiffening factor for a thin-wall cylinder will be determined from the deflections of a longitudinal strip of skin, which is treated as a beam on an elastic foundation. The equation 10, shows that the deflection under a single force P at the origin is

$$y_0 = \frac{P\Lambda}{2k}$$

When no axial force is acting equation (113) on Page 134 of Hetenyi gives the deflection with the axial force present:

$$y_1 = \frac{P\Lambda}{2k} \frac{\Lambda}{\alpha}$$

The stiffening factor is defined as

$$m = \frac{y_1}{y_0} = \frac{\Lambda}{\alpha}$$

in which $\alpha = \left[\Lambda^2 + \frac{N}{4EI}\right]^{1/2}$

$$m = \frac{1}{\left[1 + \frac{N}{4EI\Lambda^2}\right]^{1/2}} \quad (13)$$

The definition of given by equation (9) holds true also for a longitudinal strip with stiffness EI:

$$4EI\Lambda^2 = 4EI \left[\frac{k}{4EI} \right]^{1/2} = [4EIk]^{1/2}$$

Using expression for

$$k = \frac{2\pi Et}{zR}, \quad (\text{foundation modulus})$$

For a continuously loaded skin and

$$Ik = \frac{t^3}{12} \frac{Et}{R^2} = \frac{Et^2}{12R^2}, \quad \text{gives:}$$

$$4EI\Lambda^2 = \left[4E \frac{Et^2}{12R^2} \right]^{1/2} = \frac{Et^2}{\sqrt{3}R}$$

In considering skin stiffness, the Poisson's ratio of skin is assumed equal to zero setting $\nu=0$ in the expression for buckling stress of a cylinder:

$$N_{cr} = t\sigma_{cr} = \frac{1}{\sqrt{3}} \frac{Et^2}{R}$$

But this is the same value as previously derived value of $4EI\Lambda^2$. Substituting in the expression for m:

$$m = \frac{1}{[1 + \sigma/\sigma_{cr}]^{1/2}} \quad (14)$$

In which σ_{cr} is the theoretical value of the cylinder buckling stress:

$$\sigma_{cr} = Et/(\sqrt{3}R)$$

and σ is positive, when in tension.

Instead of saying that the deflections of skin decreased m times, one can say that the foundation modulus was changed to \bar{k} :

$$\bar{k} = \frac{k}{m} = k[1 + \sigma/\sigma_{cr}]^{1/2} \quad (15)$$

The inclusion of the effect of the axial force has the following impact on the previously derived expressions:

1. In equation $\Lambda^b = \frac{k}{4Et_c}$, k and I_c are replaced by \bar{K} and \bar{I}_c .

$$\bar{\Lambda}^b = \frac{\bar{K}}{4E\bar{I}_c}$$

2. In equation 12, k and Λ are replaced by \bar{K} and $\bar{\Lambda}$.

General Solution

In accordance with the definition of Δ in equation $\Delta_s + \Delta_f = \Delta$,

$$\Delta = \frac{pR^2}{Et} \quad (16)$$

p = internal pressure, uniform.

Substituting:

$$\Delta_f = \frac{wR^2}{EAt} = \frac{zPR}{2\pi EA_f} \quad \text{and equations 11 and 16}$$

in $\Delta_s + \Delta_f = \Delta$,

$$\frac{zPR}{2\pi EA_f} + \frac{P\bar{\Lambda}}{2\bar{K}} F(\bar{\Lambda}l) = \frac{pR^2}{Et}$$

In which:

$$F(\bar{\Lambda}l) = \frac{\sinh \bar{\Lambda}l + \sin \bar{\Lambda}l}{\cosh \bar{\Lambda}l - \cos \bar{\Lambda}l} \quad (17)$$

$$p \left[\frac{zR}{2\pi EA_f} + \frac{\bar{\Lambda}}{2\bar{K}} F(\bar{\Lambda}l) \right] \frac{Et}{R^2} = p$$

$$p = \left[\frac{nt}{2\pi RA_f} + \frac{Et}{2\bar{K}R^2} F(\bar{\Lambda}l) \right]^{-1} p \quad (18)$$

APPENDIX J Standards

Alum. Alloy: 7050-T76 Alclad

$$\sigma_{tu} = 73,000, \text{ lb/in}^2$$

$$\sigma_{ty} = 64,000, \text{ lb/in}^2$$

$$\sigma_{cy} = 61,000, \text{ lb/in}^2$$

$$\tau_{su} = 44,000 \text{ lb/in}^2$$

$$e = 7\%$$

$$E = (10.2)(10)^6, \text{ lb/in}^2$$

$$E_c = (10.6)(10)^6, \text{ lb/in}^2$$

$$\nu = .33$$

$$\gamma = .102, \text{ lb/in}^3$$

Air: NASA Std

At sea level: (Dry Air)

$$t_o = 59.00, ^\circ\text{F}$$

$$T_o = 518.688, ^\circ\text{R}$$

$$p_o = p_o 2116.22, \text{ lb/ft}^2$$

$$= 14.695.97, \text{ lb/in}^2$$

$$\gamma_o = .076475, \text{ lb/ft}$$

$$\mu_o = (37452)(10)^{-9}, \text{ lb.s/ft}^2$$

$$\nu_o = (1.5757)(10)^{-4}, \text{ ft}^2/\text{s}$$

$$a_o = 1116.89, \text{ ft/sec}$$



$$c_{p0} = .24067, \text{ BTU/lb}^{\circ}\text{R}$$

$$R = 53.3505, \text{ ft}^{\circ}\text{R}$$

$$k = 1.4021$$

Air:

NASA STD

at 5,000ft altitude: (dry air)

$$t_5 = 41.169, ^{\circ}\text{F}$$

$$T_5 = 500.857, ^{\circ}\text{R}$$

$$P_5 = p_5 = 1760.79, \text{ lb/ft}^2$$

$$= 12.2277, \text{ lb/in}^2$$

$$\gamma_5 = .065896, \text{ lb/ft}^3$$

$$\mu_5 = (36422)(10)^{-11}, \text{ lb.s/ft}^2$$

$$v_5 = (1.7783)(10)^{-4}, \text{ ft}^2/\text{sec}$$

$$a_5 = 1097.53, \text{ ft/sec}$$

$$c_{p5} = .234241, \text{ BTU/lb}^{\circ}\text{F}$$

$$R = 53.3505, \text{ ft}^{\circ}\text{R}$$

$$K = 1.40215$$

Air:

NASA STD

at 10,000ft altitude: (Dry air)

$$t_{10} = 23.338, ^{\circ}\text{F}$$

Air:

NASA STD

at 10,000ft altitude: (Dry air)

$$T_{10} = 483.026, {}^{\circ}\text{R}$$

$$P_{10} = p_{10} = 1455.33, \text{ lb/ft}^2$$

$$= 10.10646, \text{ lb/in}^2$$

$$\gamma_{10} = .056475, \text{ lb/ft}^3$$

$$\mu_{10} = (35374)(10)^{-11}, \text{ lb.s/ft}^2$$

$$\nu_{10} = (2.0153)(10)^{-4}, \text{ ft}^2/\text{s}$$

$$a_{10} = 1077.81, \text{ ft}^2/\text{s}$$

$$c_{p_{10}} = .240166, \text{ BTU/lb}^{\circ}\text{R}$$

$$R = 53.3505, \text{ ft}^2/{}^{\circ}\text{R}$$

$$k = 1.40215$$

Helium:

Pure He at sea level:

$$t_0 = 59.00, {}^{\circ}\text{F}$$

$$T_0 = 518.688, {}^{\circ}\text{R}$$

$$P_0 = p_0 = 2116.22, \text{ lb/ft}^2$$

$$= 14.69597, \text{ lb/in}^2$$

$$\gamma_{\text{He}_0} = .0105631, \text{ lb/ft}^3$$

$$\mu_{\text{He}_0} = 13.34(10)^{-6} \text{ at } 77.36^{\circ}\text{F}$$

Helium:

Pure He at sea level:

$$v_{He_0} =$$

$$a_{He_0} = 3271, \text{ ft/s}$$

$$c_{p_{He_0}} = 1.25, \text{ BTU/lb}^\circ\text{R}$$

$$R_{He} = 386.24496, \text{ ft}^\circ\text{R}$$

$$k_{He_0} = 1.66$$

Helium:

Pure He at 5,000ft altitude:

$$t_{He_5} = 41.169, ^\circ\text{F}$$

$$T_{He_5} = 500.857, ^\circ\text{R}$$

$$p_{He_5} = p_{He_5} = 1760.79, \text{ lb/ft}^2$$

$$= 12.2277, \text{ lb/in}^2$$

$$\gamma_{He_5} = .0091018, \text{ lb/ft}^3$$

$$\mu_{He_5} =$$

$$v_{He_5} =$$

$$a_{He_5} = 3214, \text{ ft/sec.}$$

Helium:

pure He at 5,000ft altitude:

$$c_{p_{He_5}} \approx 1.2484, \text{BTU/lb}^{\circ}\text{R}$$

$$R_{He} = 386.24496, \text{ft}/^{\circ}\text{R}$$

$$k_{He_{10}} \approx 1.66$$

Helium:

Pure He at 10,000ft altitude

$$t_{He_{10}} = 23.388, ^{\circ}\text{F}$$

$$T_{He_{10}} = 483.026, ^{\circ}\text{R}$$

$$p_{10} = p_{10} = 1455.33, \text{lb}/\text{ft}^2$$

$$\approx 10.10646,$$

$$\gamma_{He_{10}} = .0078006 \text{ lb}/\text{ft}^3$$

$$\mu_{He_{10}} =$$

$$\nu_{He_{10}} =$$

$$a_{He_{10}} = 3157, \text{ft}/\text{sec.}$$

$$c_{p_{He_{10}}} \approx 1.25, \text{BTU/lb}^{\circ}\text{R}$$

$$R_{He} = 386.24496, \text{ft}/^{\circ}\text{R}$$

$$k_{He_{10}} \approx 1.66$$

Lift of He:

At sea level: temp. of air and He is the same, gases are dry.

Pure He: $k_{He_0} = \gamma_{Air_0} - \gamma_{He_0} = 0.76475 - .0105631$

$$k_{He_0} = .065912, \text{ lb/ft}^3$$

$$.95 \text{ pure He: } k_{He_0} = .076465 - \frac{.0105612}{.95}$$

$$k_{He_0} = .065358, \text{ lb/ft}^3$$

$$\approx .06535, \text{ lb/ft}^3, \text{ used value}$$

At 5,000ft altitude:

$$.95 \text{ pure He: } k_{He_5} = \gamma_{Air_5} - \gamma_{He_5} = .065896 - .0091018/.95$$

$$k_{He_5} = .0563142, \text{ lb/ft}^3$$

$$\approx .05631, \text{ lb/ft}^3, \text{ used value}$$

At 10,000ft altitude:

$$.95 \text{ pure He: } k_{He_{10}} = \gamma_{Air_{10}} - \frac{\gamma_{He_{10}}}{.95} = .056475 - .0078006/.95$$

$$k_{He_{10}} = .0482856, \text{ lb/ft}^3$$

$$\approx .04828, \text{ lb/ft}^3, \text{ used value}$$

APPENDIX K Notations

CAPITAL LETTERS

A, ft^2 or in^2 = area

B, in. = width

C. = coefficient

C, in. = distance from NA to extreme fiber of a beam

D, lb = drag force on a hull

E, lb/in^2 = modulus of elasticity

F, lb = force

G, lb/in^2 = modulus of shear

H, in. = height

I, in^4 = moment of inertia

J, 778.156 ftlb/BTU = mechanical equivalent of heat

L, lb = lift

L, in. = length

M, ftlb = moment

P, lb/in^2 = absolute pressure

P, lb = load

P, ft = perimeter

Q, lb = shear force

R, $\text{ft}/^\circ\text{R}$ = gas constant

R, ft or in. = radius

R, degrees = Rankine temperature

T, degrees = total temperature

V , lb/ft = shear flow

V , ft³ = volume

SMALL LETTERS

a , ft/s = velocity of sound

$2a$, ft = major axis of an ellipsoid

a_s , ft or in. = semi-axis of bow ellipsoid

b , ft or in. = distance between longerons

$2b$, ft = minor axis of an ellipsoid

a/b = finess ratio of an ellipsoid hull

c , ft/s = gust velocity

d , ft or in. = diameter

e , $\sqrt{\frac{n^2 - 1}{n}}$ = eccentricity of an ellipse

g , ft/s² = gravitational acceleration

h , ft or in. = height of a frame or longeron

h , ft = head of gas

i = an individual number

k , lb/ft³ = specific lift of gas

k , c_p/c_r = ratio of specific heats

k , lb/in = spring constant

l , ft or in. = length

n , a/b

p , lb/ft² or lb/in² = static pressure

q , $\rho u^2/2$ or lb/ft² = dynamic pressure

q , lb/ft or lb/in = shear flow

r , ft or in. = radius
 t , in. = thickness
 u , knots or ft/s = airship forward velocity
 v , ft³/lb = specific volume
 w , lb = weight
 x , ft or in. = Cartesian abscissa
 x = longitudinal axis of a hull
 y = port-starboard axis of a hull
 z = vertical axis of a hull
 z = a fixed number

SUBSCRIPTS

a_e = aerodynamic
 av = average
 all = allowable
 b = for bending stress
 B = bow or bottom
 c = compression
 cr = critical
 d = doubler
 des = design
 D = drag
 e = Eulerian load
 f = frame
 g = gas head
 h = hoop



i = individual
ic = inner chord
L = longitudinal or longeron
LS = longitudinal skin direction
m = for gust moment
max = maximum
M = maximum
o = total or absolute value
oc = outer chord
S = stern
S = skin
ST = in the skin at top of the hull
SB = in the skin at bottom of the hull
t = tension
T = transverse or top
TS = in transverse direction in the skin
x = in x direction
y = in y direction
YP = yield point
z = in z direction

GREEK LETTERS

α , degrees = radial angle in the transverse plane of hull
 γ , lb/ft³ = weight density
 Δ = difference
 ϵ , in. = deformation

θ , degrees = pitch angle of the hull

θ , degrees or radians = perimetral station on a frame at a fixed load

λ = (weight of hull)/(gross displacement lift)

λ , $1/\rho$ = slenderness ratio of a column

μ , lb sec/ft² = dynamic viscosity

ν = Poisson's Ratio

ν , ft²/s = kinematic viscosity

ξ = elastic parameter

π = Ludolf's number

ρ , ft or in. = radius of gyration

ρ , lb sec²/ft⁴ = mass density

σ , lb/in² = tension or compression stress

τ , lb/in² = shear stress

Φ , degrees = angle above equator

ω , 1/s = circular velocity

Σ = summation symbol



APPENDIX L Ellipses And Ellipsoids

x, Longitudinal Axis

y, Horizontal Axis

z, Vertical Axis

Elevational Profile

Bow Ellipsoid

$$\frac{x^2}{a_B^2} + \frac{z^2}{R_T^2} = 1$$

Stern Ellipsoid

$$\frac{x^2}{a_S^2} + \frac{z^2}{R_T^2} = 1$$

Origin at max. R_T station of the hull

$$\text{Excentricity } e = \frac{\sqrt{a^2 - R_T^2}}{a}$$

Osculatory Radius of Bow

$$R_B = \frac{R_T^2}{a_B}$$

of Stern

$$R_S = \frac{R_T^2}{a_S}$$

Volume of Bow Ellipsoid:

$$V_B = (2/3) \pi a_B R_T^2$$

of Stern Ellipsoid

$$V_S = (2/3) \pi a_S R_T^2$$

Center of buoyancy from the origin at maximum diameter R_T station.

Bow Ellipsoid

$$B_B = (.375)a_B$$

Stern Ellipsoid

$$B_S = (.375)a_S$$

Area of Ellipse

$$\text{Bow } A_B = \pi a_B R_T$$

$$\text{Stern } A_S = \pi a_S R_T$$

Perimeter of Ellipse

$$\text{Bow } P_B = 2\pi a_B \left[1 - (1/2)^2 \epsilon_B^2 - \left(\frac{1 \times 3}{2 \times 4} \right)^2 \frac{\epsilon_B^4}{3} - \left(\frac{1 \times 3 \times 5}{2 \times 4 \times 6} \right)^2 \frac{\epsilon_B^6}{5} \dots \right]$$

$$\epsilon_B = \sqrt{\frac{a_B^2 - R_T^2}{a_B^2}}$$

$$\text{Stern } P_S = 2\pi a_S \left[1 - (1/2)^2 \epsilon_S^2 - \left(\frac{1 \times 3}{2 \times 4} \right)^2 \frac{\epsilon_S^4}{3} - \left(\frac{1 \times 3 \times 5}{2 \times 4 \times 6} \right)^2 \frac{\epsilon_S^6}{5} \dots \right]$$

$$\epsilon_S = \sqrt{\frac{a_S^2 - R_T^2}{a_S^2}}$$

Surface Area of Ellipsoid

$$\text{Bow } A_B = \pi R_T^2 + \pi a_B R_T \frac{\sin^{-1} \epsilon_B}{\epsilon_B}$$

$$\text{Stern } A_S = \pi R_T^2 + \pi a_S R_T \frac{\sin^{-1} \epsilon_S}{\epsilon_S}$$

Local Radius of Curvature of Ellipse

$$\text{Bow } R_B = \frac{(R_T^4 x^2 + a_B^4 y^2)^{3/2}}{a_B^4 R_T^4}$$

$$\text{Stern } R_S = \frac{(R_T^4 x^2 + a_S^4 y^2)^{3/2}}{a_S^4 R_T^4}$$



APPENDIX M

- M - 1 MC-100 Layout
- M - 2 MC-125 Layout
- M - 3 MC-150 Layout
- M - 4 MC-175 Layout
- M - 5 MC-200 Layout

APPENDIX N

- N - 1 Sketch - Assembly Method
- N - 2 Sketch - Final Assembly

Report NADC 76238-30 Volume I & Volume II

Volume II

METALCLAD AIRSHIP HULL STUDY



L. R. Campbell, V. H. Pavlecka, J. W. Roda,
E. V. Stephens and G. Szuladzinski

DECEMBER, 1976

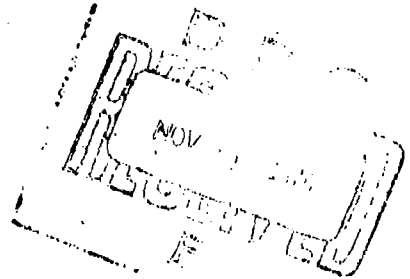
FINAL REPORT

PREPARED FOR

NAVAL AIR DEVELOPMENT CENTER

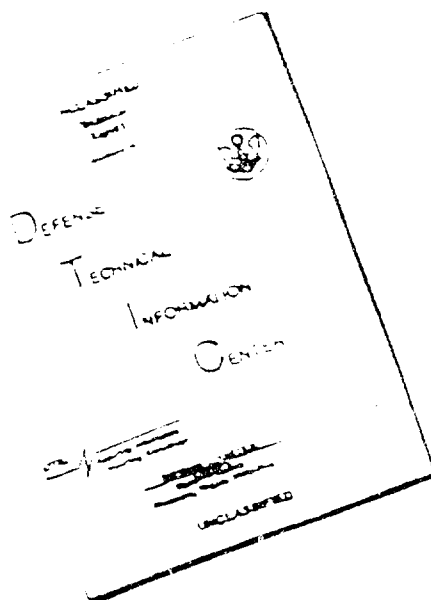
WARMINSTER, PENNSYLVANIA 18974

NADC-31P3



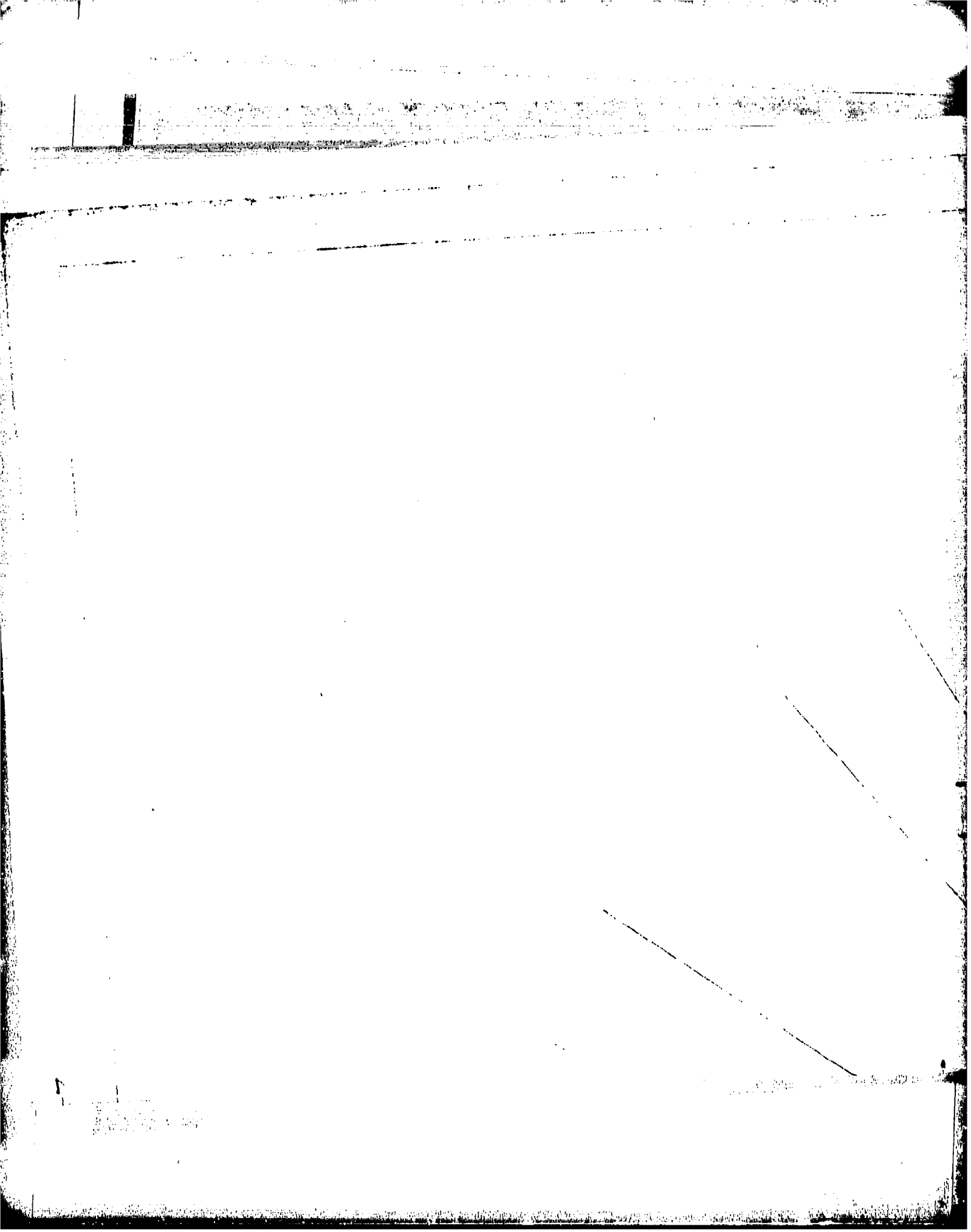
78 10 106

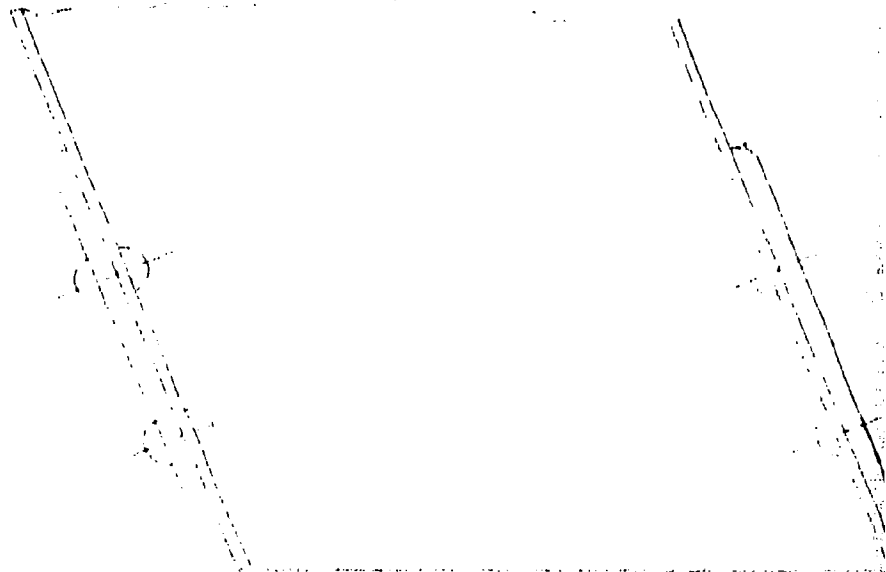
DISCLAIMER NOTICE



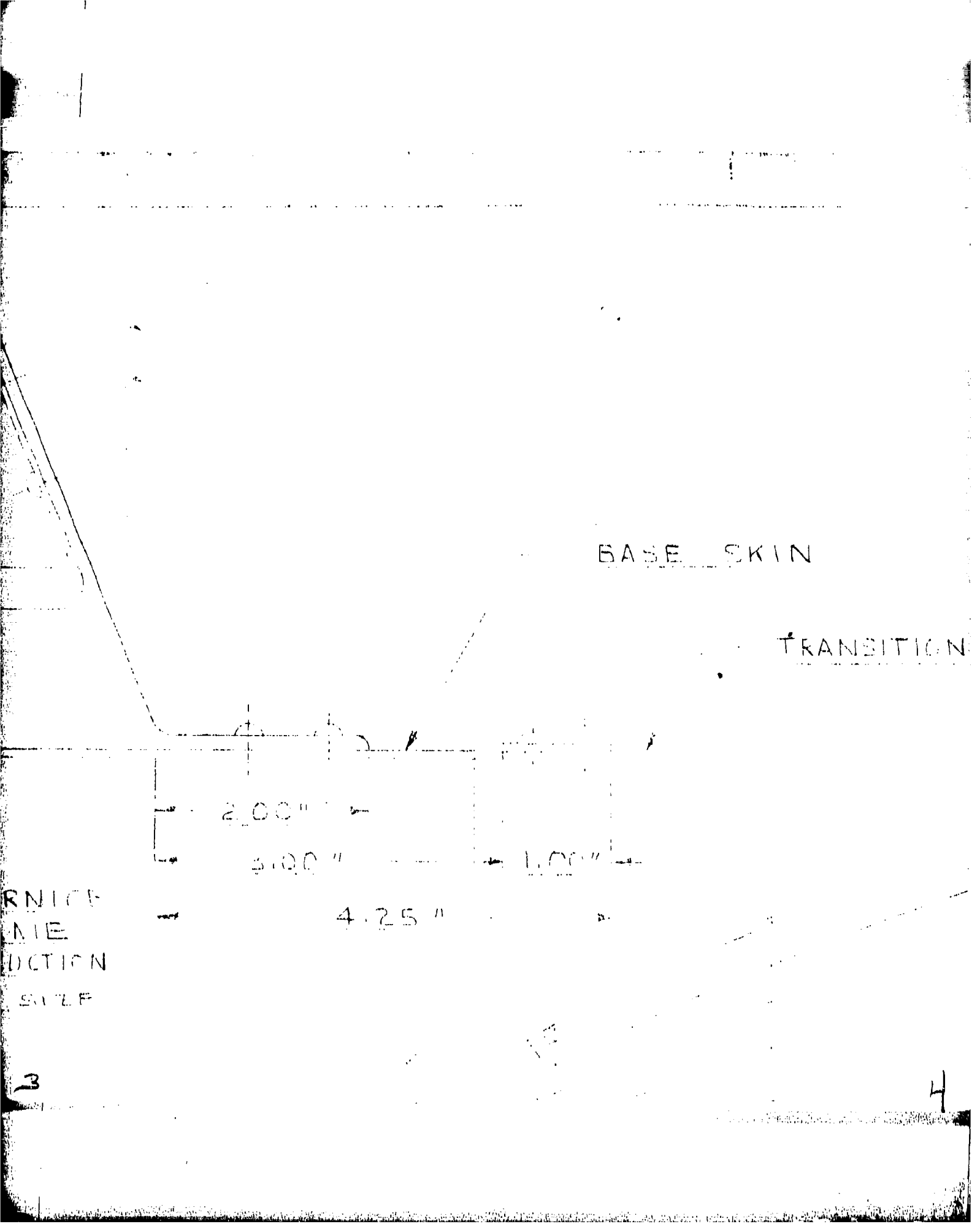
THIS DOCUMENT IS BEST
QUALITY AVAILABLE. THE COPY
FURNISHED TO DTIC CONTAINED
A SIGNIFICANT NUMBER OF
PAGES WHICH DO NOT
REPRODUCE LEGIBLY.

REPRODUCED FROM
BEST AVAILABLE COPY





BASE CORNICE
MAIN FRAME
TYPE CONSTRUCTION
SCALE: FULL SIZE



BASE SKIN

TRANSITION

2.00"

3.00"

1.00"

4.25"

RNIC
ME
DUCTION
SELF

3

4

ION SWIN

4

5

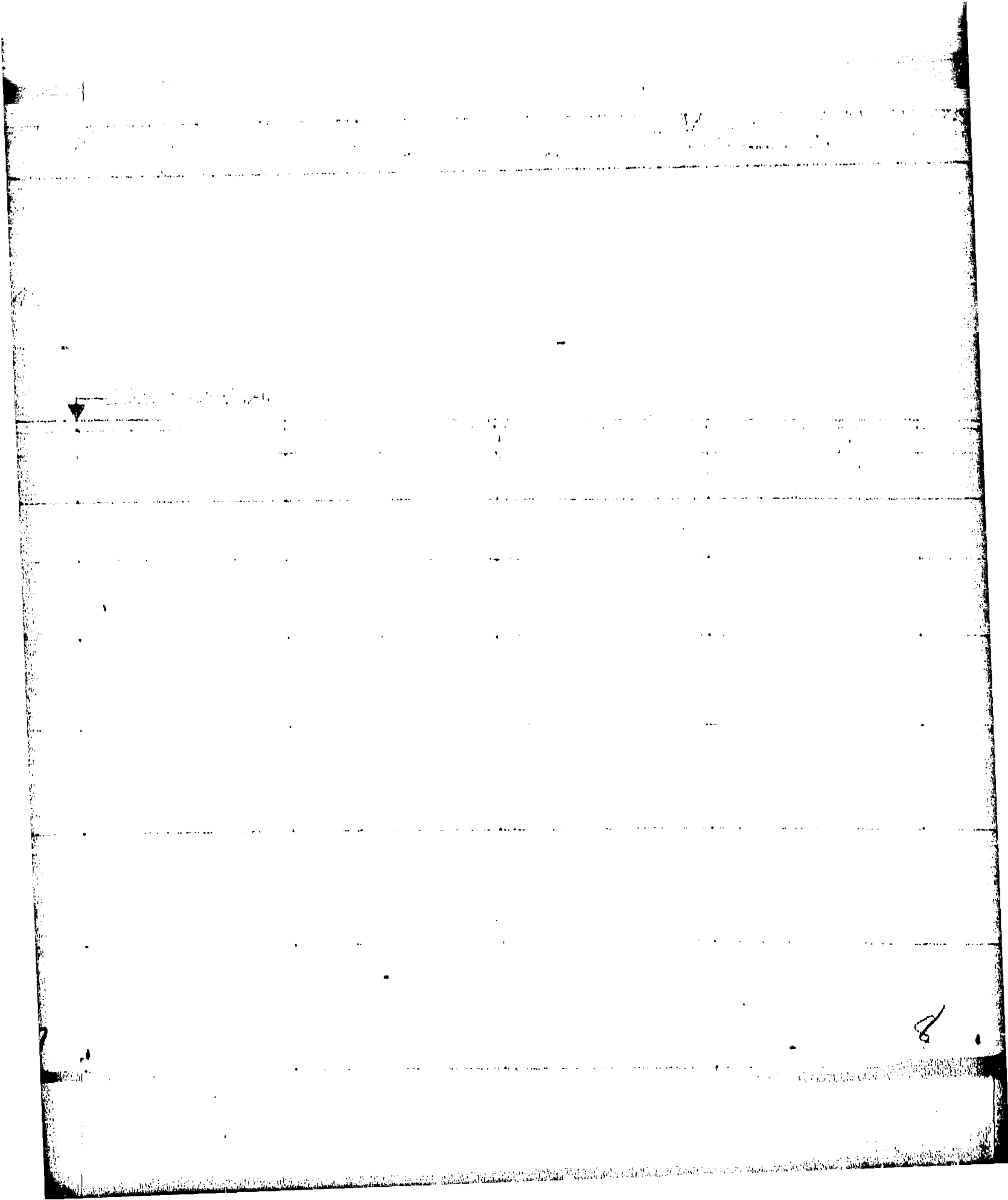
5.

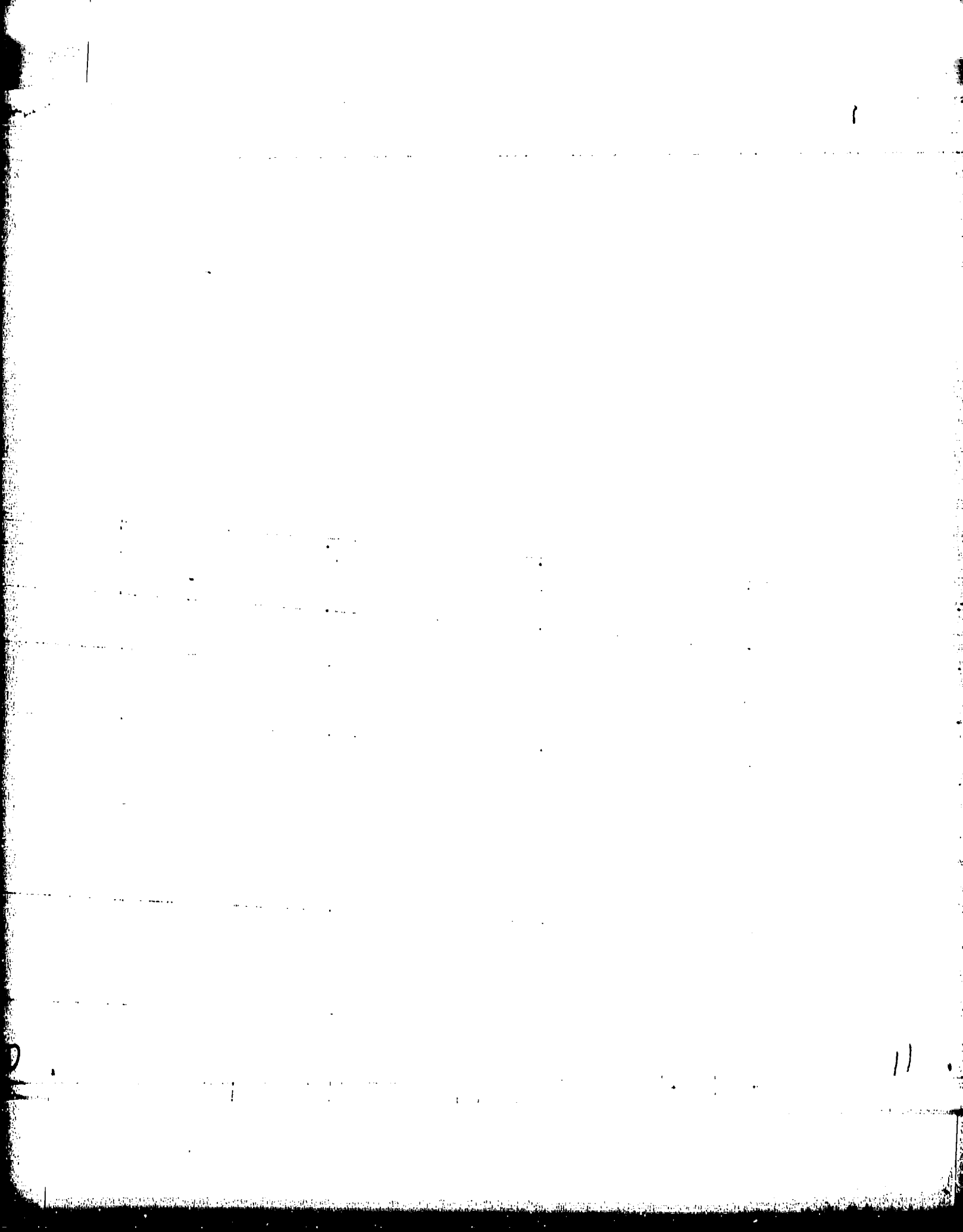
6.

8

6.

7





FASTER
SEAL
LEAF

SECONDARY
BASE

12

DOOR EDGE
STIFFENER

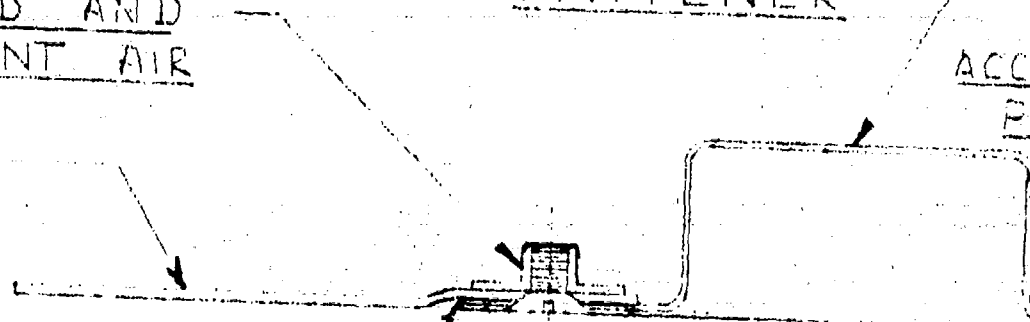
FASTENER - CAPPED AND
SEALED TO PREVENT AIR
LEAKAGE

ACCESS
PAN

SECONDARY FRAME
BASE SKIN

GASKET —

SECTION 12



SECONDARY FRAME

ACCESS DOOR
PANEL

D
↓

D
↓

ACCESS DOOR

TYPICAL CONSTRUCTION OF
LOCATED BETWEEN THE FO
ARY FRAMES :

976.15	\$	8
757.76	\$	8
683.21	\$	8
578.06	\$	8
475.16	\$	8
370.70	\$	8
245.85	TOTAL	

13.

SECONDARY FRAME

C LONGERON

C LONGERON

OF ACCESS DOOR
FOLLOWING SECOND.

828.06

820.76

715.09

611.08

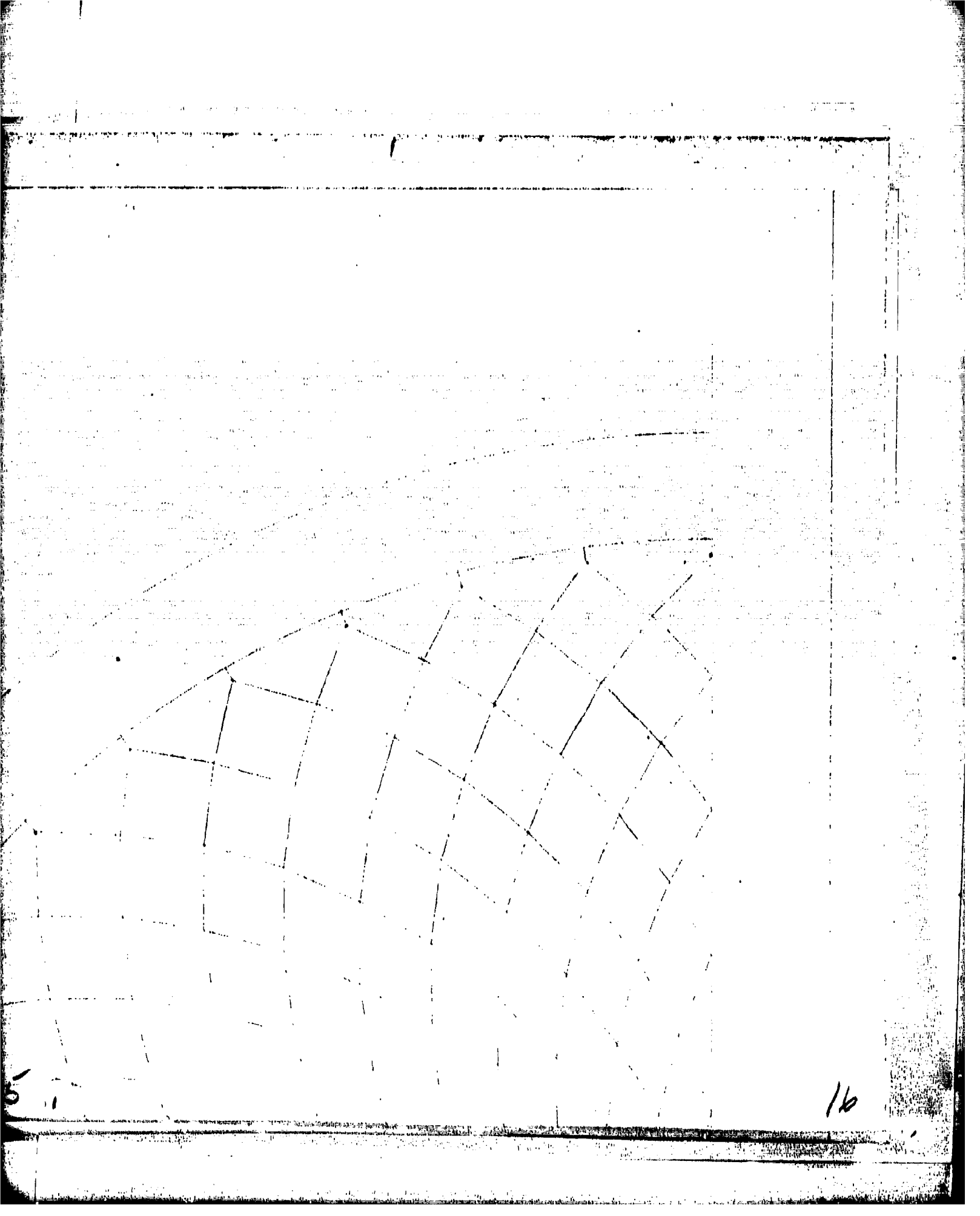
508.26

404.06

226.00

TOTAL NUMBER OF WAS CELLS : 2

15



5

16



7.5° T

DIAPHRAGM

18

5° TYP

AGM

21

21

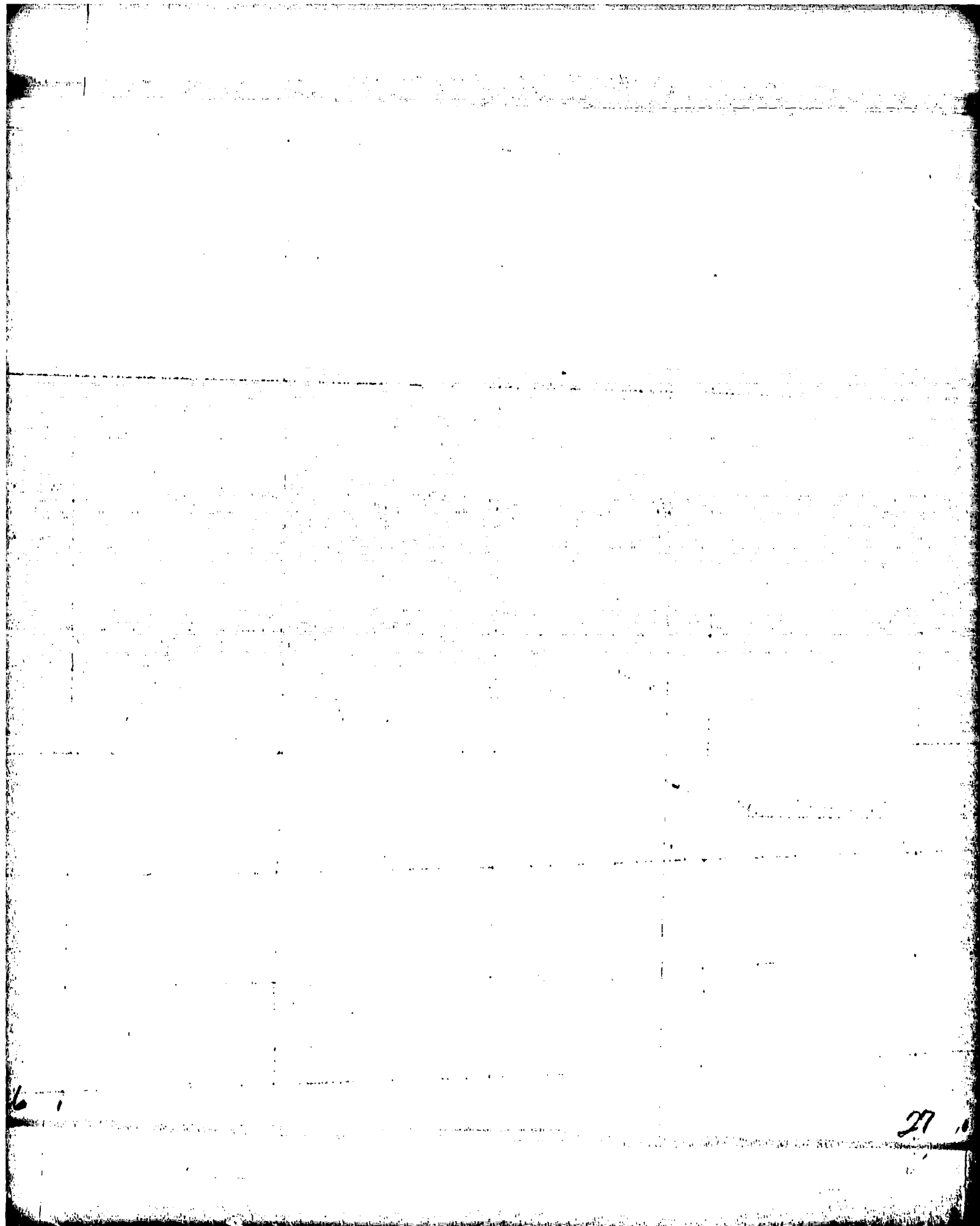
21

22

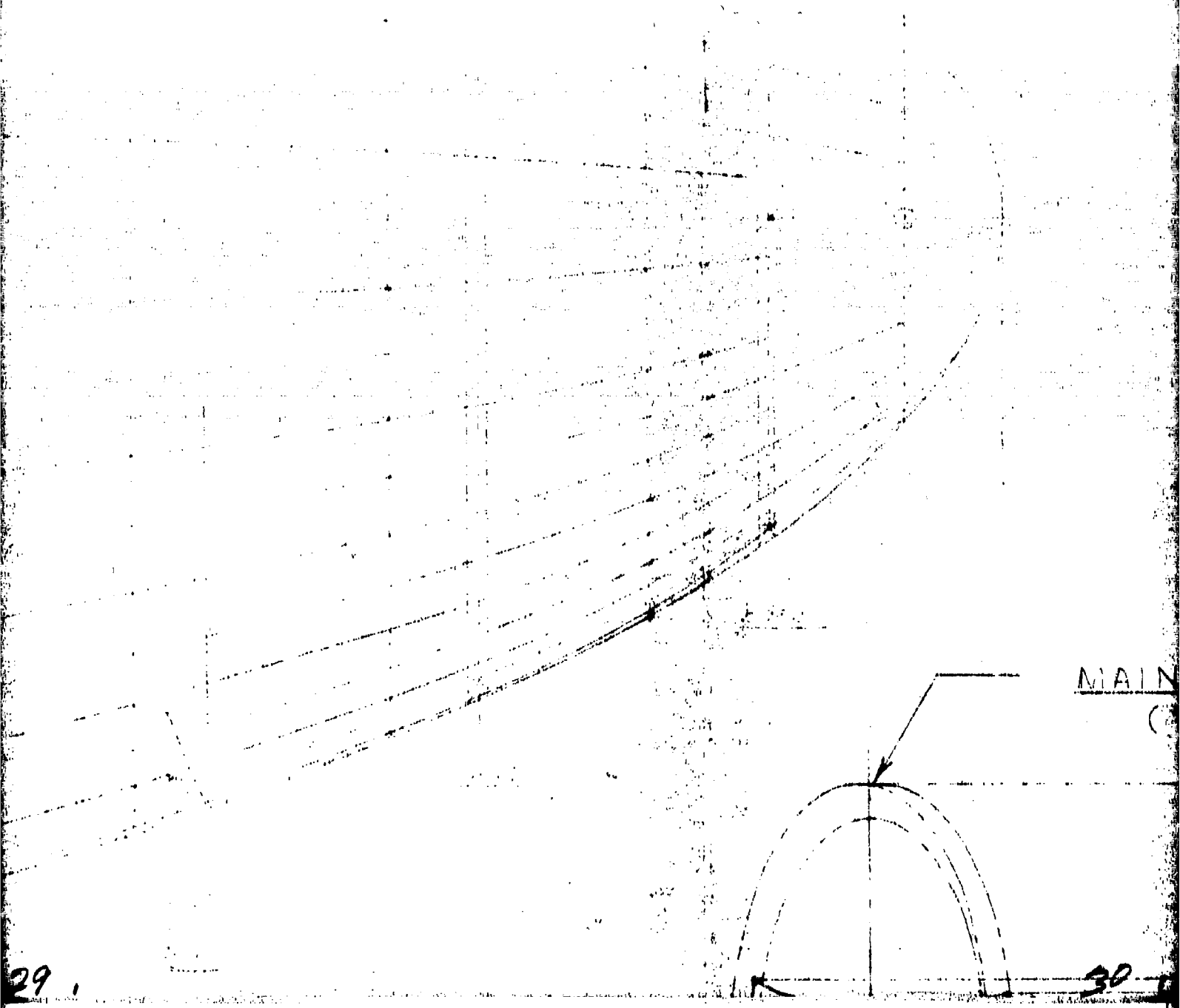
22.

23

MS. A. 1. 1. 1.



26.3135	4	2.5015
158.38	7	102.74
61.87	4	22.50



MAIN

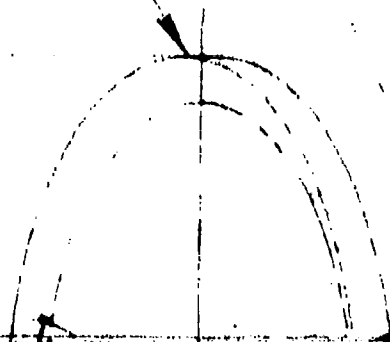
29.

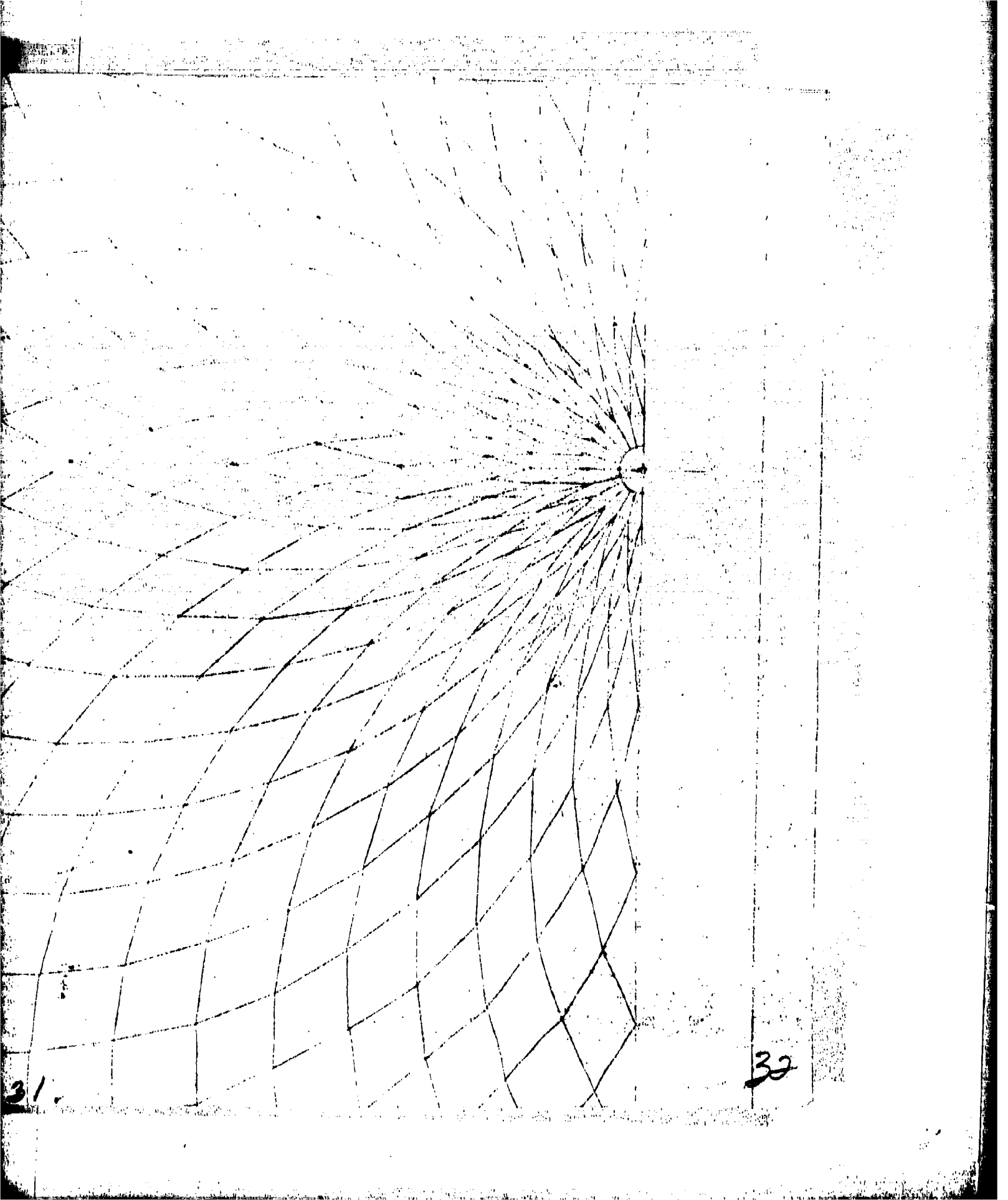
30

2.74

8.50

AIN FRAMES
(REF.)





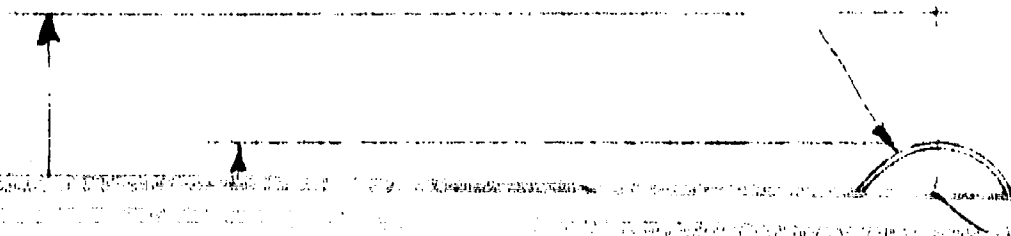
31.

32

LONGERON & LOCATION
AT MAXIMUM DIAMETER
OF HULL

SCALE: 1 INCH = 10 FEET

CAP ASSEMBLY



BALLONET
COMPARTMENT
NUMBER 1

BALLONET
COMPARTMENT
NUMBER 2

BALLO
COMPART
NUMBER

CELL 1

CELL 2

CELL 3

CELL 4

CELL 5

RESTRAINING NET

RESTRAINING NET
ANCHOR ASSEMBLY

LONGIT
MENT
NUMBER 3

BALLONET
COMPARTMENT
NUMBER 4

CELL 6 CELL 7 CELL 8 CELL 9

20
RESTRAINING NET

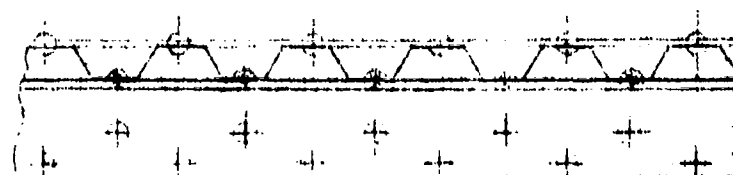
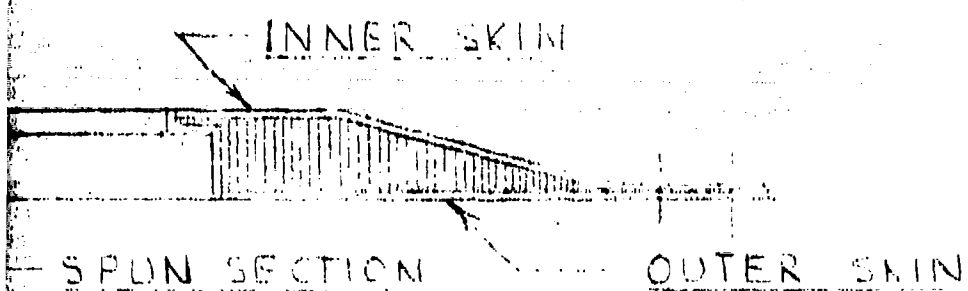
CAP ASSEMBLY

IF NECESSARY, A SPRING
SHOCK ABSORBER CAN BE
IN THIS LOCATION

HONEYCOMB

-22°

NO TYPE
N BE ADDED



SECTION

37

22
C LONG
LOCATED
EQUATO
STARBO
HULL

A - A

0.005" THICK SHEET RIVETED
AND SPOTWELDED TO CORRUGATIONS
THIS SHEET ALSO BONDED TO
PREVENT LEAKAGE

37
38

LONGERON

FIXED AT 7.5° ABOVE
HORIZONTAL ON PORT AND
BOARD SIDES OF

L

DIAPHRAGM

LONGERON
BASE SKIN

GAS CELL
MATERIAL

CLAMPING

39

8.

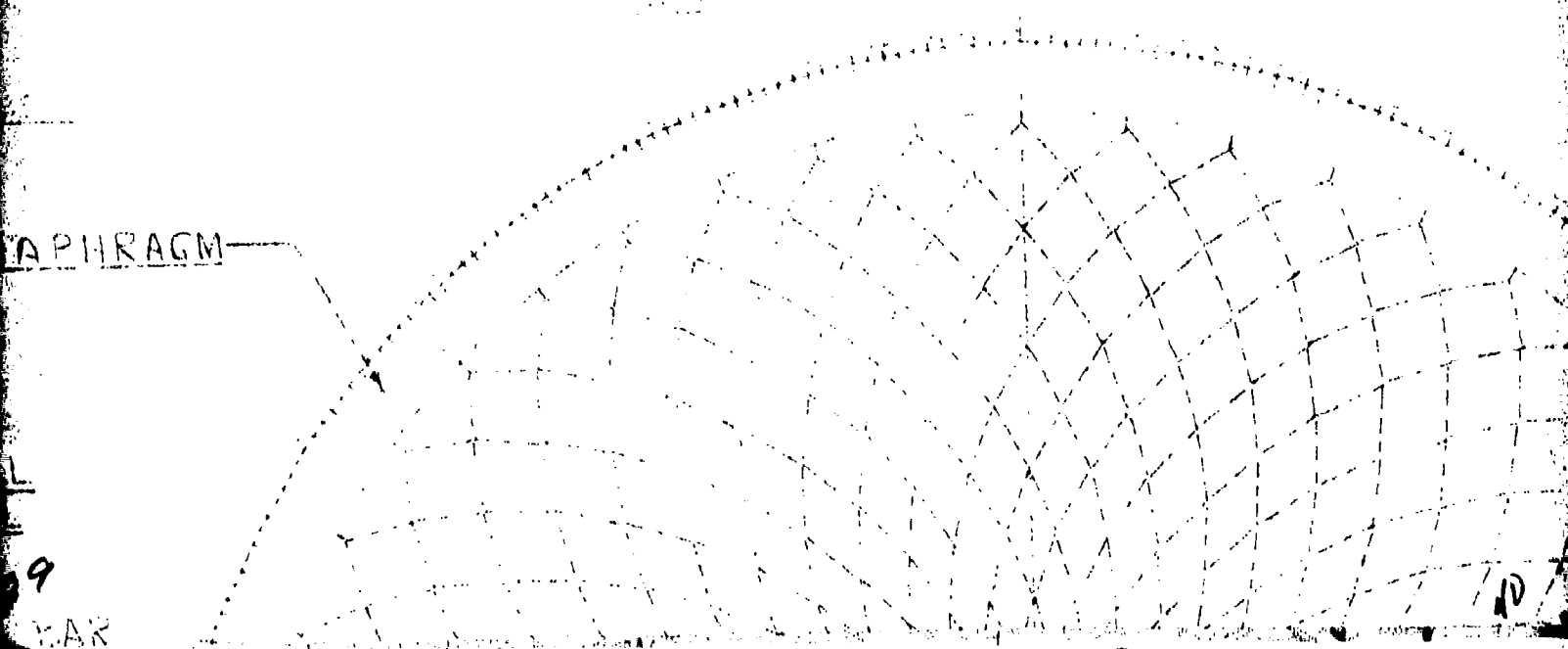
41

APHRAGM

9

KAR

10





HULL

SCALE: 1 INCH

DIAPHRAGM AND
GAS CELL TO BE
CLAMPED AND STAINED
ALONG THIS INTER-
FACE

41

26

LAYOUT

1 INCH = 10 FEET

SECTION B-B

42

42.

BUTT
JOINT

43

38.

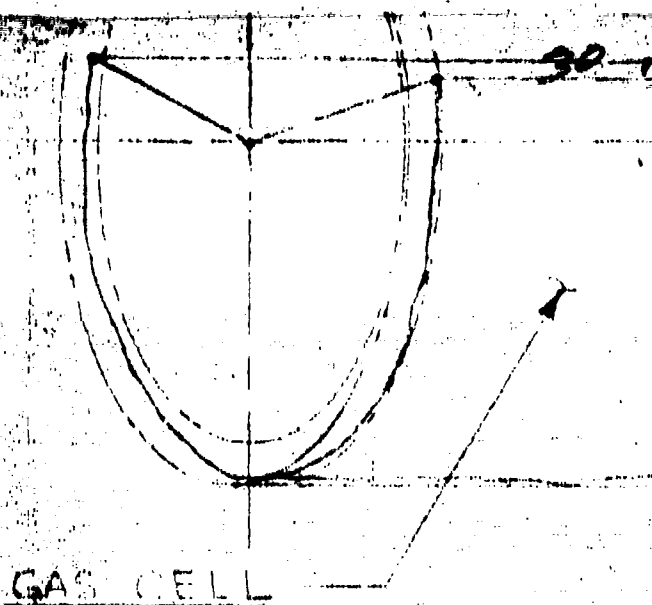
43.

44

29.

TYPE II
LAP JOINT

45

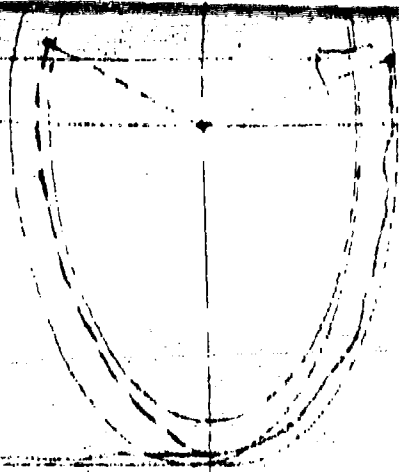


GAS CELL

GAS CELL L.C.
WHEN ASSEMBLED
AIRSHIP

TYPE I
LAP JOINT

1. FOR DESCRIPTION OF
IGN. & C. OF THE R
2. TOTAL DISPLACEMENT
3. EXTERNAL SURFACE
4. SURFACE LENGTH
5. CENTER OF BUOYANCY
6. TOTAL NUMBER OF



LOCATION
MBLED IN

VIEW LOOKING AFT OF
STARBOARD HALF OF
MAIN FRAME AT STATION
334.50 (RESTRAINING
NET SHOWN)

NOTES -

IF TYPES OF JOINTS IN SKIN STRUCTURE ARE SECT-
REPORT

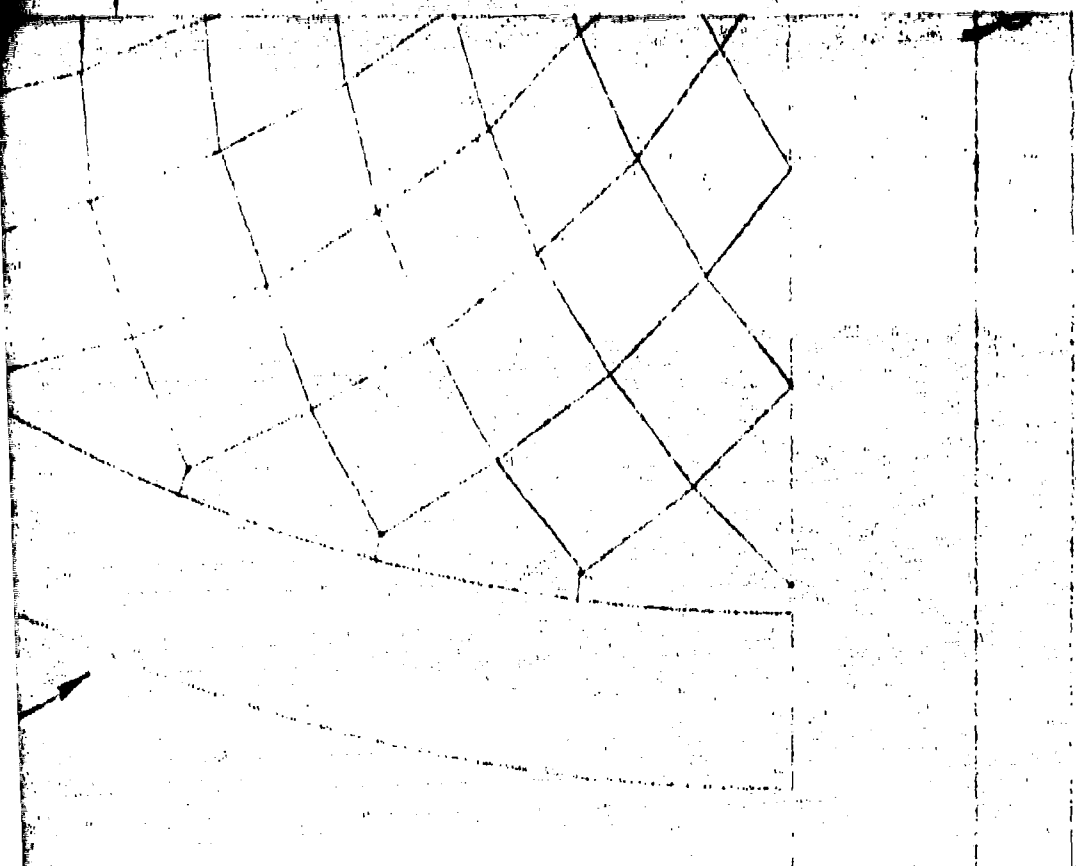
WEIGHT : 20,000 LBS

ICE AREA : 472.200

BOW TO STERN : 375.20

ANCHY : 426.85 FEET FROM BOW ALONG CENTRAL AXIS

GAS CELLS : 9



NADC 76238 30

46